The molecular requirements of the Gβγ-SNARE interaction.

By

Zack Zurawski

Dissertation
Submitted to the Faculty of the
Graduate School of Vanderbilt University
in partial fulfillment of the requirements
for the degree of

DOCTOR OF PHILOSOPHY
in

Pharmacology
May, 2016
Nashville, Tennessee

Approved: Date:

_____ _____
Heidi Hamm, Ph.D

_____ _____
Brian Wadzinski, Ph.D

_____ _____
Kevin Currie, Ph.D

_____ _____
Qi Zhang, Ph.D

_____ _____
Craig Lindsley, Ph.D

ACKNOWLEDGEMENTS

There are a great many people without whom my graduate career would not have been possible. I would like to thank my mentor, Heidi Hamm, Ph.D, first and foremost, as well as all of the Hamm lab members who helped me along the way, including Christopher Wells, M.D. Ph.D, Katherine Betke, Ph.D, Susan Yim, Karren Hyde, and the rest of the lab. The lab of Simon Alford, Ph.D, including Brian Page, Ph.D and Shelagh Rodriguez, at the University of Illinois at Chicago, conducted the studies performed in lamprey neurons. Next, the expertise of Craig Lindsley, Ph.D, and his lab, was essential for the chemical development of Gβγ-SNARE inhibitors. These chemists include Shaun Stauffer, Ph.D, Tim Senter, Ph.D, Kayla Temple, Ph.D, Changho Han, Ph.D, and others. The services of the Vanderbilt High-throughput Screening Core were very important for many of the assays described within. I would like to thank Joshua Bauer, Ph.D for his assistance in this regard. The Vanderbilt Islet Procurement and Analysis Core was very helpful for all of the studies included within pertaining to pancreatic islets. For this, credit goes to Anastasia Coldren, Greg Poffenberger, and Marcela Brissova, Ph.D. I would also like to thank Qi Zhang, Ph.D, and Claire Delbove for their assistance in conducting fluorescence microscopy studies in neurons. Finally, the other members of my dissertation committee, including Kevin Currie, Ph.D, and Brian Wadzinski, Ph.D, were essential in providing advice and guidance along the way.

TABLE OF CONTENTS

PAGE

LIST OF TABLES

LIST OF FIGURES

LIST OF ABBREVIATIONS

5-HT	serotonin
AMPA	2-Amino-3-(3-hydroxy-5-methyl-isoxazol-4-yl)propanoic acid
α_{2a}AR	α_{2a} adrenergic receptor
ATP	adenosine triphosphate
AUC	area under the curve
BoNT	botulinum neurotoxin
BSA	bovine serum albumin
cAMP	cyclic adenosine monophosphate
CAPS	3-(cyclohexylamino-1-propanonesulfonic acid
CaV	voltage-gated calcium channel
cGMP	cyclic guanosine monophosphate
CNS	central nervous system
CSP	cysteine string protein
CI	confidence interval
DTT	dithiothreitol
EC_{50}	half maximal effective concentration
EDTA	ethylenediaminetetracetic acid
EGTA	ethyleneglycoltetracetic acid
EPSC	excitatory postsynatptic current
GABA	gamma-aminobutyric acid
GGL	G protein γ-like

GDP	guanosine diphosphate
GIRK	G protein-coupled inwardly rectifying potassium channels
GPCR	G protein-coupled receptor
GRK	G protein-coupled receptor kinase
GST	glutathione S-transferase
GTP	guanosine triphosphate
HBSS	Hank's buffered salt solution
HEPES	4-(2-hydroxyethyl)-1-piperazineethanesulfonate
IC_{50}	half maximum inhibitory concentration
K_{ir}	inwardly rectifying potassium channel
LTD	long term depression
MAP	Mitogen-activated protein (kinase)
mGluR	metabotropic glutamate receptor
$MeSO_3$	methanesulfonate
$MeSO_4$	methanesulfate
MHD	Munc homology domain
NMDA	n-methyl D-aspartate
OG	n-octylglucoside
PMSF	phenylmethylsulfonyl fluoride
RGS	regulator of G protein signaling
PLC	phospholipase C

RGS	regulator of G protein signaling
SD	standard deviation
SM	Sec-1/Munc-18
SNAP	synaptosome-associated protein
SNARE	soluble N-ethylmaleimide-sensitive factor attachment protein receptors
Tris	2-Amino-2-hydroxymethyl-propane-1,3-diol
TBS	tris-buffered saline
VAMP	vesicle-associated membrane protein
VDCC	voltage-dependent calcium channel

CHAPTER I

INTRODUCTION

GPCRs: structure and function.

G-protein coupled receptors (GPCRs) are the largest family of transmembrane receptors, which transduce extracellular signals into intracellular responses. There are over 800 different GPCRs, many of which are "orphan" receptors with no identifiable ligand [1,2]. For the receptors that have identifiable ligands, a large diversity of chemotypes is observed, with neurotransmitters, peptide hormones, polypeptide hormones, the steroid hormone estrogen, odorants, light-sensitive tethered molecules, and tethered peptides that must be proteolytically cleaved for activity [1,2]. All GPCRs share basic structural motifs, the best-known of these being seven hydrophobic transmembrane domains that adopt an alpha-helical conformation, giving the receptors the alternative name "7-transmembrane receptors". In addition to this, they contain an extracellular N-terminus, an intracellular C-terminus, and three intrahelical loops on each side of the membrane[1,3]. The structures of over 127 GPCRs have been solved[4]: the beta-2 adrenergic receptor is amongst the most well-studied GPCRs from a structural perspective, with high-resolution crystal structures available in both the inactive[5,6] and active high-affinity[7] states. Unique residues and motifs on extracellular regions are responsible for ligand specificity for any given GPCR. A critical feature is the (E/D)RY ionic lock motif that forms a salt bridge between $R^{3.50}$ of helix III and $E^{6.30}$ of helix VI[8]. Receptor activation results in outward movement of helix VI by 14 Ă and extension of helix V by two helical turns, breaking the salt bridge[7,9]. In addition, changes occur to a structurally important rotamer toggle switch $W^{6.48}$ and a conserved NPxxY motif as a consequence of GPCR activation [1-3]. This altered configuration permits G protein heterotrimer binding and activation, with numerous interactions between residues of the GPCR and residues on the αN helix of the Gα subunit, the β2-β3 loop, and the α5 helix, but not the Gβγ subunit[7]. The primary function of GPCRs is to transduce an extracellular small molecule signal into an intracellular response through the generation or activation

of one or more second messenger molecules. GPCRs are nucleotide exchange factors: in response to agonist binding, they form a ternary complex consisting of agonist, receptor and heterotrimeric G-protein[7,10]. In this ternary complex, nucleotide exchange is favored. (Fig. 1Most GPCRs couple to one or more types of receptor-specific heterotrimeric G-proteins: the molecular requirements for heterotrimeric G protein coupling have not been completely elucidated, but are thought to be related to the C-terminus of Gα[11 12,13].) Active-state GPCRs also promote GRK phosphorylation and arrestin binding, leading to receptor desensitization as a feedback mechanism[14]. β-Arrestins can link GPCRs to MAP kinase (including ERK, p38, and JNK) signaling via this interaction[15], producing MAP kinase activation. This signaling is GRK-isoform dependent: GRK2/3 phosphorylation are thought to promote internalization via interactions with clathrin and AP2, while GRK5/6 promote MAP kinase scaffolding[16,17]. Receptor internalization may lead to recycling or proteolytic degradation[16]. Another important GPCR function involves homo-or hetero-dimerization of two or more receptors. This is observed in multiple families of GPCRs, but is most important for the Class C family of GPCRs, which contain an N-terminal VFT domain implicated in agonist recognition[18]. Of these receptors, metabotropic glutatmate receptors are obligate homodimers linked by a disulfide bond[19], while $GABA_B$ receptors are heterodimers consisting of a $GABA_{B1}$ and $GABA_{B2}$ receptor, the latter of which makes contact with the G protein heterotrimer[18]. The $GABA_{B1}$ subunit is thought to improve coupling efficacy through allosteric interactions[18,20]. Some GPCRs do not efficiently activate G protein signaling and are thought of as scavengers for their ligands: one example of these receptors is the chemokine receptor CXCR7, which is thought to scavenge and internalize CXCL12, preventing it from activating other chemokine receptors[21,22]. A novel class of functions is observed in the class F GPCRs, which include the Frizzled and Smoothened(Smo) receptors. The Smo receptor does not directly interact with its secreted ligand hedgehog (Hh). Instead, it exists in an inherently repressed state mediated by the transmembrane protein Patched, which is not thought to interact with Smoothened directly[23]. ,Hh binds to Patched, reducing the inhibition upon Smo[24]. Smo is then free to interact with a multi-protein complex consisting of Cos2 and

several protein kinases, including PKA, that phosphorylates the transcription factor Ci/Gli , targeting it for proteolytic degradation. Active Smo binding to this complex reduces Ci/Gli phosphorylation and degradation, allowing the transcription factor to reach the nucleus[23]. Much like traditional GPCRs, Smo also activates heterotrimeric $G_{i/o}$ G proteins, which is thought to be important for the activation of Gli transcriptional modulation in fibroblasts[25], potentially through inhibition of adenylyl cyclase to inhibit PKA-dependent Gli phosphorylation[26]. A great diversity of GPCR function is observed throughout the different families of receptors.

Heterotrimeric G proteins: structure and function.

The overwhelming majority of GPCRs transduce extracellular signals through heterotrimeric G proteins. Heterotrimeric G proteins consist of a nucleotide-binding Gα subunit and a heterodimeric Gβγ subunit consisting of Gβ and Gγ polypeptides. There are 16 different genes with additional splice variants that code for 27 unique Gα subunits[27,28]. These Gα subunits are divided into four families on the basis of function, with each family activating a unique and characteristic set of downstream effectors: $G\alpha_s$ activates adenylyl cyclases, $G\alpha_{i/o}$ inhibits adenylyl cyclases, $G\alpha_q$ activates phospholipase Cβ, and $G\alpha_{12/13}$ activates RhoGEFs[29,30]. The effectors of Gα subunits are able to generate second messenger molecules to amplify a signaling response. One well-studied second messenger would be cyclic AMP (cAMP), which is generated from adenylyl cyclase. Numerous proteins contain cAMP-binding sites, notably the regulatory subunit of PKA. cAMP binding to the regulatory PKA subunit causes it to dissociate from the catalytic subunit, allowing the catalytic subunit to phosphorylate a wide variety of proteins to alter cellular function[31]. In general, second messengers are capable of modulating the activity of numerous cell processes, such as excitability and transcription. Gα subunits are thought to be considered active in the GTP-bound state and inactive in the GDP-bound state. All Gα subunits contain a GTPase domain that hydrolyzes GTP to GDP and inorganic phosphate: this domain is conserved between all G proteins[1]. Certain effectors, termed GTPase-activating proteins, are capable of enhancing

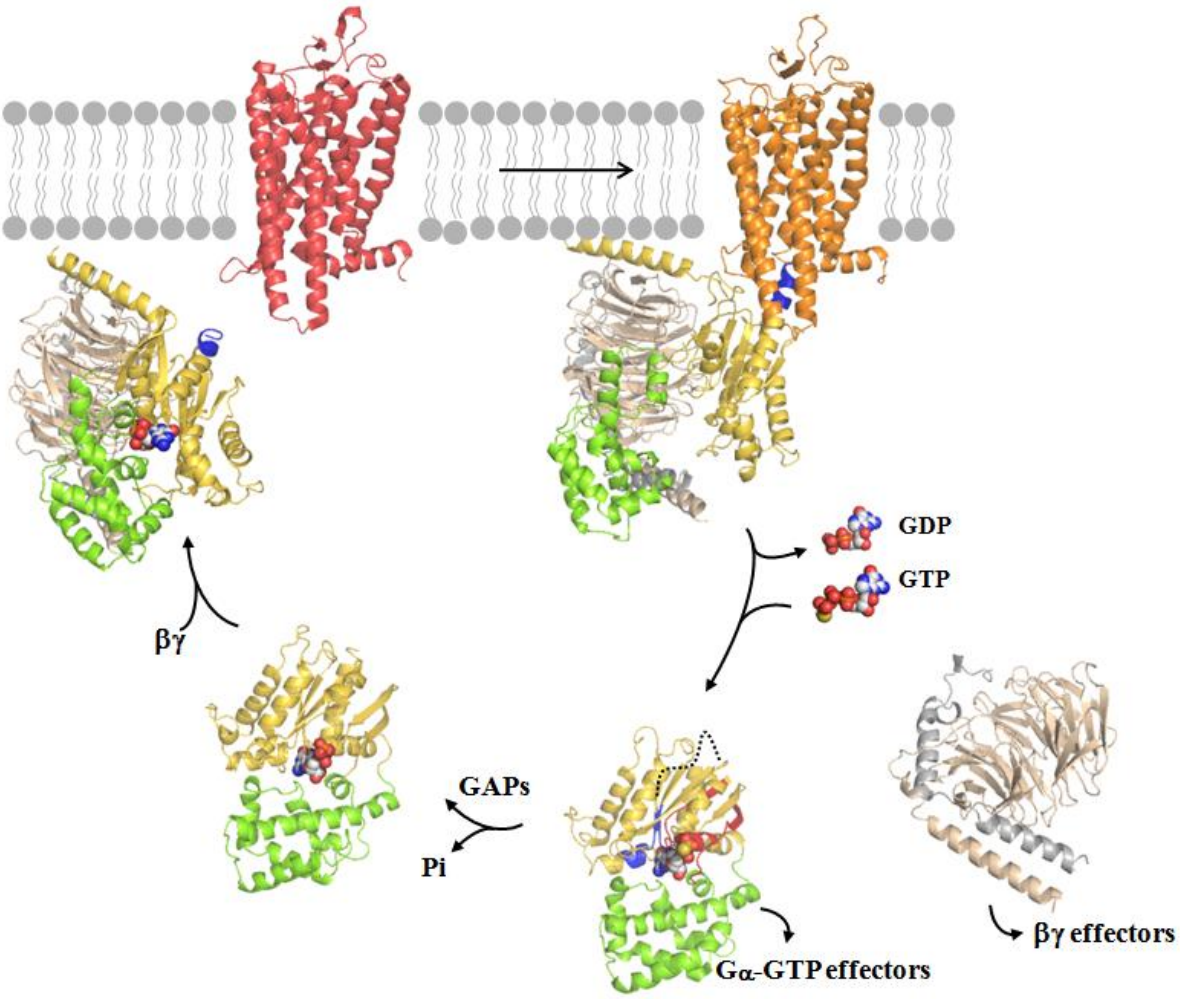

Fig. 1: The G protein cycle.

Heterotrimeric GDP-bound Gαβγ (the two domains of Gα in yellow and green, Gβ brown, Gγ gray) binds to an agonist-bound GPCR (red) to form a high-affinity ternary complex (orange). The GPCR acts as a nucleotide exchange factor for Gα, causing it to release GDP. GTP binds to the nucleotide binding pocket and promotes heterotrimer dissociation, allowing both G protein subunits to bind to their effectors. GTPase-activating proteins (GAPs) can encourage hydrolysis of GTP to GDP, resulting in heterotrimer reassociation. Illustration by Heidi Hamm, Ph.D.

the rate of which GTP hydrolysis occurs, altering the magnitude and duration of G protein signaling: one example of these are the Regulators of G protein Signaling (RGS) family of proteins, which contain an RGS-box domain that binds to and stabilizes conformations of the GTPase domain conducive to hydrolysis[32] . The GTPase domain also contains essential structural motifs for binding to effectors and GPCRs, in addition to this important catalytic activity. They also all contain a helical domain consisting of 6 α-helices that forms a cap over the nucleotide binding pocket, blocking nucleotide diffusion into the cytosol[1]. Gα subunits are subject to post-translational modification: most are palmitoylated at the N-terminus, with $G\alpha_i$ subunits subject to additional myristolation at the N-terminus.[33 34]. These post-translational modifications tether the Gα subunit to the membrane, where GPCRs and downstream effectors reside[1]. The structural characteristics listed above are well-conserved across the different Gα families.

The structure of the Gβγ subunit is well-characterized, much like Gα.. There are 5 different Gβ subunits and 12 Gγ subunits, with Gβ 1-4 being highly conserved , while $G\beta_5$ only shares 50% sequence identity with $G\beta_1$ ([35,36]). The Gγ subunits are generally grouped as Gγ1-like gammas and Gγ2-like gammas on the basis of structure and whether they are geranylgeranylated or farnesylated [35,37]. In addition, $G\beta_5$ interacts with the RGS9 family proteins to form a functional heterodimer in cells: RGS9 family members contain a Gγ-like domain for this process[38]. Gβγ is an obligate dimer with many co-chaperones required for dimer assembly, with each of the individual subunits being unstable in the absence of the other[39]. The complex features two structural regions: at the amino terminus, the N-terminal helices of Gβ and Gγ form a coiled-coil with each other[40,41]. Gβ forms a 7-bladed β-propeller structure consisting of anti-parallel β-strands termed WD-repeats[40 41]. Not all Gβ subunits form functional dimers with all Gγ subunits: $G\beta_1$ and $G\beta_4$ do, while $G\beta_2$ and $G\beta_3$ only form dimers with select gammas [42]. Some groups have reported $G\beta_5$-containing Gβγ dimers, while other groups have not [42,43]. Gβγ signaling is well-studied and it is accepted within the field of signal transduction that Gβγ subunits

play important roles in many types of GPCR signaling. Functionally, Gβγ interacts with many different effectors through binding directly to them and inducing a conformational change that modulates their activity: these effectors include adenylyl cyclases, phospholipase Cβ, phosphoinositide-3-kinase, ion channels, both Ser/Thr and Tyr kinases, and SNAREs, amongst other proteins[40,44]. These effectors that are pertinent to exocytosis, and the molecular requirements for Gβγ binding to them, will be covered in detail in other sections. Many effectors bind to Gβγ through a pleckstrin homology (PH) domain, such as phospholipase D, although numerous Gβγ effectors lack such a domain and instead bind to Gβγ via other structural features[45,46]. It is speculated that different Gβγ dimers have different signaling properties: Gβγs made with different Gγ subunits couple with differing potencies for A_1 adenosine and 5-HT_{1a} receptors, while $G\beta_1\gamma_2$ binds SNAREs with a 20- fold higher potency than $G\beta_1\gamma_1$[47,48]. Residues on Gβ are a major determinant of Gβγ-effector interactions, particularly those on the Gα-binding surface[44]. In addition, it is thought that the prenyl moiety on Gγ may be implicated in Gβγ dimer functionality. The ability of Gβγ to activate the phosphoinositide-3-kinase is reduced in $G\beta_1\gamma_2$ mutants in which the CAAX box is mutated so that $G\gamma_2$ is farnesylated instead of geranylgeranylated[49]. Similar studies were conducted with phospholipase Cβ: mutant farneysylated $G\beta_1\gamma_2$ is less potent at activating the enzyme than wild-type, while mutant geranylgeranylated $G\beta_1\gamma_1$ was better than wild-type at activating phospholipase Cβ[50]. A striking dissimilarity was observed in studies of activation of adenylyl cyclase II. Wild-type $G\beta_1\gamma_2$ activates it more potently than farnesylated $G\beta_1\gamma_2$. However, $G\beta_1\gamma_1$ or the structurally related $G\beta_1\gamma_{11}$ cannot activate ACII even in the geranylgeranylated state[50]. From this, it is clear that both the amino acid sequence and the posttranslational modifications are important for Gβγ-effector interactions. Further studies are needed in this area, as many cell types express a large number of different Gβ and Gγ subunits. One critical cellular function that is subject to intense regulation by Gβγ is exocytosis: Gβγ alters exocytic activity through its effects at and downstream of ion channels.

Exocytosis and synaptic transmission.

Exocytosis, or vesicle fusion, is divided into two categories, constitutive Ca^{2+}-independent exocytosis, and regulated Ca^{2+}-dependent exocytosis[51]. Constitutive exocytosis occurs in all cells and is required for the delivery of newly synthesized proteins from the translation machinery. Regulated exocytosis is found in certain populations of more specialized cells, such as small clear synaptic vesicles in neurons[51], and large dense-core granules found in neurons, platelets, as well as the alpha, beta, and delta cells of the pancreatic islet and chromaffin cells of the adrenal medulla, amongst other cell types[52,53]. Synaptic transmission is a ceullar process through which one neuron communicates with a second postsynaptic neuron utilizing chemical neurotransmitters. In this process, an action potential-a depolarizing electrical signal- is converted into a chemical signal at the synapse. To achieve the release of this chemical signal into the synaptic cleft, neurotransmitter-filled vesicles fuse with the plasma membrane of the cell, releasing neurotransmitter into the extracellular space, where it may bind to and activate cellular receptors on the postsynaptic cell, including G-protein coupled receptors and ion channels such as AMPA and NMDA receptors[51]. (Fig. 2) Activation of these receptors may create excitatory or inhibitory postsynaptic currents (EPSCs or IPSCs) in the postsynaptic cell, ensuring (or inhibiting) action potential propagation between the pre- and postsynaptic neurons connected via a given synapse. Exocytosis refers to the docking, priming, and fusion of the neurotransmitter or other hormone-filled vesicles with the plasma membrane at the active zone, resulting in the opening of a fusion pore through which the contents of each vesicle can diffuse into the extracellular space, which may include the synaptic cleft for neurons or the bloodstream for endocrine cells. There are three types of regulated exocytosis that are known to play a role in synaptic transmission: evoked (also known as *synchronous*) release, in which one or several vesicles fuse within a millisecond of an action potential, evoked asynchronous release, which sets in after a delay during a depolarizing stimulus, and spontaneous mini release, in which single vesicles fuse with the plasma membrane in the absence of a depolarizing stimulus

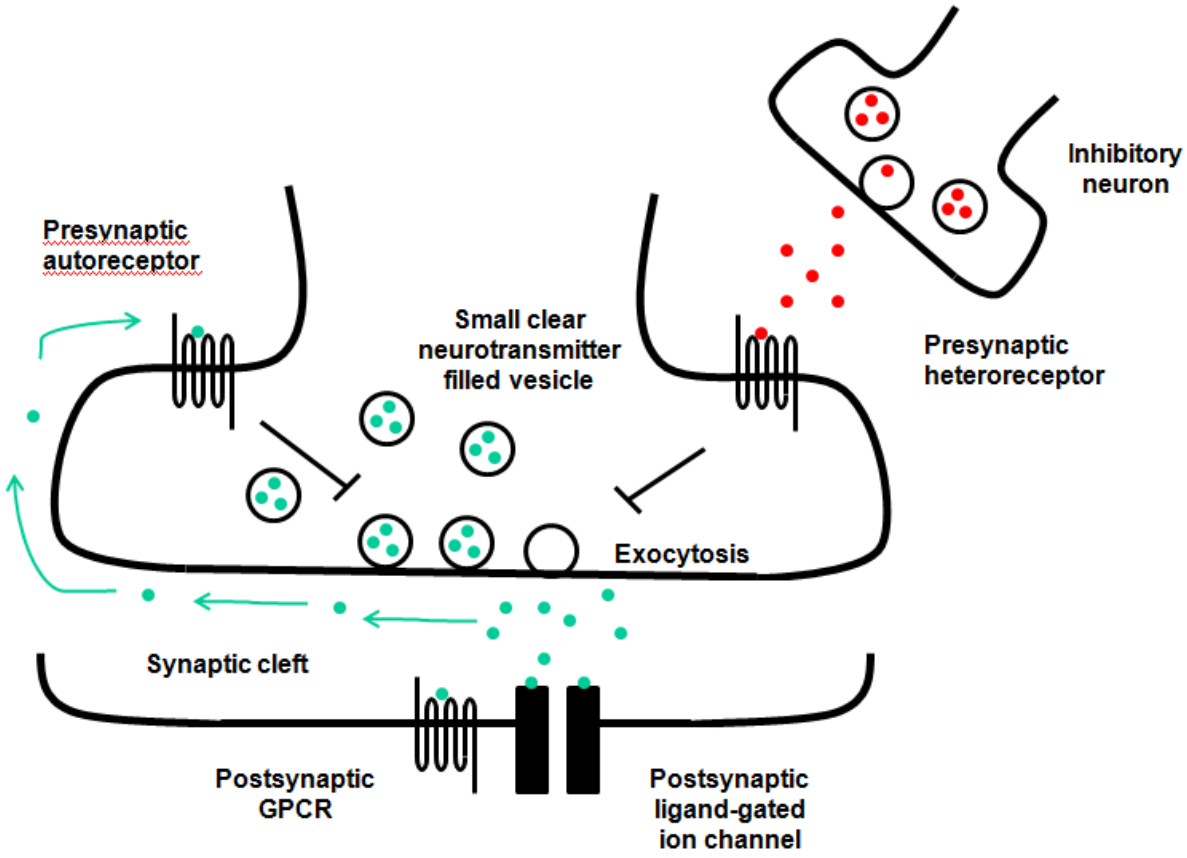

Fig. 2: Exocytosis and synaptic transmission.

In synaptic transmission, when a depolarizing signal arrives at a synapse, small clear neurotransmitter-filled vesicles at a synapse fuse at the active zone, resulting in neurotransmitter being released into the synaptic cleft. Neurotransmitters can activate postsynaptic receptors, including GPCRs and ligand-gated ion channels. Inhibition of exocytosis can occur through presynaptic autoreceptors, activated by the same neurotransmitter released from the presynaptic neuron as a form of negative feedback, or from heteroreceptors, which are activated from neurotransmitters from adjacent inhibitory neurons.

[54]. Evoked release is thought of as being the primary mechanism through which neurons communicate with each other, with spontaneous release acting to improve the fidelity of the signal[54]. Exocytosis is subject to numerous regulatory steps and many proteins participate in this process, including SNAREs, calcium sensors, and many other proteins[55-57].

SNAREs:molecular machines for exocytosis.

The SNARE complex proteins are the central force generators for exocytosis[58]. The SNARE hypothesis is a central hypothesis for our current understanding of exocytosis, in which the fusion of the vesicle and cell plasma membrane is driven by formation of a four-helix SNARE bundle, generating the necessary physical forces to merge the amphiphilic vesicle and cell membranes together and complete the fusion processes[56]. Three groups of proteins form the SNARE complex: the transmembrane t-SNAREs syntaxin, the membrane-associated t-SNARE SNAP25, and the v-SNARE synaptobrevin. The transmembrane t-SNARE syntaxin, contains three domains: a N-terminal helical H_{abc} domain, which plays a regulatory role in SNARE complex assembly and priming, the H_3 or SNARE-forming domain, which contributes a single helix to the four-helix bundle, and a C-terminal hydrophobic transmembrane domain (for SNARE domain structure, see Fig. 3) [59,60]. Syntaxin is described as a Q-SNARE, as it contributes a conserved Gln residue essential for SNARE formation at the zero ionic layer inside the four-helix bundle. There are 15 members of the syntaxin family in humans, and expression may differ between cell types and subcellular localization[59]. The membrane-associated t-SNARE SNAP25 consists of two helical SNARE domains joined by a flexible, unstructured Cys-rich linker region. It contributes 2 helices to the four-helix bundle and is also a Q-SNARE. SNAP25 lacks a transmembrane domain, with four palmitoylation sites within the linker region serving to anchor it to the membrane[60]. There are three SNAP isoforms, including SNAP25: SNAP23 plays an important role in nonneuronal exocytosis in many tissues [61-63] SNAP29 lacks palmitoylation sites [64] and has been shown to participate in exocytosis in

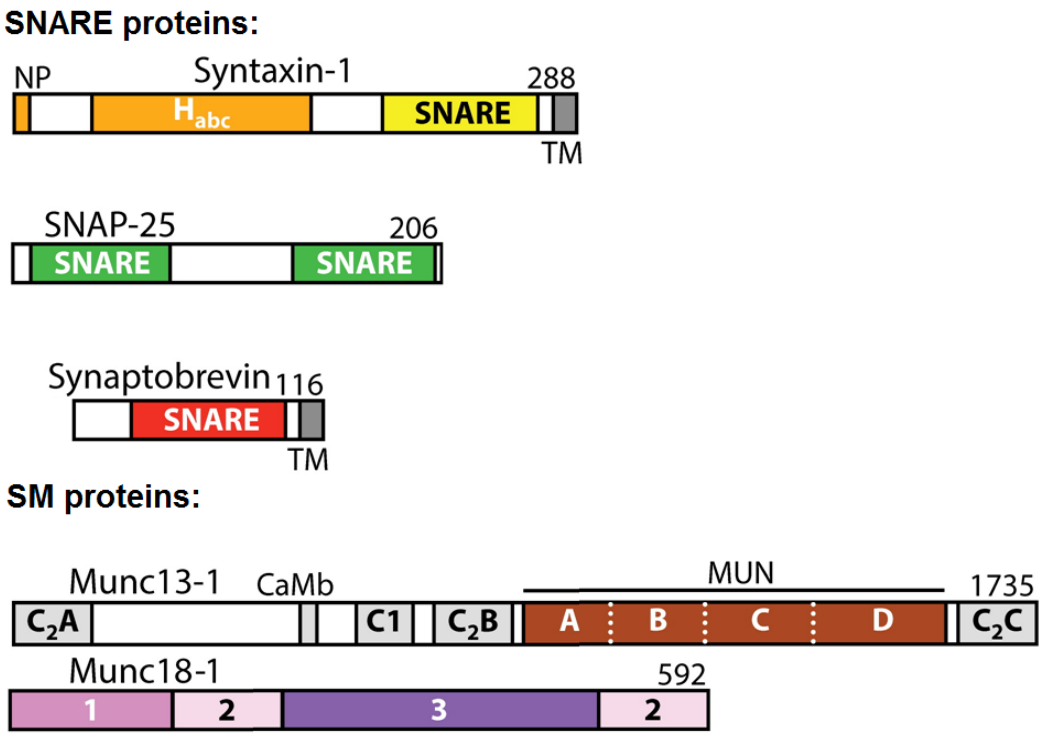

Fig. 3: SNARE and SM protein domain structure.

Visual representation of the domains of each of the SNARE proteins syntaxin, SNAP25, synaptobrevin/VAMP, and the SM proteins Munc 18-1 and Munc-13-1. Numbers in black represent the order of residues within the primary structure, while numbers and letters in white refer to the names for each domain. Figure adapted with edits for the purpose of formatting from Rizo, J, Xu J. 2015. *Annu. Rev. Biophys* 44:339-67.

several types of tissue[65,66]. Finally, the v-SNARE synaptobrevin (alternatively known as VAMP2) contains a single helical SNARE domain and a C-terminal transmembrane domain. It is localized to the vesicle and is termed an R-SNARE as it contributes an arginine residue to the "zero layer "of the elaborate series of layered protein-protein interactions that holds the SNARE complex together[60]. In most versions of the SNARE hypothesis, the t-SNAREs SNAP25 and syntaxin form a three-helix t-SNARE complex, followed by four-helix ternary complex formation with synaptobrevin. At this point, the loose trans-SNARE complex (a "SNAREpin") catalyzes fusion by zippering up into a tight cis-SNARE complex [67,68], releasing energy to drive fusion processes and form a water-filled region 1nm in diameter through which small molecules can diffuse outwards termed the fusion pore[69]. The SNARE hypothesis is supported by studies in which increasing the distance between the SNARE domains and the transmembrane domains impairs fusion [70,71]. However, the transmembrane domain in and of itself is dispensible: palmitoylated lipid-anchored SNAREs lacking a transmembrane domain are still fusion-competent. Slow fusion is observed between liposome populations containing v-SNAREs and t-SNAREs[72], but in order to achieve fast, synchronous release, many other proteins are required[73].

The role of calcium sensors in exocytosis.

Regulated exocytosis is Ca^{2+}-driven[74]. Ca^{2+} exists at low concentrations inside the cell, and considerably higher concentrations outside the cell. Within milliseconds after Ca^{2+} entry, vesicle fusion occurs[75 76]. Katz postulated that a "calcium sensor" existed within the cell that triggered vesicle fusion in response to elevated intracellular Ca^{2+}. The C2 domain protein synaptotagmin 1 was investigated as a calcium sensor after it was shown that it could bind both lipid membranes and Ca^{2+} [77,78], which would be required for such a protein. Functional evidence for this was derived from transgenic mouse studies, in which evoked release was shown to be marked deficient in homozygous syt1 knockout mice. Syt1 mutations that alter Ca^{2+} affinity alter the Ca^{2+} dependence of vesicle fusion [79,80], strongly implying that synaptotagmin 1 was the calcium sensor required for evoked release in neurons. Localized to secretory

vesicles, they all contain an N-terminal transmembrane domain and two cytosol-facing tandem C2 domains at the C-terminus, labeled C2A and C2B. These domains are responsible for both the calcium and lipid-binding functionality[54]. Synaptotagmins bind the SNAREs SNAP25 and syntaxin in a calcium-dependent manner [81,82], with low calcium-independent binding observed with apo-Syt1 and high binding with Syt1-Ca^{2+}. Biochemical studies show that the calcium-dependent binding of Syt1 to SNARE is mediated through three aspartate residues at the C-terminus of SNAP25: D179, D186, and D193[81]. Crystallographic studies of the Syt1-SNARE complex demonstrate contacts between Syt1 and two clusters of SNAP25 residues largely located midway between the N and C termini of the SN1 and SN2 helices. These residues include E37, K40, N159, M163 and D166 in the first region of contact, and D51, E52 and E55 on the second region[83]. Residues on SNAP25 that are important for calcium-independent binding are less well known. On Syt1, basic residues within both the C2A and C2B domain are important for SNARE binding. For C2A, residues R198 and K200 were important for calcium-dependent SNARE binding, while on C2B, K297 and K301 are important[84]. In addition, R398 mutants have lower Ca^{2+}-triggered fusion and t-SNARE binding[85]. R398 and R399 were also shown to be highly important residues for the interaction in the crystal structure[83]. The binding of anionic lipids to calcium sensors such as Syt1 is key to their functionality[78]. Phosphatidylserine, in particular, is a key regulator of fusion, with fusion rates tied to phosphatidylserine levels within the membrane during Syt1-triggered fusion[86] and studies showing that Syt1 demixes phosphatidylserine molecules in lipid membranes[87], potentially mediating fusion. It is thought that Syt1 may perform a "clamping" function[56]. Deletion of Syt1 causes a 10-fold enhancement in spontaneous release, termed "unclamping" [88,89]. The fusion-activating and clamping function of Syt1 are thought to be independent[56]: autapses do not exhibit unclamping in the Syt1 KO[90]. Interestingly, mutation of the Ca^{2+} -binding sites on the C2A domain inhibit synchronous release by 50% but Ca^{2+} binding-impaired C2B domain mutants block synchronous release fully [91 92,93],. However, these same mutations abolish the clamping activity to the same extent[93,94]. The functional relevance of Syt1 clamping is to ensure release only occurs in response to an intended

signal: high levels of unstimulated release from synapses would add considerable "noise" to neurotransmission [56]. The molecular functions of synaptotagmin are diverse and characterization of them is still ongoing.

There are a large number of synaptotagmins and related synaptotagmin-like C2 domain proteins that are thought of as calcium sensors for exocytosis, with over 17 synaptotagmin isoforms observed in the human genome[58]. Synaptotagmin VII is thought to be a crucial synaptotagmin for exocytosis in non-neuronal cells[95-97]. Differences in the cooperativity of calcium binding for synchronous and asynchronous release has led to the dual- Ca^{2+} sensor model of exocytosis, in which Syt1 is the calcium sensor for synchronous release and a second, unidentified calcium sensor mediates asynchronous release[98]. One candidate is Doc2, which is thought to be an important Ca^{2+} sensor for asynchronous release[99] or spontaneous release [100], although other groups have found no role for the protein in asynchronous release and instead emphasize synaptotagmin VII[101]. Interestingly, mutants in Doc2β that have impaired Ca^{2+} binding have enhanced synchronous and asynchronous release in syt1-KO neurons, and localize to the membrane constitutively[102]. Genetic ablation of both Doc2 isoforms in mice results in partially impaired glucose-stimulated insulin secretion from beta cells[103]. It is clear that calcium sensors play an essential role in all forms of regulated exocytosis.

The role of vesicle docking/priming proteins in exocytosis.

It is estimated that the readily releasable pool of vesicles within a given cell comprises a minority of the total number of vesicles [104-106]. There are thought to be four "pools"[107]: a depot pool consisting of vesicles more than 200nm from the plasma membrane, and three docked pools, located within this distance. Most vesicles are in the depot pool. The docked pools consist of the unprimed pool, which is large in size and slow to release, comprising the sustained component of release that occurs one second after calcium entry. There are two primed pools: the readily releasable pool, consisting of the fast burst phase of exocytosis that occurs within 20-40 ms of calcium entry, and the slowly releasable pool, which is

responsible for the slow burst phase that occurs within 200ms[107]. This leads to the question of the identity of the molecular determinants of each pool. Docking is defined formally as the transfer of vesicles from the depot pool to the unprimed pool[107]. It has been shown that, as a monomer, syntaxin forms a "closed" conformation that is inhibitory towards SNARE complex formation. The SM protein Munc18 binds "closed" syntaxin and enables SNARE complex formation[108,109 110] . After SNARE complex formation, Munc18 remains attached to the SNARE through the N-terminus of syntaxin[109]. SM protein domain structure is shown in Fig. 3[57]. Munc18 promotes trans-SNARE complex assembly from syntaxin1A and SNAP25[111], clasping both the v-SNARE and the t-SNARE during SNARE assembly. Genetic ablation of Munc18-1 in mice results in a block of neurotransmission[112] and a reduction in LDCVs at the plasma membrane[113]. From this, it is inferred that Munc18 plays a role in docking.

Priming is defined as the maturation of a docked vesicle in the unprimed pool to a vesicle within the slowly releasable pool or readily releasable pool[107]. The formation of the four-helix SNARE complex is considered to be the priming reaction[107]. The complex zippers up from its N to C terminus, pulling the plasma membrane and vesicle membrane into close proximity[107]. The individual steps of docking and priming are shown in Fig.4 [56]. The Munc13 family of SM proteins, of which four isoforms exist in man, are essential for the priming reaction[114,115]. It has been shown that Munc13-1-null mice lack all forms of vesicle release, while retaining docked vesicles at the synapse[115], strongly implying that the protein plays a role downstream of docking. Munc13's role in the priming reaction is facilitated through the central MUN domain , which is required for priming[116,117]. Munc13 has also been implicated in maintaining SNARE integrity throughout exocytosis, with no fusion occurring in *in* vitro models containing αSNAP and NSF to disassemble SNAREs unless Munc18 and Munc13 were present[57]. This demonstrates a role for Munc18/Munc13 as components of the minimum necessary release machinery, despite fast fusion being achievable without these proteins being present[73]. A current proposed mechanism involves Munc13 mediating the conversion between Munc18-closed syntaxin and Munc18-

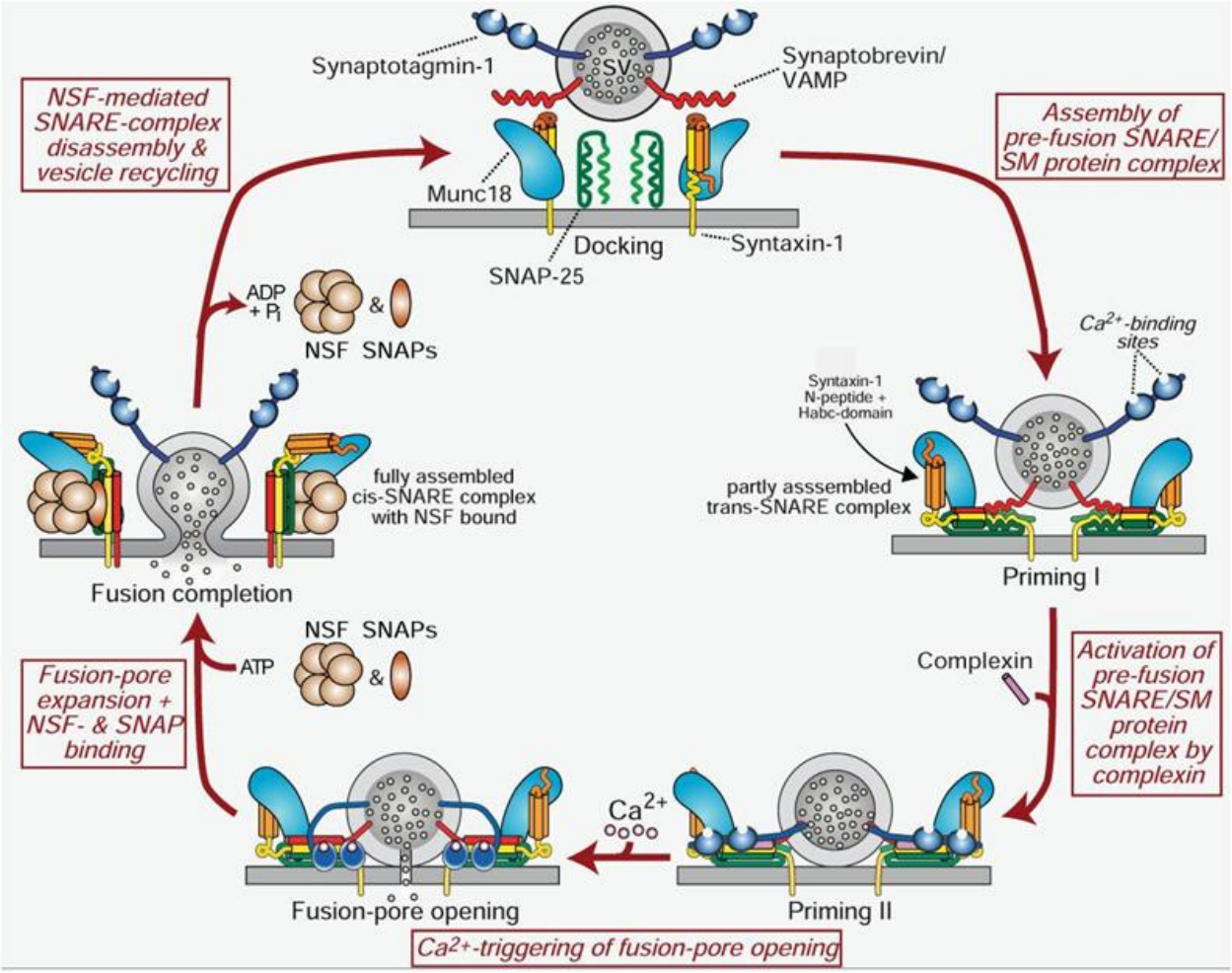

Fig. 4: Vesicle docking and priming.

Sequential representation of each of the steps required to dock and prime a vesicle for release. The pre-fusion SNARE-SM protein complex begins to dock the vesicle to the plasma membrane and is mediated by Munc18-SNARE interactions. Next, priming occurs, where the four-helix *trans*-SNARE bundle is formed, followed by activation of the pre-fusion SNARE/SM protein complex by complexin. After this, calcium triggers the opening of the fusion pore, forming a tight *cis*-SNARE complex. NSF and SNAP bind to the *cis*-SNAREs to disassemble them in an ATP-dependent manner. Figure adapted from Sudhof, *Neuron*. 2013 Oct 30; 80(3).

SNARE [55,118]. Despite functional importance, a firm biophysical role for the SM proteins in fusion has yet to be fully defined[55].

A major scaffold of the fusion machinery is the protein RIM [56]. RIM binds to Munc13, the voltage-gated calcium channel (both directly and indirectly via RIM-BP) , as well as binding to the vesicle-bound GTPase Rab3/27 in a GTP-dependent manner[56]. RIM's interactions with Munc13 are thought to keep Munc13 from autodimerizing in an inhibitory manner[119]. The functional relevance of the RIM-calcium channel interaction is to position the vesicle closely adjacent to the voltage-gated calcium channel, allowing for tight spatial regulation of calcium concentration at the active zone[56]. Deletion of RIM or RIM-BP produces a loss of calcium channels at presynaptic active zones[120,121], highlighting the importance of this scaffold in vesicle priming. The structure of the presynaptic active zone, including RIMs, is shown in Fig. 5.

The second step in priming involves the conversion from the slowly releasable pool to the readily releasable pool. Some data suggests that complexin may be implicated in this step. Complexin contains an n-terminal accessory helix and a central helix[122]. Complexin binds to the SNARE complex in a Ca^{2+}-independent manner between syntaxin and synaptobrevin[122]. The role of complexin in exocytosis was initially controversial, with uncertainty existing over whether the protein was stimulatory or inhibitory towards exocytosis. Fittingly, its role was found to be multifaceted and complex: depletion of complexin impairs fast synchronous release [123,124] but not asynchronous or spontaneous release, and complexin levels are lowered in Munc13-1-deficient animals, suggesting that this protein acts at a later step. In general, synaptotagmin-mediated fusion is also dependent upon complexin as a cofactor[125,126]. It is thought to act as a clamp upon fusion by preventing complete SNARE complex assembly until Ca^{2+} binds to synaptotagmin[54,127,128]. Complexin can bind concurrently to synaptotagmin in reconstituted membranes[129,130]. A model for complexin function has been proposed with Syt1 and complexin bound

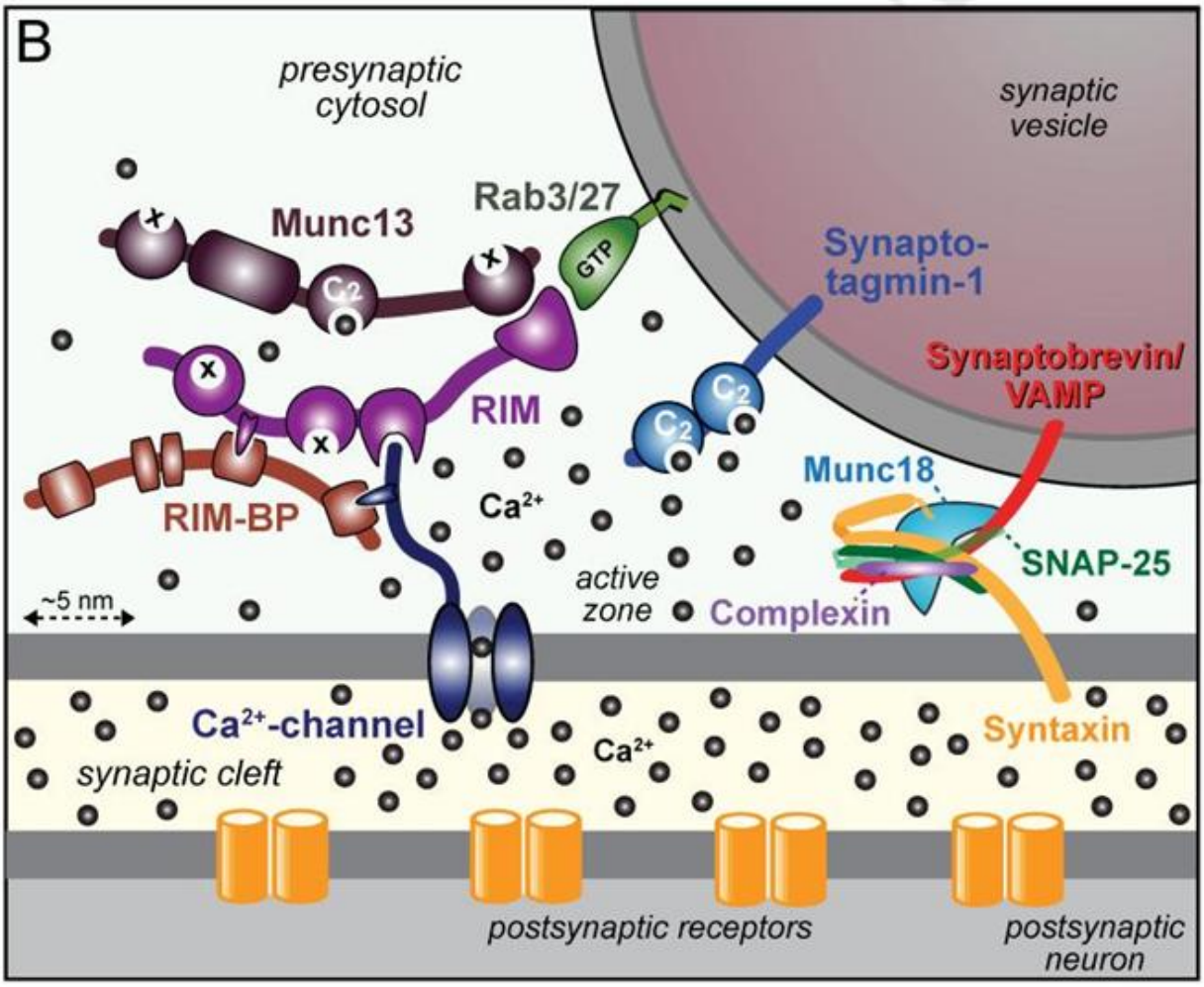

Fig. 5: Structure of the presynaptic active zone.

Diagram showing the approximate location and binding partners of each protein in the multi-protein complex of the presynaptic active zone. Cell membranes are depicted in dark grey, while vesicular membranes are depicted in medium grey. Figure adapted from Sudhof, *Neuron*. 2013 Oct 30; 80(3).

simultaneously to a partially formed SNARE complex. In the absence of Ca^{2+}, membrane fusion is inhibited through electrostatic and steric repulsion of the C2B domain of synaptotagmin and the accessory helix of complexin. In the presence of Ca^{2+}, C2B binds to the membrane, forcing the melting of the complexin accessory helix, relieving the electrostatic and steric repulsion [57,131,132] (Fig. 6) This model is in accord with studies showing that complexin inhibits fusion at low Ca^{2+} and promotes it at high Ca^{2+} in a synaptotagmin-dependent manner[73,133].

Other accessory proteins that play key roles in exocytosis.

A large number of proteins are implicated as being important for the regulation of exocytosis. This section is not meant to be a comprehensive list of all accessory proteins for exocytosis, but to rather list several major ones that are of interest to the project. After exocytosis, the ternary SNARE exists in a cis-SNARE conformation that is not conducive to further fusion events. SNARE disassembly and recycling is mediated by the ATPase NSF, which disassembles cis-SNAREs in an ATP-dependent manner[107,134]. NSF is a large, hexameric AAA+-family ATPase that forms a complex with the protein SNAP (not related to SNAP25). Three to four SNAPs form a right-handed helix around the left-handed helices of the SNARE into the central pore of NSF, where the hydrolysis of 10-50 ATPs per SNARE provides the energy for a concerted disassembly in spring-like fashion[134 135,136]. A second protein of interest is tomosyn-1, a protein with two distinct domains: an N-terminal B-propeller domain structurally similar to Gβγ, and a C-terminal R-SNARE, but no transmembrane domain[137] .Tomosyn-1 is thought to perform an inhibitory role in vesicle priming by forming a unique complex with SNAP25, syntaxin, and synaptotagmin that does not permit synaptobrevin to bind [137-139]. Finally, cysteine string protein is a neuroprotective chaperone protein that acts to prevent SNAP25 degradation within the cell[140]. It is also a GEF for Gα subunits, but interestingly, interacts with Gβγ as well at its C-terminus. Finally, it can also bind to voltage-gated calcium channels. Functionally, cysteine string

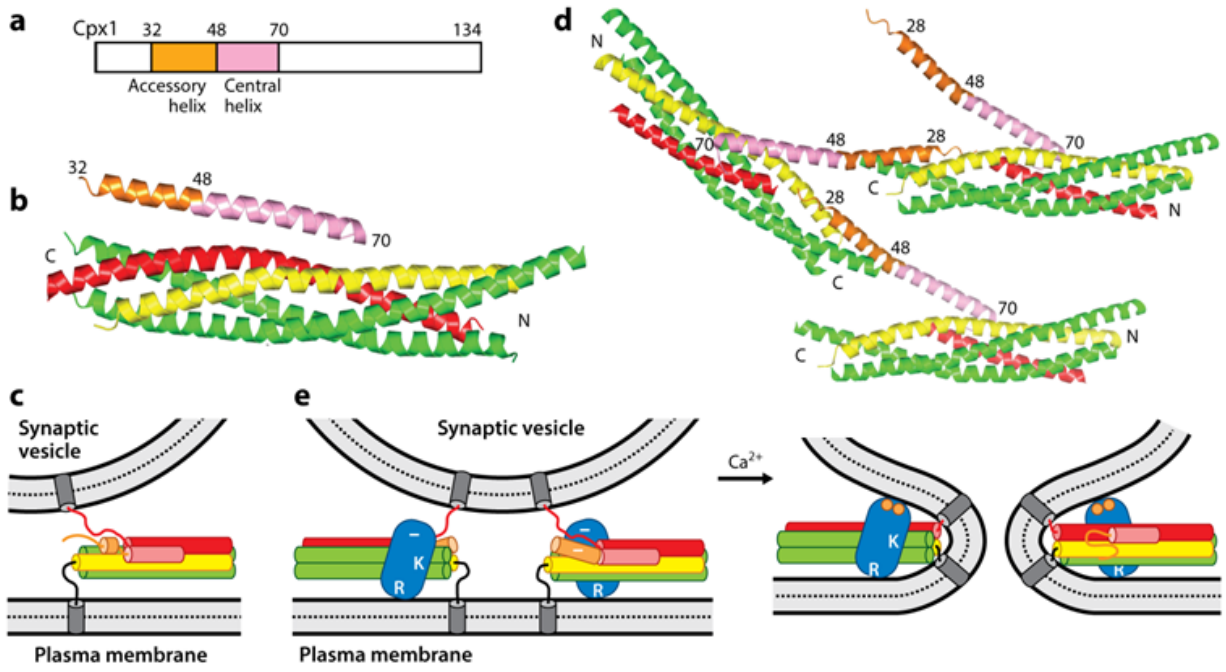

Fig. 6: The role of complexin in exocytosis.

a: Domain structure of complexin. b: Three-dimensional structure of complexin interacting with a single four-helix SNARE bundle. c: Visual representation of complexin bound to a SNARE. d: Three-dimensional structure of complexin linking multiple SNARE complexes. (PDB: 3RK3) e: Docked and primed complexin-bound SNARE fusing in the presence of Ca^{2+}. Synaptotagmin is represented in blue. Figure adapted from Rizo, J, Xu J. 2015. *Annu. Rev. Biophys* 44:339-67.

protein produces a tonic G protein inhibition of voltage-gated calcium channels in a Gβγ-dependent manner[141], limiting calcium-dependent processes in the cell.

Modulation of exocytosis by GPCRs.

G-protein coupled receptors are key regulators of exocytosis[142]. A large number of GPCRs can alter exocytosis, both in stimulatory and inhibitory fashion. GPCRs are generally thought to work through agonist-mediated stimulation of nucleotide exchange within heterotrimeric G proteins, resulting in the separation of Gα-GTP and Gβγ. Both subunits are capable of the modulation of exocytosis. For Gα, multiple families of Gα subunits play important roles in exocytosis. $G\alpha_s$ stimulates adenylyl cyclase to produce cyclic AMP, which binds to the regulatory subunit of protein kinase A and releases the catalytic subunit, capable of phosphorylating downstream effectors. Exocytosis may be perturbed by $G\alpha_s$ signaling, both in a PKA-dependent and PKA-independent manner via the cAMP-sensitive nucleotide exchange factor Epac1[143]. PKA phosphorylation of K^+ channels perturbs cell voltage, activating voltage-gated calcium channels[144,145]. CSPa is phosphorylated by PKA at S10 to reduce its binding to syntaxin and synaptotagmin, prolonging opening of the fusion pore [146,147]. SNAP25 is phosphorylated at T138 by PKA, with this phosphorylation being key to the size of the readily releasable pool[148].

Much like G_s-coupled GPCRs, G_q-coupled GPCRs also play crucial roles in the regulation of exocytosis. $G\alpha_q$ can activate phospholipase Cβ to convert PIP_2 into inositol triphosphate and diacylglycerol. Inositol phosphate (IP_3) can bind to the IP_3 receptor to mediate calcium release from internal cellular stores, while diacylglycerol can recruit the calcium-dependent protein kinase C to the cell membrane to phosphorylate other downstream effectors. Similar to PKA, phosphorylation of numerous exocytic proteins by protein kinase C, can affect their activity, such as the docking/priming protein Munc18 at S313[149], and the I-II linker of the voltage-gated calcium channel [150]. Many steps of vesicle docking, priming, and release can be perturbed by protein kinase C, with phosphorylation of S187 on the SNAP25 SN2 helix reducing

SNAP25 binding to syntaxin to regulate SNARE formation[151]. Activated GPCRs may also recruit arrestins, which can act as scaffolds to promote MAP kinase signaling to influence exocytosis[152].

The focus of my dissertation will be on $G_{i/o}$-coupled GPCRs: the $G\alpha_i$ subunit these GPCRs couple to can inhibit exocytosis through its inhibitory action on adenylyl cyclase to reduce levels of cyclic AMP and the activity of protein kinase A. Inhibition of exocytosis via reduction of cytosolic cAMP levels occurs on a slower timescale than the fast regulation required for precise temporal control of neurotransmitter release. Specific isoforms of $G\alpha_i$ can inhibit exocytosis through reduction of the refilling of the readily releasable pool in beta cells of the islets of Langerhans: this effect is thought to be independent of adenylyl cyclase as it can still occur in the presence of high intracellular cAMP[153]. Importantly, Gi/o-coupled GPCRs generate free $G\beta\gamma$ subunits, which can modulate exocytosis through several different mechanisms (Fig. 7)[142].

The regulation of G-protein coupled inwardly rectifying potassium channels by Gβγ.

G-protein coupled inwardly rectifying potassium channels were the first $G\beta\gamma$-binding proteins to be identified other than $G\alpha$ subunits. The muscarinic potassium channels in the atrium of the heart can be activated by acetylcholine to hyperpolarize the cell in a GTP- and pertussis toxin-dependent manner, leading researchers to suspect the involvement of G proteins. Injection of purified G proteins showed that the $G\beta\gamma$ subunit to be responsible for the effect[154]. Today, it is known that GIRK channels are multimeric transmembrane proteins that consist of various GIRK1-4 heterotetramers. Each of the four subunits in the complex contains two transmembrane domains and a large cytoplasmic channel domain capable of binding one $G\beta\gamma$ subunit and a Na^+ ion [155]. $G\beta\gamma$ binding to the cytoplasmic channel domain produces a rotation within this domain and movement within the inner helices, opening the channel to K^+

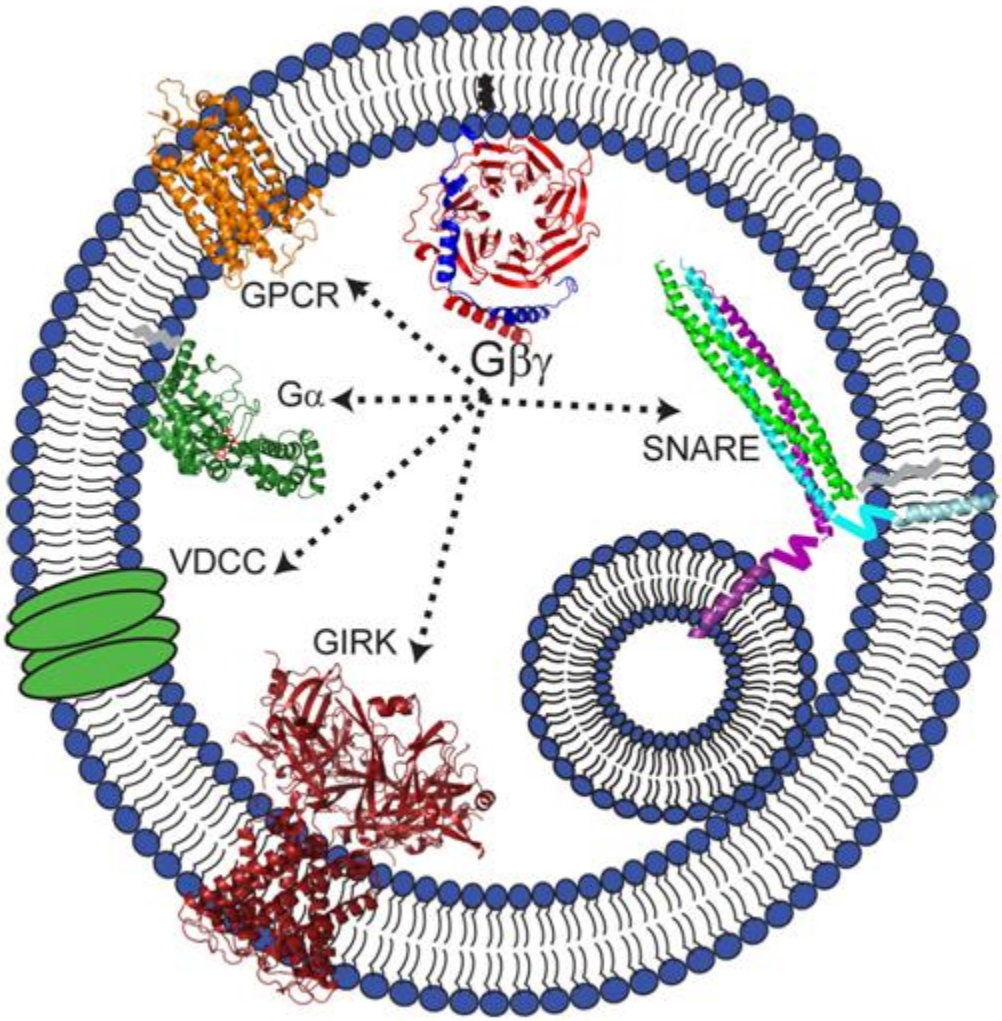

Fig. 7: Gβγ as a master regulator of exocytosis.

Gβγ (red and blue), when activated from $G_{i/o}$-coupled GPCRs (orange), can modulate exocytosis via several mechanisms, including voltage-dependent calcium channels (green), GIRK channels (red), and SNARE complexes (green, blue, and purple). Figure adapted from Betke KM, Wells CA, Hamm HE. *Prog Neurobiol*. 2012 Mar;96(3):304-21.

conductance[155]. Binding to Gβγ is mediated by interactions between the residues Q248, T249, E251, G252, and E253 on the GIRK cytoplasmic channel domain [156] [155], as well as the hydrophobic residue L344[155,157,158]. On Gβγ, the residues adjacent to the Gβ amino terminus L55, K78, I80, K89, S99, and W99 are all crucial for binding to the GIRK cytoplasmic channel domain. The $G\beta_5$ subunit, the most divergent Gβ isoform with regards to primary sequence, is incapable of activating GIRKs, instead inhibiting them [159] [160] [161,162], despite conservation of all of the important residues listed above between the two isoforms on the surface of Gβ other than L55. GIRK channels are activated by the M2 muscarinic receptor and purinergic receptors in the heart[163] and by numerous GPCRs on neurons, including serotonin, dopamine, opiate, and GABA receptors, amongst others[164,165]. GIRK channels are generally not thought of as components of the presynaptic release machinery, and in the brain, they are often localized to somatodendritic areas [166,167] They modulate exocytosis through cell-wide changes in cell voltage, making it harder for cells to fire action potentials[167,168] and activate voltage-dependent calcium channels. Despite this, some GIRK channels are found to localize presynaptically [169,170], where they act to inhibit exocytosis by decreasing the amplitude and duration of the action potential. It is uncertain whether these presynaptic GIRKs are activated by Gβγ or are G-protein mediated: evidence exists that they are pertussis-toxin resistant[169] . GIRKs are a critical mechanism for $G_{i/o}$-coupled GPCR-mediated regulation of cell voltage.

The regulation of voltage-dependent calcium channels by Gβγ.

The most well-accepted mechanism of $G_{i/o}$-coupled GPCR-mediated inhibition of exocytosis is through direct binding of Gβγ to the voltage-gated calcium channel [171-174] The $G_{i/o}$-coupled GPCR agonist norepinephrine was first reported to inhibit action-potential evoked calcium currents in chicken neurons [175,176]. Other $G_{i/o}$-coupled GPCR agonists, including GABA, somatostatin, and opioid receptors, have also been shown to function via this mechanism[174,177]. Gβγ binds directly to N-($CaV_{2.2}$) or P/Q($CaV_{2.1}$)-type voltage-gated calcium channels to inhibit calcium influx into the presynaptic cell, preventing the

activation of calcium-dependent proteins of the exocytic fusion machinery[178] [172]. Recently, it has been discovered that the R-type calcium channel ($CaV_{2.3}$) is also subject to Gβγ modulation in response to opioid receptor signaling [179]. Gβγ-mediated inhibition of these channels is voltage-dependent, with less inhibition being observed in the depolarized state [180]. Inhibition can be overcome through increasing depolarization [177,181,182]. The kinetics of the inhibition occur faster than a metabolic pathway such as $G\alpha_i$-mediated inhibition of adenylyl cyclase, occurring on the order of tens of milliseconds[172]. Beyond this, $G_{i/o}$-coupled GPCRs may also modulate calcium channels in a voltage-independent fashion through phosphorylation or trafficking [171].

The molecular requirements for Gβγ binding to the channel are fairlywell characterized. The Gβγ binding site on the channel is located on the α1 subunit of the channel on the cytosolic loops between the I-II linker region [150,183]. Two binding sites for Gβγ exist in this region, including a QXXER motif similar to that found on adenlylyl cyclase 2 and GIRKs that is implicated in Gβγ binding [150,183,184], as well as a distal site that is less well understood. Despite the presence of two sites, kinetic data suggests that the stoichiometry of binding involves a 1:1 ratio between Gβγ subunit and channel[185]. Charge-reversal mutations of residue R387 within this motif abolish Gβγ-mediated regulation of the channel[183]. Protein kinase C is a key modulator of Gβγ interactions with the binding site C-terminal to the QXXER motif: application of phorbol ester to activate PKC reduces the ability of somatostatin to inhibit calcium currents[186], while phosphorylation of Ser and Thr residues in the α1 416-434 peptide removes its ability to block Gβγ-mediated inhibition of calcium currents[150]. These data imply that phosphorylation of the PKC site in this region reduces Gβγ binding. N and P/Q-type calcium channels are anchored to SNAREs via the N-terminus of syntaxin1A binding to the synprint region on the II-III linker of the a1 subunit of the calcium channel. Upon syntaxin binding, the channel undergoes a hyperpolarizing change in the voltage dependence of inactivation[187,188]. Interestingly, cysteine string protein may have a similar effect to syntaxin1A upon Gβγ-mediated inhibition of calcium currents [141]. The channel-syntaxin

interaction enables Gβγ-mediated inhibition of these channels, with tonic inhibition of calcium currents by Gβγ being reduced by proteolytic cleavage of Stx1A with botulinum toxin C[189,190]. It is currently believed that the Gβγ binding site on Stx1A is present at the N-terminus of the H_3 domain of the channel[191]. The mutagenesis of a number of key Gα-binding residues on the surface of Gβγ revealed that the residues K78, M101, N119, T43, D186, and W332 on Gβ were all important for calcium channel modulation[44], although this was not intended to be a comprehensive list of all residues required for binding but only those residues involved in binding to Gα. Overall, the regulation of voltage-dependent calcium channels by Gβγ subunits is well-understood and a crucial mechanism for $G_{i/o}$-coupled GPCR-mediated inhibition of exocytosis.

$G_{i/o}$-coupled GPCR-mediated regulation of exocytosis downstream of calcium channels.

A number of groups have observed that inhibition of exocytosis can occur distal to Ca^{2+} entry at the synapse. The first G-protein mediated inhibition of exocytosis was observed in the beta cells of the islets of Langerhans, where catecholamines and somatostatin were shown to inhibit insulin release downstream of calcium channels [192,193]. $G_{i/o}$-coupled GPCRs were also shown to act downstream of calcium entry to block neurotransmitter release. Adenosine was found to inhibit acetylcholine release from motor neurons of the Northern leopard frog [194]. Miniature end-plate potentials could still be reduced even in Ca^{2+}-free solutions. Evidence for G protein involvement in these phenomena were derived from studies in which GTP analogues were introduced into the cell to produce a similar effect as $G_{i/o}$-coupled GPCR agonists[195]. However, further studies were needed to demonstrate which subunit was responsible for the effect: Gα, Gβγ, or another G protein distal to these. It was shown that Gβγ mediated the distal effect through direct injection of purified Gβγ into lamprey reticulospinal axons. Gβγ-binding scavenger peptides were able to block the inhibitory effect of the lamprey 5-HT_1-type receptor[196]. Importantly, no inhibition of Ca^{2+} entry was observed in these studies. This effect was corroborated by multiple independent groups. Similar studies with Gβγ-binding peptides and antibodies were conducted for the α_{2a} adrenergic receptor

in the beta cell [153], as well as for presynaptic Schaffer collateral sites in rat hippocampal CA3 slice culture[86]. The inhibitory effect of the α_2 adrenergic receptor on neurotransmission at the synapse between nociceptive pontine parabrachial nucleus and neurons of the central amgydala was bypassed through administration of a Gβγ-binding peptide [197]. Inhibitory group II metabotropic glutamate receptors (mGluRs) were shown to act distal to Ca^{2+} entry at the interneuron-Purkinje cell synapse [198], although no studies were conducted connecting this system with Gβγ. In a second study, the endogenous κ-opioid receptor agonist dynorphin released from dendritic vesicles acts in a retrograde manner to inhibit glutamate release in a manner downstream of Ca^{2+}-entry[199]. However, no studies were conducted definitely tracing this effect to Gβγ binding to any one effector, although the effect was shown to be independent of cAMP levels or voltage-gated calcium channel activity. Together, these studies suggest that Gβγ is able to act downstream of Ca^{2+} channels to mediate the effect of $G_{i/o}$-coupled GPCRs.

Gβγ regulates exocytosis downstream of calcium channels by binding directly to SNAREs.

A mechanism for the distal effect of Gβγ upon exocytosis downstream of calcium channels has been proposed. It is proposed that this occurs through direct binding of Gβγ subunits to the SNARE proteins of the vesicle fusion machinery [48,196,200]. The purified SNAREs SNAP25, syntaxin1A, and VAMP2 could directly bind Gβγ *in vitro* as both monomers and formed t-SNAREs and tertiary SNAREs [48,201]. The H_3 domain of syntaxin 1A was shown to bind Gβγ in a concentration-dependent manner on its own, while the H_{abc} domain was not[191,201]. The mechanism was shown to also involve the exocytotic calcium sensors in addition to Gβγ and SNAREs. It was also shown that the calcium sensor synaptotagmin 1 displaces Gβγ in a calcium-dependent manner, with greater displacement occurring under conditions of high calcium[201] (Fig. 8). Cleavage of the C-terminus of SNAP25 by botulinum toxin A (BoNT/A) attenuated the inhibitory effect of the lamprey serotonin receptor [200]. This effect was similarly

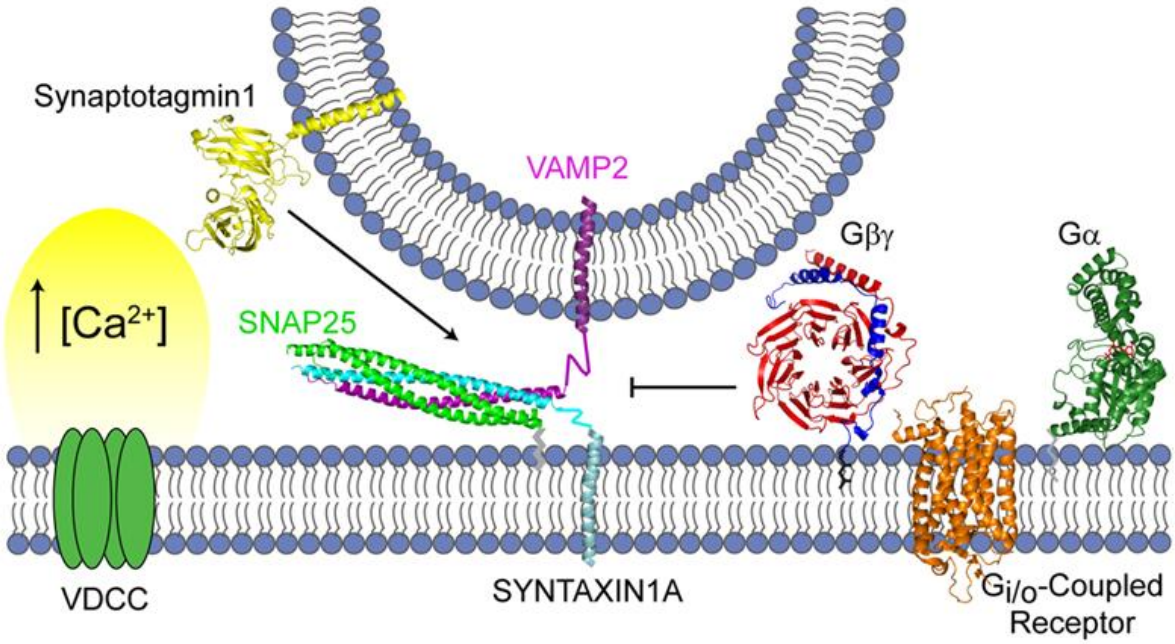

Fig. 8: Gβγ inhibits exocytosis by competing with synaptotagmin for binding sites upon SNAREs.

Visual representation of the current hypothesis for Gβγ-mediated inhibition of exocytosis downstream of calcium channels. Gβγ (red and blue) binds to the SNARE complex (green, blue, and purple), competing with apo-synaptotagmin (yellow) under conditions of low Ca^{2+}. At high Ca^{2+}, Ca^{2+}-synaptotagmin displaces Gβγ. Figure adapted from Wells CA, Zurawski Z, Rodriguez SM, Betke KM, Yim YY, Hyde K, Alford ST, Hamm HE. *Mol Pharmacol.* 2012 Dec;82(6):1136-49

corroborated by several groups in multiple cell types [86,153,197,202]. BoNT/A cleaves the C-terminal 9 amino acids from SNAP25 to create SNAP25Δ9 [203]. SNAP25Δ9 has roughly 1.7-fold lower affinity for Gβγ than full-length SNAP25[201]. The ability of the calcium sensor synaptotagmin 1 to displace Gβγ is increased for t-SNAREs containing SNAP25Δ9 relative to SNAP25WT [201]. Dye-labeling studies with vesicle populations showed that the lamprey serotonin receptor in this system acted through reducing the full fusion of vesicles with the plasma membrane , changing the mode of fusion to kiss-and run-type fusion[204]. From this, it is clear that the C-terminus of SNAP25 is crucial for the Gβγ-SNARE interaction, and that other, then unknown, parts of the SNARE complex were also involved. The precise molecular requirements of the Gβγ-SNARE interaction had yet to be elucidated. I elected to identify them as part of my dissertation project.

Physiological relevance of the Gβγ-SNARE interaction.

At the moment, limited information exists on what physiological processes may be regulated by the Gβγ-SNARE interaction. Generally, inhibition of exocytosis is essential for tight control over hormone and neurotransmitter release. For this section, we will limit our focus strictly to cellular systems that have affirmatively shown a role for the Gβγ–SNARE interaction. It has been shown that the Gβγ-SNARE interaction is important for long-term depression in the hippocampus[205]. Long-term depression in this area of the brain between Schaffer collaterals and CA1 pyramidal cells is thought to play a role in the cellular basis for learning and memory [206,207]. BoNT/A-mediated cleavage of SNAP25 blocked the presynaptic activity of group II mGluRs, which can produce presynaptic long-term depression in the presence of elevated cyclic GMP.[205] Other groups have also found a role for the Gβγ-SNARE interaction in the hippocampus. The presynaptic 5-HT_{1b} receptor at the synapse between CA1 hippocampal neurons and the subiculum was found to signal through Gβγ-SNARE[208], similarly to the lamprey serotonin receptor, despite this receptor sharing more homology to the human 5-HT_{1f} receptor. Researchers were

also able to identify a second receptor in this system that inhibited exocytosis through the Gβγ-calcium channel interaction, the $GABA_b$ receptor. It was also shown that cleavage of Stx1A by BoNT/C was sufficient to enable 5-HT_{1b} receptors to inhibit voltage-gated calcium channels, hinting at the microarchitecture of the presynapse. Projections from the CA1 area to the subiculum are implicated in long-term potentiation [209], a phenomenon also implicated in learning and memory. The subiculum is not as well-studied as other hippocampal areas, with implications for spatial navigation and mnemonic processing[210].

The Gβγ-SNARE interaction has also been shown to be associated with pain and fear processing in the amygdala. The pontine parabrachial nucleus contains fibers that carry important pain and stress information and synapse onto neurons of the lateral central amygdala. α_2 adrenergic receptors at this synapse inhibit glutamate release here via the Gβγ-SNARE interaction[197]. The amygdala is important in assigning emotional valence to sensory stimuli such as pain[211,212]. It has been shown that the parabrachio-amygdaloid nociceptive pathway integrates the emotional and sensory aspects of pain [213]. Furthermore, stress produces noradrenaline release in the central amygdala, producing stress-induced analgesia[212,214]. From this, it may be hypothesized that the Gβγ-SNARE interaction may be an important regulatory mechanism for the perception of pain. Chronic pain is a significant health problem today, being a significant source of disability and public health expenditure[215].

Outside of the brain, the Gβγ-SNARE interaction has been identified as being of importance in the endocrine system. The chromaffin cell is a neuroendocrine cell located within the medulla of the adrenal gland. They secrete catecholamines- epinephrine and norepinephrine- from large dense core vesicles into the bloodstream in response to signals from the splanchnic nerve of the sympathetic nervous system. This release is a central feature of the acute stress response that is triggered in response to dangerous situations. These cells contain several GPCRs that can inhibit catecholamine release, such as

the P2Y and μ-opioid receptor [216,217] . It was shown that the action of these inhibitory receptors was mediated by Gβγ in a calcium-independent manner[202], although crucial studies with botulinum toxins demonstrating a role for the Gβγ-SNARE interaction that were performed in other studies cited here were not included in this study.

The beta cells of the islets of Langerhans are very well studied, with their ability to release insulin in response to elevated glucose being universally accepted. The loss of this glucose-stimulated insulin secretion is a hallmark of type II diabetes[218]. It is well-known that the α_2 adrenergic receptor can inhibit glucose-stimulated insulin release in this cell type [219,220]downstream of calcium entry[153,192].This inhibition was shown to be mediated by a minimum of two mechanisms, including the Gβγ-SNARE interaction[153]. Other mechanisms include the inhibitory effect of $G\alpha_i$ on adenylyl cyclases and the readily releasable pool[153]. Considerable evidence exists implicating the inhibition of glucose-stimulated insulin release by catecholamines to type II diabetes, with α_2 antagonists selectively increasing glucose-stimulated insulin release in type II diabetics, but not healthy subjects, and genetic variants of the α_{2a} adrenergic receptor that raise receptor expression producing an inhibition of insulin secretion[221-223].

In summary, while the Gβγ-SNARE interaction has been shown to be important in a variety of tissues, data linking it with relevance in specific disease states is limited, and an ongoing goal of our research group. Most studies with the Gβγ-SNARE interaction have been with proteins or isolated tissues, whereas many chronic illnesses are complex dysregulated states involving multiple organ systems. Since $G_{i/o}$-coupled GPCR signaling is so important to the regulation of exocytosis in numerous cell types throughout the body, a central goal of our research group is to identify potential pathophysiological conditions in which the Gβγ-SNARE interaction may be dysregulated. Two of the most rigorous methods to investigate the role of a protein-protein interaction within pathophysiological disease states are to generate a transgenic organism deficient in that protein-protein interaction or to

create a small molecule inhibitor of that interaction. I opted to make both of these strategies central aims of my dissertation project: I would continue existing development of small molecule inhibitors of the Gβγ-SNARE interaction, and I would develop and begin to characterize a transgenic mouse that was deficient in the Gβγ-SNARE interaction. It is anticipated that animals treated with a Gβγ-SNARE inhibitor should develop a similar phenotype to that of a Gβγ-SNARE deficient mouse, assuming adequate pharmacokinetic and ancillary pharmacological properties. Together, this approach would provide strong verification for whether the Gβγ-SNARE interaction was important in a given cell type or dysregulated in a specific disease state.

Conclusion

The Gβγ-SNARE interaction is one essential mechanism through which $G_{i/o}$-coupled GPCRs may mediate exocytosis. Limited data is available for the binding sites for the interaction within Gβγ, SNAP25, and syntaxin. Identifying the molecular requirements for the interaction would improve our understanding of $G_{i/o}$-coupled GPCR function and yield potential gain-of-function/loss-of-function mutations that would allow us to examine whether the interaction is important in other tissues. Very little data is known about the pathophysiological relevance of the Gβγ-SNARE interaction. Could there be a specific disease state in which the interaction is dysregulated? Is it possible to develop potent and selective small molecule inhibitors of the interaction? Would small molecule inhibitors of the Gβγ-SNARE interaction be a viable therapeutic strategy for conditions in which exocytosis is heavily implicated, such as type II diabetes? Questions such as these form the basis for the studies I elected to conduct for my dissertation research.

CHAPTER II

Gβγ INHIBITS EXOCYTOSIS VIA INTERACTION WITH CRITICAL RESIDUES ON SOLUBLE N-ETHYLMALEIMIDE-SENSOR FACTOR ATTACHMENT PROTEIN-25

(Portions of this chapter appear in the journal article "Gβγ inhibits exocytosis via interaction with critical residues on soluble N-ethylmaleimide-sensitive factor attachment protein-25." in the December 2012 issue of *Molecular Pharmacology*, vol. 82, pp 1136-49, PMID 22962332.)

Introduction

Exocytosis, in which a lipid vesicle fuses with a plasma membrane in such a way to release the vesicle's contents into the extracellular space, is a complex cellular process involving many types of proteins: the SNARE proteins responsible for providing the physical forces of fusion themselves, accessory proteins involved in docking, priming, assembly, and disassembly of the SNARE proteins, kinases and phosphatases to act s regulatory enzymes, ion channels for voltage-dependent regulation, and both inhibitory and excitatory G protein coupled receptors (GPCRs). It is well-documented that the Gβγ subunit of the heterotrimeric G protein complex, in response to GPCR activation and heterotrimer dissociation, can bind to and modulate the activity of a variety of effectors. In secretory cells, Gβγ has been shown to be a central regulator of exocytosis through its action upon K^+ and Ca^{2+} channels [171,172,174] and downstream of Ca^{2+} entry via binding to SNAREs[48,142,196,200,201]. Gβγ binds directly to the ternary SNARE complex (consisting of the membrane-associated t-SNARE such as SNAP25, the transmembrane t-SNARE syntaxin, and the vesicle-associated transmembrane v-SNARE VAMP), shown in both *in vitro* binding studies and *ex vivo* exocytosis assays.

Presynaptic injections of lamprey reticulospinal axons with BoNT/A reduced exocytosis, but also bypassed the inhibitory effect of the lamprey serotonin receptor to inhibit excitatory postsynaptic action

potentials[200]. A 14-mer peptide corresponding to residues 193-206 of human SNAP25 was able to bypass Gβγ-mediated inhibition[48,200]. Cleavage of SNAP25 with BoNT/A reduces its ability to bind Gβγ maximally and its affinity for Gβγ by 1.8-fold[201], while partially retaining exocytosis. In addition, cleavage of t-SNARE by BoNT/A increases the ability of the calcium sensor synaptotagmin 1 to compete with Gβγ for binding sites upon SNARE[201]. Multiple independent groups have found similar results in various types of secretory cells[86,196,197], chromaffin cells[202], and pancreatic β cells[153].

A series of peptides that cumulatively and progressively scans the entire sequence of SNAP25 was tested for its ability to bind purified Gβγ subunits. Gβγ-binding peptides then underwent alanine scanning mutagenesis to identify individual residues that would cause the interaction to weaken when mutated to alanine. These residues were then mutated on full-length recombinant SNAP25 proteins, which were analyzed for their ability to bind Gβγ. Full-length SNAP25s were introduced into functional exocytosis assays, where the effect of $G_{i/o}$-coupled GPCRs was then determined. Beyond this, initial studies for key Gβγ-binding residues on Stx1A were also conducted. A Gβγ-binding deficient Stx1A was identified and is awaiting characterization in cell-based assays. Finally, to address the importance of SNAP25-binding residues on Gβγ, a series of peptides corresponding to Gβγ was screened for its ability to disrupt the Gβγ-SNAP25 interaction. These studies provide key insights into the molecular requirements for the Gβγ-SNARE interaction and provide key mechanistic linkage between Gβγ binding and $G_{i/o}$-coupled GPCR-mediated inhibition of exocytosis.

Methods

Plasmids. The open reading frame for SNAP-25 was subcloned into the glutathione-S-transferase (GST) fusion vector pGEX-6p-1 (GE Healthcare) for expression in bacteria. Mutagenesis of SNAP-25 was accomplished via the overlapping primer method. The SNAP-25(8A) mutant was subcloned from pGEX-6p-1 into the pRSFDuet-1 plasmid, a dual expression vector that contains cDNAs for both full-length

syntaxin 1A and SNAP-25 that results in concomitant expression and formation of t-SNARE complexes (kindly provided by E. Chapman). Plasmids were verified to contain desired mutations via Sanger sequencing utilizing BigDye Terminator dyes and resolved on an ABI 3730 DNA Analyzer (Applied Biosystems).

Antibodies. The antibody for rabbit Gβ (T-20; sc-378), was obtained from Santa Cruz Biotechnology, Inc. The HRP-conjugated goat anti-rabbit antibody was obtained from Perkin-Elmer (NEF812001EA). The anti-synaptotagmin-1 antibody subclone 41.1 was obtained from Synaptic Systems (105 011). Anti-GST (goat) Antibody DyLight™ 800 Conjugated (#600-145-200) and the anti-mouse IgG (goat, H&L) Antibody IRDye700DX® Conjugated Pre-adsorbed (#610-130-121) were both from Rockland Immunochemicals, Inc.

Protein Purification. For SNAP25 and Syt1 C2AB, recombinant bacterially-expressed glutathione-S-transferase (GST) fusion proteins were expressed in *Escherichia coli* strain Rosetta 2 (EMD Biosciences). Protein expression was induced with 100 μM isopropyl β-D-1-thiogalactopyranoside for 16 h at room temperature. Bacterial cultures were pelleted and washed once with phosphate-buffered saline before undergoing resuspension in lysis buffer (25 mM potassium 4-(2-hydroxyethyl)-1-piperazine ethanesulfonate (HEPES-KOH) pH 8.0, 150 mM KCl, 5mM 2-mercaptoethanol, 10.66 μM leupeptin, 1.536 μM aprotenin, 959 nM pepstatin, 200 μM phenylmethylsulfonyl fluoride, and 1mM ethylenediaminetetracetic acid (EDTA)). Cells were lysed with a sonic dismembranator at 4°C for 5 min. Lysates were cleared via ultracentrifugation at 26,000 x g for 20 min in a TI-70 rotor (Beckman Coulter). GST-SNAP-25 fusion proteins were purified from cleared lysates by affinity chromatography on GE Sepharose 4 FastFlow (GE Healthcare). Lysates were allowed to bind to resin overnight before being washed once with lysis buffer containing 1% Triton X-100 (Dow Chemical). The resin was then washed once with elution buffer (25 mM HEPES-KOH pH 8.0, 150 mM KCl, 5 mM 2-mercaptoethanol, 0.5% n-octyl glucoside, 1 mM EDTA, 10% glycerol). SNAP25 proteins were eluted from GST-fusion

proteins immobilized on resin via proteolytic cleavage with a GST-tagged fusion of rhinovirus 3C protease. Protein concentrations were determined with a Bradford assay kit (Pierce) and purity was verified by SDS-PAGE analysis.

t-SNARE Protein Purification. For the t-SNARE with full-length syntaxin with SNAP-25, this was expressed using the tandem vector pRSFDuet-1[224]. Purification of this SNAP-25/syntaxin 1A dimer was performed as previously described[225] utilizing a 6xHis tag present upon the N-terminus of SNAP-25. After elution, the t-SNARE was dialyzed into a final buffer consisting of: 25 mM HEPES-KOH pH 8.0, 50 mM NaCl, 5 mM 2-mercaptoethanol, 0.5% n-octyl glucoside, 5% glycerol. The n-octyl glucoside was used to prevent aggregation that may occur due to the hydrophobic transmembrane domain of syntaxin 1A that is present in this construct. After dialysis, the purified t-SNARE was divided into aliquots and frozen at -80°C.

Gβγ Purification. $G\beta_1\gamma_1$ was purified from bovine retina as described previously[226]. Recombinant $G\beta_1\gamma_2$ was expressed in Sf9 cells and purified via a 6xHis tag on $G\gamma_2$ using Talon™ immobilized metal affinity chromatography (Clontech, Mountain View, CA).

Peptide array synthesis. Peptide array synthesis was performed using the Respep SL (Intavis AG) according to standard SPOT synthesis protocols[227]. Briefly, the robotics-driven computer-directed device (Respep SL) managed complex timing, mixing, additions, and washing of the membrane over the course of the peptide synthesis. Peptides were 15 residues in length. The sequences of the peptides for SNAP-25 were based on the sequence available from the UniprotKB/Swiss Protein Database for human *SNAP-25*, P60880. After the peptides were synthesized coupled to the membranes, membranes were processed with a final side chain deprotection step. Membranes were placed in an acid-safe container in a chemical hood and submerged in a solution of 95% trifluoroacetic acid, 3% tri-isopropylsilane for 1 hour with intermittent agitation. After the trifluoroacetic acid solution was removed, the membrane was then put through a series of washes: 1) dichloromethane for four 10-minute washes; 2) dimethylformamide for

four 10-minute washes, 3) ethanol for two 2-minute washes. The membrane was allowed to dry in the hood. For the alanine-mutagenesis screening of peptides, the peptides were synthesized to be 14 residues in length.

Peptide membrane Far-Western. After membranes had dried from the synthesis de-protection washes, they were first soaked in ethanol for 5 minutes, and then re-hydrated over two washes for 5 minutes in water. The membranes were then blocked with slight agitation for 1 hour in a buffer of tris-buffered saline (TBS) with 5% milk and 0.1% Tween-20 (Sigma-Aldrich). The membranes were then washed 5 times for 5 minutes in TBS with 0.1% Tween-20 on a shaker at RT. The membranes were then incubated overnight at 4°C with $G\beta_1\gamma_1$ at a final concentration of 0.44 μM in a binding buffer of 20 mM HEPES, pH 7.5, and 5% glycerol. The next morning, membranes were washed at room temperature (RT) on a shaker three times for 5 minutes in TBS with 5% milk and 0.1% Tween-20. Membranes were then exposed to primary antibody against Gβ (T-20, SC-378; Santa Cruz Biotechnology, Inc.) at 1:5000 dilution in TBS with 0.2% Tween-20 with mixing on a shaker table at RT for 1 hour before being washed three times for 5 min each on a shaker table in TBS with 0.1% Tween-20 also at RT. The appropriate secondary antibody was then diluted into TBS to 1:10,000 dilution with 5% milk and 0.2% Tween-20 followed by gentle agitation on a shaker with membranes for 1 hour at RT. Finally, membranes were washed twice for 5-minutes in TBS with 0.1% Tween-20, followed by two 10-minute washes in TBS at RT.

Chemiluminescence. The Western Lightning™ Chemiluminescence Reagent Plus (NEL104) from Perkin-Elmer and the Immun-Star™ WesternC™ Chemiluminescence Kit (#170-5070) from Bio-Rad was used to visualize western blots following published protocols. Western blot images were obtained utilizing a Bio-Rad Gel Doc Imager. Images were analyzed for densitometry using ImageJ (available from http://rsbweb.nih.gov/ij/index.html) ANOVA calculations comparing alanine mutant peptide spot intensity with wild type peptide reactivity were determined using GraphPad Prism4 software (GraphPad Software, San Diego, CA).

Peptide synthesis. Peptides were synthesized using the Respep SL (Intavis AG) using the Tentagel amide resin as the solid support using standard Fmoc/HBTU chemistry. After the last round of synthesis, the peptides on the columns were treated with 5% acetic anhydride in dimethylformamide to acetylate the N-terminus of the peptides. After washing with dimethylformamide followed by chloromethane and overnight drying, the peptides were cleaved from the resin over the course of 3-4 hours using a mixture of 92.5% trifluoroacetic acid (TFA) and 5% tri-isopropylsilane with gentle mixing. The peptides dissolved in the TFA mixture were precipitated using ice-cold tert-butyl methyl ether. After spinning and overnight drying, the peptides were dissolved either in water or a mixture of water with acetonitrile or 0.1% TFA. The dissolved peptides were snap-frozen in an ethanol/dry ice bath followed by overnight evaporation in a vacuum-assisted evaporative centrifuge with cold trap (Centrivap from Labconco). Samples were re-solubilized in a mixture of water/acetonitrile/0.1%TFA, and subjected to preparative HPLC (Gilson) on a reverse phase C18 column (Phenomenex Luna, 30x50mm) at 50ml/min, 10-90% acetonitrile in water gradient with 0.1% TFA over five minutes. Samples were then subjected to LC/MS (Agilent 1200 LCMS) for purity and mass spec identification of the peptide. HPLC fractions were evaporated to retrieve the peptide of interest.

Gβγ labeling. Fluorescence labeling of $G\beta_1\gamma_1$ and binding assays were conducted as described previously[228]. In brief, purified $G\beta_1\gamma_1$ was exchanged via a Centricon 10,000 MW concentrator into labeling buffer (20 mM HEPES, pH 7.4, 5 mM MgCl2, 150 mM NaCl, and 10% glycerol), then mixed with 2-(4'-maleimidylanilino)naphthalene-6-sulfonic acid (MIANS) in a 5-fold molar excess. The reaction proceeded for 3 h at 4°C before quenching with 5 mM 2-mercaptoethanol. The MIANS-$\beta_1\gamma_1$ complex was separated from unreacted MIANS using a PD-10 desalting column (GE Healthcare). MIANS-$G\beta_1\gamma_1$ was stored in aliquots at -80°C.

Fluorescence Binding. All fluorescence measurements were performed in a fluorescence spectrophotometer (Cary Eclipse; Varian, Inc., Palo Alto, CA) at 17°C. MIANS-$G\beta_1\gamma_1$ was diluted into

0.1 ml of assay buffer (20 mM HEPES, pH 7.5, 5 mM $MgCl_2$, 1 mM DTT, 100 mM NaCl, 1 mM EDTA, and 0.5% n-octyl glucoside) to a final concentration of 20 nM. This assay buffer included 0.5% n-octyl glucoside to limit aggregation of the t-SNARE complexes which contain full-length t-SNARE that includes the hydrophobic transmembrane domain of syntaxin 1A. The MIANS fluorescence was monitored with excitation at 322 nm and emission at 417 nm. Fluorescence changes caused by the addition of SNARE complexes to MIANS-$G\beta_1\gamma_1$ were monitored continuously. The amplitude of the fluorescence reflects the specific site on fluorescently labeled Gβγ and its interaction with each protein. There was no nonspecific binding of the free probe to the SNARE proteins and MIANS-Gβγ was resistant to photobleaching under experimental conditions (data not shown). The EC_{50} concentrations were determined by sigmoidal dose-response curve fitting with variable slope.

GST-pull down Assay. 5 μg of each GST-SNAP-25 protein immobilized on glutathione-sepharose resin was incubated with 400 μM of the C2AB domain of synaptotagmin-1 (residues 96-422) for 1 h at 4°C and washed three times with assay buffer (20 mM HEPES, pH 7.0, 80 mM KCl, 20 mM NaCl, and 0.1% n-octyl glucoside) in a 1.5 mL Eppendorf tube. Immobilized protein complexes were then transferred to a second 1.5mL Eppendorf tube to reduce non-specific binding. The complex was eluted with 20 μl of SDS sample buffer followed by separation via SDS-PAGE. Precipitated Gβ was detected via western blot with a rabbit anti-Gβ antibody (T-20, Santa Cruz Biotechnology, Inc. (sc-378)). Precipitated synaptotagmin-1 C2AB was detected via Western blot using a mouse anti-synaptotagmin-1 antibody (subclone 41.1, Synaptic Systems (105 011)). Western blots were imaged with labeled secondary antibodies: Anti-GST (goat) Antibody DyLight™ 680 Conjugated and the mouse IgG (H&L) Antibody IRDye700DX® Conjugated using the Licor Odyssey imager (Licor Biosciences).

Electrophysiology and microinjections. Experiments were performed on the isolated spinal cords or spinal cords and brainstems of lampreys (*Petromyzon marinus*). The animals were anesthetized with tricaine methanesulfonate (MS-222; 100 mg/l; Sigma Chemical, St. Louis, MO), sacrificed by decapitation, and

the spinal cord dissected in a cold saline solution (Ringer) of the following composition (in mM): 100 NaCl, 2.1 KCl, 2.6 CaCl2, 1.8 MgCl2, 4 glucose, 5 HEPES, adjusted to a pH of 7.60. Procedures conformed to institutional guidelines (University of Illinois at Chicago, Animal Care Committee).

Paired cell recordings were made between reticulospinal axons and neurons of the spinal ventral horn. Axons of reticulospinal neurons were recorded with sharp microelectrodes containing 1M KCl, 5 mM HEPES buffered to pH 7.2 with KOH and a SNAP-25 and BoNt/E mixture as defined below. Electrode impedances ranged from 20 to 50 MΩ. Postsynaptic neurons were recorded with patch clamp in voltage clamp conditions. Patch electrodes contained in mM: Cesium methane sulfonate 102.5, NaCl 1, $MgCl_2$ 1, EGTA 5, HEPES 5, pH adjusted to 7.2 with CsOH. BoNt/E and proteins were pressure microinjected through presynaptic microelectrodes using a Picospritzer II. Presynaptic recordings were made within 100 μm of the synaptic contact to ensure protein diffusion to the region of the terminal and this was confirmed by injection of fluorescently tagged SNAP-25 protein in separate experiments. Light chain BoNT/E (List. (65 μg/mL)), was stored at –20 ^{o}C in 20 mM Na phosphate, 10 mM NaCl and 5 mM DTT at pH 6.0. The buffered toxin was diluted as 5μL with 20 μL 2 M $KMeSO_4$ and 5 mM HEPES and 20μL of solution containing one of three different variants of SNAP-25. The buffered protein mixed with BoNT/E where appropriate was diluted 1:5 with 2 M $KMeSO_4$ and 5 mM HEPES. Microinjections of buffer solutions do not affect the synaptic response or 5-HT inhibition.

Protein structure visualization. All representatives of protein structure were made using the computer program Pymol[229].

Statistics and curve fitting. All statistics (Student's t-test) and curve-fitting (sigmoidal dose-response with variable slope) were performed using GraphPad Prism version 4.03 for Windows, GraphPad Software, La Jolla California USA, www.graphpad.com.

Results

Truncation of the C-terminus of SNAP25 has a detrimental effect on the binding of Gβγ to SNAP25[201], with a 1.8-fold reduction in affinity. However, Syt1 binding to SNAP25 is also reduced [230], as is exocytosis[230] . Here, we set out to mutate SNAP25 in such a way so that Gβγ binding was inhibited but Syt1 binding and exocytosis was intact. To identify the Gβγ binding site(s) upon SNAP25, we screened individual peptides corresponding to the human SNAP25 primary sequence for their ability to bind Gβγ.

We synthesized a sequential series of peptides from SNAP-25 immobilized upon a polyvinylidinedifluoride (PVDF) membrane via an automated peptide synthesizer utilizing SPOT synthesis. We utilized a Far-Western blotting procedure where membranes were exposed to purified bovine $G\beta_1\gamma_1$ and then washed to remove unbound $G\beta_1\gamma_1$. Subsequently, they were treated with a primary antibody for Gb and a HRP-conjugated secondary antibody (Fig. 9A). Each spot on the membrane corresponded to an individual peptide 15 residues in length, shifting 3 residues with each successive spot (1–15, 4–18, 7–21, …) spanning the entire coding sequence of human SNAP25b. As a positive control, we utilized several peptides that have previously been shown to interact with Gβγ: [QEHA (QEHAQEPERQYMHIGTMVEFAYALVGK[231], SIRK (SIRKALNILGYPDY[232], the C-terminus of βARK (WKKELRDAYREAQQLVQRVPKMKNKPRS)[233], and a peptide corresponding to the Gβγ-binding sequence upon the calcium channel $CaV_{2.2}$ (GID site: KSPLDAVLKRAATKKSRNDLI)[234] . To verify that the antibody was functional, a peptide corresponding to the epitope on $G\beta_1$ (the extreme C-terminus) was used as a positive control. For a negative control, we left several areas of the membrane lacking any peptide: Gβγ binding to these regions could be considered non-specific binding of Gβγ or antibodies and subtracted from the overall signal. In Fig. 9B, a representative image of the developed membrane subsequent to the Far-Western blotting procedure , including control conditions, is depicted. A series of overlapping peptides corresponding to

specific regions upon SNAP25 showed Gβγ binding, with signal being lost as specific residues were removed (Fig. 9B, red circle). Each experiment was repeated twice for a total of three technical replicates.

To quantify the extent of Gβγ binding, we utilized densitometry with ImageJ software upon images of all of the membranes, normalizing to the areas of highest intensity on each each membrane. The results for all 65 peptides are depicted in Figure 9C. Five clustered regions upon SNAP25 were identified as being important for Gβγ binding: these clusters correspond to residues 49-75, 82-108, 121-144, 145-168, and 184-206. These regions are visualized upon the crystal structure of the docked and primed ternary SNARE complex consisting of SNAP25, syntaxin, and synaptobrevin[235]. Gβγ can bind the complex in this state[201] as well as SNARE monomers and t-SNAREs[201], and it is believed that the docked and primed vesicle is the physiologically relevant state for Gβγ binding[48]. Two super-regions are identified on the ternary SNARE complex, spanning a distance that is greater than the width of one Gβγ subunit: an N-terminal site (labeled N in Fig. 9D) or a C-terminal site proximal to the regions of Syt1 binding[230], (labeled C in Fig. 9D). These regions are labeled in red upon the crystal structure. The 82-108 peptide is localized within the flexible, unstructured region located between the SN1 and SN2 helices that is depicted as a curved line. This region is adjacent to the four pamitoylation sites located on SNAP25 that serve to tether it to the membrane.

To identify individual residues within these peptides that were important for the Gβγ-SNAP25 interaction, we utilized alanine scanning mutagenesis. In this assay, we tested the ability of any specific residue to contribute to the interaction of a peptide with Gβγ through mutation of that residue to alanine. A second series of PVDF membranes were derivatized with a peptide corresponding to one of the five Gβγ-interacting peptides from Fig. 9 where one residue within the sequence was mutated

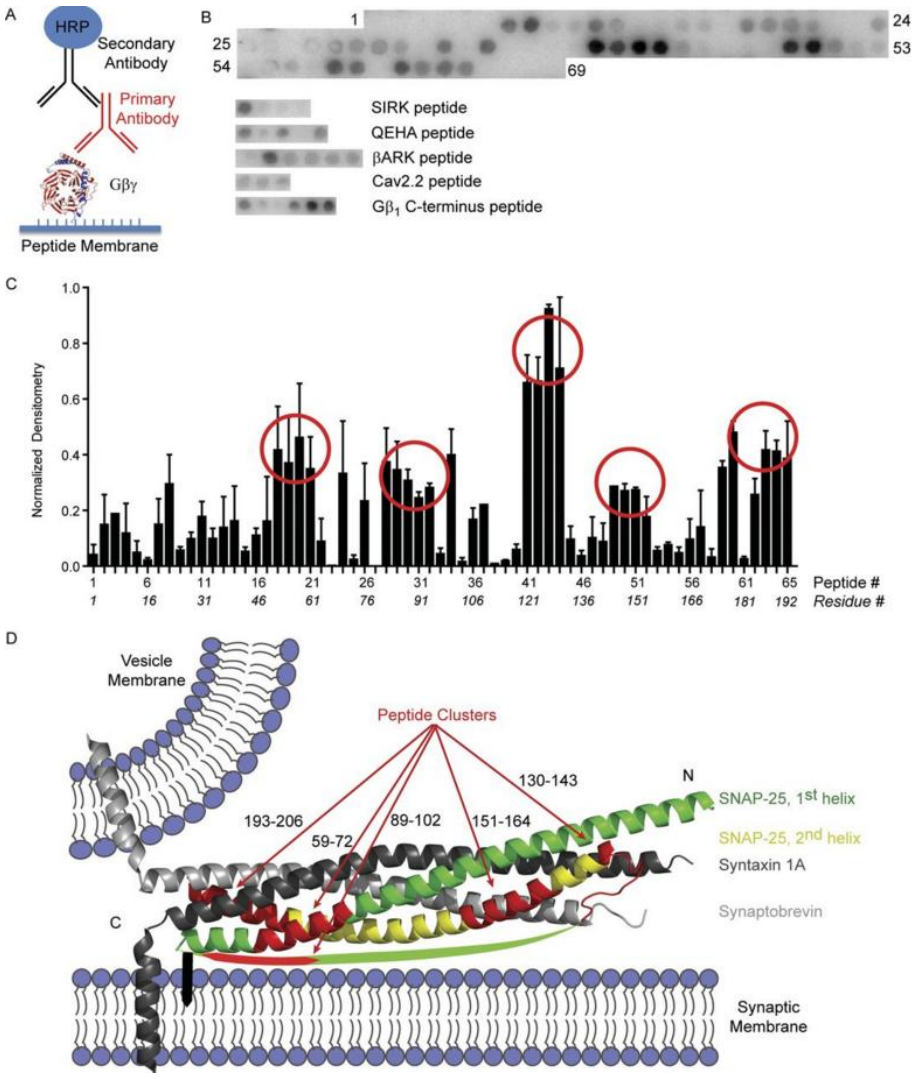

Figure 9. Screening of SNAP-25 peptides for interaction with $G\beta_1\gamma_1$.

A) The basic premise of the screening is considered a far-western. The peptide synthesizer creates peptides on a derivatized membrane. With appropriate washes in between steps, the membrane and peptides are sequentially exposed to $G\beta_1\gamma_1$, primary antibody for Gβ, and HRP-conjugated secondary antibody. B) Shown is a representative image of a membrane exposed to $G\beta_1\gamma_1$. Numbering reflects spots with successive peptides 1-65. Spots 66-69 were left without peptide synthesize on them as negative controls. Shown separately are the peptides spots derived from the sequences for the SIRK peptide, QEHA peptide, βARK peptide, the Gβγ binding domain of the calcium channel CaV2.2, and the C-terminus of $G\beta_1$. C) Densitometry was performed on the three membranes using ImageJ analysis of the image. Each membrane was normalized to the most intense spot on the membrane. The average of the three membranes was plotted for each set of 65 peptides that span the full length of SNAP-25. The x-axis reflects both the peptide number according to (B) as well as the residue number of the first residue in each respective peptide. Circles reflect clusters of peptides that had high densitometry. D) Representative sequences of the clusters of SNAP-25 peptides that were found with this screening are shown in red mapped onto the representation of the x-ray crystal structure of the core SNARE motifs (PDB ID: 2SFC); synaptobrevin, light gray; syntaxin 1A, dark gray; first SNAP-25 helix, green; second SNAP-25 helix, yellow. Syntaxin 1A and synaptobrevin each have a transmembrane domain shown as α-helices. The black bar inserted into the membrane represents the palmitoylation sites on SNAP-25. There is a green arc that represents the non-structured sequence between the two α-helices of SNAP-25. This arc includes one of the peptide clusters (red) near the palmitoylation site. "N" signifies the N-terminal end of the helices within the SNARE complex; "C" signifies the C-terminal end of the helices within the SNARE complex.Figure adapted from Wells CA, Zurawski Z, Rodriguez SM, Betke KM, Yim YY, Hyde K, Alford ST, Hamm HE. *Mol Pharmacol.* 2012 Dec;82(6):1136-49

to Ala, or a wild-type peptide to serve as a positive control. The sequence of these peptides is depicted in Table 1. Experiments were repeated twice for a total of three technical replicates per condition. We were able to identify a number of residues within each peptide that resulted in a loss of signal in the Far-Western assay when mutagenized to Ala. Densitometry values are shown for wild-type peptide and each mutant in Fig. 10B. Nine residues were shown to have significantly reduced Gβγ binding as measured by Student's *t* test when mutated to Ala in their respective peptides (Fig. 10B). Each of the nine residues, mapped upon the crystal structure of the ternary SNARE, fall within the two super-regions identified in the previous experiment. Five of the residues are proximal to the C-terminus of SNAP-25: E62, D99, K102, R198, and K201. Four of the residues are located in a second cluster at the N-terminus: R135, R136, R142, and R161. Note that E62 is located on the SN1 helix, while D99 and K102 are located in an unstructured region of SNAP25 but anticipated to be adjacent to the C-terminus due to the average distance of amide bonds and their location within the linker region spanning the SN1 and SN2 helices of SNAP25. Residues R198 and K201 are located downstream of the BoNT/A site and are lost subsequent to BoNT/A cleavage. The Syt1-binding residues D179, D186, and D193[230] were not shown to be important for Gβγ binding in this experiment, although more recent studies may suggest that residues located more centrally within SN2 may be more important for the Syt1-SNARE interaction[83].

Two residues identified in the scanning Ala mutagenesis approach, residues Gly63 and Met64, are located inside the four-helix bundle and are not solvent-exposed. As a result, these residues are not thought to be exposed to Gβγ in the four-helix bundle state, but they may be solvent-exposed in the t-SNARE complex and are solvent-exposed as a SNAP25 monomer. These residues were not investigated further in this study. The majority of the residues- seven of nine- are positively charged and highly basic R or K residues, including all four of the N-terminal residues. Two of the residues at the C-terminus are negatively charged, acidic D or E residues. Peptides may not be able to form the higher-

Peptide	Peptide Sequence
59-72	RIE**E**GMDQINKDMK
89-102	VCPCNKLKSS**D**AY**K**
130-143	SGGFI**RR**VTNDA**R**E
151-164	EQVSGIIGNL**R**HMA
193-206	DEANQ**R**AT**K**MLGSG

Table 1. SNAP-25 peptides found in screening.

SNAP-25 peptides that bound to $G\beta_1\gamma_1$ in the initial screening and had loss of binding when a residue was mutated to alanine are listed below. The residue(s) important for loss of binding is shown in boldface. Table adapted from Wells CA, Zurawski Z, Rodriguez SM, Betke KM, Yim YY, Hyde K, Alford ST, Hamm HE. *Mol Pharmacol.* 2012 Dec;82(6):1136-49

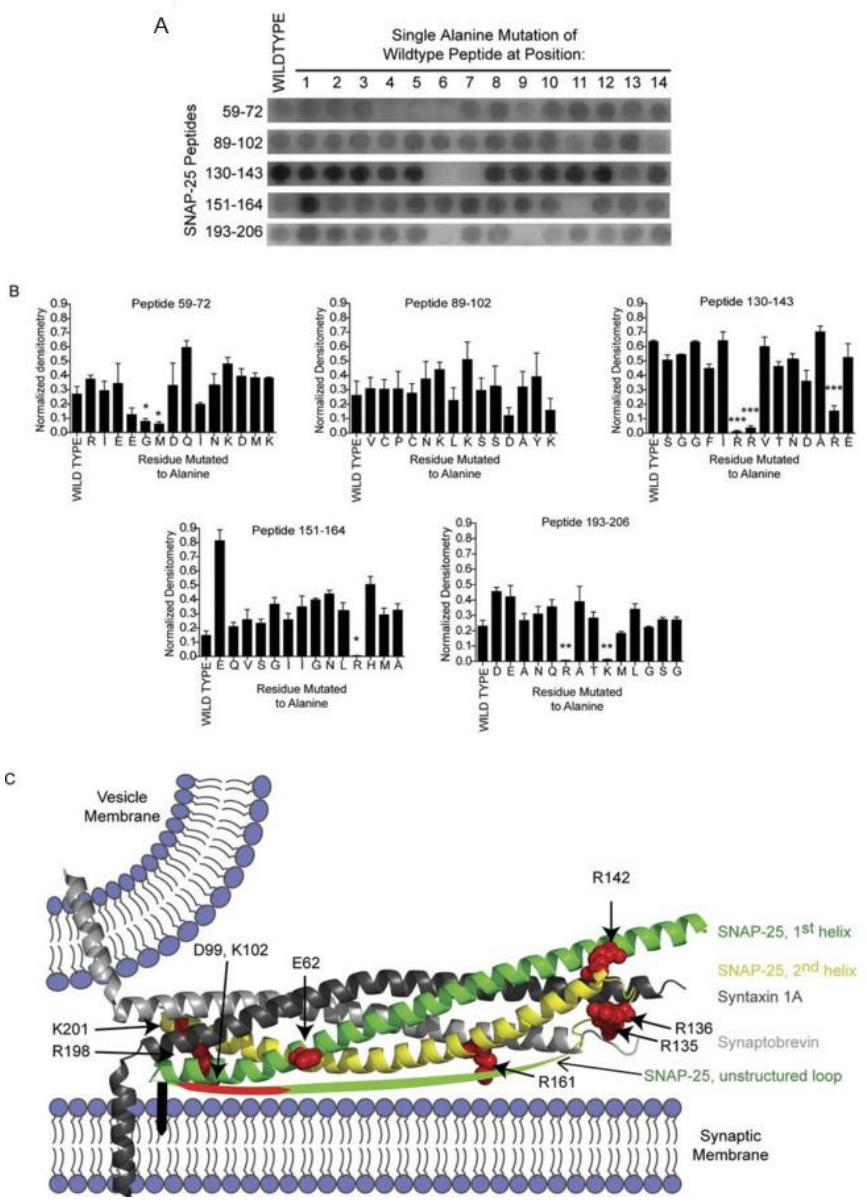

Figure 10. Alanine mutagenesis screening of SNAP-25 peptides that bind Gβγ.

A) Shown is a representative image of the alanine screening for SNAP-25 peptides synthesized on a membrane. Five peptides are identified by their sequence number shown on the left. The first spot of each row contains wild type peptide. The next 14 spots to the right are mutant peptides with a single alanine replacement of the residue at position 1, 2, 3…14 for each wild type peptide. B) Densitometry was performed across three separate membranes for each respective peptide and its series of mutants. The averaging over the three membranes is shown for the five peptides mentioned in A (Student's t-test; * - $p<0.05$, ** - $p<0.01$, *** - $p<0.001$). C) The residues (spheres, red) that had significantly reduced binding of Gβγ when mutated to alanine in their respective peptides are mapped onto the x-ray crystal structure of ternary snare (PDB ID: 1sfc). The colors signify syntaxin 1A, dark gray; synaptobrevin, light gray; first SNAP-25 helix, green; and second SNAP-25 helix, yellow; unstructured domain between the two SNAP-25 α-helices, green cartoon arc.Figure adapted from Wells CA, Zurawski Z, Rodriguez SM, Betke KM, Yim YY, Hyde K, Alford ST, Hamm HE. *Mol Pharmacol.* 2012 Dec;82(6):1136-49

order structures full-length proteins require. To investigate the importance of these residues in the binding of Gβγ to full-length SNAP25, we mutagenized a glutathione-S-transerase(GST)-SNAP25 construct and expressed it in E.coli BL21 cells. The GST-tags were proteolytically cleaved to generated purified SNAP25 proteins that were lacking the palmitoylation sites present on the mammalian protein. Starting at the C-terminal cluster (based on the prior BoNT/A studies), we generated a series of sequential mutants, with each protein containing a successive residue mutated to Ala. The R198A K201A mutant was termed "2A", with E62A/R198A/K201A being "3A" and E62A/D99A/R198A/K201A as "4A". All 5 C-terminal residues, including K102, were mutagenized to Ala in "5A". We then began to mutagenize the N-terminal binding site with "6A", featuring R135A and all other mutations. For "7A" R136A was also mutagenized to Ala. "8A" included R142A, and "9A" had all 9 residues mutagenized to Ala (E62A/D99A/K102A/R135A/R136A/R142A/R161A/R198A/K201A). The full set of mutations we made for SNAP25 mutants is defined in Table 2.

To investigate the ability of these SNAP25 mutants to bind $G\beta_1\gamma_1$ as monomers, we utilized a sensitive and quantitative fluorescence assay. $G\beta_1\gamma_1$ purified from bovine rod outer segments was labeled with sodium 2-(4'-maleimidylanilino)naphthalene-6-sulfonate (MIANS). The fluorescence of MIANS increases in hydrophobic environments, such as an interface between two interacting proteins. The fluorescence of 20 nM MIANS-$G\beta_1\gamma_1$ increased in a concentration-dependent manner when exposed to increasing amounts of wild-type SNAP25, eventually reaching saturation, with an EC_{50} of 350 nM SNAP25. (Fig. 11A). The 2A through 5A mutants display decreased affinity for $G\beta_1\gamma_1$, with 4A and 5A also displaying a decreased maximum binding. When the N-terminal mutants 6A through 9A are examined similarly, large decreases in the maximum fluorescence over baseline are observed. (Fig. 11B) 9A is still able to bind Gβγ to some extent, indicating that other residues may be present.

The 5A mutant shows us the importance of the C-terminal region alone. To test the importance of the N-terminal region, we generated a mutant that contained only the N-terminal residues mutagenized to Ala.

Mutant Name	Residues of SNAP-25 mutated	Log EC_{50} (M), (±SE)	Max (±SE)
WT	N/A	-6.45(± 0.20)	100 (±15)
2A	R198A, K201A	-6.18 (± 0.13)	96 (± 10)
3A	**E62A**, R198A, K201A	-5.93 (± 0.12)	122 (± 16)
4A	E62A, **D99A**, R198A, K201A	-6.12 (± 0.13)	71 (± 8)
5A	E62A, D99A, **K102A**, R198A, K201A	-6.08 (± 0.15)	70 (± 9)
6A	E62A, D99A, K102A, **R135A**, R198A, K201A	-5.97 (± 0.08)	88 (± 8)
7A	E62A, D99A, K102A, R135A, **R136A**, R198A, K201A	-6.12 (± 0.09)	33 (± 3)
8A	E62A, D99A, K102A, R135A, R136A, **R142A**, R198A, K201A	-5.87 (± 0.12)	20 (± 3)
9A	E62A, D99A, K102A, R135A, R136A, R142A, **R161A**, R198A, K201A	-6.36 (± 0.23)	25 (± 4)
N4A	R135A, R136A, R142A, R161A	-6.69 (± 0.14)	44 (± 3)

Table 2. SNAP-25 alanine mutants

Residues determined to be important for Gβγ binding to SNAP-25 peptides were successively introduced into the native SNAP-25 sequence. Listed are the names given to each SNAP-25 mutant with the corresponding list of residues mutated to alanine. Residues in boldface are the new mutated residue added to the previously made mutant SNAP-25. Max is the maximum fluorescence enhancement (F1/F0) of the non-linear regression for the each mutant, normalized to the maximum enhancement for wild type SNAP-25. (SE – standard error). The N4A mutant contains only the four alanine mutations near the N-terminus of the SNARE complex.Table adapted from Wells CA, Zurawski Z, Rodriguez SM, Betke KM, Yim YY, Hyde K, Alford ST, Hamm HE. *Mol Pharmacol.* 2012 Dec;82(6):1136-49

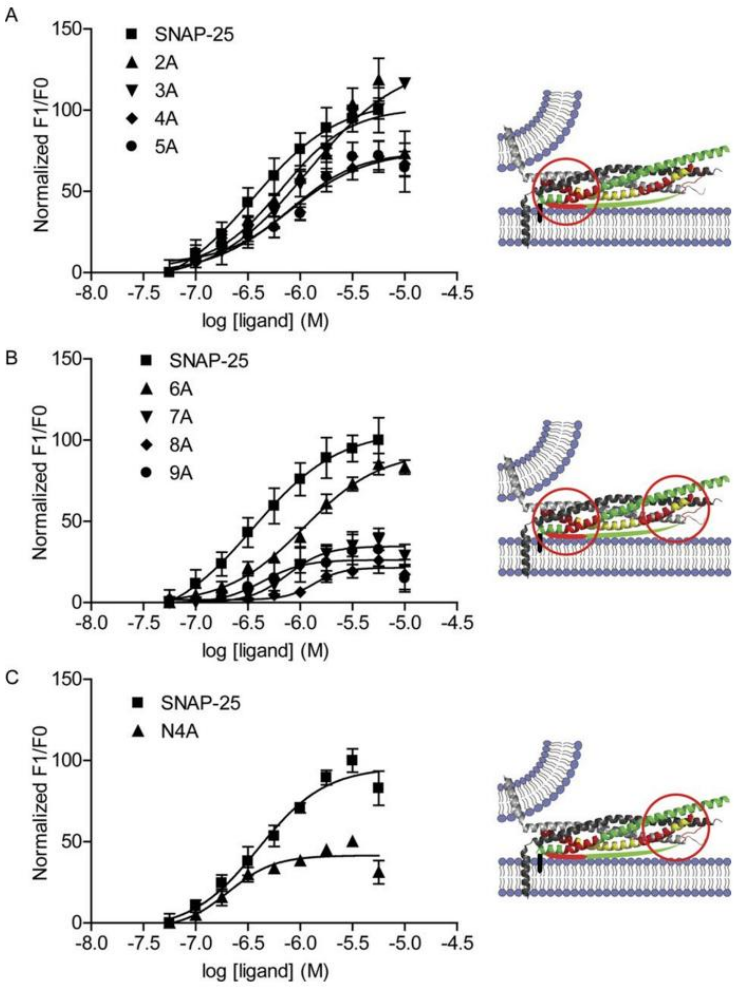

Figure 11. SNAP-25 and its alanine mutants binding to MIANS-labeled Gβγ.

A) A fixed concentration of MIANS-G$\beta_1\gamma_1$ (20 nM) was exposed to increasing concentrations of SNAP-25 with resulting increase in fluorescence, n=4. F1/F0 is the ratio of fluorescence measured in the presence of SNAP-25 over the fluorescence of G$\beta_1\gamma_1$ in the absence of SNAP-25. The fluorescence was corrected for any intrinsic fluorescence of SNAP-25 at the various concentrations. Finally, all of the curves were normalized to the highest fluorescence achieved by wild type SNAP-25 alone. (A) dose-response curves for wild-type SNAP-25, SNAP-25(2A), SNAP-25(3A), SNAP-25(4A), and SNAP-25(5A). To the right of the dose-response curves is a cartoon modified from Figure 2. The red circle denotes the area on the SNARE complex where these mutated residues are located together in the C-terminus. As in (A), the remaining previously described alanine mutants of SNAP-25 were tested with increasing concentration for binding to MIANS-G$\beta_1\gamma_1$. As compared to wild type SNAP-25, increasing numbers of mutations resulted in initially decreased EC_{50} and then decreased maximum fluorescence enhancement of MIANS-G$\beta_1\gamma_1$ (A and B). C) A SNAP-25 mutant with residues in the amino terminal region (R135A, R136A, R142A, and R161A) of the SNAP-25 protein termed N4A. When exposed to fluorescently labeled G$\beta_1\gamma_1$, this mutant (N4A) had a decreased maximal fluorescence, and its EC50 was 0.20 μM as compared to 0.35 μM . The cartoon in the right portion of (C) now shows the region with N-terminal mutated residues. Figure adapted from Wells CA, Zurawski Z, Rodriguez SM, Betke KM, Yim YY, Hyde K, Alford ST, Hamm HE. *Mol Pharmacol.* 2012 Dec;82(6):1136-49

This construct was termed "N4A" and contained the mutations R135A/R136A/R142A/R161A. Purified SNAP25 N4A displayed onlydecreased maximal fluorescence and an affinity not significantly different from wild-type for SNAP25, with an EC_{50} of 200 nM (95% CI: 100 nM-400 nM) for N4A compared to 400 nM for wild-type (95%: CI: 250 to 640 nM). From this, we can conclude that the higher-affinity C-terminal binding site is maintained, but the lower affinity N-terminal binding site features a gradual loss of interaction.

To evaluate whether the peptides identified previously could inhibit the Gβγ-SNARE interaction in a competitive manner, we utilized a competition binding assay in which 20 nM of M8-$G\beta_1\gamma_1$was reacted with an EC_{50} concentration (300 nM) of SNAP25 WT and a fixed concentration (1.5 mM) of peptide. Four of the five peptides were unable to inhibit the interaction, with only SNAP25 193-206 being able to produce a significant reduction in maximal fluorescence. (Fig. 12) This is the SNAP25 C-terminal peptide that is able to block $G_{i/o}$-coupled GPCR-mediated inhibition of exocytosis[153,200]. To examine the importance of residues R198 and K201, a mutant SNAP25 193-206 where R198 and K201 were mutagenized to Ala was similarly tested. This peptide was unable to produce a significant reduction in fluorescence. These peptides may not adopt a conformation in the assay buffer suitable for binding to Gβγ, or the peptide itself may be adequate to form the hydrophobic environment upon M8-$G\beta_1\gamma_1$. Experiments were repeated twice for three technical replicates.

The calcium sensor synaptotagmin 1 (Syt1) binding to SNARE complexes in a calcium-dependent manner has been shown to mediate exocytosis. [236] [78,90,237]. Mutations in SNAP25 have previously been shown to impair synaptotagmin 1 interactions with this protein[230]. To evaluate whether mutant SNAP25s containing residues important for Gβγ binding mutated to Ala can still bind synaptotagmin 1, we did GST-pull down assays in which GST-SNAP25 WT or GST-SNAP25 5A through 9A were immobilized on glutathione-sepharose beads and exposed to 400 nM purified synaptotagmin 1 C2AB domains, either in the presence of 2 mM of the calcium chelator

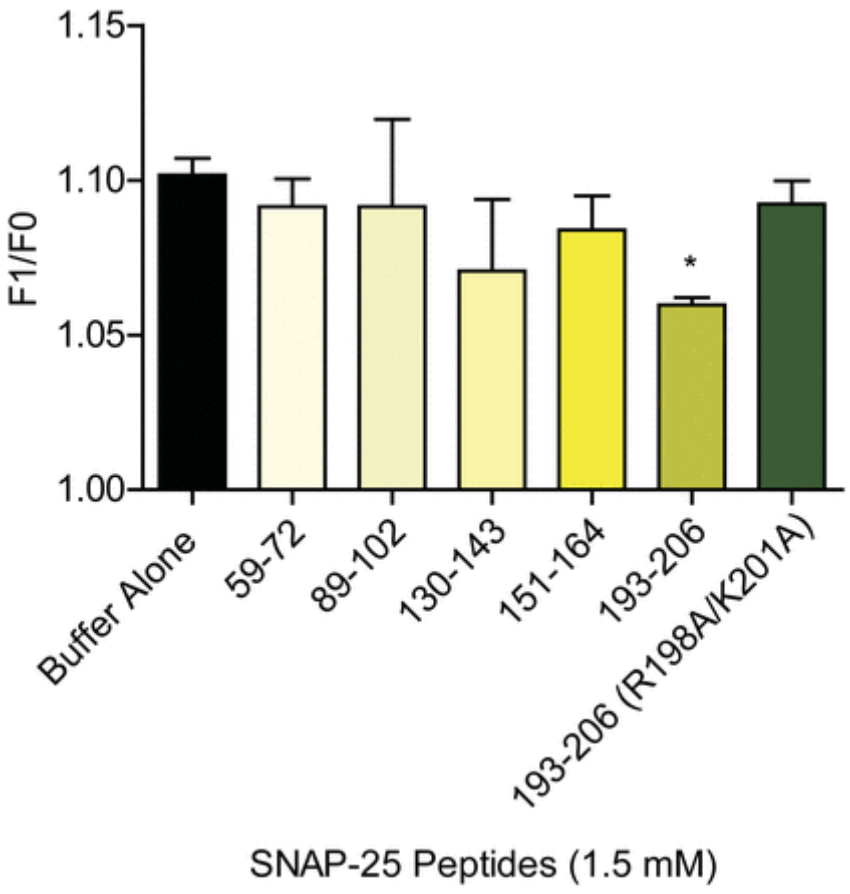

Figure 12. Inhibition of Gβγ–SNAP-25 binding by SNAP-25 peptides.

Using the fluorescence assay detecting the interaction of 20 nM MIANS-$G\beta_1\gamma_1$with 0.3 μM SNAP-25, the addition of 1.5 mM SNAP-25 peptides dissolved in water was compared to the addition of water alone. The C-terminal peptide (193-206) was the only peptide to significantly decrease the fluorescence enhancement when compared to wild type SNAP-25 (Student's t-test, $p<0.01$; $n=3$). When the residues R198 and K201 are changed to alanine in that peptide, the peptide is no longer effective at reducing fluorescence enhancement by SNAP-25 (Student's t-test, $p>0.05$; $n=3$). Figure adapted from Wells CA, Zurawski Z, Rodriguez SM, Betke KM, Yim YY, Hyde K, Alford ST, Hamm HE. *Mol Pharmacol.* 2012 Dec;82(6):1136-49

ethyleneglycoltetracetic acid (EGTA) or 1mM $CaCl_2$. In line with previous results, wild-type SNAP25 can bind both apo-Syt1 and Syt1-Ca^{2+} , with the latter showing enhanced binding (Fig. 13A). To quantify the amount of Syt1 C2AB bound, densitometric analysis was performed within the Odyssey software, normalizing the 700nm channel (I700) representing anti-Syt1 to the 800nm channel (I800) representing anti-GST . No statistically significant decrease in calcium-dependent binding was observed for any of the mutants generated in this study. (Student's *t* test, $p > 0.05$) (Fig. 13B)

The binding of Syt1 to SNAP25 and other SNARE proteins can also occur in the absence of calcium[82,92,238,239]. For the N-terminal mutants 6A and 9A, in the presence of 2 mM EGTA, the interaction between Syt1 and SNAP25 is significantly reduced (Student's *t* test,$p < 0.01$) relative to wild-type SNAP25, with the magnitude of effect being greater for the 9A mutant. The 9A mutant features the R161A mutation in addition to all of the other mutations identified in this study. Because of this, we inferred that the R161A mutation may be important for Syt1-SNAP25 calcium-independent binding. To test this, a SNAP25 containing only the R161A mutation was tested for its ability to bind apo-Syt1. SNAP25 R161A featured inhibited calcium-independent binding to Syt1(Student's *t* test,$p < 0.01$)(Fig 13C, 13D), but calcium-dependent binding was not different from wild-type. This experiment was repeated twice for a total of nine technical replicates. The basic, positively charged residue R161 is quite different in electrostatic character from the acidic residues previously shown to be important in Syt1 binding [230].

It is believed that Gβγ acts to inhibit exocytosis on assembled SNAREs rather than SNARE monomers [48]. t-SNAREs and ternary SNAREs have higher affinity for Gβγ subunits than SNARE monomers[201]. Because of this, we wanted to investigate the ability of the SNAP25 mutants to bind Gβγ when assembled into a SNARE complex. Full-length t-SNAREs containing 8 of the 9 the mutations identified earlier were expressed in *E.coli* using the pRSF-Duet tandem expression vector and purified using immobilized metal affinity chromatography. Saturation binding studies were performed with 20

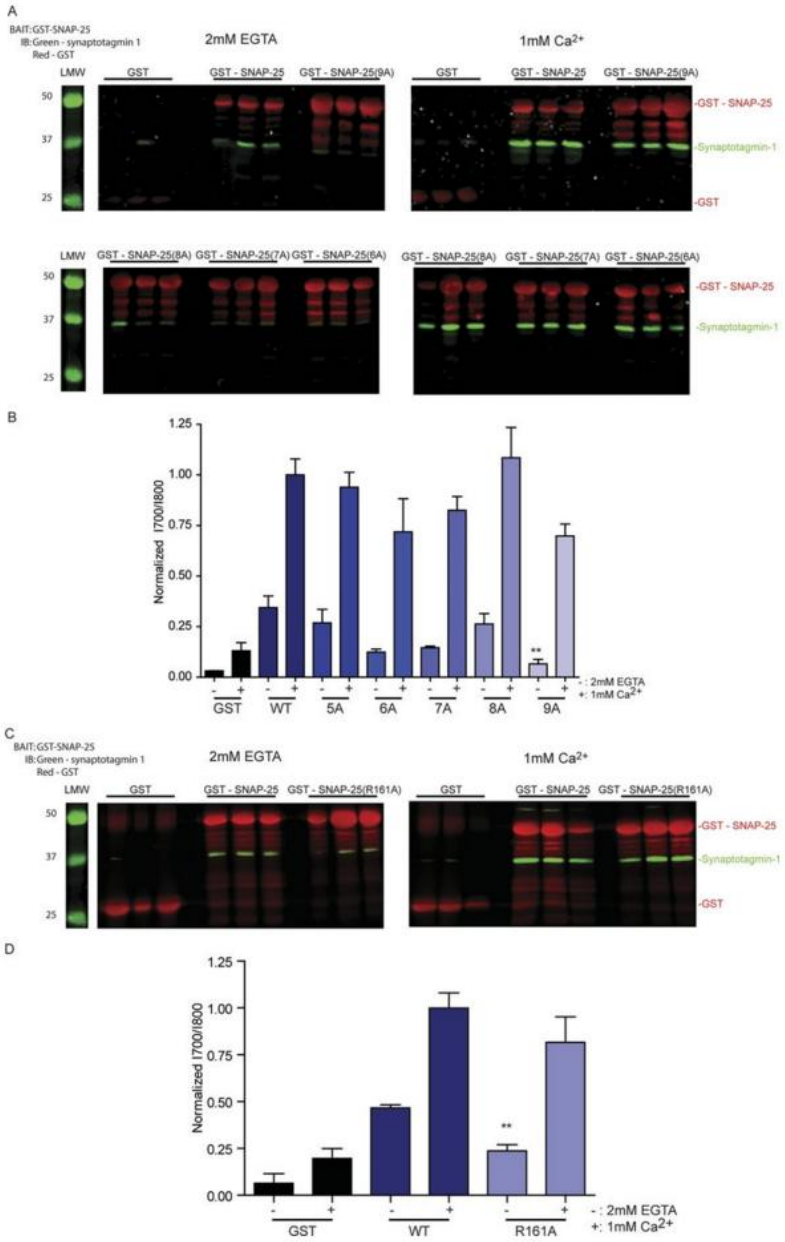

Figure 13. Ability of SNAP-25 mutants to bind to synaptotagmin-1 by GST pulldowns.

A) GST, GST-SNAP-25 wildtype, and GST-fused mutants SNAP-25(6A) through SNAP-25(9A), were glutathione purified as described in the Methods section. Shown are representative blots imaged with Odyssey for simultaneous quantitation of synaptotagmin-1 and GST signal intensity. Red is the color designated for anti-GST, and green is for anti-synaptotagmin. B) The ratio of normalized synaptotagmin-1:GST signals were averaged over three samples over the two conditions. The results are shown in the bar graph (**, $p<0.01$ when compared to WT in 2mM EGTA; one-way ANOVA, Tukey's Multiple Comparison post-test). C) GST, GST-SNAP-25 wildtype, and GST-fused mutant SNAP-25(R161A), were glutathione purified as described. Shown are representative blots imaged with Odyssey for simultaneous quantitation of synaptotagmin-1 and GST signal intensity. Red is the color designated for anti-GST, and green is for anti-synaptotagmin. D) The ratio of normalized synaptotagmin-1:GST signals were averaged over three samples over the two conditions. The results are shown in the bar graph (**, $p<0.01$ when compared to WT in 2mM EGTA; Student's t-test). Figure adapted from Wells CA, Zurawski Z, Rodriguez SM, Betke KM, Yim YY, Hyde K, Alford ST, Hamm HE. *Mol Pharmacol.* 2012 Dec;82(6):1136-49

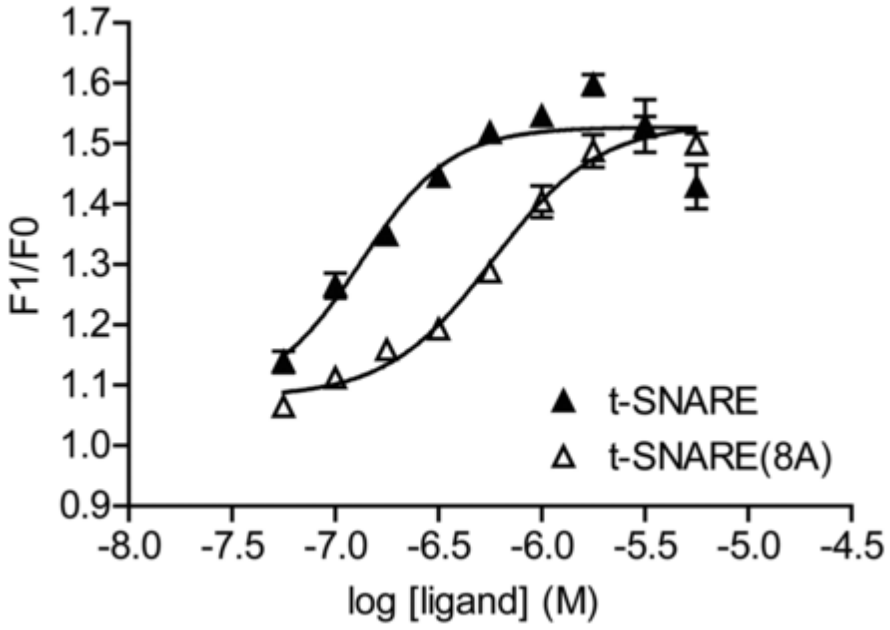

Figure 14. Wild type t-SNARE and SNAP-25 8A t-SNARE binding to MIANS-labeled Gβγ.

As in Figure 3, a fixed concentration of MIANS-$G\beta_1\gamma_1$ (20 nM) was exposed to increasing concentrations of wild-type t-SNARE with resulting increase in fluorescence, n=4. The EC_{50} for t-SNARE binding to MIANS-$G\beta_1\gamma_1$ was 0.13 μM (95% C.I., 0.07-0.26 μM). Similarly, the t-SNARE complex of syntaxin 1A with SNAP-25 8A was exposed to MIANS-$G\beta_1\gamma_1$ with the resulting increase in fluorescence shown in the figure, n=4. The EC_{50} for this complex binding to $G\beta_1\gamma_1$ is 0.58 μM (95% C.I., 0.47-0.70 μM). Figure adapted from Wells CA, Zurawski Z, Rodriguez SM, Betke KM, Yim YY, Hyde K, Alford ST, Hamm HE. *Mol Pharmacol.* 2012 Dec;82(6):1136-49

nM M8-G$\beta_1\gamma_1$ and an increasing concentration of wild-type or mutant t-SNARE. (Fig. 14) Wild-type t-SNARE bound Gβγ with an EC_{50} of 130 nM (95% CI: 67 to 260 nM), similar to previously published results[201]. t-SNARE 8A had a fourfold reduced affinity for Gβγ with an EC_{50} of 580 nM (95% CI: 470 to 700 nM) , but its maximal fluorescence was not statistically different from wild-type, unlike monomeric SNAP25. Experiments were repeated three times.

We hypothesize that one mechanism through which Gβγ inhibits exocytosis is through an interaction with SNAREs. Because of this, a mutant SNARE with a significantly reduced ability to bind Gβγ should decrease the effect of inhibitory $G_{i/o}$-coupled GPCRs that have previously been shown to work via this mechanism. To test our hypothesis, we injected purified SNAP25s or SNAP25 8As into lamprey giant axons to test their ability to impair the inhibitory effect of the lamprey serotonin receptor on vesicle release. It has previously been shown that this receptor signals through the Gβγ-SNARE interaction[48,200]. We evoked presynaptic action potentials at 30-second intervals with brief depolarizing current pulses (2ms, 1-3nA). After obtaining a minimum of 10 responses, 5-HT was added to the bath of the preparation at a concentration of 1μM and a second set of EPSCs was evoked. In the absence of BoNT/E or mutant SNAP25, 5-HT significantly reduced the EPSC amplitudes to 24± 8% of the control amplitude. Proteins were injected into the presynaptic axon utilizing pressure pulses. Injection was confirmed via imaging of injected SNAP25 that was fluorescently labeled in a separate set of paired recordings (data not shown). To replace the endogenous lamprey SNAP25 that is present at this synapse, BoNT/E was utilized to cleave SNAP25 at residue E179 (D179 in mammals). BoNT/E abolishes excitatory postsynaptic currents (EPSCs) when injected alone (Fig. 15A). BoNT/E resistance can be mediated through mutation of D179 to K without causing massive disruption to Syt1 binding [230]. SNAP25 D179K or SNAP25 8A D179K were injected presynaptically at a concentration of

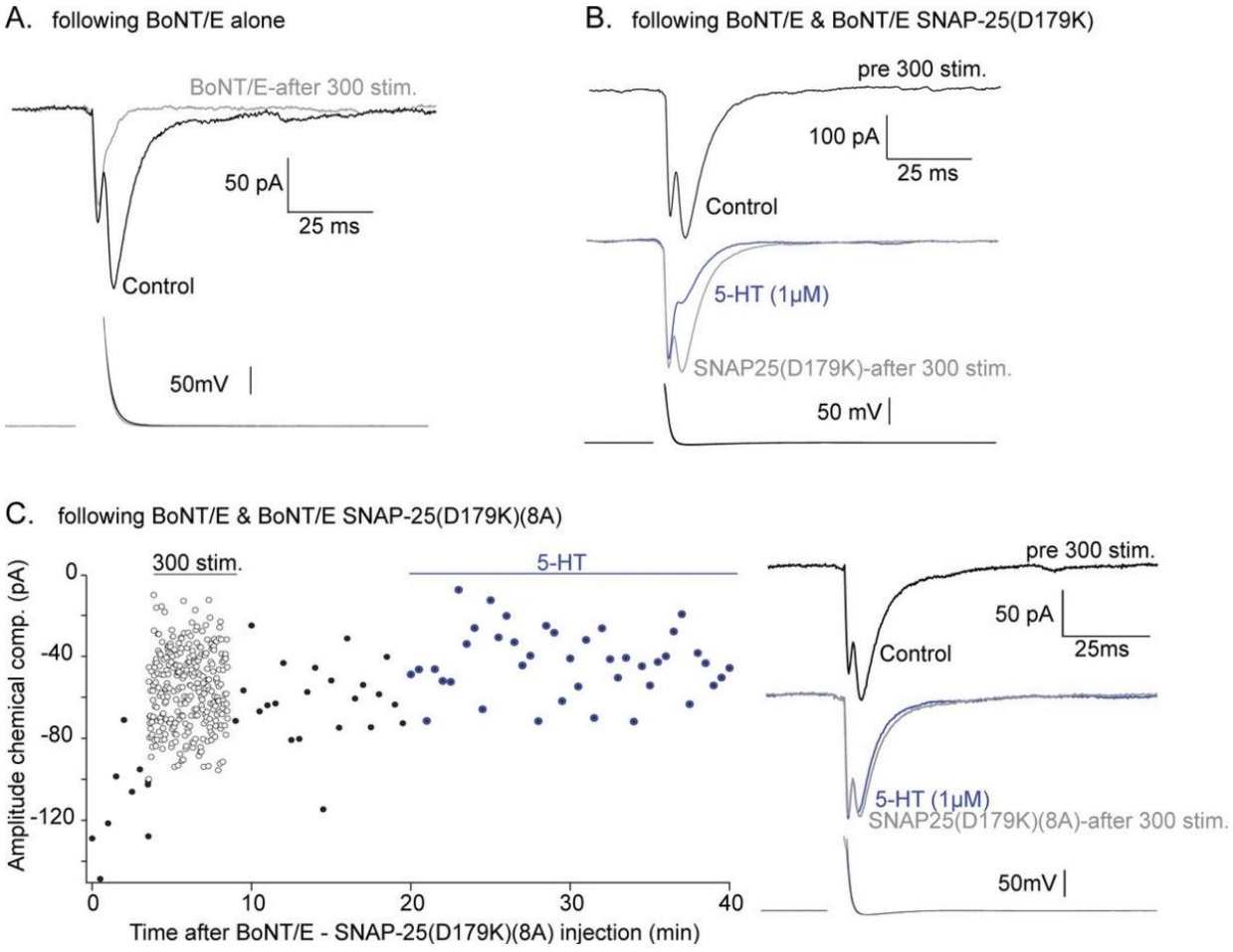

Figure 15. Effect of SNAP-25 8A on presynaptic inhibition in lamprey with 5-HT.

Paired cell recordings were made between lamprey giant reticulospinal axons and postsynaptic ventral horn target neurons. Each recording shown is the mean of at least 10 sequential responses. Overlaid presynaptic action potentials are shown below. a) In a recording in which BoNt/E was included in the presynaptic microelectrode, pressure injection of BoNt/E toxin left synaptic transmission intact (black). A period of 300 stimuli (1Hz) left no remaining chemical EPSC (early component is electrical) following loss of primed toxin resistant vesicles.b) A similar recording in which BoNt/E and SNAP-25 (D179) were included in the presynaptic electrode. A period of 300 stimuli (1Hz) reduced but did not eliminate the EPSC (gray). Addition of 5-HT (1µM) substantially reduced this remaining response (blue)c) With BoNt/E and SNAP-25 (D179) (8A) included in the presynaptic pipette. The graph shows peak chemical EPSC amplitudes recorded against time before (closed circles) during (open circles) and after closed circles 300 stimuli at 1Hz. Addition of 5-HT (1µM, blue) failed to inhibit the synaptic response. EPSC examples are means of 10 from before (black), after 300 stimuli (1Hz) gray, and after addition of 5-HT (1µM, blue). Figure adapted from Wells CA, Zurawski Z, Rodriguez SM, Betke KM, Yim YY, Hyde K, Alford ST, Hamm HE. *Mol Pharmacol.* 2012 Dec;82(6):1136-49

1mg/mL along with the light chain of BoNT/E. BoNT/E cannot cleave assembled SNARE complexes, so an additional 300 stimuli at 1Hz were applied to remove docked vesicles[200] after responses were recorded for 5 minutes. After 5 minutes of recovery, EPSCs were recorded once more. Co-injection of BoNT/E with SNAP25 D179K partially restored synaptic transmission (Fig. 15B). This can be interpreted as evidence that the injected SNAP25 can form t-SNAREs with lamprey syntaxins and VAMPs. Application of 5-HT in the bath at 1uM inhibited EPSC amplitudes to 24 ± 13% control, demonstrating that SNAP25 D179K can support Gβγ-mediated inhibition of exocytosis. Experiments were repeated twice for a total of three technical replicates. SNAP25 8A was injected presynaptically with BoNT/E in identical fashion, with EPSC amplitudes recovering to 73 ± 9% of control amplitudes (Fig. 15C). Restoration of exocytosis is evidence that SNAP258A can interact normally with the rest of the presynaptic release machinery other than Stx1A and Syt1. However, 1μM 5-HT was significantly less effective at reducing EPSC amplitudes in neurons injected with SNAP25 8A D179K than SNAP25 D179K. EPSC amplitudes were only reduced to 76 ± 5% of the amplitude before 5-HT was added. This experiment was repeated four times for a total of five technical replicates. Here, we have shown that decreasing the ability of SNARE to bind Gβγ impaires the ability of a $G_{i/o}$-coupled GPCR to inhibit exocytosis.

Discussion

Here, we have identified many of the most important residues on SNAP25 for Gβγ binding. We have created a SNAP25 with dramatically reduced ability to bind Gβγ, but still retains the ability to bind Syt1 in a Ca^{2+}-dependent manner along with being able to support exocytosis. A new N-terminal binding site for Gβγ, distinct from the previously known C-terminal site, was identified. We have shown that both Gβγ and apo-Syt1 may compete for binding at residue R161, but not at either the other Gβγ binding residues or the Syt1-Ca^{2+}-binding residues of D179, D186, or D193. Syt1 calcium-independent binding residues have not yet been previously identified. The two distinct clusters of residues, suggest a more complex interaction than a simple 1:1 binding between Gβγ and SNAP25, potentially involving two Gβγ subunits per single SNAP25. By creating a SNAP25 with reduced affinity for Gβγ that does not support $G_{i/o}$-coupled GPCR-mediated inhibition of exocytosis, we have created a linked

mechanism through which these receptors work. SNAP25 8A D179K retains its ability to form SNARE complexes and undergo exocytosis, indicating that its key interacting residues for these processes are largely intact, despite release being reduced somewhat relative to SNAP25 WT D179K. The inhibitory effect of the $G_{i/o}$-coupled GPCR upon EPSC amplitudes despite only a fourfold change in the ability of Gβγ to interact with SNARE reinforces previous studies, where BoNT/A can bypass the inhibitory effect of $G_{i/o}$-coupled GPCRs despite only cleaving SNAP25 in such a way that potency is reduced only 1.8-fold[200,201]. The effect of these mutations and /or truncations seems to be more pronounced in our cell-based assay than in *in vitro* protein binding studies. It has previously been determined that the C-terminus of SNAP25 is important in the binding of Gβγ and the ability of some, but not all, $G_{i/o}$-coupled GPCRs, to inhibit exocytosis[48,200,201,208]. Interestingly, despite major differences in the ability of SNAP25 cleaved with BoNT/A and BoNT/E to bind Gβγ[201], all Gβγ-binding residues in this region are removed by BoNT/A, with no additional residues identified from D179 to Q197. SNAP25Δ9 retains a

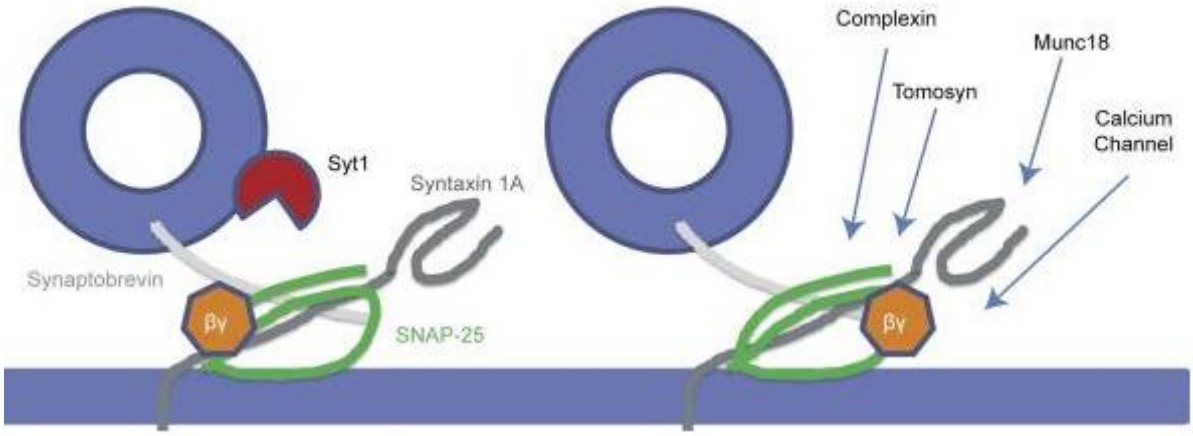

Figure 16. Gβγ - SNARE binding model.

Based on the results of this study, Gβγ appears to not only bind at or near the C-terminus of SNAP-25, but there are additional residues distal to the membrane-approximated portion of SNAP-25. Taken in the context of ternary SNARE and its proposed position at a docked synaptic vesicle, as shown in the model depicted in this figure, a single Gβγ dimer activated by a $G_{i/o}$-coupled GPCR that is bound to the C-terminus of SNAP-25 would not be able to bind the distal portion of the SNARE complex at the same time. The additional residues appear to have implications in calcium-independent binding of synaptotagmin, but they may also have importance for Gβγ modulation of other interactions with SNARE proteins. These could include calcium channels, tomosyn, complexin, and Munc18. Figure adapted from Wells CA, Zurawski Z, Rodriguez SM, Betke KM, Yim YY, Hyde K, Alford ST, Hamm HE. *Mol Pharmacol.* 2012 Dec;82(6):1136-49

substantial ability to bind $G\beta\gamma$[201]. The C-terminal peptide was able to partially inhibit wild-type SNAP25 binding to $G\beta_1\gamma_1$, while other peptides could not. The relative lack of potency of these peptides may stem from an intrinsic ability of them to bind M8-$G\beta_1\gamma_1$ and create a hydrophobic environment for the MIANS fluorophore. The Alphascreen peptide studies provide evidence for this, with the Gβ-derived peptides showing activity in the 1-100 μM range in this assay, despite the SNAP25-derived peptides being at a 15-fold higher concentration. This is an area for potential investigation for studies into putative SNAP25-binding residues on Gβ. The studies included in this chapter have highlighted a second region on SNAP25 important for Gβγ binding. This region is close to the N-terminus of the SNARE complex and located on the SN2 helix, featuring four residues R135, R136, R142, and R161 (Fig. 16). Mutagenesis of these residues to Ala produced no change in affinity for Gβγ, but a significant reduction in the maximum fluorescence. This result is interpreted as a lower-affinity N-terminal binding site. Mutation of the N-terminal residues may perturb the interaction such that the conformation of SNAP25 upon Gβγ is altered, creating a less hydrophobic environment for M8-$G\beta_1\gamma_1$. For the C-terminal binding site, while the strength of the interactions may be weakened via Ala mutations, creating a change in affinity, the hydrophobic environment is initially unchanged from wild-type, resulting in SNAP25 2A and 3A still able to achieve

maximal fluorescence. As residues within the interaction site are gradually mutated, the conformation is altered and the hydrophobicity of the environment may be perturbed, resulting in reduced maximal fluorescence. An X-ray crystal structure containing these mutants may be required to support these explanations.

It has previously been shown that the ability of Gβγ to inhibit exocytosis is not present in conditions of high calcium[201]. The increased affinity of Ca^{2+}-synaptotagmin for SNAREs may allow it to outcompete Gβγ. Syt1-Ca^{2+} can displace Gβγ from t-SNARE[201]. The residues identified in this chapter

for Gβγ binding do not interfere with calcium-dependent binding of Syt1 to SNARE. This is in line with previously published studies, in which three D residues (D179, D186, and D193) are implicated in Syt1-SNARE calcium-dependent binding[230]. Instead, Gβγ binds different residues that overlap with the Syt1 binding site. The Syt1-binding residues are acidic, while the Gβγ-binding residues are basic. Calcium-independent binding of Gβγ to SNAREs has also been reported, with calcium-independent binding being around sixfold less than calcium-dependent binding [82,92,238,239] . The molecular requirements of apo-Syt1 binding to SNAREs have yet to be elucidated, but R161 was shown to be important in our studies, with SNAP25 R161 having reduced ability to bind apo-Syt1 than SNAP25 WT and SNAP25 9A having reduced ability to bind apo-Syt1 than SNAP25 8A. Calcium-dependent binding was intact in these mutants (Fig. 13). Our data demonstrates that there are two clusters of Gβγ-interacting residues on SNAP25. It is clear that they are too far apart to simultaneously bind a single Gβγ subunit. The X-ray crystallographic structures of ternary SNARE (PDB 1SFC)[240] and $G\beta_1\gamma_1$ (PDB 1TBG [241], indicate that the greatest distance between two Gβγ-binding SNAP-25 residues, R135 and K201, is approximately 90 Å, and the diameter of a single $G\beta_1\gamma_1$ subunit is ~70 Å. Because of this, we anticipate that there are two distinct binding sites on Gβγ and that the complex can support a Gβγ:SNARE stoichiometry of greater than 1:1. Hill slope values recorded in this study support this assertion and are generally greater than 1: however, mutagenesis of a single region (N4A) does not reduce the Hill slope to 1. It is possible that Gβγ may move from the N-terminal to C-terminal binding site upon receptor activation, or the N-terminal binding site is important for Gβγ-calcium channel interactions along with previously identified Gβγ-binding domains near the N-terminus of the H_3 domain upon Stx1a[191]. An X-ray crystallographic structure of Gβγ in complex with t-SNARE or ternary SNARE is a major focus of the lab for future studies. SNAP25 and Stx1A adopted a similar conformation in larger SNARE complexes as they did with monomers [131,240 139 242].

It is currently unclear whether any of our SNAP25 mutations cause significant perturbation of the interaction of other proteins with the SNARE complex. SNARE proteins such as SNAP25 are subject to tight spatial and temporal regulation through numerous binding partners including calcium channels [243], Munc18 [108], complexin [132], and tomosyn [138]. The presence of evoked release in the SNAP25 8A D179K mutant suggests that sufficient functionality is retained for the fusion machinery to work. It remains to be seen whether Gβγ interacts with any of these components in the absence of SNARE. Conformations and binding partners enter and leave the complex as the vesicle undergoes differing stages of the cycle.

In summary, we have established novel residues on SNAP-25 for Gβγ, which implies complex binding between the two partners. Mutation of these residues to Ala led to a decreased affinity for Gβγ. This allowed us to critically test the hypothesis that $G_{i/o}$-coupled 5-HT receptors cause inhibition of vesicle fusion through Gβγ interaction with SNARE. Mutant SNAP-25 (8A) has loss of binding to Gβγ but retains its ability to form SNARE complexes and participate in exocytosis, thereby confirming the direct role of Gβγ regulation of synaptic vesicle release at the exocytotic machinery.

CHAPTER III

Gβγ BINDS TO THE EXTREME C-TERMINUS OF SNAP25 TO MEDIATE THE ACTION OF $G_{i/o}$-COUPLED GPCRs.

(Portions of this chapter appear in the journal article "Gβγ Binds to the Extreme C Terminus of SNAP25 to Mediate the Action of $G_{i/o}$-Coupled G Protein-Coupled Receptors." in the January 2016 issue of *Molecular Pharmacology* vol. 89 pp. 79-83, PMID 26519224.

Introduction:

Regulation of neurotransmitter and hormone release is an essential component of homeostasis and plasticity in many systems. Inhibitory G protein-coupled receptors protect exocytotic machinery from overstimulation by inhibiting exocytosis and the release of vesicle contents into the extracellular space. They do so by several mechanisms. One well-studied mechanism is the direct binding of G protein βγ subunits to voltage-gated calcium channels leading to voltage-dependent inhibition of calcium entry[171]. The ability of $G_{i/o}$-coupled GPCRs to inhibit exocytosis downstream of voltage-gated calcium channels is well-documented in a number of different cell types[153,196,197,202,205]. We have previously demonstrated that inhibition can also occur through the direct interaction of Gβγ with the SNARE protein SNAP25 [48,200,201]. Gβγ competes in a calcium-dependent manner with the fusogenic calcium sensor synaptotagmin 1 for binding sites on SNARE [48,201,244]. Upon calcium binding, synaptotagmin 1 binds to the SNARE complex and demixes and disorders lipid membranes to promote fusion of the vesicle membrane with the cell membrane[87,230,245]. Synaptotagmin 1 calcium-dependent binding to SNARE complexes requires three negatively-charged residues on the SN2 helix of SNAP25 located proximally to the C-terminus[230]. Both the N-terminus[244] and the C-terminus of SNAP25[200,201] contain key residues for the interaction with Gβγ. Alanine mutagenesis of 8 residues on SNAP25 reduces its ability to bind Gβγ without disrupting its

ability to bind Syt1[244]. Injection of an exogenous mutant SNAP25 containing these 8 residues mutated to Ala with a botulinum toxin E(BoNT/E) resistance site into presynaptic neurons, along with BoNT/E light chain protease, restores fusion, while abrogating serotonin's (5-HT) ability to inhibit vesicle release in lamprey reticulospinal axons[244]. Interestingly, data was recently shown supporting the notion that a distinct "microarchitecture" is prevalent at presynaptic 5-HT_{1b} receptors that predisposes them to this mode of Gβγ-driven inhibition, while other microarchitectures both within the same synapses and within other types of synapses function through other mechanisms, such as the Gβγ-mediated inhibition of calcium influx through voltage-gated calcium channels at the $GABA_B$ receptor[208]. From this, our current understanding of presynaptic inhibition is that presynaptic $G_{i/o}$-coupled GPCRs function through a variety of mechanisms, including the direct binding of Gβγ to SNAP25.

While the molecular requirements of the Gβγ-SNAP25 interaction are reasonably well-understood, much less is known about the physiology and pathophysiology of the interaction. It is not currently known which $G_{i/o}$-coupled GPCRs work through this mechanism or whether it is used in only certain cellular contexts. Further, it is not clear whether a specific disease state is dependent upon dysregulation of the Gβγ–SNARE interaction. Presynaptic $G_{i/o}$-coupled GPCRs have been shown to be relevant drug targets for anxiety and schizophrenia[246,247], but the mechanisms for these effects are not known. The Gβγ-SNARE interaction has been shown to be functionally relevant for a number of presynaptic $G_{i/o}$-coupled GPCRs[205]. To explore these and other potential areas of therapeutic relevance further, a transgenic model deficient in the Gβγ–SNARE interaction is required. The generation of such a model presents a number of challenges. A knockout-based strategy would be unsuitable. There are 5 Gβ subunits and 12 Gγ subunits[142] in the human genome, indicating a high degree of redundancy, making knockout or mutagenesis of Gβγ subunits unfeasible. While studies have been conducted pertaining to the distribution of Gβ and Gγ subunits in the brain[248], it is not currently known whether a specific combination of subunits is responsible for the Gβγ–SNARE interaction. The possibility of multiple

effectors for any given Gβγ would also be a confounding factor in such a knockout. A knockout of SNAP25 would also be unsuitable, as SNAP25 knockouts are neonatally lethal[249]. Finally, the mutations proposed in Wells *et al*, 2012, are also unsuitable for introduction into a transgenic animal, as the large number of mutations (eight) spread throughout the eight exons[250] makes homologous recombination challenging. Insertion of the 8 mutations as a minigene would also be unsuitable, as the full-length SNAP25 transcript is differentially spliced into two splice variants with differing roles, SNAP25a and SNAP25b. Thus, to obtain a mutation that was suitable for introduction as a transgene, further exploration was required. Here, we have identified an extreme C-terminal mutation suitable for introduction into the native mouse SNAP25 that reduces Gβγ binding, while retaining most Syt1 binding and supporting vesicle fusion.

Methods

Plasmids. The open reading frames for mouse SNAP25b and the C2AB domain of synaptotagmin 1 were subcloned into the glutathione transferase (GST) fusion vector pGEX-6p-1 (GE Healthcare, Chalfont St. Giles, Buckinghamshire, UK) for expression in the Rosetta DE3 strain of *Escherchia coli* (Merck Millipore, Darmstadt, Germany). Mutagenesis of SNAP25 was accomplished via the method of overlapping primers. Sequencing of all plasmids was performed using BigDye Terminator dyes and resolved on an ABI 3730 DNA Analyzer (Applied Biosystems, Foster City, CA).

Antibodies. The antibody for mouse anti-Syt1 C2AB (41.1) was obtained from Synaptic Systems (Goettingen, Germany). The goat anti-GST antibody containing conjugated DyLight 800 and the goat anti-rabbit IgG antibody containing IRDye700DX were both from Rockland Immunochemicals (Gilbertsville, PA).

SNAP25 and Synaptotagmin 1 Protein Purification. Recombinant bacterially expressed GST-fusion proteins were expressed in *Escherichia coli* strain Rosetta DE3 (Merck Millipore, Darmstadt, Germany).

SNAP25 protein expression was induced with 100 μM isopropyl β-d-1-thiogalactopyranoside (IPTG) for 16 h at 25 C. Syt1 (residues 96–422) protein expression was induced with 400 μM IPTG for 8h at 30 C. Bacterial cultures were pelleted and washed once with phosphate-buffered saline before resuspension in 25 mM HEPES-KOH, pH 8.0, 150 mM KCl, 5 mM 2-mercaptoethanol, standard concentrations of the protease inhibitors leupeptin, aprotinin, and pepstatin, 200 μM phenylmethylsulfonyl fluoride, and 1 mM EDTA. Resuspended cells were lysed with a sonic dismembranator at 4°C for 5 min. Lysates were cleared via ultracentrifugation at 26,000*g* for 20 min in a TI-70 rotor (Beckman Coulter, Fullerton, CA). For GST-Syt1, lysates were treated with 0.1 mg/mL DNAse and RNAse prior to purification to remove residual nucleic acids. SNAP25 fusion proteins were then purified from cleared lysates by affinity chromatography on Pierce Glutathione Agarose (Pierce, Rockford, IL). Lysates were exposed to resin for 4h before being washed once with resuspension buffer containing 1% Triton X-100 (Dow Chemical, Midland, MI). After centrifugation at 3000*g*, resins were then washed once with elution buffer (25 mM HEPES-KOH, pH 8.0, 150 mM KCl, 5 mM 2-mercaptoethanol, 0.5% *n*-octyl glucoside, 1 mM EDTA, and 10% glycerol). SNAP25 and Syt1 C2AB proteins were eluted from GST fusion proteins immobilized on resin via proteolytic cleavage with a GST-tagged fusion of rhinovirus 3C protease. Protein concentrations were determined with a Bradford assay kit (Thermo Fisher Scientific, Waltham, MA), and purity was assessed by SDS-polyacrylamide gel electrophoresis.

Gβγ Purification. $G\beta_1\gamma_1$ was purified from bovine retina according to previously published methods[251]. $G\beta_1$6xHis-γ_2 dimers were expressed in Sf9 cells and purified as the method of Kozasa [251]with the following exceptions: frozen Sf9 cell pellets were lysed by gentle sonication pulse, 10 seconds on 20 seconds off for 3 minutes at 30% intensity on ice. $G\beta_1$.6xHis-γ_2 dimers were affinity-purified from detergent solubilized crude cell membrane using Talon® cobalt resin (Clontech) followed by three rounds of dialysis in the following buffer: 20 mM HEPES, 100 mM NaCl, 10 mM BME, 0.8% OG, 10% glycerol pH 8.0.

Biotinylation. Purified recombinant SNAP25 or GST was diluted to 1mg/mL in 25 mM HEPES-KOH pH 8.0, 150 mM KCl, 0.5% *n*-octylglucoside, 1 mM EDTA, and 10% glycerol. A stock solution of EZ-Link NHS-SS-Biotin (Pierce, Rockford, IL) was made by dissolving 6mg in 1mL of H_2O. Biotinylation reagents were added slowly to SNAP25 proteins to a 20:1 molar excess. Reactions were allowed to proceed for 30m at 25 C before removal of excess reagent via two rounds of dialysis in 2L of 25 mM HEPES-KOH pH 8.0, 150 mM KCl, 0.5% *n*-octylglucoside, 1 mM EDTA, and 10% glycerol. Biotinylation was verified via the Pierce Biotin Quantification Kit (Pierce, Rockford, IL).

Alphascreen Binding Assays. Alphascreen luminescence measurements were performed in an EnSpire multimode plate reader (Perkin-Elmer, Waltham MA) at 27°C. Biotinylated SNAP25 was diluted into a final concentration of 20 nM in assay buffer (20 mM HEPES, pH 7.0, 10 mM NaCl, 40 mM KCl, 5% glycerol, and 0.01% triton X-100). A concentration-response curve of purified 6xHis-Gb1g2 ranging from 1μM to 1nM was made in assay buffer. After incubation while shaking for 5m, Alphascreen Histidine Detection Kit (Nickel Chelate) acceptor beads were added to a concentration of 20ug/mL in assay buffer. The assay plate was shaken for 30m. Alphascreen Streptavidin Donor Beads were then added to a concentration of 20ug/mL in low light conditions. Plates were incubated for 1H at 27 C before being read in the EnSpire. 20 nM biotinylated GST in place of SNAP25 with the four highest concentrations of $G\beta_1\gamma_2$ was used with as a negative control for non-specific binding in each assay. EC_{50} concentrations of $G\beta_1\gamma_2$ were determined by sigmoidal dose-response curve fitting with variable slope.

GST Pulldown Assay. 5μg of GST-SNAP25 protein bound to glutathione-agarose resin was incubated with a 400 μM concentration of purified recombinant Syt1 C2AB domains for 1 h at 4°C and washed 3x with assay buffer (20 mM HEPES, pH 7.2, 80 mM KCl, 20 mM NaCl, and 0.2% *n*-octyl glucoside) in a 1.5-ml Eppendorf tube. Assay buffers would contain either 2 mm EGTA or 1 mM $CaCl_2$. To reduce nonspecific binding, immobilized protein complexes were then transferred to a second 1.5-ml Eppendorf tube. Syt1-SNAP25 complexes were eluted with 20 μl of standard Laemmli sample buffer followed by

separation via SDS-polyacrylamide gel electrophoresis. The presence of Syt1 C2AB was detected via Western blot with a mouse anti-Syt1 antibody. Western blots were imaged using the LI-COR Odyssey imager (LI-COR Biosciences, Lincoln, NE) with labeled antibodies: anti-GST (goat) antibody DyLight 800 Conjugated and rabbit IgG (H&L) Antibody IRDye700DX Conjugated.

Electrophysiology and Microinjections. All studies were conducted using isolated spinal cords from sea lampreys (*Petromyzon marinus*). Sea lampreys were anesthetized with tricaine methanesulfonate (100 mg/l) and sacrificed by decapitation. Spinal cords were then dissected in an ice-cold Ringer's saline solution of the following composition: 100 mM NaCl, 2.1 mM KCl, 2.6 mM $CaCl_2$, 1.8 mM $MgCl_2$, 4 mM glucose, and 5 mM HEPES pH 7.6. All animal experiments conformed to University of Illinois at Chicago institutional guidelines.

For electrophysiological experiments, paired cell recordings were collected between reticulospinal axons and neurons of the spinal ventral horn. Recordings were obtained from axons of reticulospinal neurons with microelectrodes containing 1 M KCl, 5 mM HEPES-KOH pH 7.2, and SNAP25 and BoNT/E (65ug/mL). Electrode had impedances from 20 to 50 MΩ. Recordings were obtained from postsynaptic neurons using whole cell patch clamp under voltage-clamp conditions. Patch electrodes were filled with 102.5 mM $CsMeSO_3$, 1 mM NaCl, 1 mM $MgCl_2$, 5 mM EGTA, and 5 mM HEPES-CsOH, pH 7.2.

The light-chain of BoNT/E (65 μg/ml; List Biological Laboratories Inc., Campbell, CA) was stored at −20°C in 20 mM HEPES-NaOH pH 7.4, 50 mM NaCl, and 1mg/mL bovine serum albumin. Buffered solutions of BoNT/E were diluted as 5 μl with 20 μl of 2 M $KMeSO_4$ and 5 mM HEPES along with 20 μl of solution containing recombinant SNAP25 mutants. SNAP25 proteins were stored at −20°C in a buffer containing 25 mM HEPES-KOH pH 8.0, 150 mM KCl, 5 mM 2-mercaptoethanol, 0.5% *n*-octylglucoside, 1 mM EDTA, and 10% glycerol. SNAP25 solutions mixed with BoNT/E were diluted 1:5 with 2 M $KMeSO_4$ and 5 mM HEPES. BoNT/E and SNAP25 mutants were microinjected through presynaptic

microelectrodes using the Picospritzer II (Parker Hannifin, Hollis, NH) . All presynaptic recordings were made within 100 μm of the synaptic contact between the paired neurons.

Statistics. All statistical tests and all concentration response-curve fitting were performed using GraphPad Prism v.4.03 for Windows, (GraphPad Software, La Jolla, California, USA, www.graphpad.com)

Results

To explore the binding of a number of different SNAP25 mutants to Gβγ, we developed an Alphascreen assay (Perkin-Elmer) with higher throughput and greater dynamic range. In this assay, biotinylated recombinant mouse SNAP25 (biotinylated non-specifically upon primary amine residues with EZ-Link NHS-SS-biotin) interacts with His-tagged Gβ1γ2 subunits purified from SF9 cells inoculated with baculovirus. When the Gβγ–SNAP25 complex forms, the complex is anchored to an Alphascreen streptavidin-conjugated donor bead via the biotinylation on SNAP25 and an Alphascreen Ni-trinitriloacetic acid (NTA) acceptor bead via the His-tag on Gβγ. When the donor bead is illluminated with 680nm coherent light, dye molecules attached to it generate singlet oxygen, which can travel a short distance in solution and strike an adjacent acceptor bead. The acceptor bead generates 520-620nm light in response to singlet oxygen (Fig.17, top). High specificity for the Gβγ–SNARE interaction was observed, with minimal signal being generated in the absence of protein, but a large signal when 20 nM SNAP25 and 170 nM $G\beta_1\gamma_2$ is present in solution. As a control for non-specific binding, 20 nM glutathione-S-transferase (GST), a protein that does not interact with $G\beta\gamma^{201}$, was added to solution. 20 nM SNAP25 did not generate a signal in the presence of His-tagged 170 nM $G\alpha_i$-GDP as a second non-specific binding control (Fig. 17, bottom).

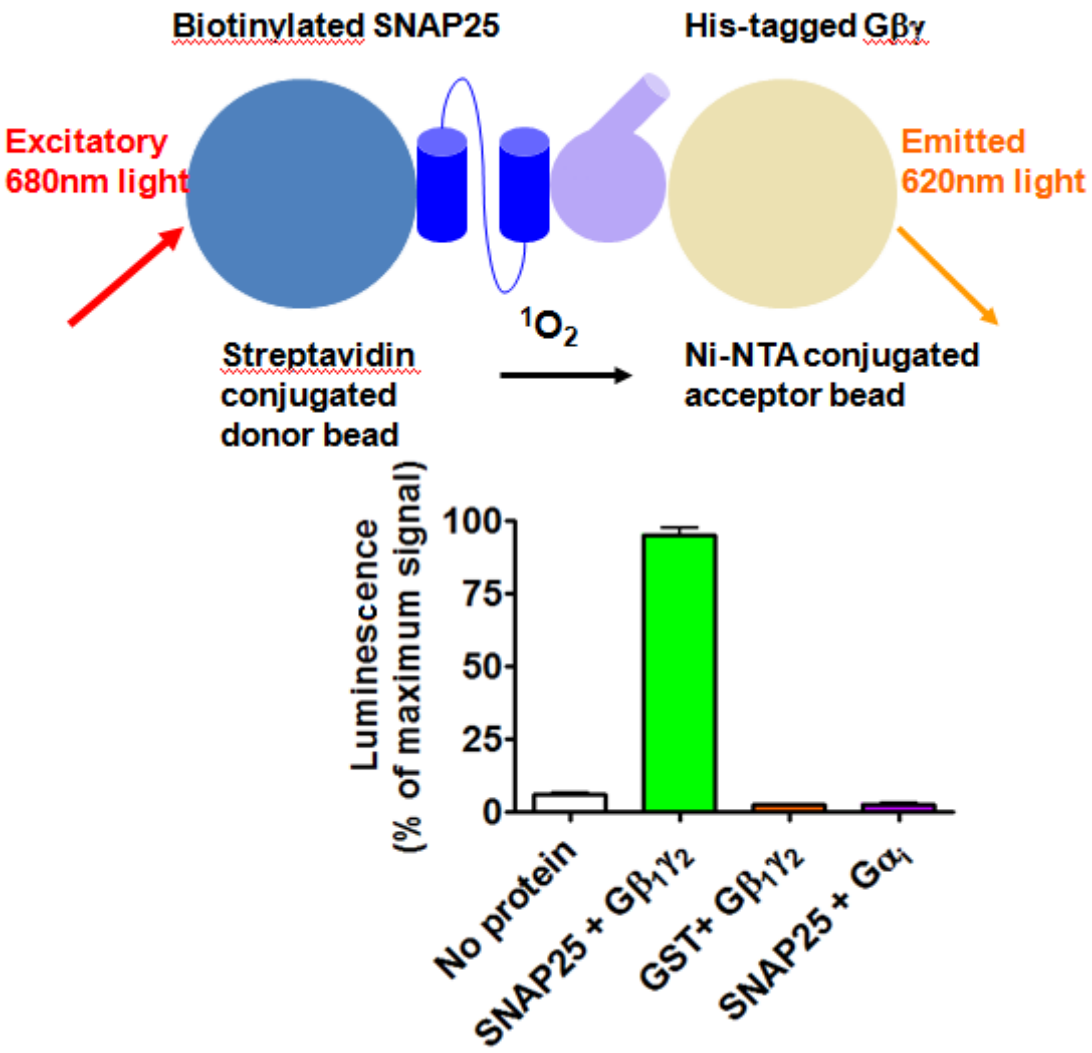

Figure 17. The Alphascreen Gβγ–SNAP25 protein-protein interaction assay.

A): Diagram of assay principle. Biotinylated SNAP25 interacts with His-tagged $G\beta_1\gamma_2$ subunits *in vitro*. The Gβγ –SNAP25 complexes are captured on Alphascreen Ni-NTA acceptor beads via the His-tag on Gβγ , while simultaneously being captured on Alphascreen streptavidin donor beads via the biotinylation on SNAP25. If 680nm light strikes a donor bead, singlet oxygen is generated and can travel a short distance in solution to strike an acceptor bead, which will generate 520-620nm light to be detected by the plate reader. B) Non-specific binding controls for the Alphascreen assay. The GST condition was repeated with each Alphascreen saturation binding and competition binding study as a non-specific binding control. Data presented as mean + S.E.M . Figure adapted from Zurawski Z, Rodriguez S, Hyde K, Alford S, Hamm HE. *Mol Pharmacol*. 2016 Jan;89(1):75-83.

The SNAP25 8A mutant (14) has 8 Gβγ-binding residues on SNAP25 mutated to Ala. Two of those residues, R198 and K201, are at the C-terminus of SNAP25, and within the final exon of the mRNA. Mutation of these two residues to Ala (termed "SNAP25 2A") produced a 1.9-fold reduction in affinity for Gβγ, while no change was observed in the ability of proteins containing these mutations to bind Syt1[244]. We hypothesized that introduction of SNAP25 2A into lamprey reticulospinal axons along with subsequent removal of endogenous SNAP25 could decrease the inhibition of glutamate release into the synapse of lamprey presynaptic 5-HT receptors. To do this, we mutated residue D179 to Lys to make SNAP25 2A resistant to BoNT/E cleavage [230].

Control experiments were first performed to ensure that terminals were filled following an injection into the presynaptic axon. Alexa 594 (1 mM) was included in the presynaptic electrode solution along with

BoNT/E. These were pressure injected into the axon. The postsynaptic neuron was filled with Alexa 488 (25 μM) by diffusion from the patch pipette. The synaptic response to presynaptic action potentials was recorded in control, prior to injection. Dye and BoNT/E were then pressure injected into the axon. The presynaptic axon was imaged using fluorescence microscopy with an excitation peak of 590 nm and a long pass emission filter (610 nm), the postsynaptic with a 488 nm excitation and a bandpass emission filter (510-550) (Fig. 18Bi). BoNT/E cannot access the primed ternary SNARE complex to cleave SNAP25. Thus, after approximately 5 minutes of recording, 300 pulses were administered at a rate of 1 Hz to remove all remaining primed vesicles[200,244]. It is clear that when labeling is present presynaptically, synaptic responses were abolished by the BoNT/E (Fig 18Bii).

It is possible to recover synaptic transmission in terminals in which a recombinant BoNT/E resistant SNAP25 is coinjected into the presynaptic axon with the BoNT/E. In a previous study, a SNAP25 containing the D179K mutation was injected into the presynaptic neuron along with BoNT/E, restoring EPSC amplitudes to 95 ± 11 % of control. In those experiments, subsequent application of 1 μM 5-HT

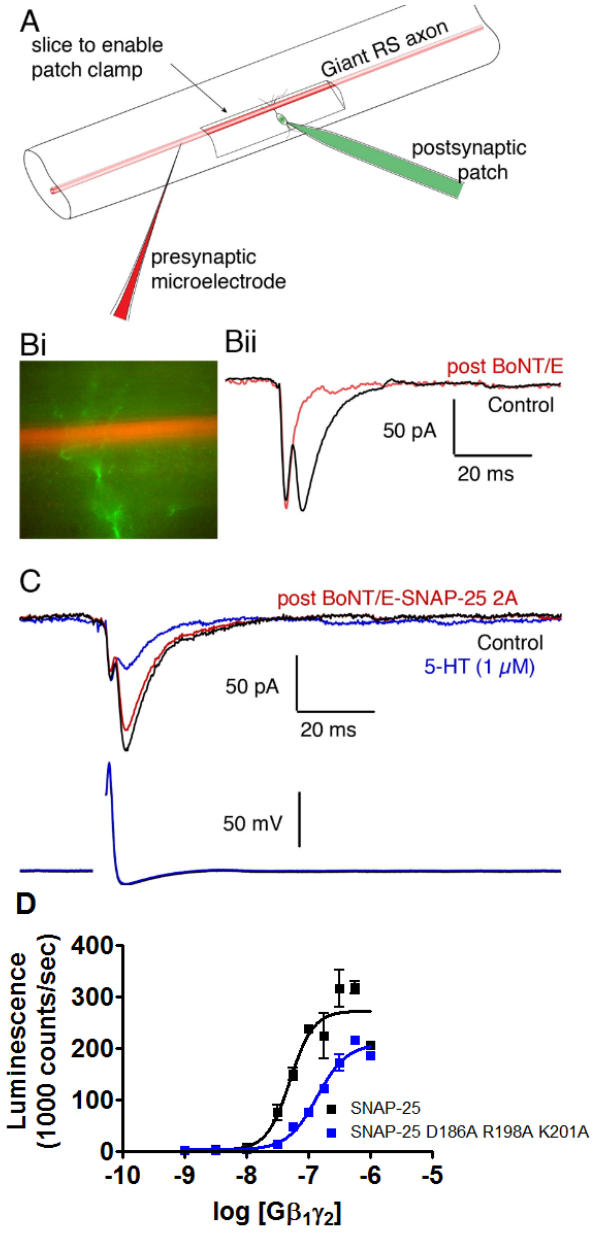

Figure 18. The SNAP25 2A mutant supports the inhibitory effect of 5-HT on glutamate release in lamprey spinal neurons.

A) Diagram of assay principle. BoNT/E resistant SNAP25 is loaded into electrodes along with BoNT/E to cleave endogenous SNAP25 and injected into the presynaptic giant RS axon. Bi) Paired recordings are taken between lamprey reticulospinal axons and neurons of the spinal ventral horn. To demonstrate that injected toxins and proteins have access to the presynaptic terminal, dye was included in the presynaptic (red, Alexa 594) and postsynaptic (green, Alexa 488). An image is shown of the dendrites of the postsynaptic cell and the axon passing through these dendrites after pressure injection into the axon. (Bii) Evoked EPSCs are shown recorded from the postsynaptic cell in control (black) and after the clearing of docked vesicles through application of 300 stimuli at 1 Hz (red) to show efficacy of BoNt/E. (C) Paired recordings from another cell in which the presynaptic electrode contained BoNt/E and a BoNt/E resistant SNAP-25-2A. After the same treatment, 5-HT is applied in the bath to inhibit EPSCs. Addition of 5-HT (1 µM) substantially reduced this remaining response by 69 ± 4% of control amplitudes. (n=4) (D) Alphascreen saturation binding for SNAP25 WT and SNAP25 2A that also contains a D186A mutation. Figure adapted from Zurawski Z, Rodriguez S, Hyde K, Alford S, Hamm HE. *Mol Pharmacol.* 2016 Jan;89(1):75-83.

reduced EPSC amplitudes to 24+/-13% of control, showing that Gβγ can still interact with recombinant SNAP25 introduced into the presynaptic terminal via pipette[244].

We repeated that experimental format in this study using the BoNT/E resistant SNAP25 2A. This was injected into axons along with BoNT/E. Paired recordings of EPSCs were then conducted between the injected reticulospinal axons and their synaptic target neurons of the spinal ventral horn (Fig. 18A). As before, 300 action potentials were evoked to deplete the primed vesicle pool. From these data it is clear that SNAP25 2A can support evoked synaptic transmission because EPSC amplitudes recovered to 81 ± 2 % of control amplitudes (n=5). In four of these recordings, subsequent application of 1 μM 5-HT reduced

EPSC amplitudes to 33 ± 5 % of the amplitude after injection and application of higher frequency stimulation. This was not different from prior studies with SNAP25 containing the D179K mutation alone[244]. (Fig. 18B) Together, these data indicate that the SNAP25 2A mutant is still capable

of forming fusion-competent SNAREs and partaking in exocytosis. Furthermore, the SNAP25 2A mutant still supports the Gβγ–SNAP25 interaction, as measured through in vitro binding assays and the effects of 5-HT on EPSC amplitudes[244], despite the reduced affinity. Correspondingly, in the Alphascreen assay, a SNAP25 containing the 2A mutation as well as a D186A mutation (a residue previously implicated in Syt1 calcium-dependent binding) had 2.7-fold lower affinity than SNAP25 WT when ran side-by-side. (EC_{50} = 50 nM (95% CI: 36-69 nM) for SNAP25WT, 137 nM (95% CI: 115-164 nM, n=3) for SNAP25 2A D186A) (Fig.18D.)

With the 2A mutant of SNAP25 still supporting the Gβγ–SNAP25 interaction, we sought to generate a set of mutants with a deleterious effect on the interaction with Gβγ . Since residues R198 and K201 are positively-charged and Ala is electrostatically neutral, we hypothesized that mutating these positively-charged residues to negatively-charged residues may have a larger effect. We generated a R198E

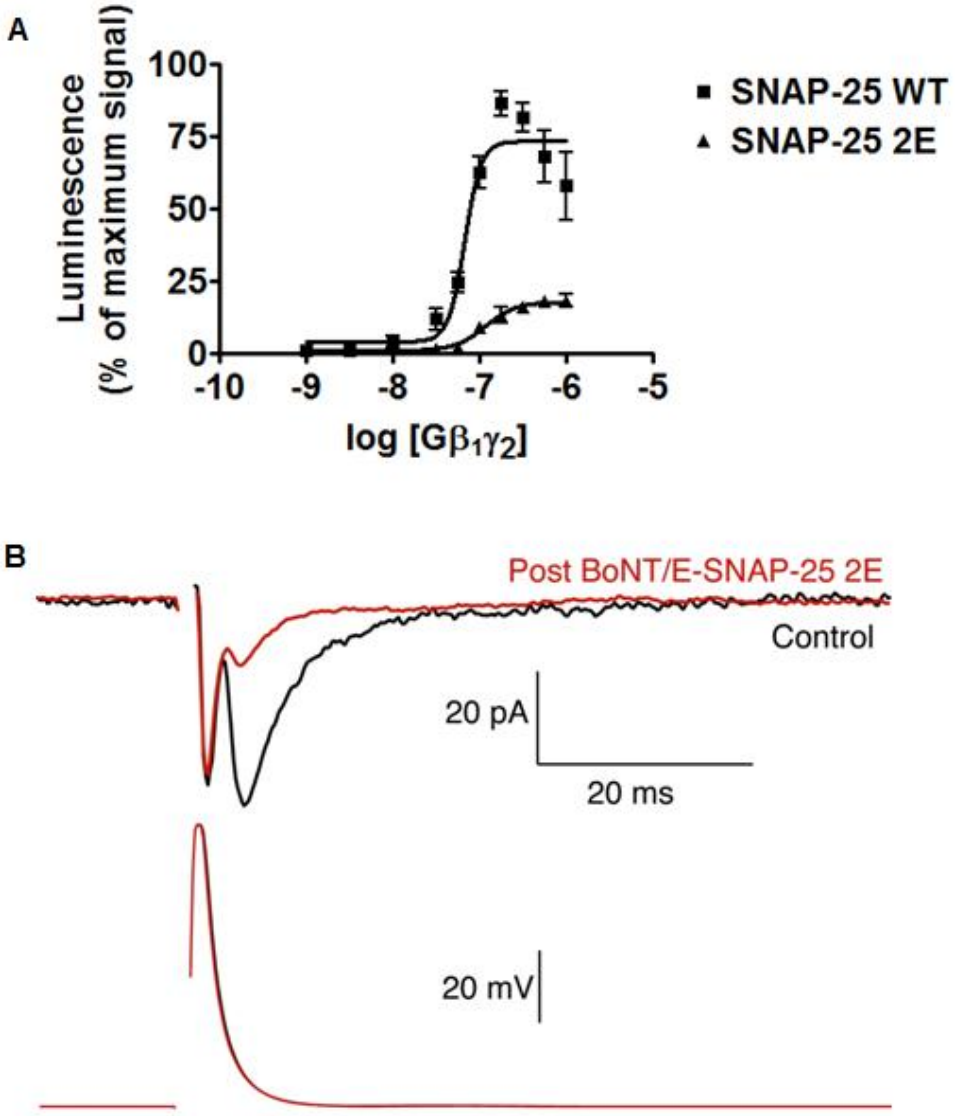

Figure 19: The SNAP25 2E mutant exhibits inhibited Gβγ -SNARE binding and inhibited neurotransmission.

A) Alphascreen concentration-response curves for SNAP25 WT and SNAP25 2E. Data normalized to the maximum luminescence signal obtained in each experiment.The EC_{50} for the binding of SNAP25 WT to $G\beta_1\gamma_2$ is 67nM (95% C.I.: 56-81nM). The EC_{50} for the binding of SNAP25 2E to $G\beta_1\gamma_2$ is 116nM (95% C.I.: 90-150nM) B) Example trace of paired recording of presynaptic neuron injected with SNAP25 2E as in Fig. 2. The chemical portion of the EPSC is reduced (to 23 ± 10% of control), indicating its inability to restore vesicle release into the synapse. Data presented as mean + S.E.M . of two independent experiments. Figure adapted from Zurawski Z, Rodriguez S, Hyde K, Alford S, Hamm HE. *Mol Pharmacol.* 2016 Jan;89(1):75-83.

K201E double mutant containing two Glu residues, SNAP25 2E. Purified recombinant SNAP25 2E had a substantially reduced ability to interact with $G\beta_1\gamma_2$ as measured in the Alphascreen assay (Fig. 19A), with a fourfold drop in efficacy and a 1.7-fold drop in potency, with an EC_{50} of 116 nM compared to an EC_{50} of 67 nM for wild-type SNAP25. Attempting to achieve an intermediate state between the 2A and 2E mutants, we made a R198Q K201Q mutant termed 2Q. We hypothesized that the 2Q mutant would contain a partial-negative charge through resonance of the amide side-chain on each glutamine residue. In the Alphascreen assay to measure the Gβγ–SNAP25 interaction, the 2Q mutant only had a small effect on Gβγ binding, with no significant difference in the EC_{50} between SNAP25 WT and SNAP25 2Q (EC_{50}= 51 nM, 95% CI: 42-63 nM, data not shown). The 2Q mutant was not chosen for cellular studies due to the lack of significance relative to SNAP25 WT. Given the promising result with SNAP25 2E, we made a BoNT/E resistant SNAP25 2E and injected it into reticulospinal axons in a similar manner to Fig. 18. Using the same approach of eliminating primed vesicles inaccessible to BoNT/E after the injection we demonstrated that the SNAP25 2E mutant could only support a substantially reduced evoked neurotransmission in this system. The peak amplitude of the response was reduced to 23 ± 10 % of the control amplitude (Fig. 19B). We hypothesized that SNAP25 2E may have had altered Syt1 binding as a result of the dramatic changes to the electrostatic character of the C-terminus of SNAP25. To test this, we utilized a GST-pull down approach similar to previously published studies[244]. We made GST-fusions of SNAP25 WT or 2E and tested them for their ability to bind Syt1 in a calcium-dependent manner. 5ug of GST-SNAP25 was incubated on glutathione-sepharose beads with 400 nM SNAP25 in the presence of either 1mM Ca^{2+} or the calcium chelator 2 mM EGTA. As a control, GST alone was incubated with 400 nM SNAP25 WT or SNAP25 2E. After incubation for 1hr, complexes were washed to remove unbound SNAP25 and analyzed via SDS-PAGE and Western blot. Antibodies against Syt1 and GST were used for detection (Fig. 20A) Both SNAP25 WT and SNAP25 2E bound Syt1 in a calcium-dependent manner. We observed a 4.6 –fold (Student's *t* test, $p< 0.001$) reduction in calcium-dependent binding for SNAP25 2E relative to SNAP25 WT. No reduction in calcium-independent binding for SNAP25 2E

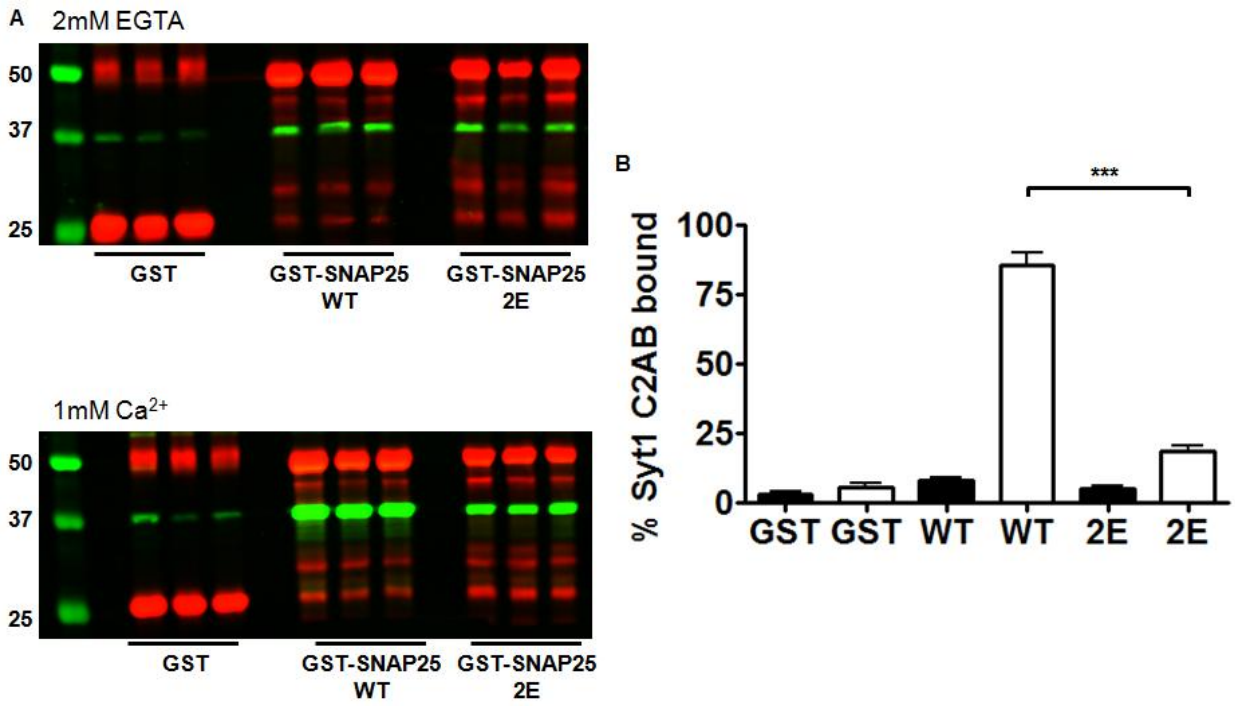

Figure 20: The SNAP25 2E mutant exhibits inhibited synaptotagmin 1 calcium-dependent binding.

A) Western blot images of GST-pull down assay. The LI-COR Odyssey system was used for simultaneous imaging of GST and Syt1. The upper blot shows samples in the presence of 2mM EGTA (black bars), while the lower blot is taken in the presence of 1mM $CaCl_2$ (white bars). Red IRDye800-labeled bands (the I800 channel) are representative of GST (26kDa) or GST-SNAP25 (51 kDa). GreenIRDye700-labeled bands (the I700 channel) are representative of Syt1 C2AB (37 kDa). B) Densitometry of bands in each sample. Densitometry performed by LI-COR Odyssey software. The amount of Syt1 C2AB present in each sample is normalized to the amount of GST or GST-SNAP25 present to correct for loading discrepancies. The resulting amount of Syt1 C2AB pulled down is then plotted as a percentage of the Syt1 pulled down by wild-type SNAP25. Error bars represent mean + S.E.M. Values measured by two-tailed Student's t-test (* $p < 0.05$, ** $p < 0.01$, *** $p < 0.001$) The experiment was repeated twice for a total of three experiments. Figure adapted from Zurawski Z, Rodriguez S, Hyde K, Alford S, Hamm HE. *Mol Pharmacol.* 2016 Jan;89(1):75-83.

was observed relative to SNAP25 WT (p= 0.076) (Fig. 20B). These data suggest that the lack of evoked neurotransmission seen in the 2E mutant may be due to impaired Syt1 calcium-dependent binding.

Finally, we sought to identify Gβγ–binding residues in other positions at the C-terminus of SNAP25. While the peptide mapping approach previously used identified several important residues, the lack of higher-order structure achieved by short peptides may lead to false-negative results. Furthermore, the Ala scanning approach previously utilized is unlikely to identify key residues that bear close structural similarity to Ala, such as Gly or Ser. Prior studies with the SNAP25Δ9 construct and BoNT/A show that this truncation has impaired Gβγ binding and reduced ability for 5-HT to inhibit vesicle release[201]. Furthermore, this mutant has impaired SNARE complex zippering[252]. Our intent was to make a smaller truncation mutant that did not exhibit these deficiencies in SNARE complex formation. The SNAP25Δ3 mutant, lacking three C-terminal residues, was previously shown to have release properties similar to wild-type SNAP25[253,254], while the SNAP25Δ4 mutant had substantially reduced exocytosis due to the critical residue L203 being truncated in this construct. We tested the ability of recombinant purified SNAP25Δ3 to bind Gβγ. This mutant exhibited a twofold reduction in the efficacy of SNAP25 binding to Gβγ compared to wild-type (Fig.21A). In the same electrophysiological assay utilized for figures 2 and 3, the BoNT/E resistant SNAP25Δ3 was able to restore exocytosis completely, with EPSC amplitudes 99 ± 4 % of control amplitudes prior to BoNT/E treatment. However, the effect of 5-HT was partially abrogated, with 1 μM 5-HT only reducing EPSC amplitudes to 48 ± 11 % of control (n=3). 5-HT was significantly less effective than in wild type conditions (Fig. 21b), while still showing an intermediate effect compared to prior results obtained with SNAP25 8A in which inhibition was almost completely lost. Together, these results suggest that SNAP25Δ3 exhibits moderately impaired ability to bind Gβγ. Finally, we tested the ability of GST- SNAP25Δ3 to bind Syt1 in the GST-pull down assay (Fig. 22). A 1.4-fold reduction in calcium-dependent binding was observed for GST- SNAP25Δ3 compared to wild-type ($p<.0001$), despite no reduction in exocytosis relative to wild-type in Fig. 21. Calcium-independent

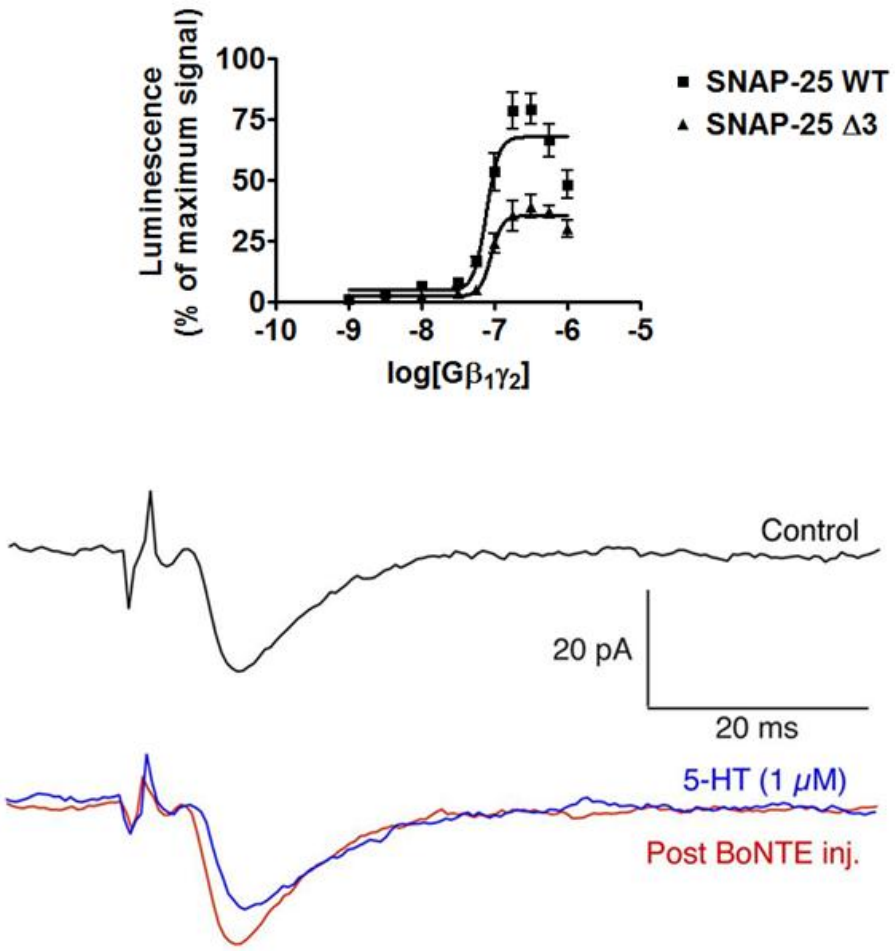

Figure 21: The SNAP25Δ3 mutant shows both impaired Gβγ binding, and an impaired inhibitory effect of 5-HT on glutamate release.

A) Alphascreen concentration-response curves for SNAP25 WT and SNAP25Δ3. The EC_{50} for the binding of SNAP25 WT to Gβ1γ2 is 76nM (95% C.I.: 64-91nM), while the EC_{50} for SNAP-25 Δ3 binding to $G\beta_1\gamma_2$ is 89nM (95% C.I.: 75-105nM). A twofold decrease was observed in the maximum luminescence signal generated by SNAP25 Δ3 compared to SNAP25 WT. Data normalized to the maximum luminescence signal obtained in each experiment. B) Example trace of paired recording of presynaptic neuron injected with SNAP25Δ3 as in Fig. 2. After 300 stimuli, EPSC amplitudes recovered to 95% of pre-injection amplitudes, indicating the ability of the mutant to restore SNAP25-dependent exocytosis. 3uM 5-HT reduced EPSC amplitudes to only 48± 11% of EPSC amplitudes recorded in the absence of 5-HT Each experiment was repeated twice for a total of three experiments. Figure adapted from Zurawski Z, Rodriguez S, Hyde K, Alford S, Hamm HE. *Mol Pharmacol*. 2016 Jan;89(1):75-83.

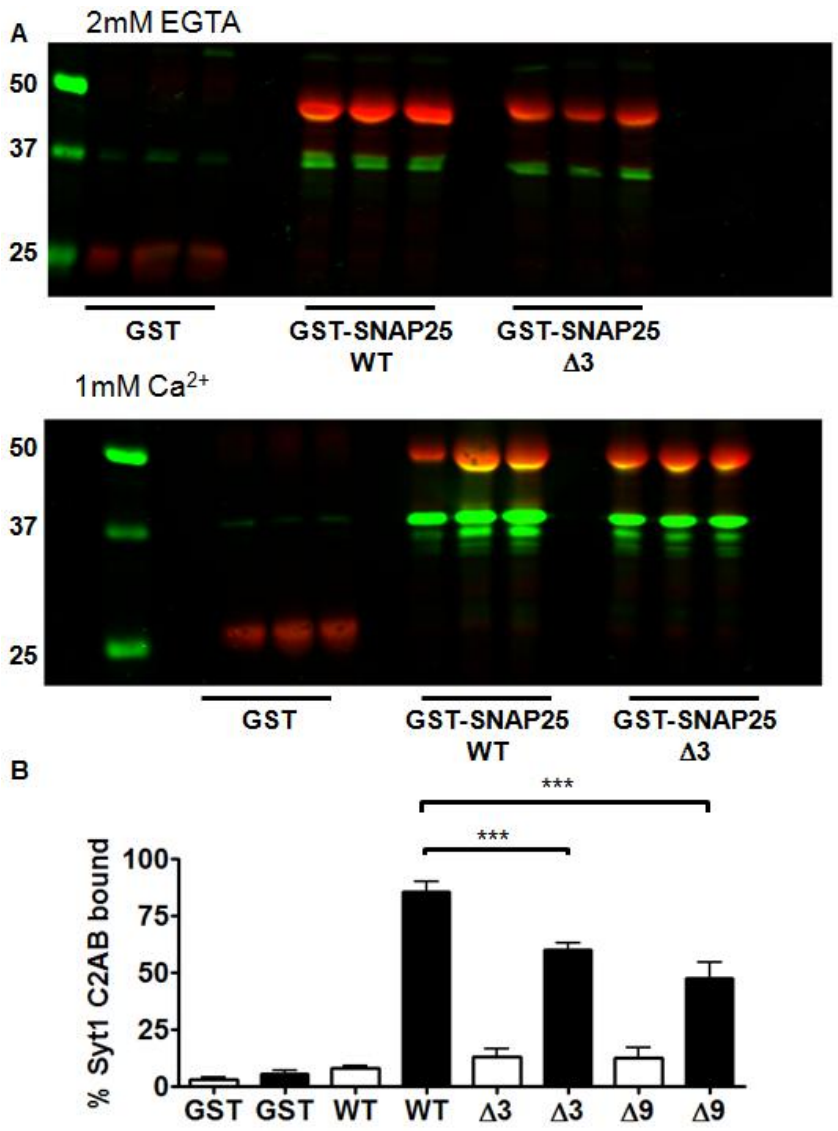

Figure 22: Syt1 calcium-independent binding is slightly reduced in the SNAP25Δ3 mutant.

A) Western blot images of GST-pull down assay as in Fig. 4. SNAP-25Δ9 immunoblot not shown. B) Densitometry for Syt1 C2AB pulled down by GST-SNAP25 WT, Δ3, or Δ9 in the presence of 2mM EGTA (white bars) or 1mM Ca^{2+} (black bars). Values for Syt1 C2AB pulled down measured by two-tailed Student's t-test (* $p < 0.05$, ** $p < 0.01$, *** $p < 0.001$) The experiments were repeated twice for three independent experiments. Figure adapted from Zurawski Z, Rodriguez S, Hyde K, Alford S, Hamm HE. *Mol Pharmacol.* 2016 Jan;89(1):75-83.

binding was not significantly different from wild-type for GST- SNAP25Δ3 (p= .065) Similarly, GST-SNAP25 Δ9 showed significantly impaired Syt1 binding in the presence of 1mM Ca^{2+} compared to wild-type, possibly suggesting that Syt1 utilizes one or more of the C-terminal residues of SNAP25 for calcium-dependent binding[82]. A 1.8-fold reduction in Syt1 calcium-dependent binding (Student's t test, $p< 0.001$) but not calcium-independent (p= .152) binding was observed, comparable to previously published results obtained with BoNT/A[82].

Discussion

We have obtained a mutant, SNAP25Δ3, which has impaired binding to Gβγ and reduced ability to support the actions of an inhibitory $G_{i/o}$-coupled GPCR upon vesicle fusion. The studies conducted here support a perturbed competition between Syt1 and Gβγ binding to SNAP25 in favor of Syt1 for the SNAP25Δ3 mutant, as maximum Gβγ binding and $G_{i/o}$-coupled GPCR activity is reduced, while exocytosis is unaffected. Given the results in Fig. 20, it would be plausible that R198 and K201 may be important for this interaction, but SNAP25 8A does not exhibit impaired calcium-dependent binding to Syt1. Neutral Ala mutations demonstrably have a smaller effect than charge-reversal mutations in these studies. A structural model of the importance of key residues in the C-terminus of SNAP25 illustrates some of the numerous regulatory mechanisms acting upon exocytosis in the C-terminus of SNAP25[48,151,240,244,253-256] (Fig. 23). Many residues at the C-terminus of SNAP25 have been associated with reduced exocytosis in mutation or truncation studies: these include R198[255], K201[255], M202[253,257], and L203[254]. The three C-terminal residues have not, with no significant difference being detected between chromaffin cells expressing wild-type SNAP25 or SNAP25Δ3[254]. Our studies echo these results, with SNAP25Δ3 being able to support exocytosis in neurons to levels similar to pre-BoNT/E-treated controls , much like the BoNT/E-resistant full-length SNAP25. There are also two important residues for exocytosis upstream of the BoNT/A cleavage site: the phosphorylation site at S187 and the SNARE-forming residue at N188.

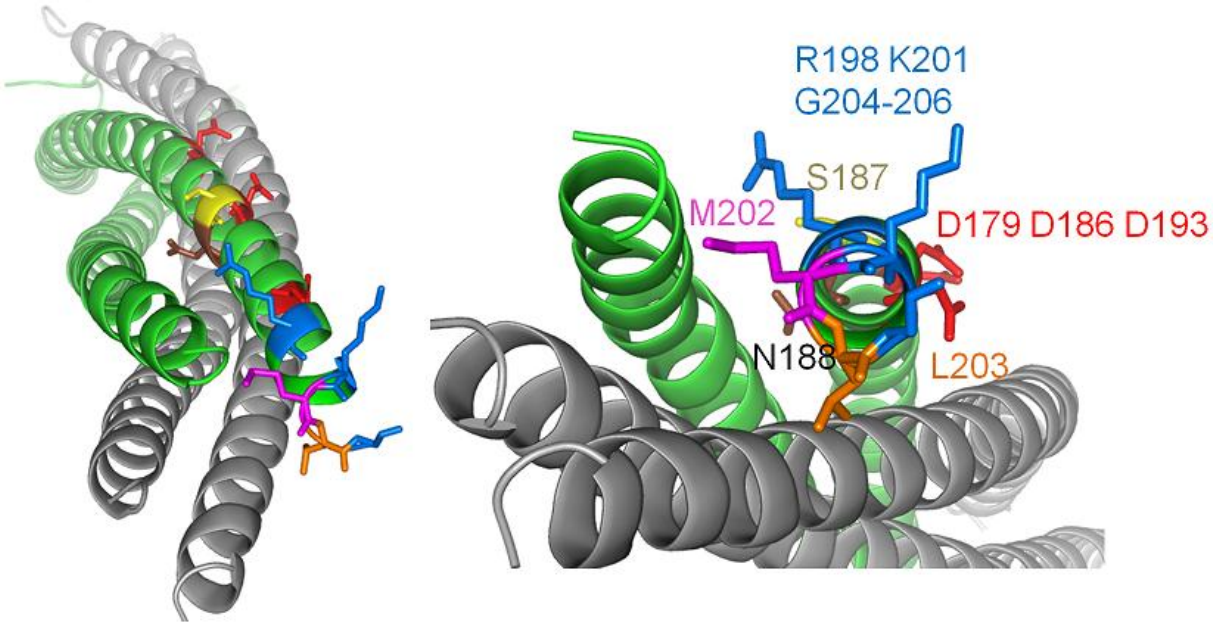

Figure 23: Functional significance of the C-terminus of SNAP25.

Left panel: 3-D crystal structure of ternary SNARE complex obtained through X-ray crystallography(PDB: 1sfc)[235] with relevant residues highlighted in different colors according to function. Right panel: Perspective through SN2 helix of SNAP25. Blue: residues implicated as being important for the Gβγ-SNARE interaction (residues S205 and G206 omitted from structure). Yellow residue S187 is phosphorylated by PKC to modulate exocytic events[151]. Brown residue N188 is important for SNARE complex interactions[256]. Residues R198 and K201 may also be important for Syt1-SNAP25 calcium-dependent binding. Red: residues implicated as being important for Syt1 calcium-dependent binding[245]. Magenta residue M202 is important for SNARE formation[257] and was shown to be important for the rapid phase of exocytosis in chromaffin cells[253]. Orange residue L203 is predicted to be involved in leucine zipper protein-protein interactions during the last stage of exocytosis[253,254]. Figure adapted from Zurawski Z, Rodriguez S, Hyde K, Alford S, Hamm HE. *Mol Pharmacol*. 2016 Jan;89(1):75-83.

The goal of these studies is to obtain a mutant with impaired Gβγ-SNARE interaction to evaluate its importance *in vivo*. The SNAP25Δ3 mutant is suitable to introduce into the endogenous SNAP25 transcript via current genome editing technologies such as the CRISPR/Cas9 system. One issue of concern is that none of the three individual residues in the extreme C-terminus of SNAP25 were identified as being important for binding Gβγ in our previous peptide mapping approach[244]. The Ala scanning approach may miss critical residues and is not optimal for identifying the importance of residues that bear structural similarities to alanine. It is apparent that mutating R198 and K201 to Ala is inadequate to disrupt the inhibitory effect of the lamprey serotonin receptor. Our results are consistent with previous studies indicating the importance of R198 and K201 as Gβγ binding residues: while the *in vitro* binding data shows a drop in potency and efficacy, the role of the 2E mutant on $G_{i/o}$-coupled GPCR-mediated inhibition of exocytosis in cells could not be studied due to the mutant not supporting exocytosis. Other possible mutants that could be considered are the R198E and K201E single mutants, since our data indicate that the 2E double mutant has extremely impaired Gβγ binding (Fig.19), as well as an impaired secretory phenotype. These single mutants have previously been shown to display an altered secretion phenotype with impaired release frequencies, slower release kinetics, and prolonged duration of the fusion pore[253,255].The R198Q single mutant also displayed this phenotype[255,257]potentially due to the partial negative charge on this mutant from resonance. Deficiencies identified in Syt1 C2AB calcium-independent or calcium-dependent binding in the GST-pull down assay for the charge-reversal R198E or K201E mutants may explain the results obtained by these groups. As a result, this makes the positively charged residues R198 and K201 unattractive candidates for our goal of mutagenesis of SNAP25 to decrease Gβγ binding in a transgenic animal. The SNAP25Δ3 mutant also leaves the key residues M202 and L203 intact, the former being shown as important for the rapid phase of exocytosis [257]and the latter being predicted as essential for leucine zipper-mediated protein-protein interactions late in exocytosis[253,257].

Prior studies conducted by our group have shown that removal of the C-terminus of SNAP25 by BoNT/A enable Syt1 to compete more effectively with Gβγ in the presence of Ca^{2+} ions[48,196,201]. SNAP25Δ9 was previously shown to have impaired calcium-dependent binding to Syt1 C2AB domains, which was also observed in our studies[82]. Tucker et al. performed reconstituted membrane fusion assays containing BoNT/A-treated SNAP25 and observed both a rightward shift in the calcium dependence and a reduction in fusion[225], even at very low levels of Ca^{2+}. Our results echo those obtained in reconstituted fusion assays, with a reduction in binding at 1 mM Ca^{2+}. Furthermore, they support cellular studies in which overexpression of the SNAP25Δ9 mutant in chromaffin cells led to slower single vesicle kinetics and reduced exocytosis[253]. Other existing data highlight the functional importance of Syt1 calcium-independent binding as a clamp for fusion[224]. Our results predict that the stimulatory effect of calcium-bound Syt1 on fusion would be reduced in a reconstituted fusion assay with vesicles containing t-SNAREs made with SNAP25 2E, and to a lesser extent SNAP25Δ3 or SNAP25Δ9. However, in cell-based studies, SNAP25Δ3 is able to support exocytosis similar to non-BoNT/E treated controls. The presence of key residues such as L203 may be required for this effect.

Peptide mapping approaches have demonstrated the importance of residues on SNAP25 on the SN2 helix located proximally to the N-terminus of the SNARE complex[244]. In that study, both the N-terminal binding sites and C-terminal binding sites were mutagenized. Selective mutagenesis of the N-terminal Gβγ binding site on SNAP25 has yet to be explored in an electrophysiological model. Two hypotheses can be envisioned as potential outcomes of this experiment: it may be possible that complete removal of the action of an inhibitory $Gi_{/o}$-coupled GPCR may only occur with disruption of both the N-terminal and C-terminal binding sites. The extent of inhibition of 5-HT receptor-mediated inhibition is greater with SNAP25 8A compared to SNAP25Δ3, consistent with this hypothesis. Another hypothesis is that N-terminal residues may be important for interaction with other proteins, for example, voltage-gated calcium channels. It has been shown that the interaction of Gβγ with voltage-gated calcium

channels is mediated by residues located near the N-terminus of the SNARE domain of syntaxin 1A[191]. Existing knowledge of the structure of formed ternary SNARE complexes suggests that these N-terminal residues on SNAP25 would be in close proximity to this region on Stx1A and may facilitate the binding of Gβγ to Stx1A for voltage-gated calcium-channel inhibition. Further studies are needed to confirm either or both of these hypotheses, however the effects of Gβγ at Ca^{2+} channels is likely to be synergistic to the inhibition of Ca^{2+} dependent Syt1 binding to the SNARE complex that we observe.

One limitation of our studies is the use of the lamprey, a non-mammalian organism. Several studies in mammalian synapses in this field have been conducted. We have previously shown that the serotonin 1B ($5\text{-}HT_{1b}$) receptor inhibits neurotransmission in rat CA1 hippocampal neurons through the interaction of Gβγ with the C-terminus of SNAP25[208]. This inhibition could be overcome via presynaptic injection of the neuron with BoNT/A, much like early studies in lamprey[200]. This mechanism of inhibition was found to not be universal across synapses, with other $G_{i/o}$-coupled GPCRs, such as the $GABA_B$ receptor, acting to inhibit exocytosis via the action of Gβγ on voltage-gated calcium channels. In lamprey, no inhibitory $G_{i/o}$-coupled GPCRs are known to inhibit release in this manner, potentially implying that the Gβγ-SNARE mechanism evolved earlier than the Gβγ-calcium channel mechanism by its presence in this primitive organism. In Delaney et al (2007), single fiber inputs from the nociceptive pontine parabrachial nucleus form glutamatergic synapses with central amygdala neurons. Inhibition of exocytosis at this synapse was shown to be mediated by the α_2 adrenergic receptor via the Gβγ-SNARE interaction[197]. Other mammalian studies include Zhang *et al*., (2011), where introduction of Gβγ-scavenging peptides into CA3 hippocampal terminals blocked group II mGluR-mediated presynaptic depression of release, and introduction of BoNT/A into Schaffer collateral CA1 synapses reduced induction of long-term depression[205]. These studies are both heavily reliant upon the introduction of Gβγ-scavening peptides and light-chain botulinum toxins to demonstrate the involvement of the Gβγ-SNARE interaction. Early studies with the Gβγ-SNARE interaction in lamprey utilized similar approaches [196,200],

and later featured the introduction of recombinant mutants of SNAP25[244] . Given the predictive value of the peptide experiments for mammalian studies, we would predict that the recombinant SNAP25 experiments would similarly extend to future mammalian studies, indicating predictive power for this approach. Beyond the pathophysiological consequences of partial disruption of the interaction of Gβγ with SNAP25, a whole-organism model bypasses many of the current limitations of existing models utilized to study this interaction. One such limitation is the dependence upon BoNT/E to remove endogenous SNAP25. The confounding effects of BoNT/E on the microarchitecture of the synapse will not be present in such a system, enabling study in a more physiologically relevant state.

CHAPTER IV

DISCOVERY AND DEVELOPMENT OF SMALL MOLECULE MODULATORS OF THE Gβγ-SNARE INTERACTION

Introduction

G protein coupled-receptors (GPCRs) are fundamental to the ability of organisms to transduce extracellular chemical signals into intracellular biochemical processes. These proteins, consisting of an N-terminal extracellular domain, seven transmembrane helices, and a C-terminal intracellular domain, are able to bind to and activate heterotrimeric G proteins. The heterotrimer G protein complex consists of the nucleotide-binding Gα subunit, and the heterodimeric Gβγ subunit, a constitutive heterodimer made of a 7-bladed B-propller Gβ subunit and a helical Gγ subunit that is anchored to the membrane through a prenyl moiety at its C-terminus.[1] The binding of an agonist to a given GPCR stabilizes the active state, to which heterotrimeric G protein can bind.[1] This binding results in the opening of the Gα subunit's nucleotide binding pocket and the exchange of bound GDP for GTP. The binding of GTP to Gα changes its conformation, resulting in a dissociation of Gα and Gβγ subunits, which are then capable of activating their respective effectors. Gβγ has been shown to interact with a wide variety of effectors via solvent-exposed residues on the Gα-binding surface of the protein[40,44,155,258-260]. These effectors include G-protein-coupled inwardly rectifying potassium (GIRK) channels, voltage-gated calcium channels, phospholipase C, the SNARE proteins SNAP-25, syntaxin, and VAMP2, along with many others[44,142,258,259,261,262]. Gβγ-mediated regulation of these effectors has been shown to play an important role in many physiological processes, including the role of the M2 receptor in decreasing contractility in atrial myocytes through the induction of inwardly rectifying K^+ currents[154] and the α_{2a} adrenergic receptor-mediated inhibition of insulin granule release in the beta cells of pancreatic islets [153,263] This process is thought to be mediated through the interaction of Gβγ with SNARE proteins [153], a well-studied

inhibitory mechanism that has been shown to occur in a wide variety of secretory cells, including neurons [196], and chromaffin cells[202]. Previously, we have determined that Gβγ inhibits exocytosis downstream of calcium release[48,196,200,201], and that this effect is mediated through direct interaction with SNARE proteins[48,201]. It has been determined by our group that the C-terminus of SNAP-25 plays an important role in the interaction between Gβγ and SNAP-25[200,201,244]. Selective mutagenesis of the Gβγ-binding site upon SNAP-25 abolished $G_{i/o}$-coupled GPCR-mediated inhibition of exocytosis in lamprey giant axons, without disrupting overall neurotransmitter release[244]. Gβγ has also been shown to inhibit exocytosis via binding to and inhibiting calcium currents from voltage-gated calcium channels, such as somatostatin-mediated inhibition of insulin release in pancreatic beta cells[171,264]. The coupling of each Gβγ subunit to its effectors within a signaling pathway is mediated by a detailed microarchitecture. 5-HT inhibits neurotransmitter release in CA1-subicular synapses via activation and subsequent interaction of Gβγ with SNARE proteins, while GABA inhibits neurotransmitter release through the interaction of Gβγ with voltage-gated calcium channels[208] , potentially allowing small molecule modulators of Gβγ signaling to take effect only in certain cell types and signaling pathways. Given the challenges of identifying which effector(s) are responsible for each phenomenon, the development of selective inhibitors of each Gβγ-effector interaction would be highly useful.

The targeting of Gβγ-effector interactions in several cell types has been shown to be a potential strategy for future drug development[265-267]. The first small molecule modulators of Gβγ signaling were the fluorescein derivatives M119 and gallein [268], identified by a screen for molecules that could compete for binding sites on Gβγ with the known Gβγ-binding peptide SIGK. These compounds were shown to inhibit Gβγ-phospholipase C beta (PLCβ) and Gβγ-PI3k interactions, without disrupting Gβγ-GIRK channel or Gβγ-calcium channel interactions[265]. These existing modulators of Gβγ-effector interactions have a number of undesirable features that would limit their ability to be optimized for clinical development, including hydrophobicity and the challenge of synthesizing derivatives of such a

complicated structure. Furthermore, while these molecules have been shown to disrupt the ability of Gβγ to interact with effectors such as phosphoinositide-3-kinase, they are inactive towards the Gβγ-SNARE (data not shown) and Gβγ-GIRK interactions[265]. Previously, label-free screening was utilized to identify low-potency inhibitors of the Gβγ-SNARE interaction[269]. Structures of previously identified Gβγ-modulatory compounds are listed in Table 3**.** With this in mind, we set out to identify new chemotypes for modulation of the Gβγ-SNARE interaction.

Methods

Small molecule chemical synthesis. Small molecule chemical synthesis was carried out in collaboration with the labs of Craig Lindsley, Ph.D, and Shaun Stauffer, Ph.D.

Plasmids. The open reading frame for SNAP-25 and residues 96-421 of rat Syt1 were subcloned into the glutathione-S-transferase (GST) fusion vector pGEX-6p-1 (GE Healthcare) for expression in bacteria. The open reading frames for Gβ1 and 6His-Gγ2 were subcloned into the baculovirus vector pVL1392 (Invitrogen). Plasmid sequences were verified to be correct with Sanger sequencing utilizing BigDye Terminator dyes and resolved on an ABI 3730 DNA Analyzer (Applied Biosystems).

Protein purification. Recombinant bacterially-expressed glutathione-S-transferase (GST) fusion proteins were expressed in *Escherichia coli* strain Rosetta 2 (EMD Biosciences). Protein expression was induced with 100 μM isopropyl β-D-1-thiogalactopyranoside for 16 h at room temperature. Bacterial cultures were pelleted and washed once with phosphate-buffered saline before undergoing resuspension in lysis buffer (25 mM potassium 4-(2-hydroxyethyl)-1-piperazine ethanesulfonate (HEPES-KOH) pH 8.0, 150 mM KCl, 5 mM 2-mercaptoethanol, 10.66 μM leupeptin, 1.536 μM aprotenin, 959 nM pepstatin, 200μM phenylmethylsulfonyl fluoride, and 1 mM ethylenediaminetetracetic acid (EDTA)). For Syt1,

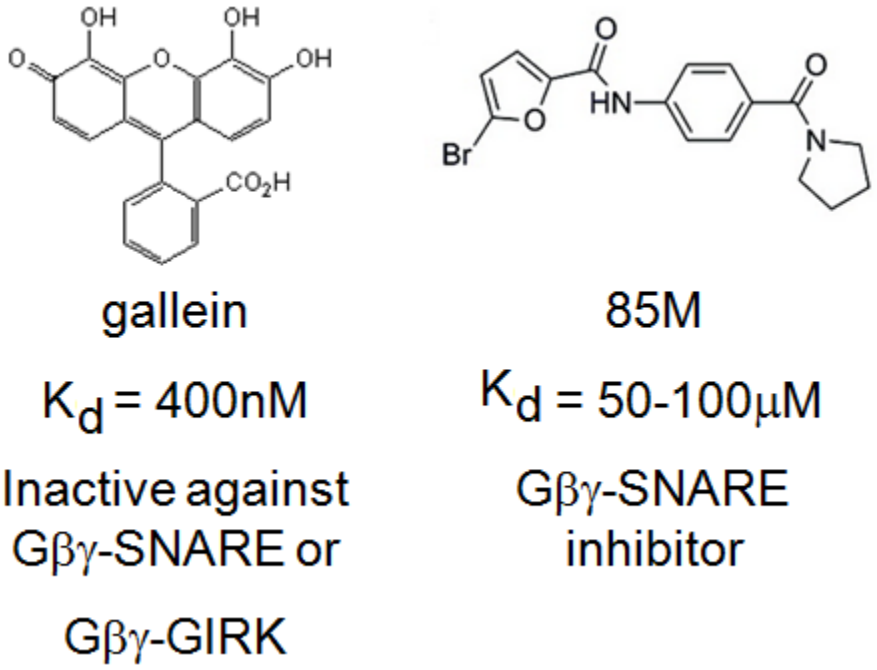

Table 3: Existing small molecule Gβγ-effector inhibitors.

Listed are the chemical structures and K_d values for two previously published inhibitors of Gβγ-effector interactions.

DNAse I(100 units/mL) and RNAse A (100 μg/mL) were added to the resuspension buffer to remove contaminating nucleic acids. Cells were lysed utilizing a sonic dismembranator at 4°C for 5 min. Lysates were cleared via ultracentrifugation at 26,000 x g for 20 min in a TI-70 rotor (Beckman Coulter). GST-SNAP-25 and GST-Syt1 fusion proteins were purified from cleared lysates by affinity chromatography on GE Sepharose 4 FastFlow (GE Healthcare). Lysates were allowed to bind to resin overnight before being washed once with lysis buffer containing 1% Triton X-100 (Dow Chemical). The resin was then washed once with elution buffer (25 mM HEPES-KOH pH 8.0, 150 mM KCl, 5 mM 2-mercaptoethanol, 0.5% n-octyl glucoside, 1 mM EDTA, 10% glycerol). SNAP25 proteins were eluted from GST-fusion proteins immobilized on resin via proteolytic cleavage with a GST-tagged fusion of rhinovirus 3C protease. After elution, SNAP25 protein was reacted with EZ-Link sulfo-NHS-SS-biotin (Pierce) at a 20:1 ratio for 30m in elution buffer lacking 2-mercaptoethanol. Excess biotin was removed via dialysis in elution buffer. Protein concentrations were determined with a Bradford assay kit (Pierce) and purity was verified by SDS-PAGE analysis. Biotinylation was performed at 25C for 30 mwith a 20-fold excess of EZ-Link Sulfo-NHS-SS Biotin (Thermo), followed by overnight dialysis of excess biotinylation reagent in elution buffer lacking 2-mercaptoethanol. Biotinyation of the substrate was verified utilizing a HABA assay kit (Pierce).

Alphascreen protein-protein interaction assays. Solutions of 100 nM SNAP25 and 212 nM $G\beta_1\gamma_2$ were prepared in assay buffer (20 mM HEPES pH7.0, 10 mM NaCl, 40 mM KCl, 0.5% glycerol, and 0.01% triton-X-100. Alphascreen Histidine Detection Kit donor and acceptor beads (PerkinElmer) were separately diluted 1:100 in assay buffer. These solutions were then plated in 384-well plates (#784201, Greiner). Compounds were dissolved in DMSO to a concentration of 10mM and plated in 384-well OptiPlates (PerkinElmer) using a Labcyte Echo 555 Omics (Labcyte) acoustic liquid handler. A Velocity Bravo liquid handler (Agilent) was utilized to add 4μL of the $G\beta_1\gamma_2$ solution to the OptiPlate. Compounds were permitted to bind to the $G\beta_1\gamma_2$ for 5m. Afterwards, 1μL of the SNAP25 solution was added to the plate and the mixture was incubated for an additional 5m. At that point, 10μL of the diluted

acceptor beads was added to the plate, and the mixture incubated for 30m at room temperature. Then, 10μL of the diluted donor beads was added to the plate. The plate was centrifuged at low RPM values to remove bubbles and the mixture incubated for 60m at room temperature. Plates were read on an EnSpire plate reader (PerkinElmer).

Thallium flux assays. HEK cells expressing the metabotropic glutamate receptor 8 and GIRK1/GIRK2 were plated on 384-well black amine-coated plates (BD Biosciences) to 90% confluence. The next day, cells were washed in Hank's balanced salt solution (HBSS) (1.26 mM $CaCl_2$, .492 mM $MgCl_2$, .407 mM $MgSO_4$, 5.33 mM KCl, .411 mM KH_2PO_4, 137.9 mM NaCl, .3358 mM Na_2HPO_4, 5.5 mM glucose, 20 mM HEPES pH 7.3). Cells were loaded with the dye Thallos-1-AM for 1 hour in HBSS. Compounds were added to 384-well plates using a Labcyte Echo 555 Omics (Labcyte) and dissolved in HBSS. An EC80 concentration of monosodium glutamate was made in thallium stimulus buffer (125 mM $NaHCO_3$, 12 mM Tl_2SO_4, 1 mM $MgSO_4$, 1.8 mM $CaSO_4$, 5 mM glucose, and 10 mM HEPES pH 7.3) and added to 384-well plates. Compounds were added to cells for 5 minutes before stimulation with glutamate in thallium stimulus buffer. Fluorescence measurements were continuously recorded using an excitation wavelength of 480nm and an emission wavelength of 540nm on a Fluorescent Drug Screening System (Hamamatsu).

Ancillary pharmacology studies. Compounds were sent to Eurofins Panlabs for radioligand binding assays against a panel of 70 G-protein coupled receptors, ion channels, and transporters.

Electrophysiology studies. Experiments were performed on isolated spinal cords or spinal cords and brainstems of lampreys (*Petromyzon marinus*). The animals were anesthetized with tricaine methanesulfonate (100 mg/l; Sigma-Aldrich) and sacrificed by decapitation, and the spinal cord was dissected in a ice-cold saline solution (Ringer's) of the following composition: 100 mM NaCl, 2.1 mM KCl, 2.6 mM $CaCl_2$, 1.8 mM $MgCl_2$, 4 mM glucose, and 5 mM HEPES, adjusted to a pH of 7.60. Procedures conformed to institutional guidelines (University of Illinois at Chicago Animal Care

Committee). Paired cell recordings were made between reticulospinal axons and neurons of the spinal ventral horn. Axons of reticulospinal neurons were recorded with sharp microelectrodes containing 1 M KCl and 5 mM HEPES buffered to pH 7.2 with KOH. Compounds were supplied at 10mM in 100% DMSO. Electrode impedances ranged from 20 to 50 MΩ. Postsynaptic neurons were recorded with a patch clamp in voltage-clamp conditions. Patch electrodes contained 102.5 mM cesium methane sulfonate, 1 mM NaCl, 1 mM $MgCl_2$, 5 mM EGTA, and 5 mM HEPES, pH adjusted to 7.2 with CsOH.

Static incubation. Static incubation was performed in part by the Vanderbilt Islet Procurement and Analysis Core. Subsequent to isolation, islets were incubated for a minimum of two hours in Dulbecco's modified Eagle medium containing 10 mM HEPES-NaOH, 500 μM $CaCl_2$, and 0.5% bovine serum albumin at a glucose concentration of 5.6 mM. 10 islets were transferred on ice to 1.5mL low retention microfuge tubes (Fisher Scientific) in 150μL of Dulbecco's modified Eagle medium containing 10 mM HEPES-NaOH, 500 μM $CaCl_2$, and 0.5% bovine serum albumin containing variable concentrations of glucose, DMSO, epinephrine, and Gβγ-SNARE inhibitors. Islets were incubated at 37 C for 45 min followed by media removal. Islets were then recovered and total insulin was extracted using sonication in acidified ethanol. Insulin content within each fraction was analyzed via radioimmunoassay (Millipore).

Results

To identify putative small-molecule inhibitors of the interaction between Gβγ and SNAP25, we developed a high-throughput assay carried out in 384-well plates. Initial approaches utilized label-free refractive index spectroscopy with the Corning EPIC technology in which purified bovine $G\beta_1\gamma_1$ was immobilized upon glass via EDC-NHS coupling and the attachment of purified recombinant t-SNAREs consisting of Stx1A and SNAP25 was observed continuously in solution[269]. This method was ultimately deemed to be unsuitable for compound screening due to high non-specific binding, with a lack of specific signal for Gβγ-t-SNARE relative to all other proteins tested. Bio-layer interferometry, in which minute changes in the thickness of immobilized layers of biomolecules upon a surface cause perturbations in the

interference patterns generated by white light, was a second protein-protein interaction technique that was also deemed unsuitable due to non-specific binding. The Alphascreen solution-based assay technology offered low non-specific binding relative to other commercially available assay systems. We used AlphaScreen technology (Perkin-Elmer) to screen the interaction between immobilized Gβγ and SNAP25 (assay described in Chapter III). The Amplified Luminescent Proximity Homogeneous Assay (Alpha) technology is a highly-sensitive assay technology conducive to screening of small molecule modulators of protein-protein interactions. In this assay, recombinant SNAP25 biotinylated on residues containing primary amines to a ratio of 1 biotin molecule per SNAP25 protein forms a complex with a His-tagged $G\beta_1\gamma_2$ subunit. These complexes are captured on Ni-NTA-conjugated acceptor beads. The protein-acceptor bead complexes are then captured on streptavidin-coated donor beads and permitted to equilibrate in solution. Upon irradiation with 680nm light, dye molecules attached to the donor beads generate singlet oxygen, which is capable of traveling up to 200 nm in solution and striking an acceptor bead. Acceptor beads are conjugated to molecules that will generate 520-620 nm light, which is then measured by the plate reader. If the SNAP25 is unable to form a complex with $G\beta_1\gamma_2$, few acceptor beads are within 200 nm and minimal 620 nm light is generated. The Alphascreen assay was readily amenable to high-throughput screening and natively exists in a 384-well format. We screened several libraries consisting of approximately 4000 compounds, including a 2000-compound library of putative protein-protein interaction inhibitors. Hits producing more than fivefold inhibition of the interaction were screened for their ability to disrupt the Gβγ-SNAP25 interaction in a single-point system, with each compound tested at 20 μM. An example of one plate from the HTS screen is shown in Fig. 24A. An Alphascreen assay in which putative hits were counterscreened for their ability to disrupt luminescence signals from a biotinylated His-tagged peptide was utilized to distinguish Gβγ-SNAP25 interaction

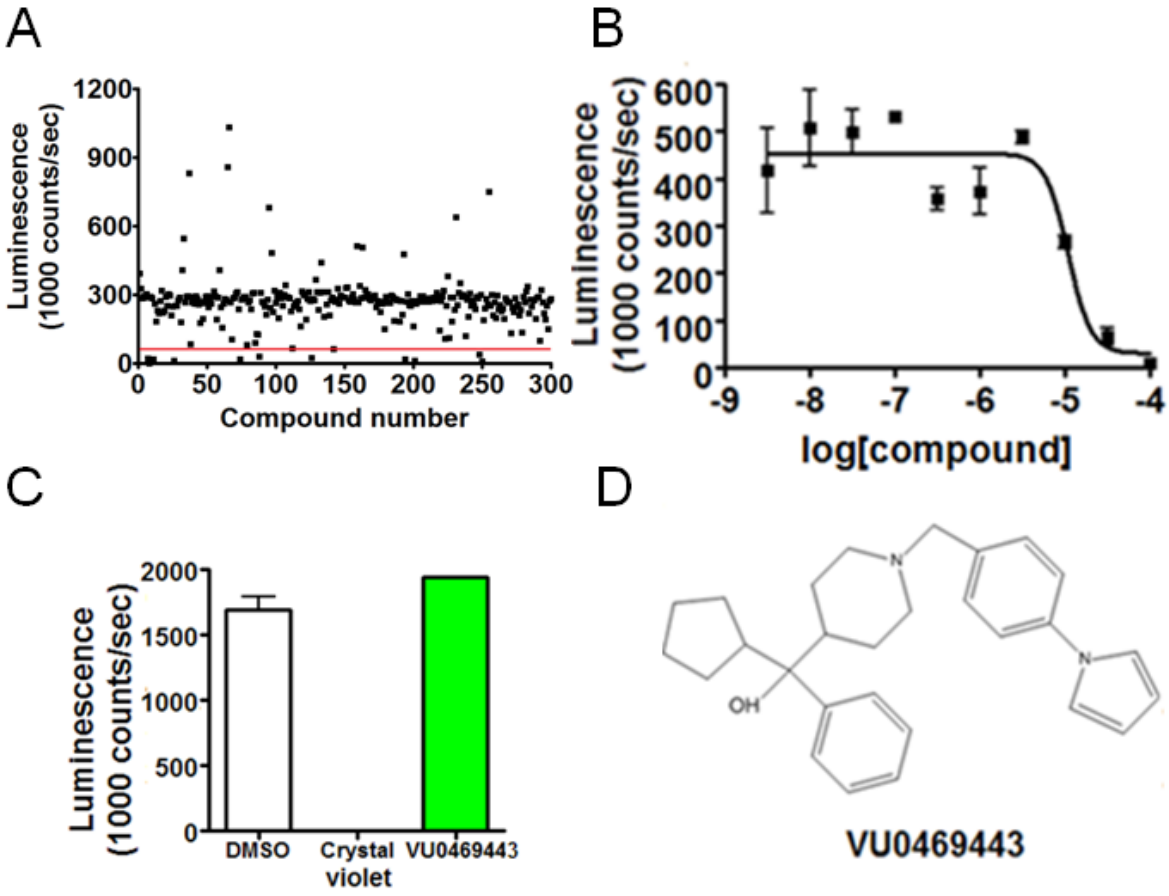

Figure 24: High-throughput screening of small molecule modulators of the Gβγ-SNAP25 interaction.

A) Example plate from the high throughput Alphascreen protein-protein interaction assay. Each dot represents one compound: the red line indicates a threshold below which compounds of interest were identified. B) Alphascreen competition binding assay with a fixed concentration of Gβγ and SNAP25 and a series of concentrations of VU0469443. C) Alphascreen counterscreen with biotinylated His-tag peptide. DMSO is a negative control, while the blue/purple light-absorbing crystal violet is a positive control for assay inhibition. D) Chemical structure of hit VU0469443.

inhibitors from compounds that produced assay interference (Fig. 24C). Crystal violet, a dye that absorbs red and orange light, was able to inhibit the counterscreen assay in a concentration-dependent manner with high potency. From our screen, a Gβγ-SNAP25 interaction inhibitor, VU0469443, was identified. (Fig. 24D) VU0469443 is a moderate (mw 414.58) molecular weight inhibitor containing a 4-carbinol N-benzyl piperidine motif. VU0469443 inhibits the Gβγ-SNARE interaction in a concentration-dependent manner with an IC_{50} of 11 μM (Fig. 24B). In tandem with the Lindsley lab, we utilized an iterative parallel synthesis protocol combining solution-phase parallel synthesis and microwave-assisted organic synthesis to generate a series of structure-activity relationships focused upon the pyrrole moiety of VU0469443.

We then sought to determine whether it was possible to generate compounds that were selective for one effector versus the other. Effector specificity for small molecule inhibitors of Gβγ has been previously documented[270]. To do this, we generated a series of analogues of VU0469443, focusing on alternatives to the 4-carbinol N-benzyl moiety, utilizing a synthesis in which pyrroles underwent reductive amination with a series of aldehydes in the presence of sodium triacetoxyborohydride in DCE We were able to generate a series of inhibitors for each interaction, including the hydroxypropyl derivative VU0476078 was sixfold more potent for Gβγ-SNAP25, with an IC_{50} of 1.8 μM in the SNAP25 assay. Other analogues were less potent, such as the decahydroquinoline-containing DK8, which was 2.8-fold less potent. (Fig. 25) These compounds show good ligand efficiency and are highly amenable to future derivatization. We then set out to examine whether VU0469443 was specific for other effectors of Gβγ, specifically GIRK channels, as these channels are amongst the best-studied and most physiologically relevant effectors of Gβγ.

We utilized thallium flux assays in a cell line containing overexpressed GIRK1 and GIRK2 along with the metabotropic glutamate receptor 8 as a $G_{i/o}$-coupled GPCR to activate Gβγ to identify potential inhibitors of the Gβγ-GIRK interaction. (Fig. 26A) Glutamate was able to activate GIRK1/2 in a

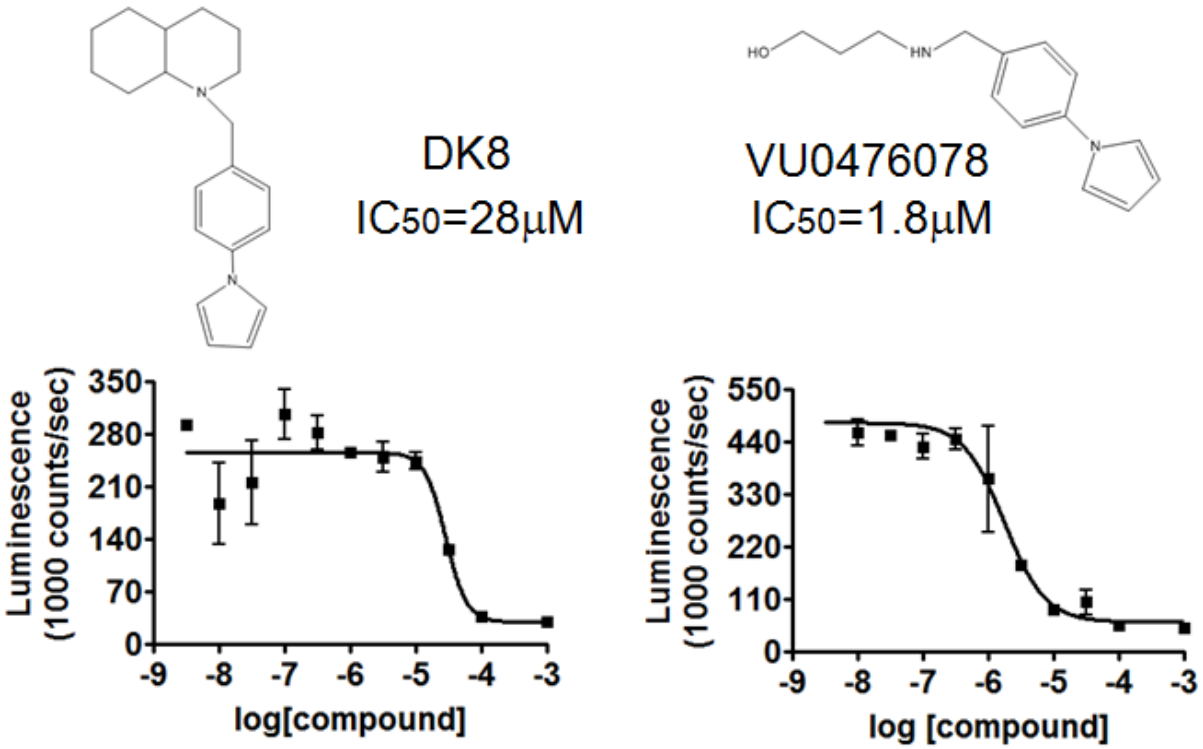

Figure 25: Structure-activity relationships yield compounds with variable ability to inhibit the Gβγ-SNAP25 interaction.

Upper panels: Chemical structures of compounds derived from the parent compound VU0469443. Lower panels: Alphascreen competition binding data for the selected derivatives DK8 and VU0476078. For the purposes of accurate IC_{50} estimation, an additional minima point is added at 1mM: actual concentrations tested end at 100μM.

concentration-dependent manner (Fig. 26B), with an EC_{50} of 8 μM. VU0469443 inhibited glutamate-evoked thallium fluxes at an EC_{80} concentration of glutamate in a concentration-dependent manner (Fig. 26C), with an IC_{50} of 4 μM. Compared to its 11 μM potency for the Gβγ-SNAP25 interaction, VU0469443 is roughly twofold selective for the Gβγ-GIRK interaction. DK8 was much more potent at Gβγ-GIRK than Gβγ-SNARE, with an IC_{50} of 2.2 μM. Both VU0469443 and the decahydroquinoline-containing analogue DK8 were selective for Gβγ-GIRK over Gβγ-SNARE in this assay, potentially implying that selective inhibitors could be developed for each interaction. However, VU0476078 was not able to generate meaningful inhibition of the Gβγ-GIRK interaction in this assay at the highest concentrations tested, implying that selective Gβγ-effector inhibitors, particularly Gβγ-SNARE, can be developed.

To examine the ancillary activity of VU0476078, we utilized a panel of assays (Eurofins Panlabs) measuring inhibition of radioligand binding at cell surface receptors and ion channels. At 10 μM, VU0476078 showed no inhibitory activity at any of the receptors or ion channels tested (Table 4) with the exception of the sigma-1 receptor. In this assay, VU0476078 was able to produce an 89% inhibition of [3H]haloperidol binding to human sigma-1 receptors in a preparation isolated from Jurkat T cells. The affinity of VU0476078 for the sigma-1 receptor may be reduced by further structure-activity studies. Finally, to demonstrate that VU0476078 inhibits Gβγ-SNAP25 interactions in an *ex vivo* system, treatment of secretory cells with VU0476078 should disrupt the inhibitory effect of Gβγ upon vesicle release. To test this hypothesis, we isolated neurons from the lamprey giant synapse and applied serotonin via the bath to inhibit vesicle release in the presence or absence of VU0476078 [48,196].

To evoke a synaptic response, presynaptic action potentials were induced with brief depolarizing current pulses (2 ms, 1-3 nA). Once 10 responses were obtained, VU0476078 was applied to the bath and excitatory postsynaptic currents (EPSCs) were measured once more. (Fig. 27A) Serotonin significantly reduced EPSC amplitudes to 25%+/-10 of control amplitudes in the presence of 1 μM VU0476078, but

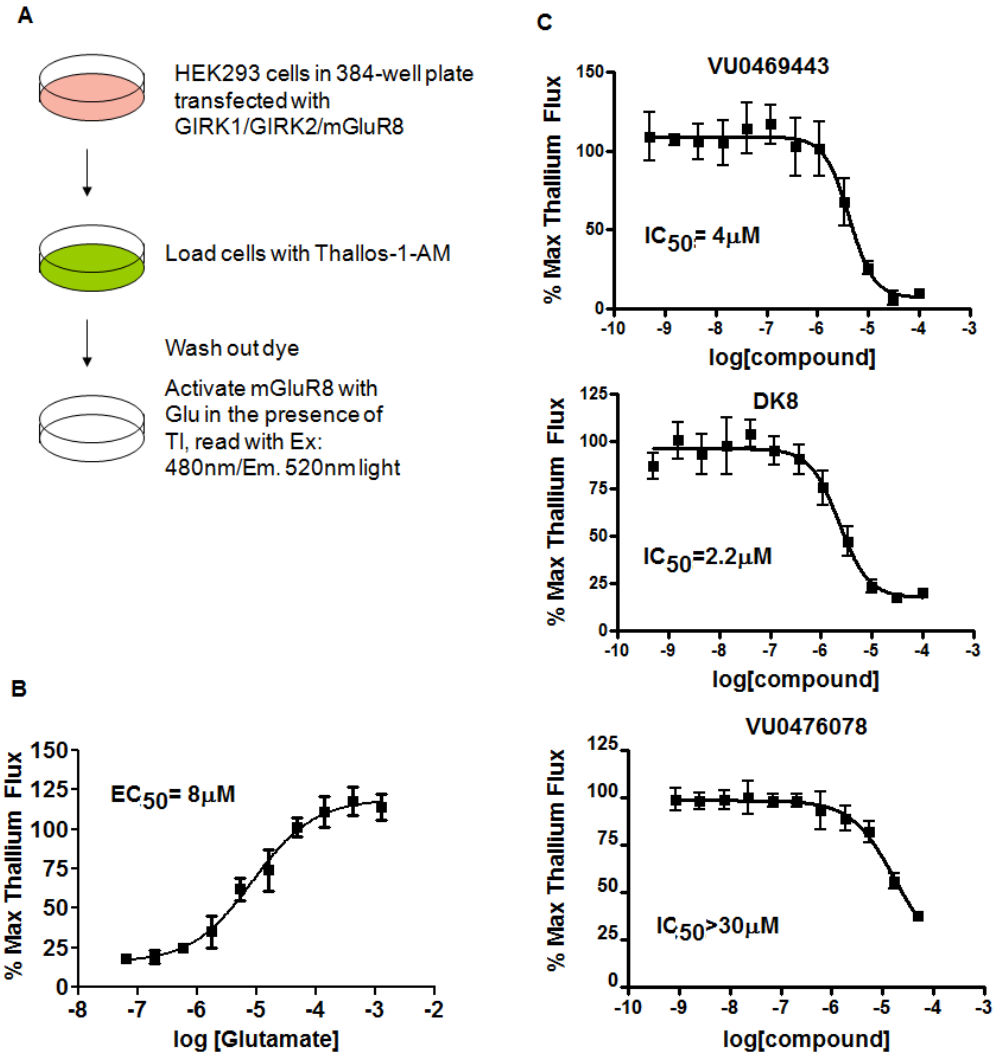

Figure 26: The ability of Gβγ-SNARE inhibitors to inhibit the Gβγ-GIRK interaction in mammalian cells.

A): Diagram of assay principle. B: Thallium flux fluorescence data showing a concentration-dependent increase in fluorescence subsequent to glutamate addition, representative of GIRK channel activation by Gβγ. After dye washout in the presence of Tl+, a baseline fluorescence is recorded, followed by continuous recording of increases in Thallos-1 fluoresence over time for 5m. Maxima from these recordings are then analyzed. C: Concentration-response curves for a fixed EC_{80} concentration of glutamate and a variable concentration of Gβγ inhibitor. Data presented as mean+ SD. For the purposes of accurate IC_{50} estimation, an additional minima point is added at 100μM: actual concentrations tested end at 30μM.

Target	Species	% Inhibition	Target	Species	% Inhibition
Adenosine A1	human	-6	Histamine H3	human	12
Adenosine A2A	human	-9	Imidazoline I2, Central	rat	10
Adenosine A3	human	10	Interleukin IL-1	mouse	10
Adrenergic A1A	rat	16	Leukotriene, Cysteinyl, CysLT1	human	6
Adrenergic A1B	rat	2	Melatonin MT1	human	-10
Adrenergic A1D	human	8	Muscarinic M1	human	12
Adrenergic A2A	human	20	Muscarinic M2	human	-4
Adrenergic B1	human	3	Muscarinic M3	human	5
Adrenergic B2	human	2	Neuropeptide Y Y1	human	6
Androgen (Testosterone)	human	-12	Neuropeptide Y Y2	human	5
Bradykinin B1	human	14	Nicotinic Acetylcholine	human	10
Bradykinin B2	human	5	Nicotinic Acetylcholine A1, Bungarotoxin	human	-3
Calcium Channel, L-Type, Benzothiazepine	rat	11	Opiate, D1	human	4
Calcium Channel, L-Type, Dihydropyridine	rat	4	Opiate K	human	7
Calcium Channel, N-Type	rat	-2	Opiate M	human	-8
Cannabinoid CB1	human	-1	Phorbol Ester	mouse	-1
Dopamine D1	human	-1	Platelet Activating Factor (PAF)	human	11
Dopamine D2S	human	-12	Potassium Channel, KATP	human	4
Dopamine D3	human	21	Potassium Channel, hERG	human	8
Dopamine D4.2	human	4	Prostanoid EP4	human	24
Endothelin ETA	human	3	Purinergic P2X	rabbit	-14
Endothelin ETB	human	2	Purinergic P2Y	rat	-18
Epidermal Growth Factor (EGF)	human	11	Rolipram	rat	9
Estrogen ERA	human	5	Serotonin 5-HT1A	human	8
GABAA, Flunitrazepam, Central	rat	-12	Serotonin 5-HT2B	human	11
GABAA, Muscimol, Central	rat	1	Serotonin 5-HT3	human	7
GABAB1A	human	-5	Sigma S1	human	89
Glucocorticoid	human	15	Sodium Channel, Site 2	rat	11
Glutamate, Kainate	rat	1	Tachykinin NK1	human	-5
Glutamate, NMDA, Agonism	rat	12	Thyroid Hormone	rat	3
Glutamate, NMDA, Glycine	rat	11	Transporter, Dopamine	human	24
Glutamate, NMDA, Phencyclidine	rat	-9	Transporter, GABA	rat	0
Histamine H1	human	7	Transporter, Norepinephrine	human	5
Histamine H2	human	-1	Transporter, Serotonin	human	17

Table 4: Ancillary pharmacology of the Gβγ-SNARE inhibitor VU0476078.

This table includes a list of every ligand binding assay performed on VU0476078 by the Eurofins company. Included is the molecular target, the species from which the receptor, transporter, or ion channel originates, and the percentage of inhibition or displacement of endogenous ligand detected at 10μM.

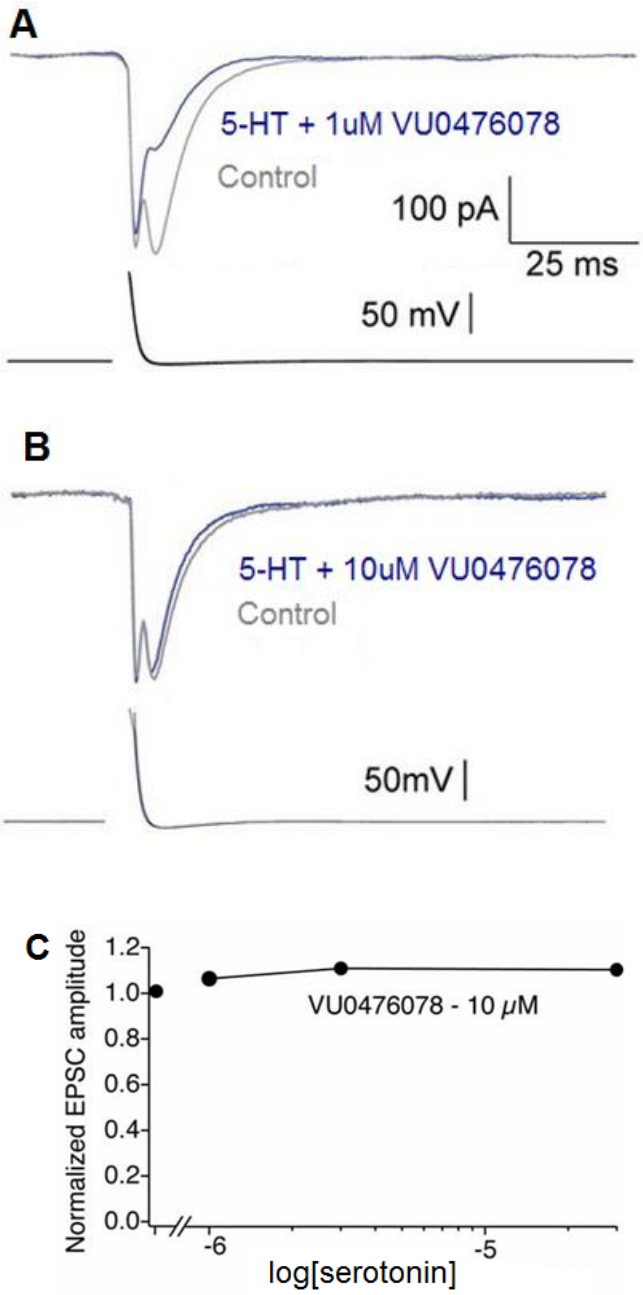

Figure 27: The ability of Gβγ-SNARE inhibitors to inhibit $G_{i/o}$-coupled GPCR activity in neurons.

A): Recording of excitatory postsynaptic currents taken from paired recordings taken from lamprey reticulospinal axons and neurons of the spinal ventral horn in the presence of 1μM VU0476078 applied to the bath. Application of 1μM 5-HT is still able to inhibit EPSC amplitudes to 25 +/- 10% of control amplitudes. B) Example trace taken from conditions in which 10μM VU0476078 was applied to the bath. C: Concentration-response curve displaying normalized EPSC amplitude as a function of 5-HT concentration. 5-HT is unable to inhibit EPSC amplitudes at all concentrations tested (1μM condition shown in panels A and B). Presynaptic action potentials shown below EPSCs.

no reduction in EPSC amplitude was observed at 10 μM VU0476078. (Fig. 27B) Taken with the negligible effects of VU0476078 upon serotonin receptors in Table 4, this data strongly implies that VU0476078 exhibits its interfering effect upon the action of the lamprey serotonin receptor by inhibiting Gβγ-SNAP25 interactions. Next, to determine whether putative Gβγ-SNAP25 inhibitors could alter physiological processes in which Gβγ-SNAP25 interactions were implicated, we measured their ability to modulate insulin secretion in intact islets of Langerhans isolated from the pancreas of 8-week old female C57BL6/J mice. Previously, the interaction of Gβγ with SNARE proteins, including SNAP25, was shown to mediate the inhibitory effect of the α_{2a} adrenoreceptor upon insulin secretion[153]. We conducted static insulin secretion assay in which high (16.7 mM) glucose-stimulated insulin secretion is measured in the presence or absence of 50uM VU0476078, along with 1 μM epinephrine. VU0476078 enhanced glucose-stimulated insulin secretion by 56% and partially blocked epinephrine-mediated inhibition. (Fig. 28A) Furthermore, VU0476078 enhanced insulin release in the presence of a low dose of the ATP-sensitive K^+ channel blocker tolbutamide, but not in the absence of tolbutamide (Fig. 28B). Together, this data suggests that the Gβγ-SNAP25 modulator VU0476078 inhibits Gβγ-SNAP25 interactions in the islet, and our overall hypothesis of Gβγ-SNARE interactions playing a key mechanistic role in the GPCR-mediated inhibition of glucose-stimulated insulin release.

While VU0476078 showed initial promise, DMPK data indicated an instability in human plasma (data not shown). Batch variability was also an issue, with an inability to generate a consistently active batch of the compound being troubling. For these reasons, we decided to look for alternatives for lead compounds. Of the compounds identified in the screen, two compounds, VU0451223 and VU0451070, were the most exciting, with an IC_{50} of 6.4 and 4.6 μM in the primary assay. (Fig. 29A) VU0451223 was able to completely inhibit the Gβγ-SNAP25 interaction, while displaying submaximal inhibition in the counterscreen at the highest concentration tested. VU0451070 was able to fully inhibit mGluR8 activation of GIRK only at the highest concentration tested (30 μM, data not shown). The compound shared structural characteristics with known Akt inhibitors and was a high molecular weight (520.8 Da),

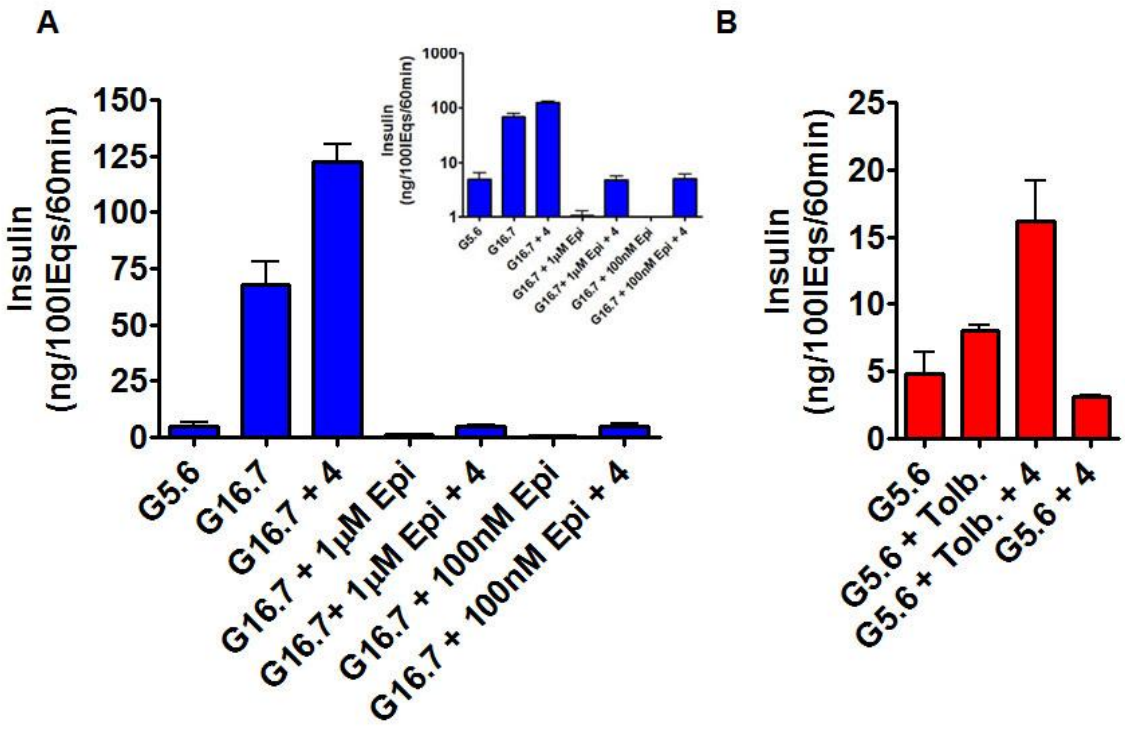

Figure 28. Gβγ-SNARE inhibitor VU0476078 enhances glucose-stimulated, but not basal, insulin secretion in mouse islets.

Islets were isolated from 8-week female C57BL/J mice and cultured overnight at 5.6mM glucose before being exposed to 16.7mM glucose in the presence or absence of two concentrations of epinephrine(epi)- 1μM or 100nM- with or without 50μM VU0476078 (abbreviated to 4 in this figure). Insulin secretion measured via RIA. A) VU0476078 enhances glucose-stimulated insulin secretion and partially reverses inhibition of GSIS by low doses of epi. Inset shows the same data but on a log scale to show the reversal by VU0476078 more clearly. There is a 4-fold reversal at 1μM epi and a 6-fold reversal at 100nM epi. B) VU0476078 enhances insulin secretion in the presence of low dose (15μM) tolbutamide. Tolbutamide enhances insulin secretion even at basal glucose, while VU0476078 does not.

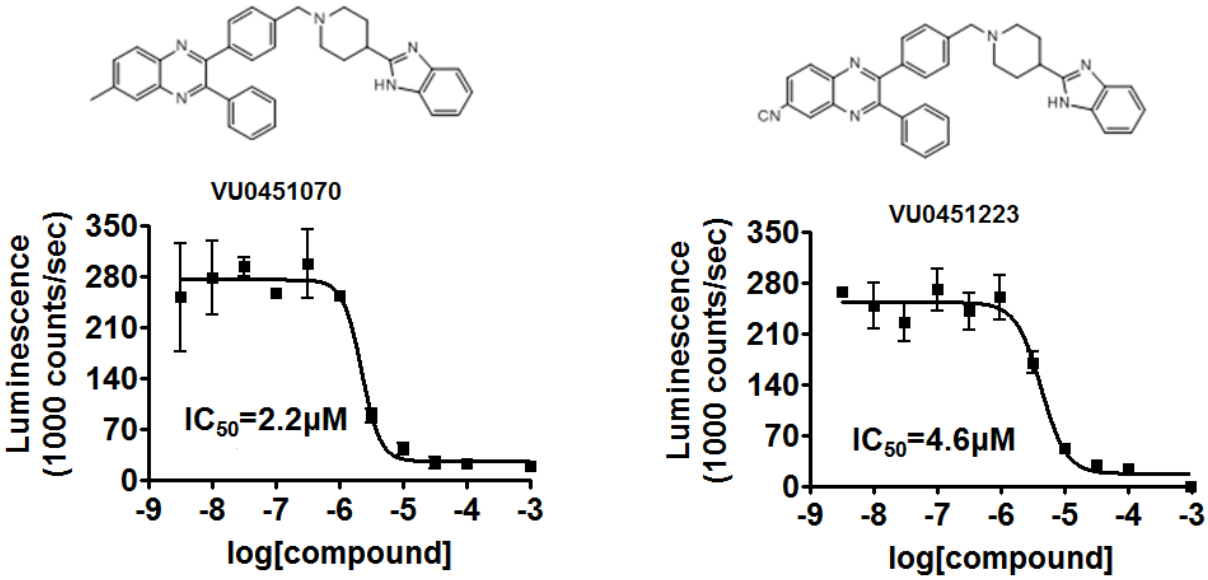

Figure 29. Gβγ-SNARE inhibitors VU0451223 and VU0451070.

Upper panels: Chemical structures of the two related "hit" compounds taken from the library of putative protein-protein interaction modulators, VU0451223 and VU0451070. Lower panels: Alphascreen competition binding curves for each compound. For the purposes of accurate IC_{50} estimation, an additional minima point is added at 1mM: actual concentrations tested end at 100μM.

so we set out to conduct minimum pharmacophore studies to reduce its molecular weight. A series of truncations of the VU0451223 chemotype were developed and tested in the Gβγ-SNAP25 primary assay The most promising compounds were the isoindolinone VU0657640. The compound had potency very similar to VU0451223 at 8 μM , but was significantly smaller (433.5 Da). Activity was lost for compounds containing a 3-hydroxymethylpiperidine tail group such as CH-E-14 or a 3,5-dimethylmorpholine such as CH-E-15. The 4-phenyl-4-cyanopiperidine tail group (CH-E-13) was also not a good inhibitor of the Gβγ-SNAP25 interaction. In contrast, the 4-(4-bromophenyl)piperidinol CH-E-17 was potent, despite the high molecular weight. (Fig.30) Our current structure-activity relationship studies are focused around derivatization of each moiety of VU0657640. Potential areas for derivatization on VU0657640 involve the two aromatic rings adjacent to the alkyne and the isoindolinone moiety. To examine the effects of VU0657640 upon $G_{i/o}$–coupled GPCR-mediated inhibition of exocytosis, in tandem with the lab of Qi Zhang, Ph.D, we examined high-K^+ evoked release in primary rat hippocampal CA1/CA3 neurons. Cultures were isolated from newborn rat pups and transfected with sypH-Tomato via calcium phosphate transfection after 2 weeks. Exocytosis was evoked via Tyrode's solution containing 90 mM K^+ in the presence or absence of 300 nM of the α_2 adrenergic agonist brimonidine. (Fig. 31) 300 nM brimonidine was able to inhibit evoked release (n=4). Pretreatment for 5m with 100 μM VU0657640 was able to partially overcome the effect of brimonidine (n=2). Interestingly, pretreatment for >1H with 100 nM tacrolimus, a calcineurin inhibitor, was also able to bypass the inhibitory effect of brimonidine (n=4), potentially suggesting that phosphorylation of one component of the synaptic machinery may disrupt α_2 AR signaling (data not shown).

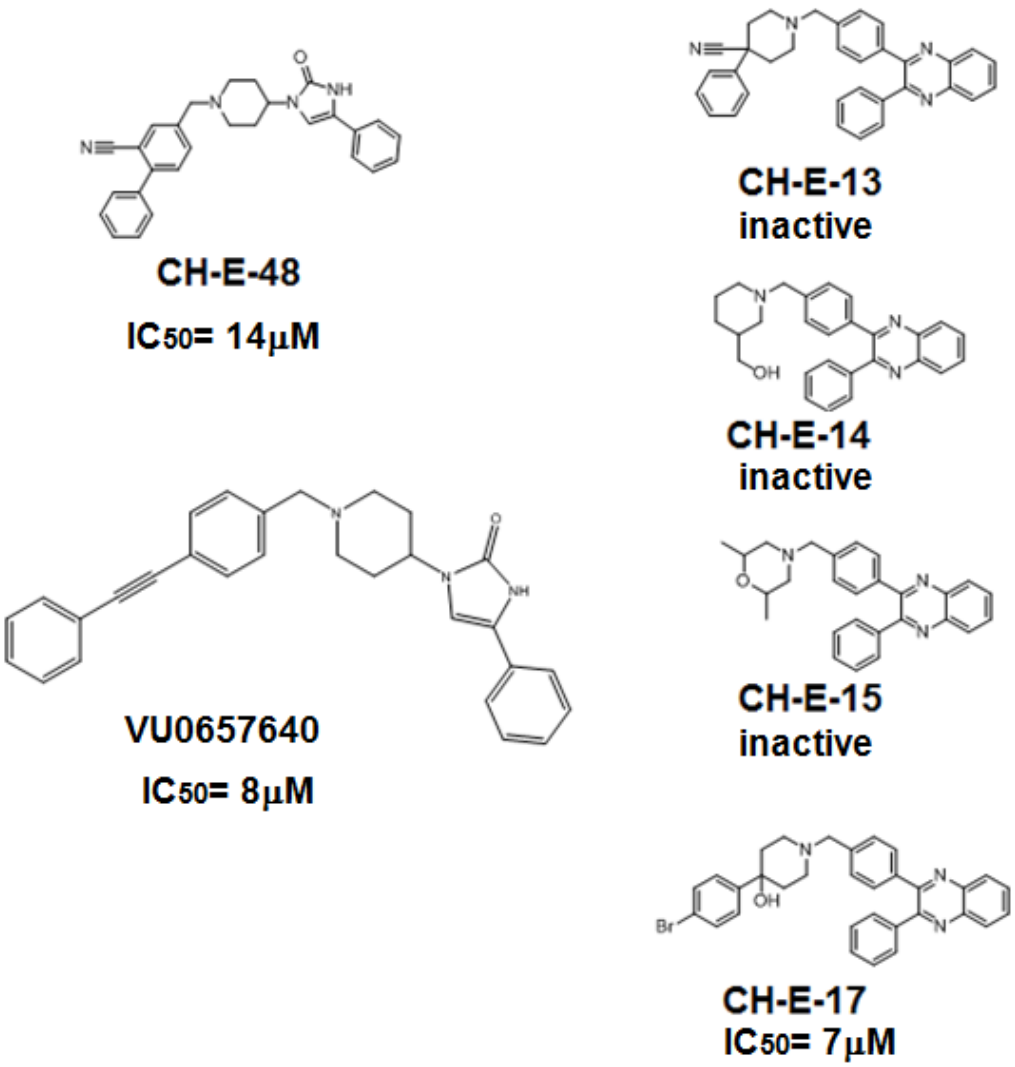

Figure 30: Structure-activity relationships of Gβγ-SNARE inhibitors derived from VU0451223.

A series of truncated analogues of VU0451223 were synthesized in a minimum pharmacophore study, resulting in lead compound VU0657640. Each compound was tested in the Alphascreen primary assay in a seven-point concentration response curve. IC_{50} values for the primary Alphascreen assay are displayed below the compound's name. Lead compound VU0657640 was tested more than four times in the primary assay with the same results, and was resynthesized twice to confirm that the active molecule was not due to impurities within the synthesis.

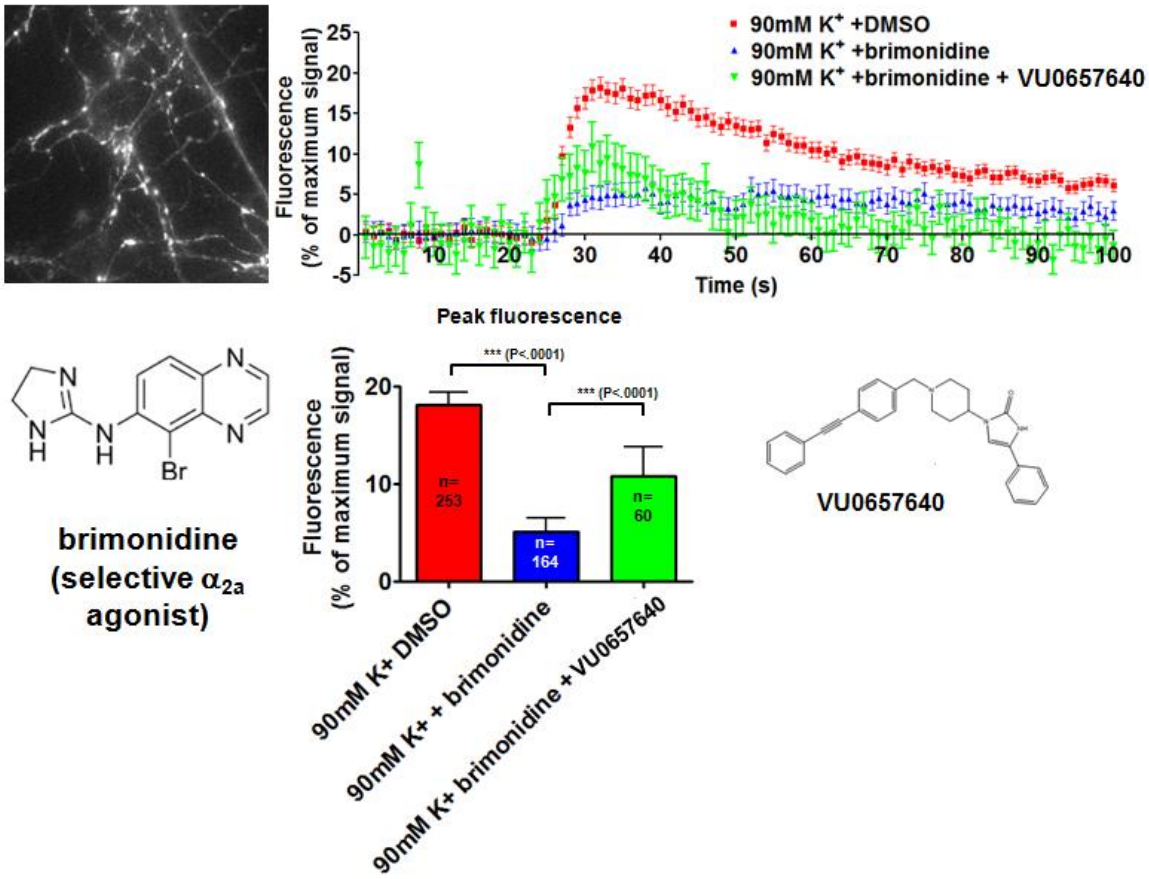

Figure 31: VU0657640 partially bypasses α_2 adrenreceptor-mediated inhibition of evoked release.

Upper left: Example image of cultures transfected with sypH-Tomato. Upper right : Bar graphs showing rise in fluorescence from exocytosis upon exposure to 90mM K+. Lower left: Chemical structure of brimonidine (300nM) in evoked release assay. Lower middle : Graph indicating peak fluorescence of each trace. Chemical structure of VU0657640 depicted below graph. DMSO and brimonidine experiments were repeated twice for a total of three experiments: VU0657650 Data analyzed by Student's t-test (*** = $p<0.0001$)

Discussion:

We have generated selective small-molecule modulators of Gβγ signaling. These compounds potently and specifically disrupt the Gβγ-SNAP25 and Gβγ-GIRK channel interactions through direct binding to Gβγ subunits. In addition, serotonin is no longer able to inhibit exocytosis in the lamprey giant synapse, an effect that has been conclusively shown to be mediated by the interaction of Gβγ with SNARE proteins. Serotonin can inhibit vesicle release in a similar manner in a variety of mammalian neurons, with this inhibitory effect being implicated in conditions such as depression. Future efforts will be devoted to improving potency and selectivity through further SAR. Indeed, every compound tested in this screen had at least an 9-fold lower potency than the fluorescein-based inhibitor M119. VU0476078 has been withdrawn from consideration due to issues of batch variability and poor DMPK properties, with the compound being unstable in human plasma. Despite the lower potency, VU0657640 does not experience similar batch variability issues, with 3 batches showing similar effects. Predictably, our Gβγ-SNAP25 inhibitors do not appear at first glance to affect SNAP25 or SNARE function with regards to Syt1. The selectivity of these molecules with regards to other critical effectors of Gβγ, such as voltage-gated calcium channels and PI3K, has yet to be determined. Furthermore, future efforts will be directed at identifying the structural determinants behind Gβγ-effector selectivity and the location of the binding site upon the Gβγ molecule. Given the differences in selectivity and potency observed compared to M119, these compounds may be binding to a different site on Gβγ from that of the SIGK peptide. The development of selective small molecule inhibitors of Gβγ-effector interactions will yield new insights into Gβγ signaling and the physiology of GPCR-mediated inhibition of exocytosis in secretory cells, as well as the basis for clinical therapies in the future. The development of substituted VU0657640 analogues is ongoing: a number of molecules have been synthesized and have undergone preliminary testing in the Gβγ-SNAP25 primary assay. Characterization of these molecules is a primary goal of the

project. Once nanomolar potency has been reached, we will test these compounds for DMPK and ancillary pharmacology, and begin studies of secretory cell function *in vivo* or in *ex vivo* systems.

CHAPTER V

THE ROLE OF THE Gβγ-SNARE INTERACTION IN METABOLISM

Introduction

Insulin is the most important hormone for glucose homeostasis. It binds to the insulin receptor on the surface of cells, causing a signal transduction cascade that results in GLUT4 glucose transporters translocating to the cell membrane, allowing cells to take up glucose. Insulin also promotes glycogen and lipid synthesis, while inhibiting gluconeogenesis. The human body's primary source of this peptide hormone are the beta cells of the islets of Langerhans in the endocrine pancreas. Type II diabetes is a chronic, metabolic disease characterized by reduced insulin secretion, insulin resistance, and hyperglycemia. T2D is a massive contributor to morbidity, mortality and health care spending, with 285 million worldwide affected by the condition[271]. The reduction in insulin secretion is a key prognostic indicator of the development of T2D, moreso than insulin resistance[218]. This reduction occurs from two mechanisms: reduction in beta cell mass, and reduced beta cell function. T2D is a progressive illness that produces additional morbidity and mortality as insulin release is reduced, with many patients becoming dependent on injectable insulin, despite the temporary beneficial effects of oral antidiabetic agents such as metformin to reduce hepatic gluconeogenesis or sulfonylureas to inhibit the K_{ATP} channel on beta cells.

Insulin secretion from the beta cells of the islets of Langerhans is highly regulated, with many processes able to alter it in a positive or negative fashion. Regulation begins at the level of transcription and translation, with numerous transcription factors able to alter transcription of the insulin gene. The initial polypeptide preproinsulin undergoes extensive post-translational modification, with disulfide bond formation and cleavage by endopeptidases. Insulin is then packaged into insulin granules, a large dense-core granule filled with crystals containing insulin, calcium, and zinc, along with GABA and ATP [272].

The release of insulin is highly regulated: it can be modulated through neurotransmitters such as norepinephrine, hormones such as somatostatin[192,264], and, most importantly, blood glucose. Glucose is taken up into the beta cell via facilitated diffusion using the glucose transporter GLUT2. In the cytosol, it undergoes glycolysis, generating ATP, which binds to the K_{ATP} channel, inhibiting its hyperpolarizing current. The beta cell depolarizes, activating voltage-gated calcium channels and triggering insulin release into the extracellular space, where it enters bloodstream and performs a number of effects through binding to the insulin receptor, a receptor tyrosine kinase[273]. Insulin receptor signaling occurs in a large number of cells in the body, including muscle cells and adipocytes. Insulin induces the uptake of glucose in these cells through a signal transduction cascade that ultimately results in the translocation of the glucose transporter GLUT4 to the plasma membrane, permitting glucose transport[273].

Much like in other cell types, GPCRs can both enhance and inhibit exocytosis. One well-studied example of a stimulatory GPCR is the Gs-coupled GLP-1 receptor, with pharmaceutical agonists thereof being used in the clinic to treat type II diabetes. GLP-1 is a neuropeptide which is released from the brain and intestinal L cells in response to food intake. It binds to and activates the GLP-1 receptor on the beta cell, leading to an accumulation of cAMP and activation of protein kinase A and Epac1 within the cell, resulting in modified ion channel activity and depolarization to produce insulin secretion[274]. Correspondingly, inhibitory GPCRs are also present on the beta cell. One of the most well-studied is the α_{2A} adrenergic receptor. This receptor, expressed on the surface of beta cells, inhibits the release of insulin in response to the neurotransmitters epinephrine or norepinephrine through a variety of different mechanisms. The α_{2A} receptor can increase the activity of the K_{ATP} channel, increasing intracellular K^+ to hyperpolarize the cell[275]. The hyperpolarizing effect was shown to be mediated through $G_{i/o}$ through studies with pertussis toxin, and specifically through multiple $G\alpha$ subunits, as antibodies against $G\alpha_i$ and $G\alpha_o$ each partially blocked the effect, while a pan-$G\alpha$ completely blocked the effect. While $G\beta$ is the subunit responsible for activating K^+ channels such as GIRK, anti-$G\beta$ had no effect [276]. A second mechanism involves the inhibition of adenylyl cyclases to reduce cyclic AMP and inhibit protein kinase

A[275]. A third involves inhibition of the refilling of the readily releasable pool by $G\alpha_i$: the subunit responsible was determined via antibody studies similar to those above[153]. Norepinephrine was found to inhibit L-type calcium channels in beta cell-derived cell lines, but not primary beta cells[275,277]. Instead, an effect distal to calcium entry was observed in primary tissue[192]. Antibodies to Gβ blocked the inhibitory effect of norepinephrine, while treatment with the Gβγ-activating cell permeable peptide mSIRK inhibited exocytosis in a non-additive manner with norepinephrine[153]. Treatment with botulinum toxin A to cleave the C-terminus from SNAP25, reducing its affinity for Gβγ, also blocked the inhibitory effect of norepinephrine[153]. Together, this data suggests that the α_{2A} adrenergic receptor inhibits glucose-stimulated insulin release via the Gβγ-SNARE interaction, along with the other mechanisms listed. One limitation of these studies is the use of primary beta cells instead of intact islets, which may have perturbed signaling due to the dissociation process. The electrophysiological methods utilized by the Sharp lab are not well-suited to work in increasingly complex tissue models such as the islet. Studies in islets or intact pancreas to implicate the Gβγ-SNARE interaction would require small molecule inhibitors of the interaction or transgenic mice deficient in the interaction.

Some data suggests that the α_{2A} adrenergic receptor may be overactive in the beta cell in type II diabetes. T2D is a disease that is partially heritable, although the consensus of modern medicine is that environment plays a significantly larger role than genetics in the determination of whether T2D will develop. Specific risk alleles for T2D exist: one such allele exists within the ADR2A gene, which codes for the α_{2A} adrenergic receptor. This allele, containing the rs5533668 SNP in the 3' UTR thought to be important for mRNA stability, results in increased receptor expression within the islet [220,278] and reduced glucose-stimulated insulin release. Beta-cell specific overexpression of the α_{2A} adrenergic receptor in mouse models results in reduced insulin release and impaired glucose tolerance[279]. α_{2-} selective antagonists enhance insulin release in subjects with type II diabetes, but not healthy subjects[222,223]. From this, we can hypothesize that overactive α_{2A} adrenergic receptor signaling is partially responsible for the

reduction in insulin release observed in T2D. This hypothesis raises two important questions: first, through which of the currently identified mechanisms is responsible for the pathophysiological overactivity of the α_{2A} adrenergic receptor in T2D? We hypothesize that the Gβγ-SNARE interaction is important for this receptor overactivity. Second, is pharmaceutical modulation of this downstream signaling mechanism (the Gβγ-SNARE interaction) a potential treatment strategy for T2D? Antagonism of the α_{2A} adrenergic receptor has been explored as a potential therapeutic option for T2D: treatment of T2D patients with the α_2 antagonist yohimbine produces increased blood insulin and reduced blood glucose[222,223,278]. However, it also results in increased blood norepinephrine, with anxiety and elevated blood pressure being reported as side effects[278]. Given the extremely common comorbidity of hypertension and T2D, direct antagonism of the α_{2A} adrenergic receptor to treat T2D while exacerbating hypertension may not be advantageous for long-term patient outcomes. Instead, we hypothesize that consecutive inhibition of two separate steps of the signaling mechanism- α_{2A} adrenergic receptor antagonism and Gβγ-SNARE inhibition- may allow us to use lower doses of the small molecules responsible for both[280,281]. This represents a novel treatment strategy that has yet to be explored by any existing antidiabetic agent on the market: while activating G_s-coupled GPCRs on the beta cell such as the GLP-1 receptor is a clinically relevant for enhancing insulin release, inhibiting $G_{i/o}$-coupled GPCRs such as the α_{2A} adrenergic receptor has not been pursued to the same extent. Both strategies may be used in tandem to provide additional enhancement of insulin release from the beta cell.

In the beta cell, the machinery for vesicle fusion resembles that found in other types of secretory cells, including neurons. The neuronal SNAREs SNAP25, syntaxin1, and VAMP2 have all been shown to play a role in insulin granule exocytosis[282]. Several SNARE proteins that differ from those found in neurons have also been implicated in insulin release, including SNAP23, syntaxin4, and VAMP3[282]. SNAP23 is a membrane-associated t-SNARE that is structurally related to SNAP25. It is normally present at low levels in beta cells, but expression levels are elevated in response to high glucose[283]. Comparatively, SNAP25 levels in genetic rat models of obesity and diabetes are reduced relative to wild-

type controls[284]. Overexpression of SNAP23 can rescue glucose-stimulated insulin secretion in response to proteolytic cleavage of SNAP25 by botulinum toxin E in beta cells[285]. However, a direct role for SNAP23 in glucose-stimulated insulin release has not been definitely conducted. In contrast, the roles of syntaxins 1 and 4 in insulin release are well-understood: syntaxin1A participates in first-phase insulin secretion, while syntaxin4 participates in both first- and second-phase insulin secretion [286,287]. Overexpression of syntaxin4 in human islets enhances glucose-stimulated insulin release[288]. The calcium sensor for insulin release is thought to be synaptotagmin VII[96,97]. Syt7 knockout mice exhibit reduced glucose-stimulated insulin secretion[289]. Studies pertaining to whether these islet SNAREs can interact with Gβγ have yet to be conducted, and it is not known whether Syt7 may compete with Gβγ for binding sites on SNAREs.

Methods

Plasmids. The open reading frame for human SNAP23, Stx2, Stx4, and VAMP8 were subcloned into the glutathione-S-transferase (GST) fusion vector pGEX-6p-1 (GE Healthcare) for expression in bacteria. The open reading frames for Gβ1 and 6His-Gγ2 were subcloned into the baculovirus vector pVL1392 (Invitrogen). Plasmid sequences were verified to be correct with Sanger sequencing utilizing BigDye Terminator dyes and resolved on an ABI 3730 DNA Analyzer (Applied Biosystems).

Protein purification. Recombinant bacterially-expressed glutathione-S-transferase (GST) fusion proteins were expressed in *Escherichia coli* strain Rosetta 2 (EMD Biosciences). Protein expression was induced with 100 μM isopropyl β-D-1-thiogalactopyranoside for 16 h at room temperature. Bacterial cultures were pelleted and washed once with phosphate-buffered saline before undergoing resuspension in lysis buffer (25 mM potassium 4-(2-hydroxyethyl)-1-piperazine ethanesulfonate (HEPES-KOH) pH 8.0, 150 mM KCl, 5 mM 2-mercaptoethanol, 10.66 μM leupeptin, 1.536 μM aprotenin, 959 nM pepstatin, 200 μM phenylmethylsulfonyl fluoride, and 1 mM ethylenediaminetetracetic acid (EDTA)). DNAse I(100 units/mL) and RNAse A (100 μg/mL) were added to the resuspension buffer to remove contaminating

nucleic acids. Cells were lysed utilizing a sonic dismembranator at 4°C for 5 min. Lysates were cleared via ultracentrifugation at 26,000 x g for 20 min in a TI-70 rotor (Beckman Coulter). GST-SNAP-25 and GST-Syt1 fusion proteins were purified from cleared lysates by affinity chromatography on GE Sepharose 4 FastFlow (GE Healthcare). Lysates were allowed to bind to resin overnight before being washed once with lysis buffer containing 1% Triton X-100 (Dow Chemical). The resin was then washed once with elution buffer (25 mM HEPES-KOH pH 8.0, 150 mM KCl, 5 mM 2-mercaptoethanol, 0.5% n-octyl glucoside, 1 mM EDTA, 10% glycerol). SNAP25 proteins were eluted from GST-fusion proteins immobilized on resin via proteolytic cleavage with a GST-tagged fusion of rhinovirus 3C protease. After elution, SNAP23, Stx2, Stx4, or VAMP8 protein was reacted with EZ-Link sulfo-NHS-SS-biotin (Pierce) at a 20:1 ratio for 30m in elution buffer lacking 2-mercaptoethanol. Excess biotin was removed via dialysis in elution buffer. Protein concentrations were determined with a Bradford assay kit (Pierce) and purity was verified by SDS-PAGE analysis. Biotinylation was performed at 25C for 30 mwith a 20-fold excess of EZ-Link Sulfo-NHS-SS Biotin (Thermo), followed by overnight dialysis of excess biotinylation reagent in elution buffer lacking 2-mercaptoethanol. Biotinyation of the substrate was verified utilizing a HABA assay kit (Pierce).

Alphascreen protein-protein interaction assays. Solutions of 100 nM SNAP25 and 212 nM $G\beta_1\gamma_2$ were prepared in assay buffer (20 mM HEPES pH7.0, 10 mM NaCl, 40 mM KCl, 0.5% glycerol, and 0.01% triton-X-100. Alphascreen Histidine Detection Kit donor and acceptor beads (PerkinElmer) were separately diluted 1:100 in assay buffer. These solutions were then plated in 384-well plates (#784201, Greiner). Compounds were dissolved in DMSO to a concentration of 10 mM and plated in 384-well OptiPlates (PerkinElmer) using a Labcyte Echo 555 Omics (Labcyte) acoustic liquid handler. A Velocity Bravo liquid handler (Agilent) was utilized to add 4μL of the $G\beta_1\gamma_2$ solution to the OptiPlate. Compounds were permitted to bind to the $G\beta_1\gamma_2$ for 5m. Afterwards, 1μL of the SNAP25 solution was added to the plate and the mixture was incubated for an additional 5m. At that point, 10μL of the diluted acceptor beads was added to the plate, and the mixture incubated for 30m at room temperature. Then,

10μL of the diluted donor beads was added to the plate. The plate was centrifuged at low RPM values to remove bubbles and the mixture incubated for 60m at room temperature. Plates were read on an EnSpire plate reader (PerkinElmer).

Islet isolation. Islet isolation was performed by the Vanderbilt Islet Procurement and Analysis Core in compliance with protocols approved by the Vanderbilt Institutional Animal Care and Use Committee. Primary mouse islets were obtained according to previously published methods[290]. Briefly, 3 mL of 0.6mg/mL collagenase P (Roche) in Hank's buffered saline solution was infused into the pancreas via the bile duct. Pancreata were then excised and immersed for digestion in collagenase P solution for 5 min at 37 C using a wrist-action shaker. Islets were then isolated from cellular debris using handpicking under a light microscope and washed three times with phosphate-buffered saline containing 1% mouse serum, followed by incubation in RPMI-1840 with 10% FBS and 5.6 mM glucose.

Static incubation. Static incubation was performed in part by the Vanderbilt Islet Procurement and Analysis Core. Subsequent to isolation, islets were incubated for a minimum of two hours in Dulbecco's modified Eagle medium containing 10 mM HEPES-NaOH, 500 μM $CaCl_2$, and 0.5% bovine serum albumin at a glucose concentration of 5.6 mM. 10 islets were transferred on ice to 1.5mL low retention microfuge tubes (Fisher Scientific) in 150μL of Dulbecco's modified Eagle medium containing 10 mM HEPES-NaOH, 500 μM $CaCl_2$, and 0.5% bovine serum albumin containing variable concentrations of glucose, DMSO, and brimonidine. Islets were incubated at 37 C for 45 min followed by media removal. Islets were then recovered and total insulin was extracted using sonication in acidified ethanol. Insulin content within each fraction was analyzed via radioimmunoassay (Millipore).

Islet perifusion. Islet perifusion was performed by the Vanderbilt Islet Procurement and Analysis Core according to previously published methods[291]. Subsequent to isolation, islets were placed in a 1mL perifusion chamber and equilibrated in Dulbecco's modified Eagle medium containing 10 mM HEPES-NaOH, 500 μM $CaCl_2$, and 0.5% bovine serum albumin in addition to 5.6 mM glucose for 30m followed

by exposure to 16.7 mM glucose plus variable concentrations of brimonidine for 9 min, at which point the glucose concentration was reverted to 5.6 mM for 24 min after each stimulus. Fractions were collected at 3m intervals at 1mL/min flow rate. Islets were then recovered and total insulin was extracted using sonication in acidified ethanol. Insulin content within each fraction was analyzed via radioimmunoassay (Millipore).

Transgenic embryo generation. The SNAP25Δ3 mouse was created with assistance from the Vanderbilt Transgenic Mouse and Embryonic Stem Cell Resource in compliance with protocols approved by the Vanderbilt Institutional Animal Care and Use Committee. Transgenic mouse embryos were generated utilizing the CRISPR/Cas9 system. The protospacer targeting construct was generated via a 24-mer oligo with a forward sequence of 5'CACCGCAACAAAGATGCTGGGAAG3' annealed to 5'AAACTTCCCAGCATCTTTGTTGC 3'. 1 μg of px330 vector (Zhang lab, MIT) was digested in a stoichiometric fashion with Bbs1 (NEB) to a final concentration of 50ng/uL for 1h at 37 C. The oligo was then ligated into the digested product with Quick Ligase (NEB) in a one-pot reaction in which oligo was added to a final concentration of 0.4 μM. and ligated for 4m at 25 C. Constructs were verified via Sanger sequencing. The single-stranded homology donor(IDT, Ultramer) was 126bp in length and spanned the C-terminal final exon of SNAP25 with 48bp of homology in either direction of the site of interest along with the G204* mutation and a HindIII site 3' of the G204* for the purposes of sequencing. The px330 vector and single-stranded homology donor were co-microinjected into the pronucleus of 587 B6D2 embryos, 447 of which were implanted into 40 B6D2 dams. 32 pups were obtained, two of which contained the G204* mutation in germline cells as measured by PCR analysis of genomic DNA. To verify that the inserted transcript was correct, PCR products were then excised and ligated into pCR2.1TOPO, which was then subjected to Sanger sequencing using M13 and T7 primers. No changes other than the addition of the G204* and HindIII site were observed.

Mouse breeding and genotyping. The presence of the G204* mutation in the SNAP25Δ3 mouse was verified via PCR and Sanger sequencing. The presence of the wild-type SNAP25 gene was verified by a

primer set with the sequence 5' GCAACAAAGATGCTGGGAAGT 3' and 5' GGATTGTGGCAGTAGCTCTG 3'. The presence of the mutant G204* gene was verified with a primer set with the sequence 5' GATGCTGTAAGCTTAGTGG 3' and 5' GGATTGTGGCAGTAGCTCTG 3'. Mouse genotypes were confirmed via the qualitative presence of a DNA band generated from a PCR reaction with Taq polymerase analyzed via agarose gel electrophoresis in gels containing 3% agarose.

Results

Based on previously published results indicating that α_{2a} antagonists are more effective at increasing GSIS in type II diabetes patients than in healthy patients[223], we hypothesized that overactive α_{2a} signaling may be responsible for the loss of first-phase insulin secretion from the islets of Langerhans observed in type II diabetes. To test this hypothesis, we measured the ability of islets extracted from lean or diet-induced obese (DIO) mice to release insulin in response to either an α_{2a}AR agonist, brimonidine (Fig. 32), or a nonselective endogenous adrenergic agonist, epinephrine. Obesity was induced in the C57BL6/J mouse via feeding for a minimum of 8 weeks on a modified diet containing 60% of its food energy from fat (Research Diets). DIO mice weighed significantly more than control mice at the time of sacrifice. Since α_2 antagonists are more effective at raising GSIS in patients with T2D relative to healthy patients[223], we anticipated that islets from the obese mice would be more sensitive to brimonidine than the control islets, and have reduced first-phase insulin secretion in response to high(16.7 mM) glucose. At 12 weeks of age, sensitivity to brimonidine and epinephrine are not statistically different between control and DIO islets , as measured by insulin secreted in static incubation (n=2, 10 islets/condition), while DIO islets secreted more insulin overall. In the perifusion insulin secretion assay, DIO islets were less sensitive to epinephrine than control islets at 12 weeks (n=2) . At an age of 24 weeks, islets extracted from DIO mice were fourfold more sensitive to brimonidine. (Fig. 32B). First-phase insulin secretion was reduced roughly threefold (Fig. 32B), but no statistically significant differences in islet insulin content were observed between lean and DIO islets (Fig. 32E).

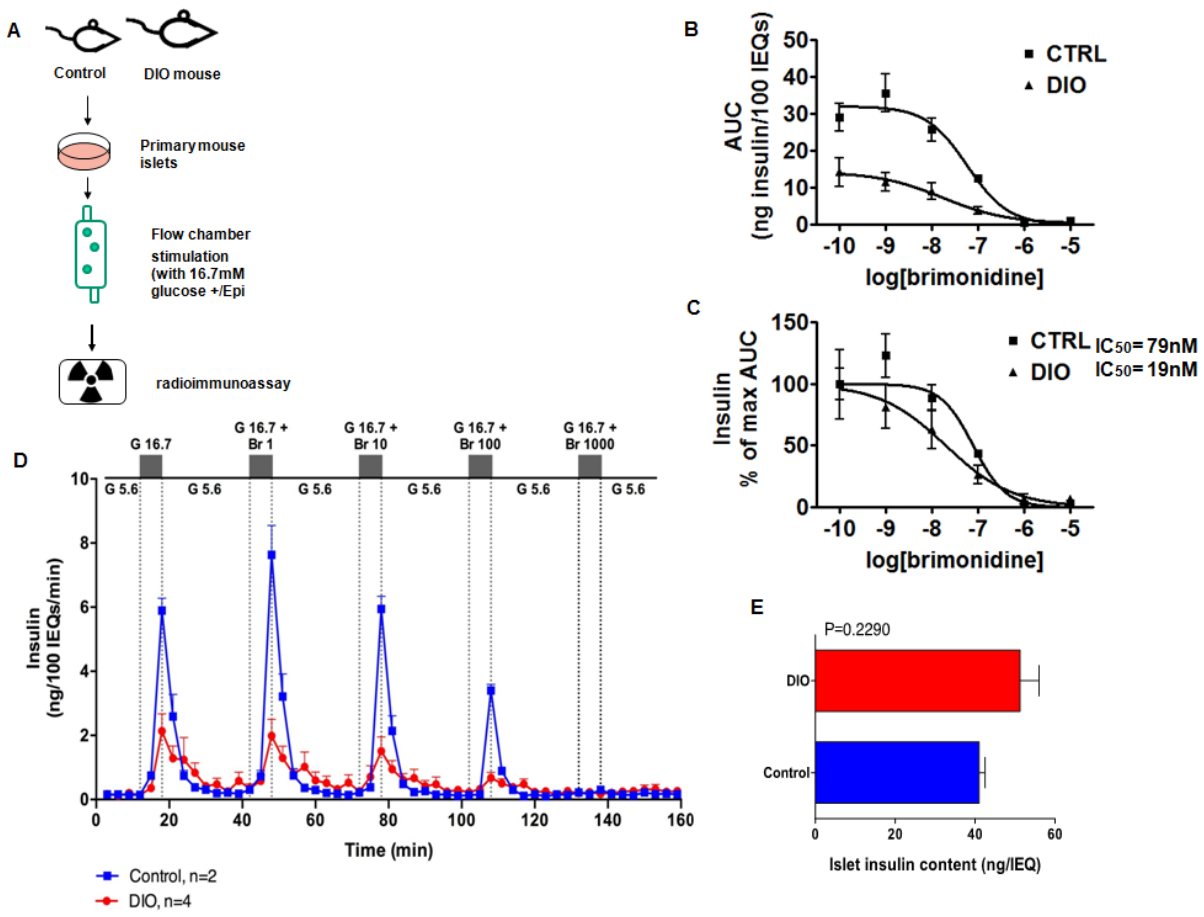

Figure 32: Aged DIO islets are more sensitive to brimonidine than control islets.

A. Diagram of perifusion assay workflow. B. Perifusion data in which CTRL and DIO islets extracted from 21-week old male mice are perifused with high glucose + an increasing concentration of brimonidine. Areas under the curve extrapolated from graph B plotted as a function of brimonidine concentration. C. AUC values normalized to the maximum within each condition. D. Raw data showing glucose-stimulated insulin secretion over time. E. Islet insulin content for each condition.

preliminary data suggests that at this age, DIO islets are more sensitive to α_{2a}AR signaling than lean islets.

We wanted to investigate the role of the Gβγ-SNARE interaction in the inhibitory effect of the α_{2a}AR on islets. To do this, we made a transgenic mouse that was deficient in the Gβγ-SNAP25 interaction. We inserted the SNAP25Δ3 allele into the wild-type SNAP25 locus using CRISPR-Cas9 technology and obtained heterozygote pups, which were bred to obtain viable and fertile homozygotes. Cleavage sites for the protospacer were identified using the assistance of Douglas Mortlock, Ph.D. sgRNAs targeting the protospacer were ligated into the Cas9-containing px330 vector utilizing a single-pot ligation reaction in which the Bbs1 endonuclease digests px330 in a stoichometric manner followed by ligation of the annealed sgRNA protospacer oligo via NEB Quick Ligase. Note the importance of both storage of Bbs1 at -80 to maintain activity and stoichiometric digestion of Bbs1. If DNA is present in excess, Bbs1 will only cut at one of two sites, permitting the DNA to reanneal or auto-ligate. Sanger sequencing of px330 can be done with U6 primer. Single-stranded homology donors contained the G204X mutation within the C-terminus of SNAP25 and a HindIII restriction site for genotyping, along with appropriate regions of homology. After ug quantities of the completed px330 construct were produced, these DNAs were co-transfected into B6D2 mouse embryos (performed by Vanderbilt Transgenic Core). Transfected embryos were implanted into dams and pups were born. PCR genotyping of the pups revealed three heterozygous mice out of 32 that had undergone homology-directed repair. Seven mice experienced neonatal lethality, an effect possibly attributed to insertion/deletion mutations within SNAP25. Heterozygous mice were fertile and were bred to yield homozygous offspring. Homozygous offspring containing the SNAP25Δ3 mutation were fertile. To determine whether the Gβγ-SNARE interaction was required for α_{2a}AR-mediated inhibition of insulin release, islets were obtained from SNAP25Δ3 mice and tested for their ability of brimonidine to inhibit insulin release, as well as their ability to secrete insulin in response to high glucose. No differences in the ability of brimonidine to inhibit glucose-

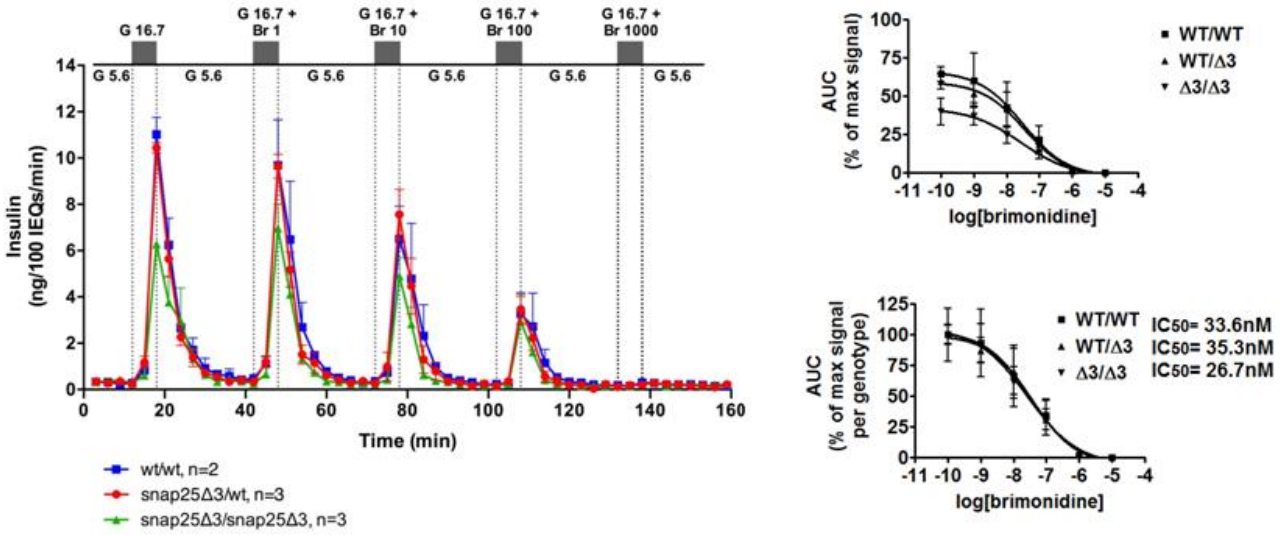

Figure 33: Inhibition of glucose-stimulated insulin secretion by brimonidine in the SNAP25Δ3 mouse.

Perifusion data of each genotype for 12 week old male mice using an identical protocol as Fig. 36. Left panel: Raw data showing glucose-stimulated insulin secretion over time. Upper right panel: Areas under the curve extrapolated from graph B plotted as a function of brimonidine concentration. Lower right panel: AUC values normalized to the maximum within each genotype.

stimulated insulin secretion, nor differences in glucose-stimulated insulin secretion itself, were detected. (Fig. 33A) Islet insulin content was identical (Fig. 33B) To investigate whether compensatory effects of SNAP23 could complicate interpretation of results observed in the SNAP25Δ3 mouse, we examined whether SNAP23 could bind Gβγ in the Alphascreen assay. SNAP23 was expressed as a GST-fusion in pGEX6.1 in E.coli and purified on glutathione-sepharose beads, followed by proteolytic cleavage of a 3C protease tag and biotinylation using EZ-Link NHS-SS Biotin. Biotinylated SNAP23 was able to bind Gβγ in a concentration-dependent manner with an EC_{50} of 78 nM (95% CI: 59 to 104 nM). (Fig. 34) In the same experiment, biotinylated SNAP25 bound Gβγ with an EC_{50} of 45 nM (95% CI: 37 to 55 nM). We then investigated whether other SNAREs found in non-neuronal cells, such as Stx2, Stx4 and VAMP8, were also able to bind Gβγ in a concentration-dependent manner. These SNAREs were expressed as full-length GST-fusions in pGEX6.1 in E. coli and purified on glutathione-sepharose beads, followed by proteolytic cleavage of a 3C protease tag and biotinylated, much like SNAP23. They were then exposed to a series of concentrations of Gβγ in the Alphascreen assay. The biotinylated Stx2 was able to bind Gβγ in a concentration-dependent manner, with an EC_{50} of 66 nM (95% CI: 55.6-78.0 nM). (Fig. 34) This experiment was repeated once for six technical replicates. Biotinylated Stx4 was able to bind Gβγ in a concentration-dependent manner with a reduced affinity compared to Stx2, with an EC50 of 134 nM (95% CI: 94.5 to 191 nM). Biotinylated VAMP8 was also able to bind Gβγ in a concentration-dependent manner with an IC_{50} of 104 nM, but a very steep Hill slope and a large response- larger than SNAP25 or Stx1A- generated a very broad 95% CI of 3.63 pM to 3 mM. Together, this data suggests that non-neuronal SNAREs can interact with Gβγ in the same fashion as the neuronal SNAREs Stx1A, SNAP25, and VAMP2.

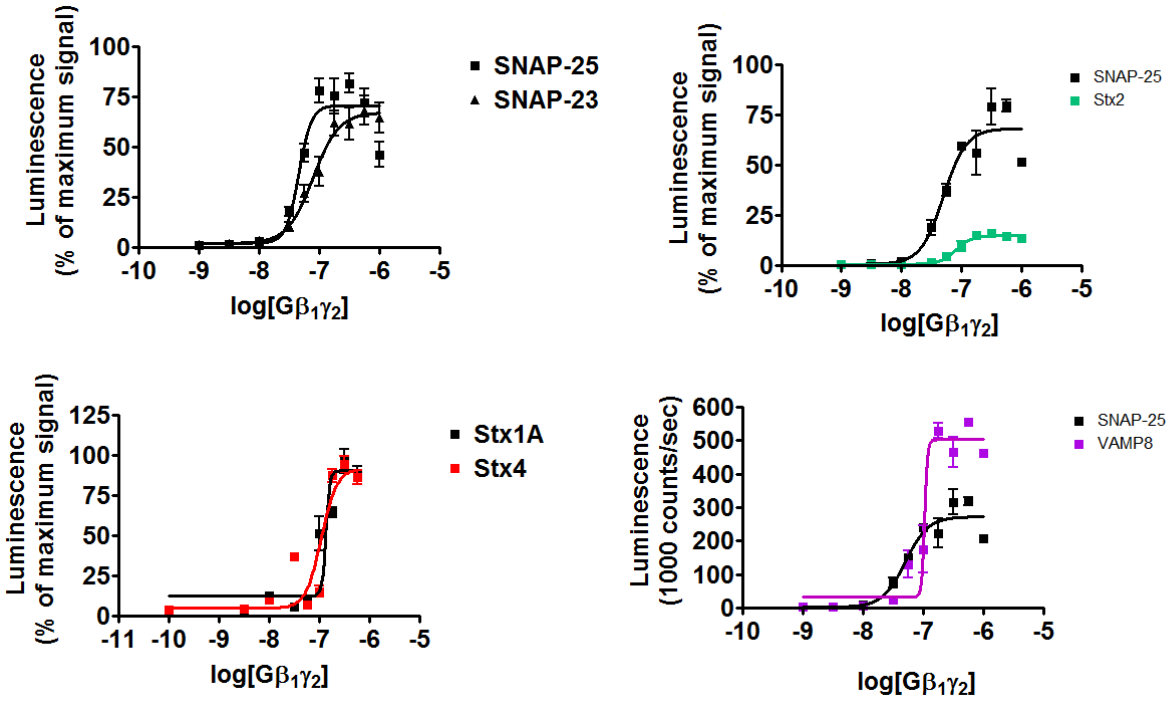

Figure 34: Non-neuronal SNAREs can also interact with Gβγ in a concentration-dependent manner.

Alphascreen concentration-response curves for Gβγ binding to SNAP25 WT , Stx1A, Stx2, Stx4, and VAMP8. Data normalized to the maximum luminescence signal obtained in each experiment except for VAMP8, in which unnormalized data is shown in order to demonstrate the difference in signal generated by VAMP8 compared to SNAP25.

Discussion

We have conducted several experiments to ascertain whether the Gβγ-SNARE interaction is essential to the functionality of the α_{2A} adrenergic receptor in intact islets. Studies conducted by other groups indicate that the distal effect of α_{2A} adrenergic receptor agonists in the beta cell (and elsewhere) are mediated through the Gβγ-SNARE interaction [153,197]. In Chapter 5, we tested the effects of a small molecule Gβγ-SNARE inhibitor, VU0476078 on glucose-stimulated insulin secretion and the inhibitory action of a non-selective adrenergic agonist, epinephrine. VU0476078 was able to stimulate glucose-stimulated insulin release roughly 70%, and conditions treated with epinephrine and VU0476078 appeared to have more insulin released than those treated with epinephrine alone, but the difference was not significant. The magnitude of the effect was only a small fraction of the inhibition produced by epinephrine. Next, we made a transgenic mouse that was partially deficient in the Gβγ-SNARE interaction. The SNAP25Δ3 mouse expresses a mutant SNAP25 in which $G_{i/o}$-coupled GPCR agonists are twofold less effective at inhibiting exocytosis in neuronal systems[292]. SNAP25Δ3 mice were not significantly different from wild-type with regards to the ability of the α_{2A} adrenergic receptor agonist brimonidine to inhibit exocytosis. Together, this data reinforces the notion that there are multiple mechanisms through which the α_{2A} adrenergic receptor signals[275], the Gβγ-SNARE interaction being one of them. The large effect of VU0476078 on GSIS alone implies that autoinhibitory signals released from the islet, potentially somatostatin, may also signal through this mechanism. It is important to note that the SNAP25Δ3 mutation contains only a twofold reduction in the ability of Gβγ to bind to SNAP25: this effect may not be strong enough to produce an observable difference for a receptor that signals through multiple mechanisms. It is also possible that Gβγ may be binding to SNAP23 in the presence of a lower-affinity SNAP25: it has been shown that SNAP23 can bind Gβγ with comparable potency for SNAP25. SNAP23 may be upregulated in SNAP25Δ3 islets, but even if it is not, exogenous levels of the protein may be adequate to sustain inhibition. The finding that non-neuronal SNAREs can bind

Gβγ, including SNAP23, Stx2 and 4, and VAMP8, is novel in and of itself. It potentially implies that tissues that do not express SNAP25 and Stx1A may also utilize the Gβγ-SNARE interaction to mediate the action of $G_{i/o}$-coupled GPCRs. We hypothesize that this mechanism is important for many different receptors and cell types, including non-neuronal cells, but not all receptors in all cell types that inhibit exocytosis [208].

In agreement with our hypothesis, we observed a loss of insulin secretion and enhanced sensitivity to α_{2A} adrenergic receptor agonists in aged DIO animals relative to healthy age-matched controls. We would anticipate that animal models of T2D may be more sensitive to α_{2A} adrenergic receptor agonists, and this seems to be the case, although DIO mice cannot be said to have T2D. It is not currently known if this effect is due to perturbation of signaling mechanisms within the beta cell, a change in receptor density, or other effects. A repeat of this experiment would still be desirable, as the change in potency has yet to reach an unambiguous 95% confidence interval between the two conditions.

Future studies in this area may involve a metabolic challenge for the SNAP25Δ3 mouse, such as the effects of α_{2A} adrenergic receptor agonists in a model of diet-induced obesity. It may also be advantageous to utilize a transgenic mouse different SNAP25 mutant that has a greater inhibition of the Gβγ-SNARE interaction, such as SNAP25Δ9 [201]or SNAP258A. The former would almost certainly be neonatally lethal, making islet extraction a challenge. The latter is challenging to introduce using current mutagenesis techniques, given the necessity of preserving SNAP25 splicing. Finally, it would be highly advantageous to use a higher potency and better-characterized Gβγ-SNARE inhibitor when such a compound is developed. While some data is known about the effects of VU0476078 on some Gβγ effectors, many others remain uncharacterized.

CHAPTER VI:

ADDITIONAL STUDIES OF THE Gβγ-SNARE INTERACTION

Introduction

In this section, we will include data of interest that is not suitable for inclusion in other chapters of the dissertation. These studies are focused on two areas: identification of residues important for the Gβγ-SNARE interaction on proteins other than SNAP25, and the ability of a calcium sensor Doc2 to compete with the Gβγ for binding sites upon SNARE. In addition to SNAP25, the SNARE proteins Stx1A and VAMP2 also interact with Gβγ[48,201]. The molecular requirements of this interaction are much less understood. Two previous studies have reported an interaction of Gβγ with the H_3 domain of Stx1A, thought to contribute one helix to the four-helix SNARE bundle[191,201]. The Gβγ-Stx1A interaction is thought to be important for $G_{i/o}$-coupled GPCRs to inhibit voltage-gated calcium currents[190]. Specifically, the N-terminal portion of the H_3 domain is thought to be crucial for the interaction[191]. Nothing is known about the individual residues that link Gβγ to Stx1A. The specific contributions of the interaction of each Gβγ subunit with SNARE is also not well-studied: does Gβγ-SNAP25 act downstream of calcium channels, while Gβγ-Stx1A acts exclusively at calcium channels? Creating mutant SNAREs that are deficient in each interaction would enable us to study the role of each in regulated exocytosis. In addition, since t-SNAREs in which eight residues from SNAP25 key for the Gβγ-SNARE interaction still interact weakly with Gβγ[244], there must be additional key Gβγ binding residues on Stx1A. Identification of these residues would increase our understanding of the Gβγ-SNARE interaction.

While it is known that Gβγ competes with Syt1 for binding sites on SNARE[201], it is not known to compete with any other C2-domain proteins in a similar fashion. Doc2 is a C2AB protein that is implicated in exocytosis, specifically asynchronous and spontaneous release[99,100]. It has been shown to

play a role in exocytosis in nonneuronal cells, notably the beta cells of the islets of Langerhans[103]. If it could be shown that Doc2 could compete with Gβγ for binding sites upon SNARE, it would expand our mechanistic understanding of Gβγ-mediated inhibition of exocytosis that may be triggered by calcium sensors other than Syt1, potentially explaining Gβγ-SNARE-mediated inhibition of exocytosis in cell systems through which Syt1 is not the primary calcium sensor, such as the beta cell[153].

Methods

Protein Purification. For SNAP25 and Doc2β C2AB, recombinant bacterially-expressed glutathione-S-transferase (GST) fusion proteins were expressed in *Escherichia coli* strain Rosetta 2 (EMD Biosciences). Protein expression was induced with 100 μM isopropyl β-D-1-thiogalactopyranoside for 16 h at room temperature. Bacterial cultures were pelleted and washed once with phosphate-buffered saline before undergoing resuspension in lysis buffer (25 mM potassium 4-(2-hydroxyethyl)-1-piperazine ethanesulfonate (HEPES-KOH) pH 8.0, 150 mM KCl, 5mM 2-mercaptoethanol, 10.66 μM leupeptin, 1.536 μM aprotenin, 959 nM pepstatin, 200 μM phenylmethylsulfonyl fluoride, and 1mM ethylenediaminetetracetic acid (EDTA)). Cells were lysed with a sonic dismembranator at 4°C for 5 min. Lysates were cleared via ultracentrifugation at 26,000 x g for 20 min in a TI-70 rotor (Beckman Coulter). GST-SNAP-25 fusion proteins were purified from cleared lysates by affinity chromatography on GE Sepharose 4 FastFlow (GE Healthcare). Lysates were allowed to bind to resin overnight before being washed once with lysis buffer containing 1% Triton X-100 (Dow Chemical). The resin was then washed once with elution buffer (25 mM HEPES-KOH pH 8.0, 150 mM KCl, 5 mM 2-mercaptoethanol, 0.5% n-octyl glucoside, 1 mM EDTA, 10% glycerol). SNAP25 proteins were eluted from GST-fusion proteins immobilized on resin via proteolytic cleavage with a GST-tagged fusion of rhinovirus 3C protease. Protein concentrations were determined with a Bradford assay kit (Pierce) and purity was verified by SDS-PAGE analysis.

Gβγ Purification. $G\beta_1\gamma_1$ was purified from bovine retina as described previously[226]. Recombinant $G\beta_1\gamma_2$ was expressed in Sf9 cells and purified via a 6xHis tag on $G\gamma_2$ using Talon™ immobilized metal affinity chromatography (Clontech, Mountain View, CA).

Peptide array synthesis. Peptide array synthesis was performed using the Respep SL (Intavis AG) according to standard SPOT synthesis protocols[227]. Briefly, the robotics-driven computer-directed device (Respep SL) managed complex timing, mixing, additions, and washing of the membrane over the course of the peptide synthesis. Peptides were 15 residues in length. The sequences of the peptides for SNAP-25 were based on the sequence available from the UniprotKB/Swiss Protein Database for human *SNAP-25*, P60880. After the peptides were synthesized coupled to the membranes, membranes were processed with a final side chain deprotection step. Membranes were placed in an acid-safe container in a chemical hood and submerged in a solution of 95% trifluoroacetic acid, 3% tri-isopropylsilane for 1 hour with intermittent agitation. After the trifluoroacetic acid solution was removed, the membrane was then put through a series of washes: 1) dichloromethane for four 10-minute washes; 2) dimethylformamide for four 10-minute washes, 3) ethanol for two 2-minute washes. The membrane was allowed to dry in the hood. For the alanine-mutagenesis screening of peptides, the peptides were synthesized to be 14 residues in length.

Peptide membrane Far-Western. After membranes had dried from the synthesis de-protection washes, they were first soaked in ethanol for 5 minutes, and then re-hydrated over two washes for 5 minutes in water. The membranes were then blocked with slight agitation for 1 hour in a buffer of tris-buffered saline (TBS) with 5% milk and 0.1% Tween-20 (Sigma-Aldrich). The membranes were then washed 5 times for 5 minutes in TBS with 0.1% Tween-20 on a shaker at RT. The membranes were then incubated overnight at 4°C with $G\beta_1\gamma_1$ at a final concentration of 0.44 μM in a binding buffer of 20 mM HEPES, pH 7.5, and 5% glycerol. The next morning, membranes were washed at room temperature (RT) on a shaker three times for 5 minutes in TBS with 5% milk and 0.1% Tween-20. Membranes were then exposed to primary antibody against Gβ (T-20, SC-378; Santa Cruz Biotechnology, Inc.) at 1:5000 dilution in TBS

with 0.2% Tween-20 with mixing on a shaker table at RT for 1 hour before being washed three times for 5 min each on a shaker table in TBS with 0.1% Tween-20 also at RT. The appropriate secondary antibody was then diluted into TBS to 1:10,000 dilution with 5% milk and 0.2% Tween-20 followed by gentle agitation on a shaker with membranes for 1 hour at RT. Finally, membranes were washed twice for 5-minutes in TBS with 0.1% Tween-20, followed by two 10-minute washes in TBS at RT.

Chemiluminescence. The Western Lightning™ Chemiluminescence Reagent Plus (NEL104) from Perkin-Elmer and the Immun-Star™ WesternC™ Chemiluminescence Kit (#170-5070) from Bio-Rad was used to visualize western blots following published protocols. Western blot images were obtained utilizing a Bio-Rad Gel Doc Imager. Images were analyzed for densitometry using ImageJ (available from http://rsbweb.nih.gov/ij/index.html) ANOVA calculations comparing alanine mutant peptide spot intensity with wild type peptide reactivity were determined using GraphPad Prism4 software (GraphPad Software, San Diego, CA).

Alphascreen protein-protein interaction assays. Solutions of 100 nM SNAP25 and 212 nM $G\beta_1\gamma_2$ were prepared in assay buffer (20 mM HEPES pH7.0, 10 mM NaCl, 40 mM KCl, 0.5% glycerol, and 0.01% triton-X-100. Alphascreen Histidine Detection Kit donor and acceptor beads (PerkinElmer) were separately diluted 1:100 in assay buffer. These solutions were then plated in 384-well plates (#784201, Greiner). Compounds were dissolved in DMSO to a concentration of 10 mM and plated in 384-well OptiPlates (PerkinElmer) using a Labcyte Echo 555 Omics (Labcyte) acoustic liquid handler. A Velocity Bravo liquid handler (Agilent) was utilized to add 4μL of the $G\beta_1\gamma_2$ solution to the OptiPlate. Compounds were permitted to bind to the $G\beta_1\gamma_2$ for 5m. Afterwards, 1μL of the SNAP25 solution was added to the plate and the mixture was incubated for an additional 5m. At that point, 10μL of the diluted acceptor beads was added to the plate, and the mixture incubated for 30m at room temperature. Then, 10μL of the diluted donor beads was added to the plate. The plate was centrifuged at low RPM values to

remove bubbles and the mixture incubated for 60m at room temperature. Plates were read on an EnSpire plate reader (PerkinElmer).

Protein Structure Visualization. All protein structures were visualized using the program Pymol (http://www.pymol.org) (Schrödinger, USA).

Results

While detailed information pertaining to the molecular basis of the interaction of Gβγ and SNAP25 is known, the individual residues on syntaxin1A required for interaction with Gβγ are unknown. The H_{abc} domain of Stx1A alone was not shown to interact strongly with Gβγ, while the H_3 domain did, as measured by a fluorescence intensity binding assay or GST-pull down assay[191,201]. To identify individual Gβγ–binding residues upon Stx1A, we began by identifying small peptides derived from the full-length Stx1A sequence capable of interacting with Gβγ. We derivatized Stx1A much in the same manner as we did for SNAP25 in Fig. 9 and Fig. 10. Several clusters of consecutive peptides upon Stx1A appeared to bind Gβγ. We performed densitometry upon images of the membranes in triplicate, with each value being normalized to the signal with the highest respective luminance of the three. Peptides that showed a high degree of reactivity towards Gβγ corresponded to 3 distinct regions on Stx1A, corresponding to residues 49-62, 116-129, and 252-265. Intriguingly, peptides derived from both the H_{abc} domain and the H_3 domain were shown to bind tightly to Gβγ. Previously, only the H_3 domain was shown to bind Gβγ, as measured by fluorescence binding assays. The consensus sequence for each cluster of reactive peptides is visualized upon the three-dimensional structure of the ternary complex of the Stx1A H_{abc} domain. With peptides of interest identified, we then performed scanning alanine mutagenesis upon these peptides to identify individual residues required for the interaction of Gβγ. In this experiment, peptides shown to interact with Gβγ were modified so that a single residue was altered to Ala. The modified peptides were then spotted onto a PVDF membrane and exposed to a Far-Western blotting procedure with Gβγ in a manner identical to that shown in Figure 1. Densitometric analysis to

determine the amount of bound Gβγ was performed in a similar fashion. Our analysis showed that four residues showed a statistically significant decrease in the amount of Gβγ bound when mutated to Ala: K55, R56, R125, and F127.(Fig. 35A). We were unable to find a single residue in the H_3 domain that showed a loss of function when mutated to Ala. These residues are labeled on the three-dimensional structure of the Stx1A H_{abc} domain depicted in Fig. 35B. Interestingly, all four of them are on the H_{abc} domain, with no single residue within Stx1A 252-265 being able to produce a significant reduction in binding when mutated to Ala.

To investigate whether these residues were important , we measured the ability of Gβγ to bind the cytosolic domains of wild-type Stx1A or mutant Stx1A where residues highlighted previously were mutated to Ala. Mutation of K55 and R125 to Ala was sufficient to abolish Gβγ binding. (Fig. 36A) K55A alone did not seem to have a significantly different ability to bind Gβγ from wild-type.This raises the question as to whether both K55 and R125 were required, or whether R125 alone was sufficient to abolish the interaction. Characterization of the R125A mutation is ongoing.

To investigate the importance of specific regions on the importance of Gβ for the Gβγ-SNARE interaction, a series of peptides corresponding to regions of Gβ and Gγ were synthesized and tested for their ability to disrupt the Gβγ-SNAP25 interaction in a concentration-dependent manner in the Alphascreen competition binding assay. 20 nM biotinylated SNAP25 was exposed to an EC_{80} concentration of $G\beta_1\gamma_2$ (180 nM). This assay is described in greater detail in Chapter 3. Ten peptides were suspended in DMSO at a concentration of 10 mM and tested at concentration ranges from 100 μM to 10 nM in the assay. Of the ten peptides tested, the peptide corresponding to residues 2-24 on $G\gamma_2$ was highly potent, with an IC_{50} of 7.7 μM (95% CI: 4.8 to 12.2 μM). (Fig. 37) $G\gamma_1$ 2-24 was 5-fold less potent with an IC_{50} of 39.3 μM (95% CI: 15.3 to 100 μM). $G\gamma_2$ 29-45 was unable to inhibit the interaction,

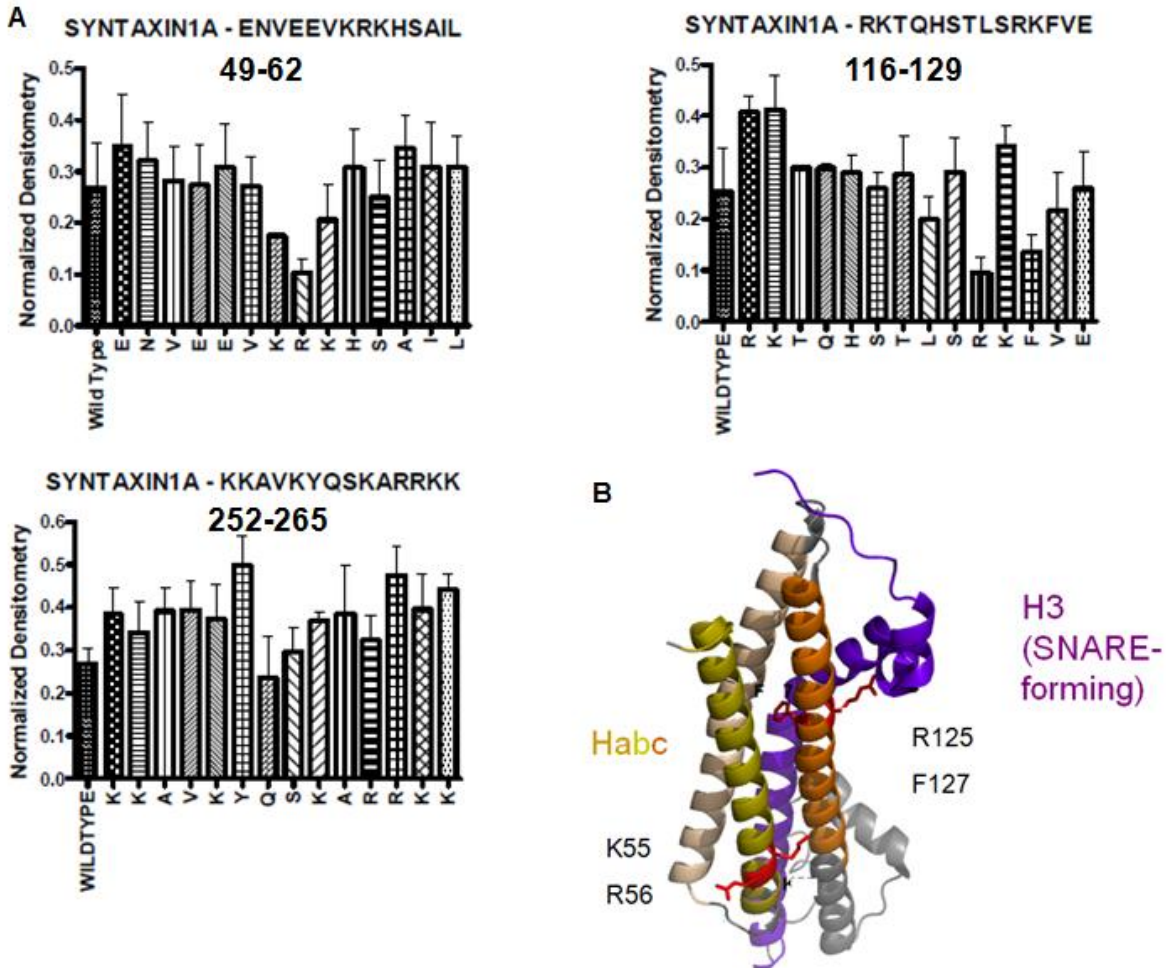

Figure 35. Peptide mapping approach for identifying Gβγ-binding residues on Stx1A.

A: Densitometric analysis of each of the three peptides identified from the ResPep peptide mapping approach. The peptides correspond to residues 49-62, 116-129, and 252-265. Each letter corresponds to a given residue mutated to Ala. Normalized densitometric values were compared to wild-type via Student's *t*-test. B: Structure of the Gβγ-binding residues of interest mapped in red onto the Habc domain of syntaxin (PDB: 1S94). Structure adapted from Bracher A, Weissenhorn W, (2004) *BMC Struct. Biol.*. **4:** 6-6

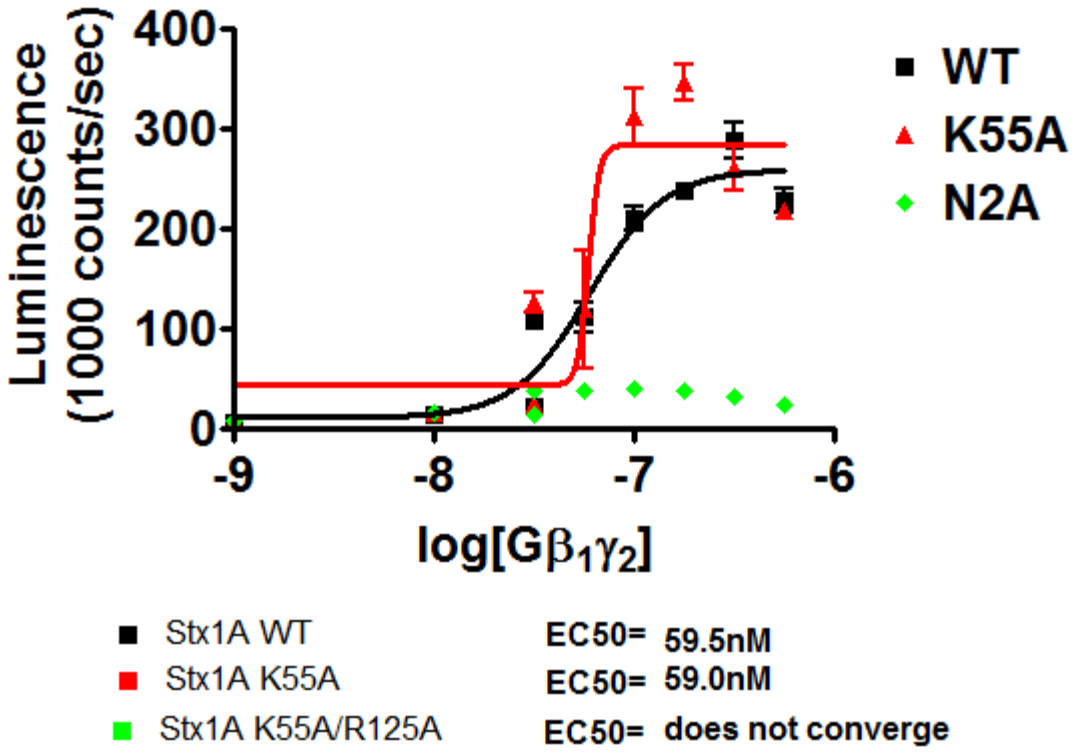

Figure 36: The Stx1A K55A R125A mutant exhibits inhibited Gβγ -SNARE binding.

Alphascreen concentration-response curves for Stx1A WT, Stx1A K55A and Stx1A K55A/R125A. .The EC_{50} for the binding of Stx1A WT to $G\beta_1\gamma_2$ is 59.5nM. The EC_{50} for the binding of Stx1A K55A to $G\beta_1\gamma_2$ is 59.0nM. To obtain accurate EC_{50} values, the 1μM condition was tested, but not included in the EC_{50} calculation, as syntaxin 1A exhibits a considerable "hooking effect" at this concentration in the Alphascreen assay that can interfere with EC_{50} estimation. The K55A/R125A mutant did not exhibit a meaningful concentration-dependent binding to $G\beta_1\gamma_2$.

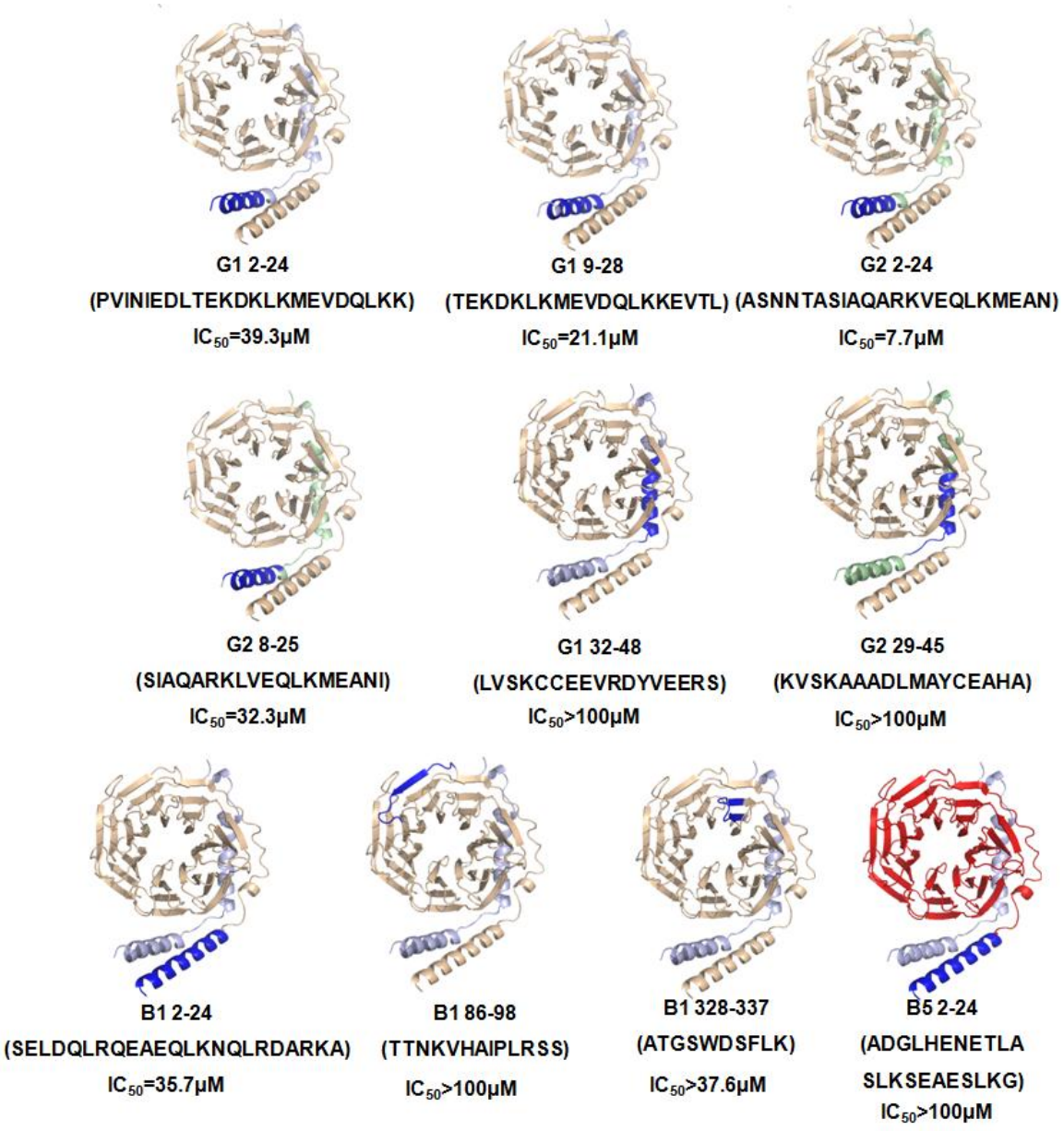

Figure 37. Gβ and Gγ peptides can disrupt the Gβγ-SNAP25 interaction in a concentration-dependent manner.

Peptides superimposed over structure of Gβγ subunit(brown for Gβ1, red for Gβ5, grey for Gγ1, green for Gγ2) with residues shown underneath. The area on the structure corresponding to each peptide is depicted in dark blue. IC_{50} values obtained from the Gβγ-SNAP25 Alphascreen competition binding assay, described in Chapter 3. For the purposes of accurate IC_{50} estimation, an additional minima point is added at 300μM: actual concentrations tested end at 100μM. Structure adapted from Sondek J, Bohm A, Lambright DG, Hamm HE, Sigler PB. *Nature.* 1996 Jan 25;379(6563):369-74. (PDB: 1TBG)

while the $G\gamma_1$ 32-48 peptide had an IC_{50} greater than 100 μM. The N-terminus of Gβ, adjacent to Gγ, was also able to inhibit the interaction in a concentration-dependent manner, with $G\beta_1$ 2-24 inhibiting the interaction with an IC_{50} of 35.6 μM (95% CI: 17.3 to 73.4 μM). $G\beta_5$ 2-24, the isoform with the least homology to $G\beta_1$, was unable to inhibit the interaction to any meaningful extent. Importantly, the $G\beta_1$ 328-337 peptide, containing the key SNARE-interacting residue W332, inhibited the interaction with a potency of 37.6 μM (95% CI: 19.0 to 74 μM). We then generated purified His-tagged $G\beta_1\gamma_2$ K78/W332A proteins from SF9 cells and measured their ability to bind GST-tagged SNAP25 in the GST-pull down assay. However, their ability to bind SNAP25 could not be ascertained by this assay, as the mutant precipitated during the assay and produced a signal in the non-specific binding controls. (data not shown) To investigate this further, other approaches, utilizing total internal reflection microscopy, to examine a fluorescently-labeled double mutant interacting with SNAREs embedded in a lipid bilayer, are currently being pursued by the Alford lab.

It is currently unknown whether Gβγ can compete with other calcium sensors for competition in the same way that it can compete with Syt1. We sought to investigate whether the calcium sensor Doc2, which is implicated in asynchronous release [99], was also able to compete with Gβγ for binding sites upon SNAP25. We purified Doc2β C2AB fragments using a similar purification scheme to Syt1 C2AB. Doc2β-Ca^{2+} C2AB is the most potent inhibitor of the Gβγ-SNAP25 interaction known, with an IC_{50} of 461 nM (95% CI: 379-562 nM).(Fig. 38),. Much like apo-Syt1 C2AB, apo-Doc2β C2AB is less potent than Doc2B-Ca^{2+} C2AB, with an IC_{50} of 1.60 μM (95% CI: 952 nM to 2.67μM), . This data suggests that Doc2 may compete with Gβγ for binding sites upon SNAREs in asynchronous or spontaneous release.

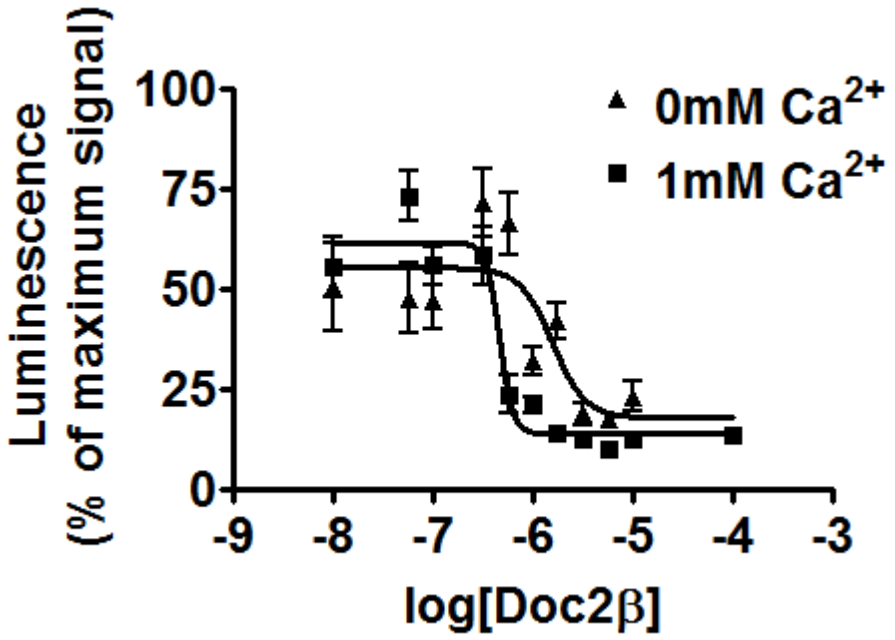

Figure 38: Doc2 can disrupt the Gβγ-SNAP25 interaction in a calcium-dependent manner.

Alphascreen competition binding experiment in which a range of concentrations of a recombinant fragment of apo-Doc2β or Doc2β-Ca^{2+} lacking the transmembrane domain along with an EC_{80} concentration of $G\beta_1\gamma_2$ (180μM) are incubated with SNAP25. Competition binding experiments were carried out in the presence and absence of 1mM $CaCl_2$. For the purposes of accurate IC_{50} estimation, an additional minima point is added at 100μM: actual concentrations tested end at 10μM. The experiments were repeated once for two independent experiments.

Discussion

Here, we have conducted preliminary studies indicating potential binding sites for Gβγ upon Stx1A. We have identified two residues upon Stx1A for which mutation to Ala abolishes the ability to interact with Gβγ. Syntaxin 1A, in tandem with Munc18, moves from a "closed" to an "open" conformation with the movement of the H_{abc} domain away from the remainder of the SNARE complex [109,293]. Given the importance of the H_{abc} domain from our mutagenesis studies, it is unclear whether the "open" or "closed" conformation is relevant to Gβγ binding. We made efforts to mutagenize the Stx1A to lock it in a "closed" conformation, but the mutagenesis PCR reaction was not successful in any of the conditions tested. Differences in the "docked" state and the fully-zipped fusion-competent SNARE complex [92,139,239] with regards to Gβγ binding have also yet to be investigated.

With regards to the residues on Stx1A identified by ResPep, curiously, the H_{abc} domain alone was unable to bind Gβγ in fluorescence intensity binding experiments[201]. It has been reported that the Gβγ binding site is located at the N-terminus of the H_3 domain[191]. Both of these studies utilize protein fragments: the H_{abc} domain may not be able to adopt the proper conformation in the absence of the H_3 domain to bind Gβγ. Our data shows an instrumental role for the H_{abc} domain in mediating the interaction of Gβγ with Stx1A. It is possible that the H_3 domain is required for the H_{abc} domain to reach the required conformation to bind Gβγ. Potentially, cell-based results could be complicated by the requirement of the Stx1A construct to contain the BoNT/C resistance mutation K253I. $G_{i/o}$-coupled GPCR-mediated inhibition of exocytosis may be bypassed in the K253I mutant alone. The K253A mutant was still able to bind Gβγ in a concentration-dependent manner: the possibility exists for the K253I mutant to have reduced ability to bind as a result of the hydrophobic nature of isoleucine with respect to alanine. BoNT/C cleaves SNAP25 at R198A, much like BoNT/A[294], and transfection with Stx1A alone may be inadequate to rescue exocytosis. To investigate the role of the K55A R125A mutation upon $G_{/o}$-coupled GPCR-mediated inhibition of exocytosis, several approaches were

considered. Injection of purified Stx1A K253I monomers into lamprey RS axons was deemed infeasible due to solubility issues with the Stx1A transmembrane domain. Injection of a palmitoylation-site containing syntaxin[71] lacking the transmembrane domain was considered, but rejected due to difficulties making the construct and issues with ensuring palmitoylation. Instead, we are developing a lamprey transfection approach in tandem with the Alford lab. To verify that transfection occurred within the intact lamprey CNS, constructs were ligated into pcDNA-IRES-GFP, a vector containing a GFP transcript after an internal ribosome entry site to ensure two polypeptides were translated: Stx1A and GFP as a fluorescent marker indicating transfection. The Stx1A N2A transcript containing a K253I mutation for BoNT/C resistance was successfully ligated into this vector. We will take this vector and express it in intact lamprey CNS using the protocol described above. After that, paired recordings between lamprey RS axons and neurons of the spinal ventral horn will be obtained.

We have identified several peptides corresponding to regions on Gβ and Gγ which can compete with full-length Gβγ subunits for binding to SNARE. Consistent with previously published studies[48,50], peptides corresponding to $G\gamma_2$ are more potent than peptides corresponding to $G\gamma_1$. These studies indicate that he binding of Gβγ to SNARE bears similarities to the binding of Gβγ to adenylyl cyclase II, in that the amino acid sequence of Gγ (and not just the prenyl modification) is important for its binding to SNARE. However, $G\gamma_1$ peptides are capable of binding to SNARE, while full-length $G\beta_1\gamma_1$ is unable to activate adenylyl cyclase II[50]. ResPep peptide binding studies in which individual residues within peptides are mutagenized to Ala are an important future experiment for identifying individual SNARE-binding residues upon Gβγ. In addition, the ability of these mutant Gβγ subunits to disrupt vesicle fusion must be investigated. Since wild-type Gβγ is present in all secretory cells, experiments for this would ideally be conducted in *in vitro* systems of reconstituted fusion, where the ability of SNARE-containing liposomes to fuse in the presence of wild-type or mutant Gβγ is investigated.

Finally, we have shown that the calcium sensor Doc2, implicated in spontaneous[100] and asynchronous release[99], may be able to compete with Gβγ for binding to SNARE. Potentially, this implies that C2AB proteins in general may able to compete with Gβγ for binding sites upon SNARE. However, in hippocampal CA1 synapses, neither the amplitude nor distribution of Sr^{2+}-evoked asynchronous release, nor spontaneous mini-EPSCs, were altered by $5\text{-}HT_{1b}$ receptor[208] activation, a mechanism thought to occur via Gβγ-SNARE. A second C2-domain containing protein of interest is Munc13, which has three C2 domains spread throughout its primary sequence. Munc13 is critical for vesicle priming and can promote fusion in tandem with Munc18 in the absence of Syt1[57]. It has yet to be determined whether Munc13 is able to compete with Gβγ for SNARE, and what role, if any, this may play in $G_{i/o}$-coupled GPCR-mediated inhibition of exocytosis.

CHAPTER VII:

SUMMARY AND FUTURE DIRECTIONS

The studies contained in this dissertation contain numerous insights into the molecular requirements of the Gβγ-SNARE interaction. To briefly summarize the conclusions, we have identified a number of residues on SNAP25 and Stx1A that are required for Gβγ binding, as well as preliminary studies to investigate certain residues that are crucial for the binding of Gβ and Gγ to SNAREs. We have generated SNAP25 mutants that are deficient in both Gβγ binding and $G_{i/o}$-coupled GPCR signaling, providing additional evidence linking the Gβγ-SNARE interaction to $G_{i/o}$-coupled GPCR-mediated regulation of exocytosis. In addition, we have developed effector-selective small molecule modulators of the Gβγ-SNAP25 interaction with micromolar potency. These small molecules are able to interfere with the action of $G_{i/o}$-coupled GPCRs in *ex vivo* systems. This is a second argument demonstrating the importance of the Gβγ-SNARE interaction to certain types of $G_{i/o}$-coupled GPCR signaling. Finally, we have begun to characterize the phenotype of a mouse that is deficient in the Gβγ-SNARE interaction, the SNAP25Δ3 mouse. These studies form the basis for futher investigations to identify potential pathophysiological states in which the Gβγ-SNARE interaction may be dysregulated, as well as future molecular studies to yield additional insights into $G_{i/o}$-coupled GPCR-mediated regulation of exocytosis.

One important key finding was the identification of a second N-terminal region on SNAP25 for Gβγ binding[244]. Four Gβγ-binding residues were found in close proximity to each other within this site, all located on the SN2 helix . The N-terminal residues R135, R136, R142, and R161 are in close proximity to the N-terminus of Stx1A, which has been shown to be important for the Gβγ-calcium channel interaction [191]. The functional importance of each of the two binding sites has yet to be fully explored: one potential area of interest is for the functional importance of the N-terminal binding site

alone. The SNAP25 N4A construct has reduced ability to bind Gβγ, but nothing is known about its ability to support $G_{i/o}$-coupled GPCR-mediated inhibition of exocytosis downstream of or at calcium channels. Functional studies with N4A and 5A in a system that expresses both Gβγ-calcium channel signaling and Gβγ-SNARE signaling would expand our understanding of the synaptic microarchitecture. Hippocampal CA1 cultures such as those used in previous studies[208], expressing both 5-$HT1_b$ and $GABA_b$ receptors, would be a viable system for such an experiment.

We were able to show that a SNAP25 lacking two C-terminal Gβγ-binding residues was still able to bind Gβγ, but binding (and the inhibitory effect on exocytosis) for a mutant lacking both the N-and C-terminal residues was almost absent. Less drastic mutations have a less severe phenotype: selective Ala mutagenesis of the two Gβγ-binding residues R198 and K201 results in a SNAP25 with partially reduced affinity for Gβγ, while proteolytic removal of the R198 and K201 and the extreme C-terminus from SNAP25 resulted in $G_{i/o}$-coupled GPCRs no longer being able to inhibit exocytosis[48,153,197,201,292] . Charge-reversal mutations to these residues block exocytosis[255,292] and reduce calcium-dependent binding of Syt1 to SNAP25. This reduced calcium-dependent binding could form the basis for the reduced secretion observed in this mutant.

A second area of inquiry is centered around the molecular requirements for Gβ and Gγ binding to SNAREs. Due to the challenge of making mutant Gβγ subunits, little is known about the residues on Gβ and Gγ required for this process. The development of transfectable secretory cell systems, such as the pHluorin studies used to test the effect of the compounds upon the α_{2a} adrenergic receptor in CA1/CA3 cultures, may assist us in investigating these residues. One limitation of this approach is that loss-of-function studies are challenging to conduct in overexpression systems, as functional wild-type Gβγ is still present.

Mechanistic studies of Gβγ-mediated inhibition of exocytosis.

We have reaffirmed the importance of previous studies suggesting that Gβγ competes with synaptotagmin for binding sites upon SNARE to inhibit exocytosis[201]. Our studies have been conducted in the absence of lipid membranes, which may result in altered functionality of SNAREs or synaptotagmin. Studies such as co-flotation or fusion assays [130]in lipid vesicles may yield additional insights into the Gβγ-SNARE mechanism. Furthermore, all of our synaptotagmin functional studies have been performed in the absence of complexin, which is now thought to be an essential component of the fusion machinery[57]. Synaptotagmin's calcium-dependent action on synchronous release is thought to involve the melting of the complexin accessory helix [132]. $G_{i/o}$-coupled GPCRs can become activated before a depolarizing signal arrives at the active zone, presumably resulting in Gβγ binding to SNARE. A critical question to be answered in the future is whether Gβγ can still bind to SNARE and compete with synaptotagmin in a calcium-dependent manner to the five-helix SNARE bundle containing complexin embedded in lipid membranes. Some evidence exists to support this hypothesis: the kinetics of studies in intact secretory cells demonstrate that Gβγ acts on the docked and primed SNARE complex. If Gβγ does not behave in this manner in a future co-flotation experiment, Gβγ must perturb the stoichiometry of this complex via an alternative, unknown mechanism. How does the presence of Gβγ affect complexin binding to the four-helix SNARE bundle? Does the presence of Gβγ on the SNARE affect the stability of the complexin accessory helix, perturbing the action of synaptotagmin? Increasingly elaborate functional studies will answer these questions.

The microarchitecture of inhibitory signaling at the synapse.

In Hamid and Alford, [208], we showed distinct differences in the signaling mechanisms for different GPCRs. The 5-HT_{1B} receptor signaled purely through the Gβγ-SNARE interaction, while the $GABA_B$ receptor acted exclusively by modulating calcium currents through Gβγ. Cleavage of SNAREs with BoNT/C resulted in the 5-HT_{1B} receptor being able to signal through calcium currents. We hypothesize that the N-terminal residues R135, R136, R142, and R161 upon SNAP25 may be required for this effect,

as these residues are in close proximity to the N-terminus of the H_3 domain on Stx1A. It may be that the proteolysis of the SNARE alters the synaptic microarchitecture in such a way to give the Gβγ access to the calcium channel. These studies are in contrast to others conducted with BoNT/C, where cleavage of syntaxin inhibited the ability of $G_{i/o}$-coupled GPCRs to inhibit calcium currents [189,191].

The action of inhibitory GPCRs in islets and neurons has been reported to be dependent upon calcineurin, with calcineurin inhibitors abolishing the ability of them to inhibit exocytosis[220,295]. We hypothesize that calcineurin may be required for $G_{i/o}$-coupled GPCRs to inhibit exocytosis. The phosphorylation target of calcineurin is currently unknown. Yakel hypothesized that the site was the PKC site on the voltage-gated calcium channel[295]. This does not explain the calcineurin dependence observed in the action of the α_{2A} adrenergic receptor in the beta cell, where this receptor has been shown to signal via Gβγ-SNARE instead of through Gβγ-calcium channel interactions[153]. It may be that the target of calcineurin is tau: a recognized calcineurin substrate, hyperphosphorylated tau results in microtubule disorganization[296]. Tubulin binds heterotrimeric G proteins, including $G\alpha_{i1}$[297]. It may be reasonable to hypothesize that perturbations in tau dephosphorylation by calcineurin may affect delivery of heterotrimeric G protein to the synaptic microarchitecture, disrupting the function of $G_{i/o}$-coupled GPCRs. Recent advances in super-resolution microscopy may make imaging of the synaptic microarchitecture feasible to confirm the hypotheses stated above.

Ongoing development of Gβγ-SNARE inhibitors.

We have developed small-molecule modulators of the Gβγ-SNARE interaction that are selective for it relative to other Gβγ effectors. Our lead compound, VU0657640, inhibits the interaction in a concentration-dependent manner with single-digit micromolar potency. Efforts to develop the potency of VU0657640 have not proven successful, with several analogues displaying potency that is not significantly different from VU0657640, and the majority thereof being weaker. This potency is roughly

fourfold lower than the previous lead compound, VU0476078. However, we can say with confidence that VU0657640 is the active molecule in the solution, as we have tested three batches of this material, all of which have similar potency. This is a significant step forward from the batch variability of VU0476078, in which two batches displayed activity, while many more did not. Structure-activity relationship studies of VU0657640 will continue. In addition, we will characterize the potency of VU0657640 at inhibiting various Gβγ-effector interactions: the Gβγ-calcium channel interaction and the Gβγ-GIRK channel interaction are two immediate studies to be conducted. Metabolism and ancillary pharmacological properties of VU0657640 may also be worth investigating, especially if it is eventually deemed appropriate to conduct *in vivo* testing of the compound. *In vivo* testing may be used to determine if the molecule could be beneficial in rodent models of mental illness, or in metabolic studies, such as glucose tolerance tests. It may be possible to utilize VU0657640 to identify new physiological systems in which the Gβγ-SNARE interaction may play a role. However, a more potent analogue would be highly advantageous, as ancillary pharmacology panels often characterize compounds at 10 μM, a concentration slightly above the IC_{50} for VU0657640. A tenfold rise in potency would probably render many of these studies feasible, since low-potency compounds may not reach the required EC_{50} values in the target tissue without excessive dosages that may result in unacceptable ancillary pharmacology. Gallein, a Gβγ inhibitor with a potency in the hundreds of nM, has been utilized for *in vivo* studies of heart failure[268], amongst others[265,298]. Development of existing small molecule Gβγ-SNARE inhibitors is an ongoing goal of our research.

The pathophysiological relevance of the Gβγ-SNARE interaction.

We have developed a number of interesting new tools to study the pathophysiological relevance of the Gβγ-SNARE interaction. Selective Gβγ-SNARE inhibitors enhanced glucose-stimulated insulin release, potentially implying a role for the interaction in the regulation of that process. The SNAP25Δ3 mouse represents the first transgenic mouse deficient in the Gβγ-SNARE interaction. We were not yet able to

use this model to complement previous studies confirming a role for the Gβγ-SNARE interaction in the role of α_{2a} adrenergic receptor-mediated regulation of insulin release[153]. However, many studies remain to be conducted. Studies of neuronal function, both electrophysiological and behavioral, have yet to be performed. Pain and the perception thereof may be a compelling area to investigate due to the importance of the Gβγ-SNARE interaction in several cell types implicated in this area[197]. Two independent groups have reported an important role for the Gβγ-SNARE interaction the hippocampus[205,208], making hippocampal functions, such as spatial memory, another highly enticing area for investigation. Our compounds represent potential therapeutic options to treat diseases in which Gi/o-coupled GPCRs have been implicated. Rodent behavioral models can have predictive value for identifying potential treatments for these conditions. Investigating Gβγ-SNARE inhibitors in these models may be of value when the compounds are more potent and better characterized. Ultimately, the development of transgenic animals and compounds enable us to investigate the importance of the Gβγ-SNARE interaction in a wide variety of secretory cells that contain inhibitory $G_{i/o}$-coupled GPCRs that regulate vesicle release.

REFERENCES

1 Oldham, W. M. & Hamm, H. E. Heterotrimeric G protein activation by G-protein-coupled receptors. *Nat Rev Mol Cell Biol* **9**, 60 (2008).

2 Rosenbaum, D. M., Rasmussen, S. G. F. & Kobilka, B. K. The structure and function of G-protein-coupled receptors. *Nature* **459**, 356-363 (2009).

3 Oldham, W. M. & Hamm, H. E. How do receptors activate G proteins? *Advances in Protein Chemistry* 74 67-93 (2007)

4 Dandan, Z., Qiang, Z. & and Beili, W. Structural Studies of G Protein-Coupled Receptors. *Mol. Cells* **38**, 836-842 (2015).

5 Cherezov, V., Rosenbaum, D. M., Hanson, M. A., Rasmussen, S. G. F., Thian, F. S., Kobilka, T. S., Choi, H.-J., Kuhn, P., Weis, W. I., Kobilka, B. K. & Stevens, R. C. High Resolution Crystal Structure of an Engineered Human β(2)-Adrenergic G protein-Coupled Receptor. *Science* **318**, 1258-1265 (2007).

6 Rasmussen, S. G. F., Choi, H.-J., Rosenbaum, D. M., Kobilka, T. S., Thian, F. S., Edwards, P. C., Burghammer, M., Ratnala, V. R. P., Sanishvili, R., Fischetti, R. F., Schertler, G. F. X., Weis, W. I. & Kobilka, B. K. Crystal structure of the human β2 adrenergic G-protein-coupled receptor. *Nature* **450**, 383-387(2007).

7 Rasmussen, S. G. F., DeVree, B. T., Zou, Y., Kruse, A. C., Chung, K. Y., Kobilka, T. S., Thian, F. S., Chae, P. S., Pardon, E., Calinski, D., Mathiesen, J. M., Shah, S. T. A., Lyons, J. A., Caffrey, M., Gellman, S. H., Steyaert, J., Skiniotis, G., Weis, W. I., Sunahara, R. K. & Kobilka, B. K. Crystal structure of the β2 adrenergic receptor-G_s protein complex. *Nature* **477**, 549-555, (2011).

8 Palczewski, K., Kumasaka, T., Hori, T., Behnke, C. A., Motoshima, H., Fox, B. A., Trong, I. L., Teller, D. C., Okada, T., Stenkamp, R. E., Yamamoto, M. & Miyano, M. Crystal Structure of Rhodopsin: A G Protein-Coupled Receptor. *Science* **289**, 739-745 (2000).

9 Farrens, D. L., Altenbach, C., Yang, K., Hubbell, W. L., Khorana H. G. Requirement of rigid-body motion of transmembrane helices for light activation of rhodopsin. *Science* **274**, 768-770 (1996).

10 De Lean, A., Stadel, J. M. & Lefkowitz, R. J. A ternary complex model explains the agonist-specific binding properties of the adenylate cyclase-coupled beta-adrenergic receptor. *Journal of Biological Chemistry* **255**, 7108-7117 (1980).

11 Conklin, B. R. & Bourne, H. R. Structural elements of Gα subunits that interact with Gβγ, receptors, and effectors. *Cell* **73**, 631-641(1993).

12 Blahos, J., Mary, S., Perroy, J., de Colle, C., Brabet, I., Bockaert, J. & Pin, J.-P. Extreme C Terminus of G Protein α-Subunits Contains a Site That Discriminates between G_i-coupled Metabotropic Glutamate Receptors. *Journal of Biological Chemistry* **273**, 25765-25769 (1998).

13 Kostenis, E., Conklin, B. R. & Wess, J. Molecular Basis of Receptor/G Protein Coupling Selectivity Studied by Coexpression of Wild Type and Mutant M2 Muscarinic Receptors with Mutant $G\alpha_q$ Subunits. *Biochemistry* **36**, 1487-1495, 1997).

14 Nygaard, R., Frimurer, T. M., Holst, B., Rosenkilde, M. M. & Schwartz, T. W. Ligand binding and micro-switches in 7TM receptor structures. *Trends in Pharmacological Sciences* **30**, 249-259, (2009).

15 Bruchas, M. R. & Chavkin, C. Kinase Cascades and Ligand-Directed Signaling at the Kappa Opioid Receptor. *Psychopharmacology* **210**, 137-147 (2010).

16 Kang, D. S., Tian, X. & Benovic, J. L. Role of β-arrestins and arrestin domain-containing proteins in G protein-coupled receptor trafficking. *Current Opinion in Cell Biology* **27**, 63-71(2014).

17 Shenoy, S. K. & Lefkowitz, R. J. β-arrestin-mediated receptor trafficking and signal transduction. *Trends in Pharmacological Sciences* **32**, 521-533(2011).
18 Gurevich, V. V. & Gurevich, E. V. How and why do GPCRs dimerize? *Trends in Pharmacological Sciences* **29**, 234-240(2008).
19 El Moustaine, D., Granier, S., Doumazane, E., Scholler, P., Rahmeh, R., Bron, P., Mouillac, B., Banères, J.-L., Rondard, P. & Pin, J.-P. Distinct roles of metabotropic glutamate receptor dimerization in agonist activation and G-protein coupling. *Proceedings of the National Academy of Sciences of the United States of America* **109**, 16342-16347 (2012).
20 Galvez, T., Duthey, B., Kniazeff, J., Blahos, J., Rovelli, G., Bettler, B., Prézeau, L. & Pin, J.-P. Allosteric interactions between GB1 and GB2 subunits are required for optimal $GABA_B$ receptor function. *The EMBO Journal* **20**, 2152-2159 (2001).
21 Sánchez-Martín, L., Sánchez-Mateos, P. & Cabañas, C. CXCR7 impact on CXCL12 biology and disease. *Trends in Molecular Medicine* **19**, 12-22(2013).
22 Balabanian, K., Lagane, B., Infantino, S., Chow, K. Y. C., Harriague, J., Moepps, B., Arenzana-Seisdedos, F., Thelen, M. & Bachelerie, F. The Chemokine SDF-1/CXCL12 Binds to and Signals through the Orphan Receptor RDC1 in T Lymphocytes. *Journal of Biological Chemistry* **280**, 35760-35766 (2005).
23 Kalderon, D. The mechanism of hedgehog signal transduction. *Biochemical Society Transactions* **33**, 1509-1512 (2005).
24 Ruiz-Gómez, A., Molnar, C., Holguín, H., Mayor Jr, F. & de Celis, J. F. The cell biology of Smo signalling and its relationships with GPCRs. *Biochimica et Biophysica Acta (BBA) - Biomembranes* **1768**, 901-912(2007).
25 Riobo, N. A., Saucy, B., DiLizio, C. & Manning, D. R. Activation of heterotrimeric G proteins by Smoothened. *Proceedings of the National Academy of Sciences* **103**, 12607-12612, (2006).
26 Kotani, T. Protein kinase A activity and Hedgehog signaling pathway. *Vitamins & Hormones* **88**, 273-291 (2012).
27 Wilkie T. M, Gilbert D. J., Olsen S. A, Chen X-N., Amatruda T. T., Korenberg J. R., Trask B. J., de Jong P., Reed R. R., Simon M. I, Jenkins N. A. & Copeland N. G. Evolution of the mammalian G protein alpha subunit multigene family. *Nature Genetics* **1**, 85-91 (1992).
28 Yokoyama S, S. W. Phylogeny and evolutionary rates of G protein alpha subunit genes. *J Mol Evol* **35**, 230-238 (1992).
29 Simon MI, S. M., Gautam N. Diversity of G proteins in signal transduction. *Science* **252**, 802-808 (1991).
30 Siehler, S. Regulation of RhoGEF proteins by $G_{12/13}$-coupled receptors. *British Journal of Pharmacology* **158**, 41-49(2009).
31 Sassone-Corsi, P. The Cyclic AMP Pathway. *Cold Spring Harbor Perspectives in Biology* **4** (2012).
32 Kach, J., Sethakorn, N. & Dulin, N. O. A finer tuning of G-protein signaling through regulated control of RGS proteins. *American Journal of Physiology - Heart and Circulatory Physiology* **303**, H19-H35 (2012).
33 Smotrys, J. E. & Linder, M. E. Palmitoylation of Intracellular Signaling Proteins: Regulation and Function. *Annual Review of Biochemistry* **73**, 559-587 (2004).
34 Chen C. A, Manning D. R. Regulation of G proteins by covalent modification. *Oncogene* **20**, 1643-1652 (2001).
35 Downes, G. B. & Gautam, N. The G protein subunit gene families. *Genomics* **62**, 544-552 (1999).
36 Hildebrandt, J. D. Role of subunit diversity in signaling by heterotrimeric G proteins. *Biochemical Pharmacology* **54**, 325-339(1997).
37 Chen, Y., Weng, G., Li, J., Harry, A., Pieroni, J., Dingus, J., Hildebrandt, J. D., Guarnieri, F., Weinstein, H. & Iyengar, R. A surface on the G protein beta-subunit involved in interactions with adenylyl cyclases. *Proc Natl Acad Sci U S A* **94**, 2711-2714 (1997).

38 Hooks, S. B., Waldo, G. L., Corbitt, J., Bodor, E. T., Krumins, A. M. & Harden, T. K. RGS6, RGS7, RGS9, and RGS11 stimulate GTPase activity of G_i family G-proteins with differential selectivity and maximal activity. *J Biol Chem* **278**, 10087-10093 (2003).
39 Willardson, B. & Tracy, C. in *GPCR Signalling Complexes – Synthesis, Assembly, Trafficking and Specificity Subcellular Biochemistry* **63** 131-153 (2012).
40 Clapham, D. E. & Neer, E. J. G protein βγ subunits. *Annu Rev Pharmacol Toxicol* **37**, 167-203 (1997).
41 Sondek, J., Bohm, A., Lambright, D. G., Hamm, H. E. & Sigler, P. B. Crystal structure of a G-protein βγ dimer at 2.1A resolution. *Nature* **379**, 369-374 (1996).
42 Dingus, J., Wells, C. A., Campbell, L., Cleator, J. H., Robinson, K. & Hildebrandt, J. D. G Protein βγ Dimer Formation: Gβ and Gγ Differentially Determine Efficiency of in Vitro Dimer Formation†. *Biochemistry* **44**, 11882-11890 (2005).
43 Fletcher, J. E., Lindorfer, M. A., DeFilippo, J. M., Yasuda, H., Guilmard, M. & Garrison, J. C. The G Protein β_5 Subunit Interacts Selectively with the G_q α Subunit. *Journal of Biological Chemistry* **273**, 636-644 (1998).
44 Ford, C. E., Skiba, N. P., Bae, H., Daaka, Y., Reuveny, E., Shekter, L. R., Rosal, R., Weng, G., Yang, C. S., Iyengar, R., Miller, R. J., Jan, L. Y., Lefkowitz, R. J. & Hamm, H. E. Molecular basis for interactions of G protein βγ subunits with effectors. *Science* **280**, 1271-1274 (1998).
45 Touhara, K., Inglese, J., Pitcher, J. A., Shaw, G. & Lefkowitz, R. J. Binding of G protein βγ-subunits to pleckstrin homology domains. *Journal of Biological Chemistry* **269**, 10217-10220 (1994).
46 Preininger, A. M., Henage, L. G., Oldham, W. M., Yoon, E. J., Hamm, H. E. & Brown, H. A. Direct Modulation of Phospholipase D Activity by Gβγ. *Molecular Pharmacology* **70**, 311-318 (2006).
47 Lim, W. K., Myung, C.-S., Garrison, J. C. & Neubig, R. R. Receptor−G Protein γ Specificity: γ_{11} Shows Unique Potency for A_1 Adenosine and 5-HT_{1A} Receptors†. *Biochemistry* **40**, 10532-10541(2001).
48 Blackmer, T., Larsen, E. C., Bartleson, C., Kowalchyk, J. A., Yoon, E. J., Preininger, A. M., Alford, S., Hamm, H. E. & Martin, T. F. G protein βγ directly regulates SNARE protein fusion machinery for secretory granule exocytosis. *Nat Neurosci* **8**, 421-425 (2005).
49 Kerchner, K. R., Clay, R. L., McCleery, G., Watson, N., McIntire, W. E., Myung, C.-S. & Garrison, J. C. Differential Sensitivity of Phosphatidylinositol 3-Kinase p110γ to Isoforms of G Protein βγ Dimers. *Journal of Biological Chemistry* **279**, 44554-44562 (2004).
50 Myung, C.-S., Yasuda, H., Liu, W. W., Harden, T. K. & Garrison, J. C. Role of Isoprenoid Lipids on the Heterotrimeric G Protein γ Subunit in Determining Effector Activation. *Journal of Biological Chemistry* **274**, 16595-16603 (1999).
51 Purves, D., Augustine, G., Fitzpatrick, D., Hall ,W.C., LaMantia, A.S., McNamara, J.O., White, L.E. *Neuroscience, 4th Edition*. (2008).
52 Hall, J.E, Guyton, A. The Textbook of Medical Physiology. 11th ed. (2005).
53 Pohorecky, L. A. & Wurtman, R. J. Adrenocortical Control of Epinephrine Synthesis. *Pharmacological Reviews* **23**, 1-35 (1971).
54 Pang, Z. P. & Südhof, T. C. Cell Biology of Ca^{2+}-Triggered Exocytosis. *Current Opinion in Cell Biology* **22**, 496-505 (2010).
55 Rizo, J. & Südhof, T. C. The Membrane Fusion Enigma: SNAREs, Sec1/Munc18 Proteins, and Their Accomplices—Guilty as Charged? *Annual Review of Cell and Developmental Biology* **28**, 279-308, (2012).
56 Südhof, Thomas C. Neurotransmitter Release: The Last Millisecond in the Life of a Synaptic Vesicle. *Neuron* **80**, 675-690 (2013).
57 Rizo, J. & Xu, J. The Synaptic Vesicle Release Machinery. *Annual Review of Biophysics* **44**, 339-367(2015).

58 Südhof, T. C. & Rothman, J. E. Membrane Fusion: Grappling with SNARE and SM Proteins. *Science* **323**, 474-477 (2009).
59 Teng, F. Y. H., Wang, Y. & Tang, B. L. The syntaxins. *Genome Biology* **2**, reviews3012.3011-reviews3012.3017 (2001).
60 Jahn, R. & Scheller, R. H. SNAREs- engines for membrane fusion. *Nat Rev Mol Cell Biol* **7**, 631-643 (2006).
61 Ravichandran, V., Chawla, A. & Roche, P. A. Identification of a Novel Syntaxin- and Synaptobrevin/VAMP-binding Protein, SNAP-23, Expressed in Non-neuronal Tissues. *Journal of Biological Chemistry* **271**, 13300-13303 (1996).
62 Zhu, Q., Yamakuchi, M. & Lowenstein, C. J. SNAP23 Regulates Endothelial Exocytosis of von Willebrand Factor. *PLoS ONE* **10**, e0118737(2015).
63 Mendez, M. & Gaisano, H. Y. Role of the SNARE protein SNAP23 on cAMP-stimulated renin release in mouse juxtaglomerular cells. *American Journal of Physiology - Renal Physiology* **304**, F498-F504 (2013).
64 Rapaport, D., Lugassy, Y., Sprecher, E. & Horowitz, M. Loss of SNAP29 Impairs Endocytic Recycling and Cell Motility. *PLoS ONE* **5**, e9759(2010).
65 Williams, C. M., Savage, J. S., Harper, M. T., Moore, S. F., Hers, I. & Poole, A. W. Identification of roles for the SNARE-associated protein, SNAP29, in mouse platelets. *Platelets*, 1-9, (2015).
66 Su, Q., Mochida, S., Tian, J.-H., Mehta, R. & Sheng, Z.-H. SNAP-29: A general SNARE protein that inhibits SNARE disassembly and is implicated in synaptic transmission. *Proceedings of the National Academy of Sciences* **98**, 14038-14043 (2001).
67 Li, F., Pincet, F., Perez, E., Eng, W. S., Melia, T. J., Rothman, J. E. & Tareste, D. Energetics and dynamics of SNAREpin folding across lipid bilayers. *Nat Struct Mol Biol* **14**, 890-896(2007).
68 Weber, T., Zemelman, B. V., McNew, J. A., Westermann, B., Gmachl, M., Parlati, F., Sollner, T. H. & Rothman, J. E. SNAREpins: minimal machinery for membrane fusion. *Cell* **92**, 759-772 (1998).
69 Jackson, M. B. & Chapman, E. R. The fusion pores of Ca^{2+}-triggered exocytosis. *Nat Struct Mol Biol* **15**, 684-689 (2008).
70 Deák, F., Shin, O.-H., Kavalali, E. T. & Südhof, T. C. Structural Determinants of Synaptobrevin 2 Function in Synaptic Vesicle Fusion. *The Journal of Neuroscience* **26**, 6668-6676 (2006).
71 Zhou, P., Bacaj, T., Yang, X., Pang, Zhiping P. & Südhof, Thomas C. Lipid-Anchored SNAREs Lacking Transmembrane Regions Fully Support Membrane Fusion during Neurotransmitter Release. *Neuron* **80**, 470-483(2013).
72 Bhalla, A., Chicka, M. C., Tucker, W. C. & Chapman, E. R. Ca^{2+}-synaptotagmin directly regulates t-SNARE function during reconstituted membrane fusion. *Nat Struct Mol Biol* **13**, 323-330(2006).
73 Diao, J., Grob, P., Cipriano, D. J., Kyoung, M., Zhang, Y., Shah, S., Nguyen, A., Padolina, M., Srivastava, A., Vrljic, M., Shah, A., Nogales, E., Chu, S. & Brunger, A. T. Synaptic proteins promote calcium-triggered fast transition from point contact to full fusion. *eLife* **1** (2012).
74 Katz, B. & Miledi, R. Ionic requirements of synaptic transmitter release. *Nature* **215**, 651 (1967).
75 Dodge, F. A., Jr. & Rahamimoff, R. Co-operative action a calcium ions in transmitter release at the neuromuscular junction. *J Physiol* **193**, 419-432 (1967).
76 Sabatini, B. L. & Regehr, W. G. Timing of neurotransmission at fast synapses in the mammalian brain. *Nature* **384**, 170-172 (1996).
77 Perin, M. S., Fried, V. A., Mignery, G. A., Jahn, R. & Sudhof, T. C. Phospholipid binding by a synaptic vesicle protein homologous to the regulatory region of protein kinase C. *Nature* **345**, 260-263 (1990).
78 Chapman, E. R., Hanson, P. I., An, S. & Jahn, R. Ca^{2+} regulates the interaction between synaptotagmin and syntaxin 1. *J Biol Chem* **270**, 23667-23671 (1995).
79 Pang, Z. P., Shin, O.-H., Meyer, A. C., Rosenmund, C. & Südhof, T. C. A Gain-of-Function Mutation in Synaptotagmin-1 Reveals a Critical Role of Ca^{2+}-Dependent Soluble N-

Ethylmaleimide-Sensitive Factor Attachment Protein Receptor Complex Binding in Synaptic Exocytosis. *The Journal of Neuroscience* **26**, 12556-12565 (2006).

80 Fernandez-Chacon, R., Konigstorfer, A., Gerber, S. H., Garcia, J., Matos, M. F., Stevens, C. F., Brose, N., Rizo, J., Rosenmund, C. & Sudhof, T. C. Synaptotagmin I functions as a calcium regulator of release probability. *Nature* **410**, 41-49(2001).

81 Zhang, X., Kim-Miller, M. J., Fukuda, M., Kowalchyk, J. A. & Martin, T. F. J. Ca^{2+}-Dependent Synaptotagmin Binding to SNAP-25 Is Essential for Ca^{2+}-Triggered Exocytosis. *Neuron* **34**, 599 (2002).

82 Gerona, R. R., Larsen, E. C., Kowalchyk, J. A. & Martin, T. F. The C terminus of SNAP25 is essential for Ca^{2+}-dependent binding of synaptotagmin to SNARE complexes. *Journal of Biological Chemistry* **275**, 6328-6336 (2000).

83 Zhou, Q., Lai, Y., Bacaj, T., Zhao, M., Lyubimov, A. Y., Uervirojnangkoorn, M., Zeldin, O. B., Brewster, A. S., Sauter, N. K., Cohen, A. E., Soltis, S. M., Alonso-Mori, R., Chollet, M., Lemke, H. T., Pfuetzner, R. A., Choi, U. B., Weis, W. I., Diao, J., Sudhof, T. C. & Brunger, A. T. Architecture of the synaptotagmin-SNARE machinery for neuronal exocytosis. *Nature* **525**, 62-67 (2015).

84 Lynch, K. L., Gerona, R. R. L., Larsen, E. C., Marcia, R. F., Mitchell, J. C. & Martin, T. F. J. Synaptotagmin C2A Loop 2 Mediates Ca^{2+}-dependent SNARE Interactions Essential for Ca^{2+}-triggered Vesicle Exocytosis. *Molecular Biology of the Cell* **18**, 4957-4968 (2007).

85 Gaffaney, J. D., Dunning, F. M., Wang, Z., Hui, E. & Chapman, E. R. Synaptotagmin C2B Domain Regulates Ca^{2+}-triggered Fusion in Vitro: CRITICAL RESIDUES REVEALED BY SCANNING ALANINE MUTAGENESIS. *Journal of Biological Chemistry* **283**, 31763-31775 (2008).

86 Zhang Z, W. Y., Wang Z, Dunning FM, Rehfuss J, Ramanan D, Chapman ER, Jackson MB. Release mode of large and small dense-core vesicles specified by different synaptotagmin isoforms in PC12 cells. **13**, 2324-2336 (2011).

87 Lai, A. L., Tamm, L. K., Ellena, J. F. & Cafiso, D. S. Synaptotagmin 1 Modulates Lipid Acyl Chain Order in Lipid Bilayers by Demixing Phosphatidylserine. *Journal of Biological Chemistry* **286**, 25291-25300 (2011).

88 Littleton, J. T., Stern, M., Schulze, K., Perin, M. & Bellen, H. J. Mutational analysis of Drosophila synaptotagmin demonstrates its essential role in Ca^{2+}-activated neurotransmitter release. *Cell* **74**, 1125-1134(1993).

89 Broadie, K., Bellen, H. J., DiAntonio, A., Littleton, J. T. & Schwarz, T. L. Absence of synaptotagmin disrupts excitation-secretion coupling during synaptic transmission. *Proceedings of the National Academy of Sciences of the United States of America* **91**, 10727-10731 (1994).

90 Geppert, M., Goda, Y., Hammer, R. E., Li, C., Rosahl, T. W., Stevens, C. F. & Südhof, T. C. Synaptotagmin I: A major Ca^{2+} sensor for transmitter release at a central synapse. *Cell* **79**, 717-727(1994).

91 Mackler, J. M., Drummond, J. A., Loewen, C. A., Robinson, I. M. & Reist, N. E. The C2B Ca^{2+}-binding motif of synaptotagmin is required for synaptic transmission in vivo. *Nature* **418**, 340-344(2002).

92 Nishiki, T.-i. & Augustine, G. J. Dual Roles of the C2B Domain of Synaptotagmin I in Synchronizing Ca^{2+}-Dependent Neurotransmitter Release. *J. Neurosci.* **24**, 8542-8550 (2004).

93 Shin, O.-H., Xu, J., Rizo, J. & Südhof, T. C. Differential but convergent functions of Ca^{2+} binding to synaptotagmin-1 C2 domains mediate neurotransmitter release. *Proceedings of the National Academy of Sciences* **106**, 16469-16474 (2009).

94 Lee, J., Guan, Z., Akbergenova, Y. & Littleton, J. T. Genetic Analysis of Synaptotagmin C2 Domain Specificity in Regulating Spontaneous and Evoked Neurotransmitter Release. *The Journal of Neuroscience* **33**, 187-200 (2013).

95 Schonn, J.-S., Maximov, A., Lao, Y., Südhof, T. C. & Sørensen, J. B. Synaptotagmin-1 and -7 are functionally overlapping Ca^{2+} sensors for exocytosis in adrenal chromaffin cells. *Proceedings of the National Academy of Sciences* **105**, 3998-4003 (2008).
96 Gao, Z., Reavey-Cantwell, J., Young, R. A., Jegier, P. & Wolf, B. A. Synaptotagmin III/VII Isoforms Mediate Ca^{2+}-induced Insulin Secretion in Pancreatic Islet β-Cells. *Journal of Biological Chemistry* **275**, 36079-36085 (2000).
97 Gauthier, B. R., Duhamel, D. L., Iezzi, M., Theander, S., Saltel, F., Fukuda, M., Wehrle-Haller, B. & Wollheim, C. B. Synaptotagmin VII splice variants α, β, and δ are expressed in pancreatic β-cells and regulate insulin exocytosis. *The FASEB Journal* **22**, 194-206 (2008).
98 Sun, J., Pang, Z. P., Qin, D., Fahim, A. T., Adachi, R. & Sudhof, T. C. A dual-Ca^{2+}-sensor model for neurotransmitter release in a central synapse. *Nature* **450**, 676-682, d (2007).
99 Yao, J., Gaffaney, J. D., Kwon, S. E. & Chapman, E. R. Doc2 Is a Ca^{2+} Sensor Required for Asynchronous Neurotransmitter Release. *Cell* **147**, 666.
100 Groffen, A. J., Martens, S., Arazola, R. D., Cornelisse, L. N., Lozovaya, N., de Jong, A. P. H., Goriounova, N. A., Habets, R. L. P., Takai, Y., Borst, J. G., Brose, N., McMahon, H. T. & Verhage, M. Doc2β Is a High-Affinity Ca^{2+} Sensor for Spontaneous Neurotransmitter Release. *Science* **327**, 1614-1618 (2010).
101 Pang, Zhiping P., Bacaj, T., Yang, X., Zhou, P., Xu, W. & Südhof, Thomas C. Doc2 Supports Spontaneous Synaptic Transmission by a Ca^{2+}-Independent Mechanism. *Neuron* **70**, 244-251(2011).
102 Gaffaney, J. D., Xue, R. & Chapman, E. R. Mutations that disrupt Ca^{2+}-binding activity endow Doc2β with novel functional properties during synaptic transmission. *Molecular Biology of the Cell* **25**, 481-494 (2014).
103 Li, J., Cantley, J., Burchfield, J., Meoli, C., Stöckli, J., Whitworth, P. T., Pant, H., Chaudhuri, R., Groffen, A. A., Verhage, M. & James, D. DOC2 isoforms play dual roles in insulin secretion and insulin-stimulated glucose uptake. *Diabetologia* **57**, 2173-2182 (2014).
104 Hua, Y., Sinha, R., Thiel, C. S., Schmidt, R., Huve, J., Martens, H., Hell, S. W., Egner, A. & Klingauf, J. A readily retrievable pool of synaptic vesicles. *Nat Neurosci* **14**, 833-839(2011).
105 Rosenmund, C. & Stevens, C. F. Definition of the Readily Releasable Pool of Vesicles at Hippocampal Synapses. *Neuron* **16**, 1197-1207 (1996).
106 Harata, N., Pyle, J. L., Aravanis, A. M., Mozhayeva, M., Kavalali, E. T. & Tsien, R. W. Limited numbers of recycling vesicles in small CNS nerve terminals: implications for neural signaling and vesicular cycling. *Trends in Neurosciences* **24**, 637-643(2001).
107 Becherer, U. & Rettig, J. Vesicle pools, docking, priming, and release. *Cell and Tissue Research* **326**, 393-407(2006).
108 Rizo, J. & Sudhof, T. C. Snares and Munc18 in synaptic vesicle fusion. *Nat Rev Neurosci* **3**, 641-653 (2002).
109 Dulubova, I., Sugita, S., Hill, S., Hosaka, M., Fernandez, I., Sudhof, T. C. & Rizo, J. A conformational switch in syntaxin during exocytosis: role of munc18. *Embo J* **18**, 4372-4382 (1999).
110 Misura, K. M. S., Scheller, R. H. & Weis, W. I. Three-dimensional structure of the neuronal-Sec1-syntraxin 1a complex. *Nature* **404**, 355-362. (2000).
111 Shen, J., Tareste, D. C., Paumet, F., Rothman, J. E. & Melia, T. J. Selective Activation of Cognate SNAREpins by Sec1/Munc18 Proteins. *Cell* **128**, 183-195.
112 Verhage, M., Maia, A. S., Plomp, J. J., Brussaard, A. B., Heeroma, J. H., Vermeer, H., Toonen, R. F., Hammer, R. E., van den, T. K., Berg, Missler, M., Geuze, H. J. & Südhof, T. C. Synaptic Assembly of the Brain in the Absence of Neurotransmitter Secretion. *Science* **287**, 864-869 (2000).
113 Voets, T., Toonen, R. F., Brian, E. C., de Wit, H., Moser, T., Rettig, J., Sudhof, T. C., Neher, E. & Verhage, M. Munc18-1 promotes large dense-core vesicle docking. *Neuron* **31**, 581-591 (2001).

114 Aravamudan, B., Fergestad, T., Davis, W. S., Rodesch, C. K. & Broadie, K. Drosophila Unc-13 is essential for synaptic transmission. *Nat Neurosci* **2**, 965-971 (1999).
115 Augustin, I., Rosenmund, C., Sudhof, T. C. & Brose, N. Munc13-1 is essential for fusion competence of glutamatergic synaptic vesicles. *Nature* **400**, 457-461(1999).
116 Madison, J. M., Nurrish, S. & Kaplan, J. M. UNC-13 Interaction with Syntaxin Is Required for Synaptic Transmission. *Current Biology* **15**, 2236-2242(2005).
117 Stevens, D. R., Wu, Z.-X., Matti, U., Junge, H. J., Schirra, C., Becherer, U., Wojcik, S. M., Brose, N. & Rettig, J. Identification of the Minimal Protein Domain Required for Priming Activity of Munc13-1. *Current Biology* **15**, 2243-2248(2005).
118 Ma, C., Li, W., Xu, Y. & Rizo, J. Munc13 mediates the transition from the closed syntaxin–Munc18 complex to the SNARE complex. *Nat Struct Mol Biol* **18**, 542-549(2011).
119 Deng, L., Kaeser, P. S., Xu, W. & Südhof, T. C. RIM Proteins Activate Vesicle Priming by Reversing Autoinhibitory Homodimerization of Munc13. *Neuron* **69**, 317-331(2011).
120 Kaeser, P. S., Deng, L., Wang, Y., Dulubova, I., Liu, X., Rizo, J. & Südhof, T. C. RIM Proteins Tether Ca^{2+} Channels to Presynaptic Active Zones via a Direct PDZ-Domain Interaction. *Cell* **144**, 282-295(2011).
121 Han, Y., Kaeser, P. S., Südhof, T. C. & Schneggenburger, R. RIM Determines Ca^{2+} Channel Density and Vesicle Docking at the Presynaptic Active Zone. *Neuron* **69**, 304-316(2011).
122 Bracher, A., Kadlec, J., Betz, H. & Weissenhorn, W. X-ray Structure of a Neuronal Complexin-SNARE Complex from Squid. *Journal of Biological Chemistry* **277**, 26517-26523 (2002).
123 Reim, K., Mansour, M., Varoqueaux, F., McMahon, H. T., Sudhof, T. C., Brose, N. & Rosenmund, C. Complexins regulate a late step in Ca^{2+}-dependent neurotransmitter release. *Cell* **104**, 71-81 (2001).
124 Xue, M., Reim, K., Chen, X., Chao, H.-T., Deng, H., Rizo, J., Brose, N. & Rosenmund, C. Distinct domains of complexin I differentially regulate neurotransmitter release. *Nat Struct Mol Biol* **14**, 949-958 (2007).
125 Cao, P., Yang, X. & Südhof, T. C. Complexin Activates Exocytosis of Distinct Secretory Vesicles Controlled by Different Synaptotagmins. *The Journal of Neuroscience* **33**, 1714-1727 (2013).
126 Jorquera, R. A., Huntwork-Rodriguez, S., Akbergenova, Y., Cho, R. W. & Littleton, J. T. Complexin Controls Spontaneous and Evoked Neurotransmitter Release by Regulating the Timing and Properties of Synaptotagmin Activity. *The Journal of Neuroscience* **32**, 18234-18245 (2012).
127 Giraudo, C. G., Eng, W. S., Melia, T. J. & Rothman, J. E. A Clamping Mechanism Involved in SNARE-Dependent Exocytosis. *Science* **313**, 676-680 (2006).
128 Maximov, A., Tang, J., Yang, X., Pang, Z. P. & Südhof, T. C. Complexin Controls the Force Transfer from SNARE Complexes to Membranes in Fusion. *Science* **323**, 516-521 (2009).
129 Xu, J., Brewer, K. D., Perez-Castillejos, R. & Rizo, J. Subtle Interplay between Synaptotagmin and Complexin Binding to the SNARE Complex. *Journal of Molecular Biology* **425**, 3461-3475 (2013).
130 Chicka, M. C. & Chapman, E. R. Concurrent Binding of Complexin and Synaptotagmin to Liposome-Embedded SNARE Complexes†. *Biochemistry* **48**, 657-659 (2009).
131 Chen, X., Tomchick, D. R., Kovrigin, E., Araç, D., Machius, M., Südhof, T. C. & Rizo, J. Three-Dimensional Structure of the Complexin/SNARE Complex. *Neuron* **33**, 397-409(2002).
132 Trimbuch, T., Xu, J., Flaherty, D., Tomchick, D. R., Rizo, J. & Rosenmund, C. Re-examining how complexin inhibits neurotransmitter release. *eLife* **3** (2014).
133 Lai, Y., Diao, J., Cipriano, D. J., Zhang, Y., Pfuetzner, R. A., Padolina, M. S. & Brunger, A. T. Complexin inhibits spontaneous release and synchronizes Ca^{2+}-triggered synaptic vesicle fusion by distinct mechanisms. *eLife* **3**, e03756(2014).

134 Zhao, M. & Brunger, A. T. Recent Advances in Deciphering the Structure and Molecular Mechanism of the AAA + ATPase N-Ethylmaleimide-Sensitive Factor (NSF). *Journal of Molecular Biology*, Epub ahead of print (2015)
135 Zhao, M., Wu, S., Zhou, Q., Vivona, S., Cipriano, D. J., Cheng, Y. & Brunger, A. T. Mechanistic insights into the recycling machine of the SNARE complex. *Nature* **518**, 61-67, (2015).

136 Ryu, J.-K., Min, D., Rah, S.-H., Kim, S. J., Park, Y., Kim, H., Hyeon, C., Kim, H. M., Jahn, R. & Yoon, T.-Y. Spring-loaded unraveling of a single SNARE complex by NSF in one round of ATP turnover. *Science (New York, N.Y.)* **347**, 1485-1489 (2015).
137 Ashery, U., Bielopolski, N., Barak, B. & Yizhar, O. Friends and foes in synaptic transmission: the role of tomosyn in vesicle priming. *Trends in Neurosciences* **32**, 275-282(2009).
138 Fujita, Y., Shirataki, H., Sakisaka, T., Asakura, T., Ohya, T., Kotani, H., Yokoyama, S., Nishioka, H., Matsuura, Y., Mizoguchi, A., Scheller, R. H. & Takai, Y. Tomosyn: a Syntaxin-1–Binding Protein that Forms a Novel Complex in the Neurotransmitter Release Process. *Neuron* **20**, 905-915 (1998).
139 Pobbati, A. V., Razeto, A., Böddener, M., Becker, S. & Fasshauer, D. Structural Basis for the Inhibitory Role of Tomosyn in Exocytosis. *Journal of Biological Chemistry* **279**, 47192-47200 (2004).
140 Johnson, J. N., Ahrendt, E. & Braun, J. E. A. CSPα: the neuroprotective J protein. *Biochemistry and Cell Biology* **88**, 157-165(2010).
141 Magga, J. M., Jarvis, S. E., Arnot, M. I., Zamponi, G. W. & Braun, J. E. Cysteine string protein regulates G protein modulation of N-type calcium channels. *Neuron* **28**, 195-204 (2000).
142 Betke K.M., Wells, C.A., Hamm H. E. GPCR mediated regulation of synaptic transmission. *Prog Neurobiol.* **3** (2012).
143 Seino, S. & Shibasaki, T. PKA-Dependent and PKA-Independent Pathways for cAMP-Regulated Exocytosis. *Physiological Reviews* **85**, 1303-1342 (2005).
144 Brunelli M, Castellucci, V. F., Kandel E.R. Synaptic facilitation and behavioral sensitization in Aplysia: possible role of serotonin and cyclic AMP. *Science* **194**, 1178-1181 (1976).
145 Castellucci, V. F., Kandel, E. R., Schwartz, J. H., Wilson, F. D., Nairn, A. C. & Greengard, P. Intracellular injection of t he catalytic subunit of cyclic AMP-dependent protein kinase simulates facilitation of transmitter release underlying behavioral sensitization in Aplysia. *Proceedings of the National Academy of Sciences of the United States of America* **77**, 7492-7496 (1980).
146 Evans, G. J. O., Wilkinson, M. C., Graham, M. E., Turner, K. M., Chamberlain, L. H., Burgoyne, R. D. & Morgan, A. Phosphoryaltion of cysteine string protein by protein kinase A. *Journal of Biological Chemistry* **276**, 47877-47885 (2001).
147 Evans, G. J. O. & Morgan, A. Phosphorylation-dependent interaction of the synaptic vesicle proteins cysteine string protein and synaptotagmin I. *Biochemical Journal* **364**, 343-347 (2002).
148 Nagy, G., Reim, K., Matti, U., Brose, N., Binz, T., Rettig, J., Neher, E. & Sorensen, J. B. Regulation of releasable vesicle pool sizes by protein kinase A-dependent phosphorylation of SNAP-25. *Neuron* **41**, 417-429 (2004).
149 Morgan, A., Burgoyne, R. D., Barclay, J. W., Craig, T. J., Prescott, G. R., Ciufo, L. F., Evans, G. J. O. & Graham, M. E. Regulation of exocytosis by protein kinase C. *Biochemical Society Transactions* **33**, 1341-1344 (2005).
150 Zamponi, G. W., Bourinet, E., Nelson, D., Nargeot, J. & Snutch, T. P. Crosstalk between G proteins and protein kinase C mediated by the calcium channel α1 subunit. *Nature.* **385**, 442-446. (1997).
151 Shimazaki, Y., Nishiki, T.-i., Omori, A., Sekiguchi, M., Kamata, Y., Kozaki, S. & Takahashi, M. Phosphorylation of 25-kDa Synaptosome-associated Protein: Possible Involvement in Protein Kinase C-Regulated Neurotransmitter Release. *Journal of Biological Chemistry* **271**, 14548-14553 (1996).

152 DeFea, K. A. Beta-arrestins as regulators of signal termination and transduction: How do they determine what to scaffold? *Cellular Signalling* **23**, 621-629(2011).
153 Zhao, Y., Fang, Q., Straub, S. G., Lindau, M. & Sharp, G. W. G. Noradrenaline inhibits exocytosis via the G protein βγ subunit and refilling of the readily releasable granule pool via the $\alpha_{i1/2}$ subunit. *The Journal of Physiology* **588**, 3485-3498(2010).
154 Logothetis, D. E., Kurachi, Y., Galper, J., Neer, E. J. & Clapham, D. E. The βγ subunits of GTP-binding proteins activate the muscarinic K^+ channel in heart. *Nature* **325**, 321-326 (1987).
155 Whorton, M. R. & MacKinnon, R. X-ray structure of the mammalian GIRK2-βγ G-protein complex. *Nature* **498**, 190-197(2013).
156 Yokogawa, M., Osawa, M., Takeuchi, K., Mase, Y. & Shimada, I. NMR Analyses of the Gβγ Binding and Conformational Rearrangements of the Cytoplasmic Pore of G Protein-activated Inwardly Rectifying Potassium Channel 1 (GIRK1). *Journal of Biological Chemistry* **286**, 2215-2223 (2011).
157 He, C., Zhang, H., Mirshahi, T. & Logothetis, D. E. Identification of a Potassium Channel Site That Interacts with G Protein βγ Subunits to Mediate Agonist-induced Signaling. *Journal of Biological Chemistry* **274**, 12517-12524 (1999).
158 Finley, M., Arrabit, C., Fowler, C., Suen, K. F. & Slesinger, P. A. βL–βM loop in the C-terminal domain of G protein-activated inwardly rectifying K^+ channels is important for Gβγ subunit activation. *The Journal of Physiology* **555**, 643-657 (2004).
159 Lei, Q., Jones, M. B., Talley, E. M., Schrier, A. D., McIntire, W. E., Garrison, J. C. & Bayliss, D. A. Activation and inhibition of G protein-coupled inwardly rectifying potassium ($K_{ir}3$) channels by G protein βγ subunits. *Proceedings of the National Academy of Sciences of the United States of America* **97**, 9771-9776 (2000).
160 Lei, Q., Talley, E. M. & Bayliss, D. A. Receptor-mediated Inhibition of G Protein-coupled Inwardly Rectifying Potassium Channels Involves Gαq Family Subunits, Phospholipase C, and a Readily Diffusible Messenger. *Journal of Biological Chemistry* **276**, 16720-16730 (2001).
161 Qiubo, L., Miller, B. J., Edmund, M. T., James, C. G. & Douglas, A. B. Molecular Mechanisms Mediating Inhibition of G Protein-coupled Inwardly-rectifying K^+ Channels. *Mol. Cells* **15**, 1-9 (2003).
162 Reuveny, E., Slesinger, P. A., Inglese, J., Morales, J. M., Iniguez-Lluhi, J. A., Lefkowitz, R. J., Bourne, H. R., Jan, Y. N. & Jan, L. Y. Activation of the cloned muscarinic potassium channel by G protein βγ subunits. *Nature* **370**, 143-146 (1994).
163 Breitweiser GE, S. G. Mechanism of muscarinic receptor-induced K^+ channel activation as revealed by hydrolysis-resistant GTP analogues. *The Journal of General Physiology* **91**, 469-493 (1988).
164 Brown, A. M. Regulation of heartbeat by G protein-coupled ion channels. *American Journal of Physiology - Heart and Circulatory Physiology* **259**, H1621-H1628 (1990).
165 Nicoll, R. A., Malenka, R. C. & Kauer, J. A. Functional comparison of neurotransmitter receptor subtypes in mammalian central nervous system. *Physiological Reviews* **70**, 513-565 (1990).
166 Fernández-Alacid, L., Aguado, C., Ciruela, F., Martín, R., Colón, J., Cabañero, M. J., Gassmann, M., Watanabe, M., Shigemoto, R., Wickman, K., Bettler, B., Sánchez-Prieto, J. & Luján, R. Subcellular compartment-specific molecular diversity of pre- and post-synaptic $GABA_B$-activated GIRK channels in Purkinje cells. *Journal of Neurochemistry* **110**, 1363-1376 (2009).
167 Lüscher, C., Jan, L. Y., Stoffel, M., Malenka, R. C. & Nicoll, R. A. G Protein-Coupled Inwardly Rectifying K^+ Channels (GIRKs) Mediate Postsynaptic but Not Presynaptic Transmitter Actions in Hippocampal Neurons. *Neuron* **19**, 687-695 (1997).
168 Lüscher, C. & Slesinger, P. A. Emerging roles for G protein-gated inwardly rectifying potassium (GIRK) channels in health and disease. *Nat Rev Neurosci* **11**, 301-315(2010).

169 Ladera, C., Del Carmen Godino, M., Cabañero, M. J., Torres, M., Watanabe, M., Luján, R. & Sánchez-Prieto, J. Pre-synaptic $GABA_B$ receptors inhibit glutamate release through GIRK channels in rat cerebral cortex. *Journal of Neurochemistry* **107**, 1506-1517 (2008).
170 Michaeli, A. & Yaka, R. Dopamine inhibits $GABA_A$ currents in ventral tegmental area dopamine neurons via activation of presynaptic G-protein coupled inwardly-rectifying potassium channels. *Neuroscience* **165**, 1159-1169 (2010).
171 Zamponi, G. W. & Currie, K. P. M. Regulation of CaV_2 calcium channels by G protein coupled receptors. *Biochimica et biophysica acta* **1828**, 1629-1643 (2013).
172 Ikeda, S. R. Voltage-dependent modulation of N-type calcium channels by G-protein βγ subunits. *Nature* **380**, 255-258 (1996).
173 Hille, B. Modulation of ion-channel function by G-protein-coupled receptors. *Trends Neurosci* **17**, 531-536 (1994).
174 Dolphin, A. C. & Scott, R. H. Calcium channel currents and their inhibition by (-)-baclofen in rat sensory neurones: modulation by guanine nucleotides. *Journal of Physiology, London* **386**, 1-17 (1987).
175 Dunlap, K. & Fischbach, G. D. Neurotransmitters decrease the calcium conductance activated by depolarization of embryonic chick sensory neurones. *J Physiol* **317**, 519-535 (1981).
176 Dunlap, K. Fischbach., G. D. Neurotransmitters decrease the calcium ocmponent of sensory neurone action potentials. *Nature* **276**, 837-839 (1978).
177 Womack, M. D. & McCleskey, E. W. Interaction of opioids and membrane potential to modulate Ca^{2+} channels in rat dorsal root ganglion neurons. *J Neurophysiol* **73**, 1793-1798 (1995).
178 Mintz, I. M. & Bean, B. P. $GABA_B$ receptor inhibition of P-type Ca^{2+} channels in central neurons. *Neuron* **10**, 889-898 (1993).
179 Berecki, G., Motin, L. & Adams, D. J. Voltage-Gated R-Type Calcium Channel Inhibition via Human μ-, δ-, and κ-opioid Receptors Is Voltage-Independently Mediated by Gβγ Protein Subunits. *Molecular Pharmacology* **89**, 187-196 (2016).
180 Bean, B. P. Neurotransmitter inhibition of neuronal calcium currents by changes in channel voltage dependence. *Nature* **340**, 153-156 (1989).
181 Brody, D. L., Patil, P. G., Mulle, J. G., Snutch, T. P. & Yue, D. T. Bursts of action potential waveforms relieve G-protein inhibition of recombinant P/Q-type Ca^{2+} channels in HEK 293 cells. *J Physiol* **499 (Pt 3)**, 637-644 (1997).
182 Tosetti, P., Taglietti, V. & Toselli, M. Action-potential-like depolarizations relieve opioid inhibition of N-type Ca^{2+} channels in NG108-15 cells. *Pflugers Arch* **437**, 441-448 (1999).
183 De Waard, M., Liu, H., Walker, D., Scott, V. E., Gurnett, C. A. & Campbell, K. P. Direct binding of G-protein βγ complex to voltage-dependent calcium channels. *Nature* **385**, 446-450 (1997).
184 Chen, J., DeVivo, M., Dingus, J., Harry, A., Li, J., Sui, J., Carty, D. J., Blank, J. L., Exton, J. H., Stoffel, R. H. & et al. A region of adenylyl cyclase 2 critical for regulation by G protein βγ subunits. *Science* **268**, 1166-1169. (1995).
185 Zamponi, G. W. & Snutch, T. P. Modulation of voltage-dependent calcium channels by G proteins. *Curr Opin Neurobiol* **8**, 351-356 (1998).
186 Swartz, K. J. Modulation of Ca^{2+} channels by protein kinase C in rat central and peripheral neurons: Disruption of G protein-mediated inhibition. *Neuron* **11**, 305-320(1993).
187 Bezprozvanny, I., Scheller, R. H. & Tsien, R. W. Functional impact of syntaxin on gating of N-type and Q-type calcium channels. *Nature* **378**, 623-626 (1995).
188 Rettig, J., Sheng, Z. H., Kim, D. K., Hodson, C. D., Snutch, T. P. & Catterall, W. A. Isoform-specific interaction of the alpha1A subunits of brain Ca^{2+} channels with the presynaptic proteins syntaxin and SNAP-25. *Proceedings of the National Academy of Sciences of the United States of America* **93**, 7363-7368 (1996).
189 Stanley, E. F. & Mirotznik, R. R. Cleavage of syntaxin prevents G-protein regulation of presynaptic calcium channels. *Nature* **385**, 340-343 (1997).

190 Jarvis, S. E., Magga, J. M., Beedle, A. M., Braun, J. E. & Zamponi, G. W. G protein modulation of N-type calcium channels is facilitated by physical interactions between syntaxin 1A and Gβγ. *Journal of Biological Chemistry* **275**, 6388-6394 (2000).
191 Jarvis, S. E., Barr, W., Feng, Z. P., Hamid, J. & Zamponi, G. W. Molecular determinants of syntaxin 1 modulation of N-type calcium channels. *J Biol Chem* **277**, 44399-44407 (2002).
192 Wollheim, C. B., Kikuchi, M., Renold, A. E. & Sharp, G. W. G. Somatostatin- and Epinephrine-Induced Modifications of $^{45}Ca^{++}$ Fluxes and Insulin Release in Rat Pancreatic Islets Maintained in Tissue Culture. *Journal of Clinical Investigation* **60**, 1165-1173 (1977).
193 Mandarino, L., Itoh, M., Blanchard, W., Patton, G. & Gerich, J. Stimulation of Insulin Release in the Absence of Extracellular Calcium by Isobutylmethylxanthine and Its Inhibition by Somatostatin. *Endocrinology* **106**, 430-433 (1980).
194 Silinsky, E. M. On the mechanism by which adenosine recptor activation inhibits the release of acetylcholine from motor nerve endings. *Journal of Physiology* **346**, 243-256 (1984).
195 Knight, D. E. & Baker, P. F. Guanine nucleotides and Ca-dependent exocytosis: Studies on two adrenal cell preparations. *FEBS Letters* **189**, 345-349 (1985).
196 Blackmer, T., Larsen, E. C., Takahashi, M., Martin, T. F., Alford, S. & Hamm, H. E. G protein βγ subunit-mediated presynaptic inhibition: regulation of exocytotic fusion downstream of Ca^{2+} entry. *Science* **292**, 293-297. (2001).
197 Delaney A. J, Crane. J. W., Sah P. Noradrenaline modulates transmission at a central synapse by a presynaptic mechanism. *Neuron.* **5**, 880-892 (2007).
198 Glitsch, M. Selective Inhibition of Spontaneous But Not Ca^{2+}-Dependent Release Machinery by Presynaptic Group II mGluRs in Rat Cerebellar Slices. *Journal of Neurophysiology* **96**, 86 (2006).
199 Iremonger, K. J. & Bains, J. S. Retrograde Opioid Signaling Regulates Glutamatergic Transmission in the Hypothalamus. *The Journal of Neuroscience* **29**, 7349 (2009).
200 Gerachshenko, T., Blackmer, T., Yoon, E. J., Bartleson, C., Hamm, H. E. & Alford, S. Gβγ acts at the C terminus of SNAP-25 to mediate presynaptic inhibition. *Nat Neurosci* **8**, 597-605 (2005).
201 Yoon, E. J., T. Gerachshenko, B.D. Spiegelberg, S. Alford, and H.E. Hamm. Gβγ interferes with Ca^{2+}-dependent binding of synaptotagmin to the soluble N-ethylmaleimide-sensitive factor attachment protein receptor (SNARE) complex. *Mol. Pharmacol.* **72**, 1210-1219 (2007).
202 Yoon, E. J., H.E. Hamm, and K.P.M. Currie. G protein βγ subunits modulate the number and nature of exocytotic fusion events in adrenal chromaffin cells independent of calcium entry. *J Neurophysiol* **100**, 2929-2939. (2008).
203 Schiavo, G., Santucci, A., Dasgupta, B. R., Mehta, P. P., Jontes, J., Benfenati, F., Wilson, M. C. & Montecucco, C. Botulinum neurotoxins serotypes A and E cleave SNAP-25 at distinct COOH-terminal peptide bonds. *FEBS Lett* **335**, 99-103 (1993).
204 Photowala, H., Blackmer, T. Schwartz, E, Hamm H. E, and Alford S.. G protein βγ-subunits activated by serotonin mediate presynaptic inhibition by regulating vesicle fusion properties. *Proc Natl Acad Sci U S A* **103**, 4281-4286 (2006).
205 Zhang, X.-l., Upreti, C. & Stanton, P. K. Gβγ and the C Terminus of SNAP-25 Are Necessary for Long-Term Depression of Transmitter Release. *PLoS ONE* **6**, e20500.
206 Braunewell, K. Manahan-Vaughan., D. Long-term depression: a cellular basis for learning? *Rev Neurosci* **12**, 121-140 (2001).
207 Bailey, C. H., Bartsch, D. & Kandel, E. R. Toward a molecular definition of long-term memory storage. *Proceedings of the National Academy of Sciences of the United States of America* **93**, 13445-13452 (1996).
208 Hamid, E., Church, E., Wells, C. A., Zurawski, Z., Hamm, H. E. & Alford, S. Modulation of Neurotransmission by GPCRs Is Dependent upon the Microarchitecture of the Primed Vesicle Complex. *The Journal of Neuroscience* **34**, 260-274 (2014).

209 Commins, S., Gigg, J., Anderson, M. & O'Mara, S. M. The projection from hippocampal area CA1 to the subiculum sustains long-term potentiation. *NeuroReport* **9** (1998).
210 Morris, R. G. M., Schenk, F., Tweedie, F. & Jarrard, L. E. Ibotenate Lesions of Hippocampus and/or Subiculum: Dissociating Components of Allocentric Spatial Learning. *European Journal of Neuroscience* **2**, 1016-1028 (1990).
211 Davis, M. Whalen, P. J. . The amygdala: vigilance and emotion. *Mol Psychiatry* **6**, 13-34 (2001).
212 Rhudy, J. M., Meagher W . Fear and anxiety: divergent effects on human pain thresholds. *Pain* **84**, 65-75 (2000).
213 Neugebauer, V., Li, W., Bird, G. C. & Han, J. S. The Amygdala and Persistent Pain. *The Neuroscientist* **10**, 221-234 (2004).
214 Morilak, D. A., Barrera, G., Echevarria, D. J., Garcia, A. S., Hernandez, A., Ma, S. & Petre, C. O. Role of brain norepinephrine in the behavioral response to stress. *Progress in Neuro-Psychopharmacology and Biological Psychiatry* **29**, 1214-1224(2005).
215 Breivik, H., Collett, B., Ventafridda, V., Cohen, R. & Gallacher, D. Survey of chronic pain in Europe: Prevalence, impact on daily life, and treatment. *European Journal of Pain* **10**, 287-287(2006).
216 Ennion, S. J., Powell, A. D. & Seward, E. P. Identification of the P2Y12 Receptor in Nucleotide Inhibition of Exocytosis from Bovine Chromaffin Cells. *Molecular Pharmacology* **66**, 601-611 (2004).
217 Hernández, A., Segura-Chama, P., Jiménez, N., García, A. G., Hernández-Guijo, J. M. & Hernández-Cruz, A. Modulation by endogenously released ATP and opioids of chromaffin cell calcium channels in mouse adrenal slices. *American Journal of Physiology - Cell Physiology* **300**, C610-C623 (2011).
218 Gerich, J. Is Reduced First-Phase Insulin Release the Earliest Detectable Abnormality in Individuals Destined to Develop Type 2 Diabetes? *Diabetes* **51**, S117-S121 (2002).
219 Porte Jr, D., Graber, A. L., Kuzuya, T. & Williams, R. H. The effect of epinephrine on immunoreactive insulin levels in man. *Nutrition* **12**, 225 (1996).
220 Rosengren, A. H., Jokubka, R., Tojjar, D., Granhall, C., Hansson, O., Li, D.-Q., Nagaraj, V., Reinbothe, T. M., Tuncel, J., Eliasson, L., Groop, L., Rorsman, P., Salehi, A., Lyssenko, V., Luthman, H. & Renström, E. Overexpression of α_{2A}-Adrenergic Receptors Contributes to Type 2 Diabetes. *Science* **327**, 217-220 (2010).
221 Rosengren, A. H., Braun, M., Mahdi, T., Andersson, S. A., Travers, M. E., Shigeto, M., Zhang, E., Almgren, P., Ladenvall, C., Axelsson, A. S., Edlund, A., Pedersen, M. G., Jonsson, A., Ramracheya, R., Tang, Y., Walker, J. N., Barrett, A., Johnson, P. R. V., Lyssenko, V., McCarthy, M. I., Groop, L., Salehi, A., Gloyn, A. L., Renström, E., Rorsman, P. & Eliasson, L. Reduced Insulin Exocytosis in Human Pancreatic β-Cells With Gene Variants Linked to Type 2 Diabetes. *Diabetes* **61**(2012).
222 Robertson, R. P., Halter, J. B. & Porte, D. A role for alpha-adrenergic receptors in abnormal insulin secretion in diabetes mellitus. *The Journal of Clinical Investigation* **57**, 791 (1976).
223 Broadstone VL, P. M., Bajaj V Alpha-adrenergic blockade improves glucose-potentiated insulin secretion in non-insulin-dependent diabetes mellitus. *Diabetes* **36**, 932-937 (1987).
224 Chicka, M. C., Hui, E., Liu, H. & Chapman, E. R. Synaptotagmin arrests the SNARE complex before triggering fast, efficient membrane fusion in response to Ca^{2+}. *Nat Struct Mol Biol* **15**, 827-835,(2008).
225 Tucker, W. C., Weber, T. & Chapman, E. R. Reconstitution of Ca^{2+}-regulated membrane fusion by synaptotagmin and SNAREs. *Science* **304**, 435-438 (2004).
226 Mazzoni, M. R., Malinski, J. A. & Hamm, H. E. Structural analysis of rod GTP-binding protein, G_t. limited proteolytic digestion pattern of G_t with four proteases defines monoclonal antibody epitope. *J. Biol. Chem.* **266**, 14072-14081 (1991).
227 Frank, R. The SPOT-synthesis technique: Synthetic peptide arrays on membrane supports:principles and applications. *Journal of Immunological Methods* **267**, 13 (2002).

228 Phillips, W. J. & Cerione, R. A. Labeling of the beta gamma subunit complex of transducin with an environmentally sensitive cysteine reagent. Use of fluorescence spectroscopy to monitor transducin subunit interactions. *J Biol Chem* **266**, 11017-11024 (1991).
229 Schrodinger, LLC. *The PyMOL Molecular Graphics System, Version 1.3r1* (2010).
230 Zhang, X., Kim-Miller, M. J., Fukuda, M., Kowalchyk, J. A. & Martin, T. F. Ca^{2+}-dependent synaptotagmin binding to SNAP-25 is essential for Ca^{2+}-triggered exocytosis. *Neuron* **34**, 599-611 (2002).
231 Weng, G., Li, J., Dingus, J., Hildebrandt, J. D., Weinstein, H. & Iyengar, R. Gβ Subunit Interacts with a Peptide Encoding Region 956-982 of Adenylyl Cyclase 2: CROSS-LINKING OF THE PEPTIDE TO FREE Gβγ BUT NOT THE HETEROTRIMER. *Journal of Biological Chemistry* **271**, 26445-26448 (1996).
232 Scott, J. K., Huang, S. F., Gangadhar, B. P., Samoriski, G. M., Clapp, P., Gross, R. A., Taussig, R. & Smrcka, A. V. Evidence that a protein-protein interaction 'hot spot' on heterotrimeric G protein βγ subunits is used for recognition of a subclass of effectors. *Embo J* **20**, 767-776 (2001).
233 Koch, W. J., Hawes, B. E., Inglese, J., Luttrell, L. M. & Lefkowitz, R. J. Cellular expression of the carboxyl terminus of a G protein-coupled receptor kinase attenuates G βγ-mediated signaling. *Journal of Biological Chemistry* **269**, 6193-6197 (1994).
234 De Waard, M., Hering, J., Weiss, N. & Feltz, A. How do G proteins directly control neuronal Ca^{2+} channel function? *Trends in Pharmacological Sciences* **26**, 427-436(2005).
235 Sutton, R. B. Crystal structure of a SNARE complex involved in synaptic exocytosis at 2.4 A resolution. *Nature* **395**, 347-353. (1998).
236 Brose, N. P., AG. Sudhof, TC. Jahn, R. Synaptotagmin: a calcium sensor on the synaptic vesicle surface. *Science* **256**, 1021-1025 (1992).
237 Mehta, P. P., Battenberg, E. & Wilson, M. C. SNAP-25 and synaptotagmin involvement in the final Ca^{2+}-dependent triggering of neurotransmitter exocytosis. *Proceedings of the National Academy of Sciences of the United States of America* **93**, 10471-10476 (1996).
238 Mahal, L. K., Sequeira, S. M., Gureasko, J. M. & Söllner, T. H. Calcium-independent stimulation of membrane fusion and SNAREpin formation by synaptotagmin I. *The Journal of Cell Biology* **158**, 273-282 (2002).
239 Rickman, C. & Davletov, B. Mechanism of Calcium-independent Synaptotagmin Binding to Target SNAREs. *Journal of Biological Chemistry* **278**, 5501-5504 (2003).
240 Sutton, R. B., Fasshauer, Jahn, R. & Brunger, A. T. Crystal structure of a SNARE complex involved in synpatic exocytosis at 2.4 A resolution . *Nature* **395**, 347-353. (1998).
241 Sondek, J., Bohm, A., Lambright, D. G., Hamm, H. E. & Sigler, P. B. Crystal structure of a G-protein βγ dimer at 2.1A resolution. *Nature* **379**, 369-374 (1996).
242 Kümmel, D., Krishnakumar, S. S., Radoff, D. T., Li, F., Giraudo, C. G., Pincet, F., Rothman, J. E. & Reinisch, K. M. Complexin cross-links pre-fusion SNAREs into a zig-zag array: a structure-based model for complexin clamping. *Nature Structural & Molecular Biology* **18**, 927-933(2011).
243 Davies, J. N., Jarvis, S. E. & Zamponi, G. W. Bipartite syntaxin 1A interactions mediate CaV2.2 calcium channel regulation. *Biochemical and Biophysical Research Communications* **411**, 562-568 (2011).
244 Wells, C.A., Zurawski, Z., Betke, K.M., Yim, Y.Y., Hyde, K., Rodriguez, S, Alford, S, Hamm, H.E. Gβγ Inhibits Exocytosis Via Interaction with Critical Residues on SNAP-25. *Mol Pharmacol.* **82**, 1136-1149 (2012).
245 Bai, J., C.T. Wang, D.A. Richards, M.B. Jackson, and E.R. Chapman. Fusion pore dynamics are regulated by synaptotagmin*t-SNARE interactions. *Neuron* **41**, 929-942 (2004).
246 Swanson, C. J., M. Bures, M.P. Johnson, A.M. Linden, J.A. Monn, and Schoepp, D. D. Metabotropic glutamate receptors as novel targets for anxiety and stress disorders. *Nat Rev Drug Discov* **4**, 131-144 (2005).
247 Patil, S. T., L. Zhang, F. Martenyi, S.L. Lowe, K.A. Jackson, B.V. Andreev, A.S. Avedisova, L.M. Bardenstein, I.Y. Gurovich, M.A. Morozova, S.N. Mosolov, N.G. Neznanov, A.M. Reznik,

A.B. Smulevich, V.A. Tochilov, B.G. Johnson, J.A. Monn, and D.D. Schoepp. Activation of mGlu2/3 receptors as a new approach to treat schizophrenia: a randomized Phase 2 clinical trial. *Nat Med* **13**, 1102-1107 (2007).

248 Betke, K. M., Rose, K. L., Friedman, D. B., Baucum, A. J., Hyde, K., Schey, K. L. & Hamm, H. E. Differential Localization of G Protein βγ Subunits. *Biochemistry* **53**, 2329-2343 (2014).

249 Washbourne, P., Thompson, P. M., Carta, M., Costa, E. T., Mathews, J. R., Lopez-Bendito, G., Molnar, Z., Becher, M. W., Valenzuela, C. F., Partridge, L. D. & Wilson, M. C. Genetic ablation of the t-SNARE SNAP-25 distinguishes mechanisms of neuroexocytosis. *Nat Neurosci* **5**, 19-26(2002).

250 Oyler, G. A., Higgins, G. A., Hart, R. A., Battenberg, E., Billingsley, M., Bloom, F. E. & Wilson, M. C. The identification of a novel synaptosomal-associated protein, SNAP-25, differentially expressed by neuronal subpopulations. *The Journal of Cell Biology* **109**, 3039-3052 (1989).

251 Kozasa, T. & Gilman, A. G. Purification of recombinant G proteins from Sf9 cells by hexahistidine tagging of associated subunits. Characterization of α_{12} and inhibition of adenylyl cyclase by α_z. *Journal of Biological Chemistry* **270**, 1734-1741 (1995).

252 Fang, Q., Berberian, K., Gong, L.-W., Hafez, I., Sørensen, J. B. & Lindau, M. The role of the C terminus of the SNARE protein SNAP-25 in fusion pore opening and a model for fusion pore mechanics. *Proceedings of the National Academy of Sciences* **105**, 15388-15392,(2008).

253 Gil, A., Gutiérrez, L. M., Carrasco-Serrano, C., Alonso, M. T., Viniegra, S. & Criado, M. Modifications in the C Terminus of the Synaptosome-associated Protein of 25 kDa (SNAP-25) and in the Complementary Region of Synaptobrevin Affect the Final Steps of Exocytosis. *Journal of Biological Chemistry* **277**, 9904-9910 (2002).

254 Criado, M., Gil, A., Viniegra, S. & Gutiérrez, L. M. A single amino acid near the C terminus of the synaptosomeassociated protein of 25 kDa (SNAP-25) is essential for exocytosis in chromaffin cells. *Proceedings of the National Academy of Sciences* **96**, 7256-7261(1999).

255 Fang, Q., Zhao, Y., Herbst, A. D., Kim, B. N. & Lindau, M. Positively Charged Amino Acids at the SNAP-25 C Terminus Determine Fusion Rates, Fusion Pore Properties, and Energetics of Tight SNARE Complex Zippering. *The Journal of Neuroscience* **35**, 3230-3239(2015).

256 Chen, Y. A., Scales, S. J., Duvvuri, V., Murthy, M., Patel, S. M., Schulman, H. & Scheller, R. H. Calcium Regulation of Exocytosis in PC12 Cells. *Journal of Biological Chemistry* **276**, 26680-26687 (2001).

257 Sørensen, J. B., Wiederhold, K., Müller, E. M., Milosevic, I., Nagy, G., de Groot, B. L., Grubmüller, H. & Fasshauer, D. Sequential N- to C-terminal SNARE complex assembly drives priming and fusion of secretory vesicles. *EMBO J* **25** (2006).

258 Hamm, H. E. The many faces of G protein Signaling. *J. Biol. Chem.* **273**, 669-672 (1998).

259 Cabrera-Vera, T. M., Vanhauwe, J., Thomas, T. O., Medkova, M., Preininger, A., Mazzoni, M. R. & Hamm, H. E. Insights into G protein structure, function, and regulation. *Endocr Rev* **24**, 765-781 (2003).

260 Lodowski, D. T., Pitcher, J. A., Capel, W. D., Lefkowitz, R. J. & Tesmer, J. J. G. Keeping G proteins at bay: A complex between G protein-coupled receptor kinase 2 and Gβγ. *Science* **300**, 1256-1262 (2003).

261 Smrcka, A. V. G protein βγ subunits: Central mediators of G protein-coupled receptor signaling. *Cellular and Molecular Life Sciences* **65**, 2191-2214 (2008).

262 Clapham, D. E. Intracellular signaling: more jobs for Gβγ. *Curr. Biol.* **6**, 814-816 (1996)

263 Winzell, M. S. r. & Ahrën, B. G-protein-coupled receptors and islet function: Implications for treatment of type 2 diabetes. *Pharmacology & Therapeutics* **116**, 437 (2007).

264 Schwetz, T. A., Ustione, A. & Piston, D. W. Neuropeptide Y and somatostatin inhibit insulin secretion through different mechanisms. *American Journal of Physiology - Endocrinology And Metabolism* **304**, E211.

265 Lehmann, D. M., Seneviratne, A. M. P. B. & Smrcka, A. V. Small Molecule Disruption of G Protein βγ Subunit Signaling Inhibits Neutrophil Chemotaxis and Inflammation. *Molecular Pharmacology* **73**, 410 (2008).
266 Malik, S., deRubio, R. G., Trembley, M., Irannejad, R., Wedegaertner, P. B. & Smrcka, A. V. G protein βγ subunits regulate cardiomyocyte hypertrophy through a perinuclear Golgi phosphatidylinositol 4-phosphate hydrolysis pathway. *Molecular Biology of the Cell* **26**, 1188-1198(2015).
267 Lin, Y. & Smrcka, A. V. Understanding Molecular Recognition by G protein βγ Subunits on the Path to Pharmacological Targeting. *Molecular Pharmacology* **80**, 551-557,(2011).
268 Bonacci, T. M., Mathews, J. L., Yuan, C., Lehmann, D. M., Malik, S., Wu, D., Font, J. L., Bidlack, J. M. & Smrcka, A. V. Differential Targeting of Gβγ-Subunit Signaling with Small Molecules. *Science* **312**, 443-446 (2006).
269 Wells C.A., Betke, K. M., Lindsley C.W, Hamm H.E. Label-free detection of G protein-SNARE interactions and screening for small molecule modulators. *ACS Chem Neurosci* **1**, 69-78 (2012).
270 Seneviratne, A., Burroughs, M., Giralt, E. & Smrcka, A. V. Direct-reversible binding of small molecules to G protein βγ subunits. *Biochimica et biophysica acta* **1814**, 1210-1218, (2011).
271 Ashcroft, FrancesÂ M. & Rorsman, P. Diabetes Mellitus and the β Cell: The Last Ten Years. *Cell* **148**, 1160.
272 Suckale, J. & Solimena, M. The insulin secretory granule as a signaling hub. *Trends in Endocrinology & Metabolism* **21**, 599-609(2010).
273 Boucher, J., Kleinridders, A. & Kahn, C. R. Insulin Receptor Signaling in Normal and Insulin-Resistant States. *Cold Spring Harbor Perspectives in Biology* **6** (2014).
274 Holst, J. J. The Physiology of Glucagon-like Peptide 1. *Physiological Reviews* **87**, 1409-1439 (2007).
275 Straub, S. G. & Sharp, G. W. G. Evolving insights regarding mechanisms for the inhibition of insulin release by norepinephrine and heterotrimeric G proteins. *American Journal of Physiology - Cell Physiology* **302**, C1687-C1698 (2010).
276 Zhao, Y., Fang, Q., Straub, S. G. & Sharp, G. W. G. Both Gi and Go Heterotrimeric G Proteins Are Required to Exert the Full Effect of Norepinephrine on the β-Cell KATP Channel. *Journal of Biological Chemistry* **283**, 5306-5316 (2008).
277 Hsu, W. H., Xiang, H., Rajan, A. S. & Boyd, A. E. Activation of α_2-Adrenergic Receptors Decreases Ca^{2+} Influx to Inhibit Insulin Secretion in a Hamster β-Cell Line: An Action Mediated by a Guanosine Triphosphate-Binding Protein. *Endocrinology* **128**, 958-964, doi:10.1210/endo-128-2-958 (1991).
278 Tang, Y., Axelsson, A. S., Spégel, P., Andersson, L. E., Mulder, H., Groop, L. C., Renström, E. & Rosengren, A. H. Genotype-based treatment of type 2 diabetes with an α2A-adrenergic receptor antagonist. *Science Translational Medicine* **6**, 257ra139-257ra139 (2014).
279 Devedjian, J. C. Pujol, A., Cayla, C., George, M., Casellas, A., Paris, H., Bosch, F.. Transgenic mice overexpressing alpha2A-adrenoceptors in pancreatic beta-cells show altered regulation of glucose homeostasis. *Diabetologia* **43** (2000).
280 Tallida, R. Drug synergism: its detection and applications. *J Pharmacol Exp Ther* **298**, 865-872 (2001).
281 Tallida, R. Interactions between drugs and occupied receptors. *Pharmacol Ther* **113**, 197-209 (2007).
282 Leung, Y. M., Kwan, E. P., Ng, B., Kang, Y. & Gaisano, H. Y. SNAREing Voltage-Gated K^+ and ATP-Sensitive K^+ Channels: Tuning β-Cell Excitability with Syntaxin-1A and Other Exocytotic Proteins. *Endocrine Reviews* **28**, 653-663,(2007).
283 Torrejón-Escribano, B., Escoriza, J., Montanya, E. & Blasi, J. Glucose-Dependent Changes in SNARE Protein Levels in Pancreatic β-Cells. *Endocrinology* **152**, 1290-1299, (2011).

284 Chan, C. B., MacPhail, R. M., Sheu, L., Wheeler, M. B. & Gaisano, H. Y. Beta-cell hypertrophy in fa/fa rats is associated with basal glucose hypersensitivity and reduced SNARE protein expression. *Diabetes* **48**, 997-1005 (1999).
285 Sadoul, K., Berger, A., Niemann, H., Weller, U., Roche, P. A., Klip, A., Trimble, W. S., Regazzi, R., Catsicas, S. & Halban, P. A. SNAP-23 Is Not Cleaved by Botulinum Neurotoxin E and Can Replace SNAP-25 in the Process of Insulin Secretion. *Journal of Biological Chemistry* **272**, 33023-33027 (1997).
286 Spurlin, B. A. & Thurmond, D. C. Syntaxin 4 Facilitates Biphasic Glucose-Stimulated Insulin Secretion from Pancreatic β-Cells. *Molecular Endocrinology* **20**, 183-193 (2006).
287 Ohara-Imaizumi, M., Fujiwara, T., Nakamichi, Y., Okamura, T., Akimoto, Y., Kawai, J., Matsushima, S., Kawakami, H., Watanabe, T., Akagawa, K. & Nagamatsu, S. Imaging analysis reveals mechanistic differences between first- and second-phase insulin exocytosis. *The Journal of Cell Biology* **177**, 695-705 (2007).
288 Oh, E., Stull, N. D., Mirmira, R. G. & Thurmond, D. C. Syntaxin 4 Up-Regulation Increases Efficiency of Insulin Release in Pancreatic Islets From Humans With and Without Type 2 Diabetes Mellitus. *The Journal of Clinical Endocrinology and Metabolism* **99**, E866-E870, (2014).
289 Gustavsson, N., Lao, Y., Maximov, A., Chuang, J.-C., Kostromina, E., Repa, J. J., Li, C., Radda, G. K., Südhof, T. C. & Han, W. Impaired insulin secretion and glucose intolerance in synaptotagmin-7 null mutant mice. *Proceedings of the National Academy of Sciences* **105**, 3992-3997 (2008).
290 Brissova, M., Fowler, M., Wiebe, P., Shostak, A., Shiota, M., Radhika, A., Lin, P. C., Gannon, M. & Powers, A. C. Intraislet Endothelial Cells Contribute to Revascularization of Transplanted Pancreatic Islets. *Diabetes* **53**, 1318-1325 (2004).
291 Zhao, A., Ohara-Imaizumi, M., Brissova, M., Benninger, R. K. P., Xu, Y., Hao, Y., Abramowitz, J., Boulay, G., Powers, A. C., Piston, D., Jiang, M., Nagamatsu, S., Birnbaumer, L. & Gu, G. $G\alpha_o$ Represses Insulin Secretion by Reducing Vesicular Docking in Pancreatic β-Cells. *Diabetes* **59**, 2522-2529 (2010).
292 Zurawski, Z., Rodriguez, S., Hyde, K., Alford, S. & Hamm, H. E. Gβγ Binds to the Extreme C Terminus of SNAP25 to Mediate the Action of Gi/o-Coupled G Protein–Coupled Receptors. *Molecular Pharmacology* **89**, 75-83 (2016).
293 Hammarlund, M., Palfreyman, M. T., Watanabe, S., Olsen, S. & Jorgensen, E. M. Open Syntaxin Docks Synaptic Vesicles. *PLoS Biology* **5**, e198, (2007).
294 Vaidyanathan, V. V., Yoshino, K., Jahnz, M., Dorries, C., Bade, S., Nauenburg, S., Niemann, H. & Binz, T. Proteolysis of SNAP-25 isoforms by botulinum neurotoxin types A, C, and E: domains and amino acid residues controlling the formation of enzyme-substrate complexes and cleavage. *J Neurochem* **72**, 327-337 (1999).
295 Yakel, J. L. Calcineurin regulation of synaptic function: from ion channels to transmitter release and gene transcription. *Trends in Pharmacological Sciences* **18**, 124-134, doi:http://dx.doi.org/10.1016/S0165-6147(97)01046-8 (1997).
296 Conde, C. & Caceres, A. Microtubule assembly, organization and dynamics in axons and dendrites. *Nat Rev Neurosci* **10**, 319-332, (2009).
297 Schappi, J. M., Krbanjevic, A. & Rasenick, M. M. Tubulin, actin and heterotrimeric G proteins: Coordination of signaling and structure. *Biochimica et biophysica acta* **1838**, (2014).
298 Casey, L. M., Pistner, A. R., Belmonte, S. L., Migdalovich, D., Stolpnik, O., Nwakanma, F. E., Vorobiof, G., Dunaevsky, O., Matavel, A., Lopes, C. M. B., Smrcka, A. V. & Blaxall, B. C. Small Molecule Disruption of Gβγ Signaling Inhibits the Progression of Heart Failure. *Circulation Research* **107**, 532.